Models for flexible building operation in the Nordhavn district energy system

Kyriaki Foteinaki

Models for flexible building operation in the Nordhavn district energy system

PhD thesis
by
Kyriaki Foteinaki

DTU

Section for Energy and Services, Department of Civil Engineering, Technical University of Denmark

February 2019

Declaration

I hereby declare that this thesis was written by myself entirely. All sources and materials I have used are enclosed. The thesis has not been submitted further in this form or any other form, and has not been used to obtain any other equivalent qualifications at any other organization/institute.

Kyriaki Foteinaki
14 February 2019
Kgs. Lyngby, Denmark

Acknowledgements

Abstract

As part of the transition from a traditional carbon-intensive energy system to a sustainable energy system, a high proportion of electricity production from renewable energy sources has already been achieved in many countries and it is anticipated to increase further. This means that the controllability of the supply side is limited, which reduces the stability of the power grid and increases the need for balancing strategies. Energy flexibility is proposed as a way to facilitate the management of the energy system while integrating a large proportion of renewable energy sources. In this way, the traditional energy management approach, in which demand dictates the production, can be extended to decentralized energy storage and flexible load shifting, so that both demand and production are controlled to some extent to stabilize the energy network. The residential building sector has a great potential for flexibility, as it is responsible for a very large share of all energy consumption and part of this energy demand can, with appropriate control, be shifted in time, in order to increase the flexibility of the demand side. There are both thermal and electrical loads in buildings that can become flexible. The potential energy flexibility of a building depends on its physical characteristics, the local energy grid and on occupants energy-related activities.

The present research forms part of the "EnergyLab Nordhavn – New urban energy infrastructure" project, which is a smart city research and demonstration project based on the newly developed Nordhavn district in Copenhagen, Denmark. The present thesis analyses the potential flexibility of low-energy residential buildings as a contribution to design and operational decisions, considering the relation of the building with the energy infrastructure and the occupants. The main objectives of the thesis were:

i) to investigate the physical potential of low-energy buildings to facilitate flexible heating operation by using the thermal mass of the buildings as heat storage, while maintaining thermal comfort;

ii) to investigate the operational flexibility potential of low-energy buildings by proposing methodologies that make it possible for the heating system to be operated in such a way as to meet the flexibility requirements of a given district energy supply system;

iii) to address the occupants' energy-related activities in relation to flexible electricity loads, using Danish time-use survey data to create a realistic daily electricity demand profile for Danish households, which can be used when modelling energy flexibility of dwellings.

The most important findings of the research performed in this thesis may be summarized as follows:

In the first part of the work, it was shown that by using only the inherent structural thermal mass of the buildings as storage, there is physical potential for flexible heating operation of low-energy buildings. In cases of abundant production of renewable energy in the system, the buildings can act as storage absorbing thermal energy in the structural thermal mass. In addition, low-energy buildings can remain without any heat supply for many hours without jeopardizing thermal comfort, if there is need to withhold the heat supply for a certain period of time. The results depend on the duration of the change in the heating system and the time of the day that it was performed. It was observed that the energy flexibility potential is strongly affected by the boundary conditions, namely the ambient temperature, solar radiation and internal heat gains.

Focusing on the thermal mass of different concrete elements, measurements from a custom-made set of temperature sensors cast inside concrete walls and ceilings at different depths, confirmed that all the internal concrete layers examined contributed to the physically available heat storage potential of a building.

In the next step of the work, the operational flexibility potential of low-energy buildings using their thermal mass as heat storage was evaluated in relation to the local district heating. The demand of the district heating system was used for rule base scheduling and the marginal heat production cost was used for cost based scheduling of the building's heating system. It was shown that highly effective heat load shifting can be achieved to reduce consumption during the district heating system's peak load hours, and that costs decrease can be achieved. Some possibly adverse effects were identified, as increasing the flexibility of heating system operation may result in increased total energy use and new peaks in the heating load of the building. Nevertheless, higher energy use may be considered acceptable, if it costs less to be produced and can be beneficial for the environment because the additional energy comes from renewable sources. The magnitude

of the benefits that could be achieved was found to be associated with acceptable changes in energy use and in thermal comfort of the occupants of the building.

The role of building occupants was addressed in relation to household electricity loads, as there is some potential for achieving flexible electricity loads in buildings by rescheduling the use of domestic appliances and possibly the heating system, i.e. heat pumps or electric heating. Creating realistic daily household electricity demand profiles was undertaken as the basis for flexibility modelling of electricity household loads. Using information collected from a large group of Danes, i.e. Danish time-use survey (DTUS) data, about the timing of household activities, two modelling approaches were implemented to model the occupant energy-related activities. The resulting occupant energy-related activities profile was linked to electricity demand by using data on appliance ownership and power ratings. A realistic daily electricity load profile for Danish households was obtained, one that can be used in future modelling of energy flexibility of dwellings.

Resumé

Som en del af overgangen fra et traditionelt energisystem baseret på intensiv brug af fossile brændsler til et bæredygtigt energisystem er der allerede i mange lande opnået, at en stor andel af el-produktionen hidrører fra vedvarende energikilder, og andelen forventes at stige yderligere. Dette medfører en begrænset mulighed for at kontrollere forsyningssiden, hvilket reducerer el-nettets stabilitet og øger behovet for strategier, der kan balancere energisystemet. Energifleksibilitet er foreslået som en måde at gøre det muligt at styre energisystemet, samtidig med at der integreres en stor andel vedvarende energikilder. På denne måde kan den traditionelle energistyringsmetode, hvor efterspørgslen dikterer produktionen, udvides med decentraliseret energilagring og fleksibel forskydning af belastningen, så både efterspørgsel og produktion styres til en vis grad for at stabilisere energinettet. Boligsektoren har et stort potentiale for at bidrage til energisystemets fleksibilitet, da det står for en meget stor andel af alt energiforbrug, og en del af dette energibehov kan med passende kontrol flyttes tidsmæssigt for at øge forbrugssidens fleksibilitet. Der er både termiske og elektriske forbrug i bygninger, der kan blive fleksible. En bygnings potentielle energifleksibilitet afhænger af dens fysiske egenskaber, det lokale energinet og af beboernes energirelaterede aktiviteter.

Denne forskning er en del af projektet "EnergyLab Nordhavn - New urban energy infrastructure", der er et forsknings- og demonstrationsprojekt om smarte byer baseret på den nyligt udviklede Nordhavn-bydel i København. Den foreliggende afhandling analyserer den mulige fleksibilitet af lavenergiboliger som et bidrag til beslutninger om design og drift under iagttagelse af bygningers relation til beboerne og til bydelens energiinfrastruktur. Hovedopgaverne for afhandlingen har været:

i) at undersøge lavenergibygningers fysiske potentiale for at muliggøre fleksibel opvarmning ved at bruge bygningernes termiske masse som varmelagring og samtidig opretholde termisk komfort;

ii) at undersøge potentialet for fleksibilitet i lavenergibygninger ved at foreslå metoder, der gør det muligt at opvarme en lavenergibygning på en sådan måde, at det opfylder behovet for fleksibilitet i et givet energiforsyningssystem;

iii) at betragte beboernes energirelaterede aktiviteter i relation til fleksible el-belastninger, ved hjælp af "Danish time-use survey" data ved at opstille realistiske daglige el-forbrugsprofiler for danske husstande, der kan bruges til modellering af energifleksibilitet i boliger.

De vigtigste resultater af den forskning, der er udført i denne afhandling, kan opsummeres som følger:

I den første del af arbejdet blev det vist, at ved kun at bruge den iboende strukturelle termiske masse af bygningerne til varmelagring, er der fysisk potentiale for fleksibel opvarmning af lavenergibygger. I tilfælde af rigelig produktion af vedvarende energi i energisystemet kan bygningerne fungere som lagre, der optager varme i den strukturelle termiske masse. Desuden kan lavenergibygninger forblive uden varmeforsyning i flere timer uden at det går ud over den termiske komfort, hvis der skulle være behov for at afbryde varmetilførslen i en vis periode. Resultaterne afhænger af, hvor længe ændringen i varmetilførslen opretholdes, og af hvilket tidspunkt på dagen den gennemføres. Det blev observeret, at potentialet for energifleksibilitet er stærkt påvirket af randbetingelserne, nemlig den udendørs temperatur, solstrålingen og de interne varmetilskud.

Med fokus på den termiske masse af forskellige betonelementer, blev der brugt målinger fra et specialfremstillet sæt temperatursensorer, der var støbt ind i betonvægge og lofter i forskellige dybder, til at bekræfte at alle de undersøgte interne betonlag har bidraget til det fysisk tilgængelige varmelagringspotentiale i en bygning.

I det næste trin af arbejdet vurderedes det operationelle fleksibilitetspotentiale i lavenergibygger med deres termiske masse som energilagring i forhold til lokal fjernvarme. Fjernvarmesystemets behov for fleksibilitet blev brugt til regelbaseret planlægning, og marginalvarmeproduktionen blev anvendt til omkostningsbaseret planlægning af en bygnings varmesystem. Det blev vist, at ved en effektiv forskydning af varmebelastningen kan opnås en reduktion af forbruget i fjernvarmesystemets maksimale belastningstimer, og der kan opnås en omkostningsreduktion. Nogle muligvis negative virkninger blev identificeret, idet øget fleksibilitet i varmesystemets drift kan resultere i et højere totalt energiforbrug, og der kan forekomme nye toppe i bygningens varmelast. Ikke desto mindre kan højere energiforbrug betragtes som acceptabelt, hvis det koster mindre at producere og kan være gavnligt for miljøet, fordi den ekstra energi kommer fra vedvarende

energikilder. Størrelsen af de fordele, der kunne opnås, viste sig at være forbundet med acceptable ændringer i energiforbruget og i den termiske komfort for beboerne i bygningen.

Den rolle, som bygningens beboere spiller, blev behandlet i forhold til husholdningers el-belastninger, idet der er potentiale for at opnå fleksible el-belastninger i bygninger ved at omlægge brugen af husholdningsapparater og muligvis varmesystemet, dvs. varmepumper eller elvarme. Oprettelse af realistiske dagligdags el-forbrugsprofiler blev udført som grundlag for fleksibilitetsmodellering af husholdningers el-forbrug. Ved hjælp af oplysninger indsamlet fra en stor gruppe af danskere, dvs. data fra "Danish time-use survey", DTUS, (dansk tidsforbrugsundersøgelse), om timingen af aktiviteter i husstande, blev der implementeret to metoder til modellering af beboeres energirelaterede aktiviteter. Den resulterende energirelaterede aktivitetsprofil for beboere blev knyttet til efterspørgslen efter elektricitet ved at bruge data om ejerskab og effektbehov af apparater. Der blev opnået et realistisk dagligt belastningsprofil for danske husstande, som kan bruges ved fremtidig modellering af boligers energifleksibilitet.

Table of Contents

List of figures

List of tables

List of Abbreviations

Acronym	Abbreviated words
ACH	Air Change per Hour
ASHRAE	American Society of Heating, Refrigerating and Air-Conditioning Engineers
BTM	Building Thermal Mass
CO_2	Carbon Dioxide
DH	District Heating
DR	Demand Response
DSM	Demand Side Management
DTUS	Danish Time-Use Survey
e.g.	Exempli gratia, meaning "for example"
EBC	Energy in Buildings and Communities
et al.	et alia, meaning "and others"
EV	Electric Vehicle
GHG	Greenhouse Gas
HP	Heat Pump
HVAC	Heating, Ventilation, and Air Conditioning
i.e.	Id est, meaning "that is"
IEA	International Energy Agency
MOBO	Multi-Objective Building Optimization tool
MPC	Model Predictive Control
NMF	Neutral Modelling Format
O&M	Operation and Maintenance
PCM	Phase Change Material
PhD	Doctor of Philosophy
RERM	Roadmap for a Resource Efficient Europe
RES	Renewable Energy Sources
SFH	Single-family House
TABS	Thermally Activated Building Systems
TES	Thermal Energy Storage
TUS	Time-Use Survey
UN	United Nations
VAT	Value-Added Tax

List of publications: Journal articles, Conference papers

- Foteinaki, K., Li, R., Heller, A. and Rode, C. (2018) 'Heating system energy flexibility of low-energy residential buildings', *Energy and Buildings*. Elsevier B.V. doi: 10.1016/j.enbuild.2018.09.030.
- Foteinaki, K., Li, R., Péan, T., Rode, C. and Salom, J. (2018) *'*Evaluation of energy flexibility of low-energy residential buildings connected to district heating'. S*ubmitted to a peer-reviewed journal (December 2018)*
- Foteinaki, K., Li, R., Rode, C. and Andersen, R. K. (2018) 'Modelling household electricity load profiles based on Danish time- use survey data'. S*ubmitted to a peer-reviewed journal (December 2018)*
- Foteinaki, K., Li, R., Heller, A., Christensen, M. H. and Rode, C. (2019) 'Dynamic thermal response of low-energy residential buildings based on in-wall measurements'. A*ccepted to the 13th REHVA World Congress CLIMA 2019*. Bucharest, Romania.
- Sarran, L., Foteinaki, K., Gianniou, P. and Rode, C. (2017) 'Impact of Building Design Parameters on Thermal Energy Flexibility in a Low-Energy Building', *in the Proceedings of the 15th IBPSA Conference.* San Francisco, CA, USA, pp. 239–248.
- Zilio, E., Foteinaki, K., Gianniou, P. and Rode, C. (2017) 'Impact of Weather and Occupancy on Energy Flexibility Potential of a Low-energy Building', *in the Proceedings of the 15th IBPSA Conference*. San Francisco, CA, USA, pp. 1493–1502.
- Gianniou, P., Foteinaki, K., Heller, A. and Rode, C. (2017) 'Intelligent Scheduling of a Grid-Connected Heat Pump in a Danish Detached House, *in the Proceedings of the 15th IBPSA Conference*. San Francisco, CA, USA, pp. 95–102.
- Foteinaki, K., Heller, A. and Rode, C. (2016) 'Modeling energy flexibility of low energy buildings utilizing thermal mass', *in the Proceedings of* the *9th International Conference on Indoor Air Quality Ventilation & Energy Conservation In Buildings (IAQVEC)*. Songdo, Incheon. Republic of Korea.

List of publications that are not included in the thesis

- Luc, K. M., Foteinaki, K., Rode, C. and Christensen, M. H. (2017) 'Prosumer Analysis Report', *EnergyLab Nordhavn Delivery no. 3.2 a.* url*:* http://www.energylabnordhavn.com/publications-and-deliverables.html

Chapter 1 Introduction

1.1   Framework

Climate change is widely acknowledged to be a major challenge worldwide and we live in an era in which efforts are being made to transition from a traditional carbon-intensive energy system to a sustainable energy system. The energy sector emits 62% of the total greenhouse gases (GHG) [1], so it is a crucial area for the development and application of regulatory policies. Europe is a main driver in this, and the European Council reached agreement in 2014 on the "2030 climate and energy framework", endorsing, among others, three important targets [2]:

- at least 40% less greenhouse gas emissions by 2030 compared to 1990
- at least 27% renewable energy consumption by 2030
- at least a 27% improvement in energy efficiency by 2030

A high proportion of electricity production from renewable energy sources (RES) has already been achieved in many countries and it is expected to increase further. In these countries, decentralized electricity production from RES is currently being integrated into the energy system as part of a sustainable solution. At the same time, electrification of the demand side is expected to increase, and fossil-fuelled vehicles are being gradually replaced with electric vehicles and fossil-fuelled heating systems are being replaced by heat pumps [3]. As a consequence of these changes, managing energy systems becomes more difficult, as they limit the controllability of the supply side and the stability of the power grid, increasing the need for balancing strategies [4].

Many published studies have proposed energy flexibility as a way to facilitate secure operation of the energy system while integrating a large proportion of energy from renewable sources, e.g. [5], [6]. In this context, the traditional energy management approach, in which demand dictates production, is extended with decentralized energy storage, and flexible load shifting with demand response [3], so that both demand and production are controlled to some extent to stabilize the energy network. In this respect, the concept of demand-side management (DSM) has been developed, according to which consumers would have a key role in increasing the flexibility of the whole energy system [7]. This concept was introduced by Gellings [8] as "the planning and implementation of those electric utility activities designed to influence customer uses of electricity in ways that will produce desired changes in the utility's load shape". Methods for shifting demand have attracted great attention, developing the framework for appropriate markets and introducing new control strategies and end use technologies for energy storage in the system [7].

The residential building sector has great potential for flexibility. It is responsible of a large proportion of all energy consumption as it constituted 27 % of the final energy consumption in Europe in 2016 [9]. Some of this energy demand can, by introducing appropriate controls, be shifted in time and/or scale, in order to increase the flexibility of demand in the energy system. There are both thermal and electrical loads in buildings that could become flexible. Buildings have an inherent thermal mass in their construction which could be used for energy storage, in order to postpone the heating or cooling of a building for a certain period of time without jeopardizing the thermal comfort of the building occupants. In addition, the operation of certain domestic appliances could be shifted in time to make electricity loads more flexible. The potential building energy flexibility depends on the physical characteristics of a building, the local energy supply grid and the occupant's activities in the building.

The aim of the present research was *to analyse the potential energy flexibility of residential buildings to provide a basis for informed design and operational decisions, by considering the relation of the building to its energy infrastructure and the occupants' activities.*

1.1.1 EnergyLab Nordhavn project

The present PhD project forms part of the "EnergyLab Nordhavn – New urban energy infrastructure" project, launched in 2015. EnergyLab Nordhavn is a smart city research and demonstration project based in the Nordhavn district of Copenhagen, Denmark. Several companies and research groups intend to make Nordhavn a globally visible real-life laboratory that will become an example of a sustainable city of the future, while also contributing to the City of Copenhagen's goal of becoming carbon-neutral by 2025. This requires innovation in urban design - not least of the energy infrastructure. "The project focuses on a cost-effective future smart energy system that integrates multiple energy infrastructures (electricity, thermal, transportation) and provides an intelligent control of subsystems and components – providing necessary flexibility for efficient utilisation of renewable energy" (Figure 1) [10]. Specifically, this PhD project relates to Work Package 3 on "Smart Energy Buildings". The objective of WP3 is to increase our understanding of the role of low-energy buildings in a smart energy system, and to develop and demonstrate novel control solutions for smarter operation and monitoring of energy and the indoor environment in modern buildings, integrating otherwise problematic fluctuations of the various energy forms into an interconnected system.

Since the Nordhavn district has only recently been developed, the buildings are designed according to the most recent building regulations. According to the Danish Building Regulation 2015 (BR15), and later to the Building Regulation 2018 (BR18), "the total demand of the building for energy supply for heating, ventilation, cooling and domestic hot water must not exceed 30.0 kWh/m² per year plus 1000 kWh per year divided by the heated floor area in m²" [11], [12]. The focus of the present thesis is on low-energy buildings. After an economic evaluation of the available options [13], the municipality selected district heating as the heat supply in the area, so this was the heat supply network considered in the present thesis.

Figure 1. Components of EnergyLab Nordhavn project [10]

1.2   Research hypothesis and objectives

The main hypothesis of this thesis was that *low-energy residential buildings can be induced to operate as energy flexible elements in a district energy system*. The hypothesis was addressed via modelling and data analysis of residential buildings and their heating systems in Denmark and specifically in Nordhavn, with a collective summary of the individual findings.

There were three main <u>objectives</u> in this thesis, which collectively examine the truth of the research hypothesis:

1. To investigate the physical potential of low-energy buildings to facilitate flexible heating operation by using the thermal mass of the buildings as heat storage while maintaining thermal comfort.
2. To investigate the operational flexibility potential of low-energy buildings by proposing methodologies that make it possible for the heating system to be operated in such a way as to meet the flexibility requirements of a given district energy supply system.
3. To address the occupants' energy-related activities in relation to flexible electricity loads, using Danish time-use survey data to create a realistic daily electricity demand profile for Danish households, which can be used when modelling energy flexibility of dwellings.

1.3   Thesis structure

This paragraph describes the structure of the thesis. <u>Chapter 1</u> is an introduction that presents the framework that led to the research hypothesis of the thesis and its main objectives. <u>Chapter 2</u> provides the background and state-of-the-art of the topics that are examined in the present thesis. In particular, the concept of energy flexible buildings, the role of the thermal mass of the buildings, and the relationship of the building with its heat supply system and the influence of occupants. The building modelling approaches are also introduced. The third, fourth and fifth chapters summarize the main findings of the reports published in the course of this PhD: <u>Chapter 3</u> summarises the results of an evaluation of physically available energy flexibility in the thermal mass of the buildings, in terms of energy and thermal comfort; <u>Chapter 4</u> assesses different control strategies for flexible operation of a building connected to a district heating system and the flexible operation of a building equipped with a heat pump; and <u>Chapter 5</u> links occupant energy-related activities to their resulting electricity demand, in order to obtain a realistic daily electricity load profile for Danish households, which can be used for flexibility modelling of household electricity loads. <u>Chapter 6</u> summarizes the key findings of all the research, while the final <u>Chapter 7</u> suggests future research topics. The publications that were produced in the context of this work appear in the <u>Appendix</u>.

Table 1 lists the reports published during the course of this PhD. Each publication is related to the relevant research objective of the thesis and it is stated whether it was addressed by simulation modelling or measurements.

Table 1: Overview of publications included in the thesis

Paper	Title	Objective	Simulation	Measurements	Chapter
# I	Heating system energy flexibility of low-energy residential buildings	#1	X		3.1
# II	Evaluation of energy flexibility of low-energy residential buildings connected to district heating	#2	X		4.1
# III	Modelling household electricity load profiles based on Danish time-use survey data	#3	X		5
# IV	Dynamic thermal response of low-energy residential buildings based on in-wall measurements	#1		X	3.4
# V	Impact of Building Design Parameters on Thermal Energy Flexibility in a Low-Energy Building	#1	X		3.2
# VI	Impact of Weather and Occupancy on Energy Flexibility Potential of a Low-energy Building	#1	X		3.2
# VII	Intelligent Scheduling of a Grid-Connected Heat Pump in a Danish Detached House	#2	X		4.2
# VIII	Modeling energy flexibility of low energy buildings utilizing thermal mass	#1	X		3.3

Chapter 2 Background

This chapter provides the background and state-of-the-art of the topics that are examined in the present thesis. In particular, a definition for energy flexible buildings is provided and possible sources of energy flexibility in buildings are presented. In this context, the role of the thermal mass of buildings is emphasised, together with the relation of the building with its heat supply system and the occupants' activities. Finally, a brief overview of building modelling approaches and simulation tools for building energy modelling is provided.

2.1 Energy flexible buildings

2.1.1 Definition of energy flexible buildings

The building sector is listed as one of the three key sector that must be addressed in "Roadmap for a Resource Efficient Europe" (RERM),), which is an environmental policy document that outlines the ways to transform Europe's economy into a sustainable one by 2050 [14]. RERM states that buildings have significant potential for resource conservation by better construction and use of buildings, as they could impact 42% of final energy consumption, 35% of total GHG emissions, 50% of extracted materials and 30% of water in some regions. In addition, the large thermal mass that is inherent in buildings, together with the different technologies that can be integrated with buildings, can be used for thermal energy storage. Buildings thus have the potential to provide flexibility services to the energy system by suitable control of their thermal and electrical loads. The concept of the energy flexibility of a building is not new, but has recently attracted more attention and is defined by 'International Energy Agency (IEA) Energy in Buildings and Communities Program (EBC) Annex 67 *Energy Flexible Buildings*' as "the ability to manage its demand and generation according to local climate conditions, user needs and grid requirements" [15]. Hence, energy flexible buildings will be able to respond to load control strategies determined by the requirements of the relevant energy network. The main properties that are often evaluated when a building is operated flexibly are the amount of energy use that can be shifted in time (added/withheld), the start time and duration of the shift, and the costs incurred by or saved by this shift when the entire energy supply system is considered [15].

To date, there is no market structure for flexibility services. However, there are possible actors that could participate and benefit from them: distribution and/or transmission system operators, balancing actors that could be developed, building owners and/or occupants whose tolerance of discomfort could reduce their energy bills or be increased by environmental awareness, building management operators, policy makers.

2.1.2 Building loads and storage technologies

Buildings consist of different types of shiftable loads requiring different control approaches, i.e. space heating and cooling, domestic hot water, electric appliances, charging of electric vehicles, etc. Some of those loads are directly flexible and can be displaced in time either via a grid-connected automatic controller or manually by users in response to incentive mechanisms, such as smart domestic appliances and the charging of electric vehicles [16]. Some loads are not directly flexible in time; instead, the required energy load must be met at the most convenient time for the system and the energy must be stored so that it can be used when needed. This can be achieved by using different storage technologies, which can be divided into two main categories: electricity storage and thermal energy storage.

For electricity storage, electric batteries of different scales can be used. Small scale batteries installed into domestic electronic devices have an affordable cost, provide increased mobility during use and have a momentary impact on the grid level. Large scale batteries, with enough capacity to store enough energy to meet a household's demand for several hours, have a highly debatable cost efficiency and environmental impact [17], and a less predictable lifetime that depends on repetitive charging and discharging [18]. Intermediate scale batteries include those of electric vehicles (EVs), which are expected to gain a considerable share of the market in the future, i.e. over 35 million vehicles in the world in 2022 according to

the International Energy Agency [19]. The fact that the use of EVs is limited to a small fraction of the day, with the need for charging being most often flexible in time, enables these batteries to offer considerable potential for grid flexibility. Different solutions and optimisation algorithms for coupling EVs with the grid have been reviewed, e.g. [20]. This technology, however, still presents some problems, including battery disposal, costs and social acceptance. Using "second-hand" batteries, which have been used in EVs, in buildings has been proposed as a cost-effective solution for building flexibility [21].

Concerning thermal energy storage, many different technologies are available, as reviewed by [22]. Those most broadly used are the inherent thermal mass of the building structure [22], [23], with or without the integration of phase change materials (PCMs) [24], and HVAC systems such as hot water tanks [25], [26]. In order to use the structural mass of the building as thermal heat storage, a sensible heat storage approach is used. Sensible heat storage is the most common and simple technique, for which a temperature gradient is applied to a material in order for it to accumulate or release heat. The amount of energy stored and the time characteristics of the process depend on the thermodynamic properties of the material and the temperature gradient to which it is exposed. Construction materials, primarily concrete, have considerable storage potential. Concrete building components, i.e. floors, walls, ceilings, could thus contribute to load shifting, by being exposed to higher temperatures in order to accumulate heat, which they would release later when the air temperature decreases. To increase the storage capacity of the building mass, the incorporation of latent heat storage components has become increasingly popular among researchers, i.e. integrating phase change materials in the building structure. These materials use the latent heat of the liquid to solid phase change. Although this technology has been widely researched, e.g. [24], [27], there are still many constraints on its large scale application. The most common application of heat storage in a HVAC system is hot water storage. This technology uses the sensible heat storage approach and due to the high heat capacity of water, it is possible to store enough hot water to respond to the large variations in DHW demand. Hot water storage may be used for space heating as well. Many studies, e.g. [23], couple the hot water tank with the use of heat pumps, in order to enhance the load shifting potential. In combined systems which include solar thermal, hot water tanks are often a key element [28]. Another HVAC approach to storage is used in Thermally Activated Building Systems (TABS), which is an active heat storage system that uses building elements, i.e. walls, floor, ceiling, as the sensible heat storage medium [22]. Hot water pipes, ducts for air circulation or heating cables are embedded in the building elements and charge them when appropriate. The heat is then released to the indoor environment by conduction, convection and radiation.

Integration of PCMs and storage systems in the HVAC may require new investments. Although domestic hot water storage tanks are common in Danish households, especially in apartment blocks, they are not necessarily available in every building; instantaneous heat exchangers are also used to supply domestic hot water from the district heating network. Heat storage in phase change materials is an emerging technology and as research is still needed, applications in buildings are rare [22], [29], [30]. On the other hand, the thermal mass of the building stock is available and can be used as short-term thermal energy storage with a limited investment in appropriate control installations for the heating system. In existing residential buildings such controllers are usually missing. Commercial buildings and new residential buildings frequently have the heating system connected to a building/home management system, which would have to be reprogrammed to provide building flexibility in response to an external signal. The objective of this thesis, in terms of thermal energy flexibility, is to use the physically available thermal energy storage of buildings, so the thermal mass of the building structure is the focus of this work.

2.2 Thermal mass of buildings as heat storage

Building thermal mass is the mass of the building that consists of such materials that are able to store thermal energy. The components that are typically included in the estimation of the thermal mass are the building structure, interior partitions and furniture. The thermal mass is divided into external and internal. The former is exposed to the ambient conditions directly, while the latter is exposed to the indoor conditions only.

Heat storage in the thermal mass can be achieved by simply exposing it to a temperature gradient. The thermal mass absorbs or releases heat through the basic heat transfer mechanisms: conduction, convection,

radiation. Heat transfer by convection takes place at the surface of the thermal mass. The radiation process takes place between the thermal mass and the rest of the surfaces in the room, while conduction takes place within the interior body of the thermal mass.

Different physical properties of the materials of the thermal mass are involved in the effectiveness of thermal storage, including their density, specific heat capacity, thermal conductivity and surface heat transfer rate. The heat transfer rate depends on the available surface area of the material and the coefficients of convective and radiative heat transfer. The temperature difference between the participating media, as well as the air flow speed around the thermal mass, define the convective heat transfer coefficient. During one cycle, the penetration depth through the interior body of the thermal mass is limited by the diffusivity of the material, which is the thermal conductivity divided by density and specific heat capacity at constant pressure [31].

The thermal mass of the building usually consists of multiple layers of different materials and it is exposed to various heat gain sources, such as domestic equipment, lighting, occupants, solar gain, and incoming air supplied either by natural ventilation or by mechanical HVAC systems. The heat transfer processes and the dynamic thermal response of the building mass can thus be highly complicated.

2.2.1 Application of thermal mass to indoor comfort and energy conservation

Buildings with high thermal mass have been used for many years in research and in real applications, as this property has been shown to have a positive impact on occupant comfort. It has the ability to mitigate the indoor effect of outdoor temperature fluctuations, maintaining the indoor air temperature in a narrower range [32]–[34]. If passive heating or cooling techniques are implemented, high thermal mass can contribute to energy conservation. One typical example of the application of thermal mass during summer is night time cooling with natural ventilation, in order to minimize the need for mechanical cooling. Many studies, simulations and measurements, have been performed within this field, e.g. [35]–[38], and their conclusion was that in high thermal mass buildings, with night time natural ventilation indoor air temperatures are decreased and the use of energy for cooling is reduced. Studies have been also performed for winter time; for example [39] monitored a timber and a concrete building and concluded that the concrete building had considerably lower heating energy use due to the higher thermal mass.

2.2.2 Application of thermal mass to flexible load operation

In Sweden, as early as 1982, a pilot test was performed, which involved two buildings whose response to an absence of heating that lasted several hours was studied [40]. For durations less than 24 hours, a temperature drop of less than 3°C was observed, which was considered acceptable. Since then, there have been many studies showing the potential for using the structural thermal mass of buildings for heat storage in order to achieve energy flexibility [23], [41]–[47]. Most studies perform simulations of shifting heating loads in time to reduce demand in peak load periods, or to promote demand in off-peak periods, imposing heating strategies that exploit the dynamic thermal response of the building mass. Research to date has been mainly focused on typical examples of the building stock, namely old or moderately old buildings, as case studies to assess the flexibility potential, such as [43], [45], [47]–[49]. In order for the concept of energy flexibility to be used on the energy system scale and across sectors, a portfolio with different potentials and dynamics must be developed including building categories that offer different flexibility options. Regarding the new generation of buildings, a few studies have compared the potential of older buildings to that of newer buildings [23], [44], [46], and [50], a study of a low-energy single-family house in France. In-depth analysis of the flexibility potential of low-energy buildings is the target of the present work.

2.3 Flexible buildings in relation to the local energy supply system

In order for buildings to provide flexibility to the energy grid, they should function in a grid context and this should serve as basis of the control algorithms. The interaction between the energy infrastructure and a building should preferably take place via two-way communication platforms. The full potential of a group of buildings can then be exploited in terms of the timing and magnitude of the available flexibility by implementing appropriate demand response strategies in buildings.

2.3.1 Approaches for implementation of demand response in buildings

There are two main approaches to implementing demand response in the building sector: direct and indirect load control [51], [52]. In direct load control, the supplier directly controls the loads of the consumers and has the right to perform load modulations in order to facilitate the operation of the system. Consumers may be provided with incentives, for example a lower fixed cost in the contract, in order to accept participation in such a demand response scheme. A tolerable thermal comfort range should be agreed upon and/or the consumers should have the possibility to override the control, possibly with an associated price penalty. The indirect load control refers to ways of motivating consumers to participate in demand response, by adjusting the timing and/or the magnitude of their energy use [53]. Indirect control is usually achieved by offering financial inducements; the supplier provides variable tariff schemes that will motivate the consumer to benefit from low-cost periods and avoid high-cost periods. The dynamics of the tariff scheme may vary, including time-of-year (seasonal) pricing, time-of-use pricing (daily or weekly variations), critical-peak pricing and real-time pricing, depending on the requirements of the energy system. The consumers are informed about the price of energy one day or some hours in advance and decide whether or not to participate in the demand response activity. More demand response types are described in the literature [54], and the different methods could also be combined.

2.3.2 Flexible buildings in relation to the district heating system

Initially, the focus of energy flexibility was on the electricity sector, though a multi-carrier energy system gradually developed. The need for the electricity grid to be seen as part of an integrated smart energy system is explained in [55] and the importance for the stability of the grid of including flexible Combined Heat and Power (CHP) production is emphasized. An integrated cross-sector approach was used in [56] to identify optimum storage solutions that make it possible to use a larger proportion of renewable energy, as opposed to focusing on individual sub-sectors, such as electricity storage solutions, which are less cost-efficient. In [57] they concluded that a district heating (DH) system can cost-effectively contribute to the security of supply and to the sustainability of future energy systems.

One very important element of DH networks is the potential for short-term heat storage, facilitating the optimization of the CHP cogeneration in relation to the electricity sector without compromising the heating sector [58], [59]. Using heat storage, when there is sufficient electricity production in the system from intermittent renewable energy, for example wind turbines, CHP can decrease their production since heat can be supplied from storage. The CHP plant can increase electricity production when there is higher demand for electricity. In that case, if the heat production is higher than the heat demand, the heat storage can be charged; conversely, if the heat production is lower than the heat demand, the heat storage can be discharged. This provides flexibility to the energy system, which is a significant aspect for the integration of a larger proportion of intermittently available renewables, which is economically and environmentally crucial for the optimal operation of the system. The thermal energy infrastructure, with its existing energy storage and the potential for extension, is thus considered a great asset for energy flexibility.

The building sector, because of the large thermal mass of the existing building stock, appears to have potential for short-term thermal energy storage, as previously mentioned. Most often, case study buildings connected to the electricity grid have been used, with heat pumps [45], [60]–[63] or with electric space heating systems [64]. Only a few studies have concerned buildings which are connected to a district heating grid. Compared to the electricity system, the available information and expertise on demand shifting for DH is limited. An important impediment to this is that the market structure for heat is not as developed and transparent as it is for electricity, so it is not yet sufficiently mature to manage demand response. In [65] the authors discussed the Swedish situation, in which although district heating pricing has been liberalized over the past two decades, the district heating market has not yet evolved to become a nationally integrated market. In [66] existing heat pricing models and methods were reviewed and [67] reported a survey to capture the current structure of DH price models in Sweden, in an effort to improve the DH market and promote heat pricing transparency. Both studies [66], [67] state that market transparency will have to be improved before effective demand shifting strategies can be implemented in DH systems.

Important benefits would be obtained by managing demand response in DH systems. For the system, reduced heat production costs by minimising start-ups and avoiding the use of peak load boilers. Capacity issues in the existing network could be handled by more efficient use of the existing pipes and installations, thus reducing network investment costs. In addition, CHP plants would able to adjust the heat production to in order to benefit from high proportion of renewable energy in the electricity system, in such a way that the CHP plants still run along the curve of the most efficient states of cogeneration, which makes it possible to increase the revenue of the CHP plants from electricity sales. In addition, environmental benefits would be achieved by minimising the use of carbon-intensive peak load boilers and increasing the use of renewable energy sources in the system. However, in order for the consumer to benefit from participating in managed demand response, monetary incentives would probably have to be offered. In [66] it was stated that engaging consumers on the demand side is as important as renovating a DH supply and distribution system, in order to achieve energy and CO_2 emissions reduction, so the development of a real-time pricing mechanism in the DH sector is suggested.

Previous work on managing demand response in buildings connected to DH was focused on the load shape rather than real-time heat pricing. In [68] a multi-agent system to control a DH network with 14 buildings was reported; the goal was to achieve peak shaving without reducing the quality of services, and the importance of taking many small local decisions to impact the overall system performance was emphasized. In continuation, [69] described the implementation of load control based on a multi-agent system in three DH systems in Sweden, and showed that the system achieved a reduction of peak loads of up to 20% of the total load. In [70] an optimization algorithm was simulated, using the thermal capacity of buildings with a certain flexibility in the time taken to reach the set-point. The results estimated peak reductions of up to 35% with about 2% increased heat use. In [71] an optimization model of a case study energy system in a Danish city was described, focusing on the impact of storage in the building thermal mass on DH energy supply. It was found that the building thermal mass was used as intra-day storage and that it facilitated effective use of a larger proportion of solar thermal heating energy. Evaluating the potential of individual buildings to act as thermal energy storage by adjusting the signals of the supply temperature to the radiator system, [43] reported results from 5 case study multifamily residential buildings and showed that heavy concrete buildings can tolerate changes in heat delivery without significant deterioration of their indoor climate. In [72] a field study was performed in 28 households connected to a DH network in England, implementing load shifting, which improved the load factor (ratio of mean to maximum demand) from 0.29 to 0.44, with a consequently increased energy use of approximately 3%. It was estimated, however, that the network cost reductions would exceed this amount. Only a few studies have reported demand response based on dynamic heat production costs. In [73] they proposed and simulated an implementation of demand response, with a sensor network that exchanged information between the heat supplier and the building substation. In a 5-day simulation of a building the indoor temperature set-point was modulated according to variable pricing for heating in order to reduce energy use during peak load hours. The study showed an energy use reduction of 20% during peak load hours, while the indoor temperature was reduced by 1°C with an outdoor temperature of -15°C. In [51] the results of three case study buildings in which demand response demonstrations were carried out are reported; it was recommended that DH tariff structures that encourage the use of DSM should be adopted, and that the tariffs in DH should reflect the suppliers' marginal heat production costs and should be understandable by the customers and should remain within legal constraints.

2.3.3 Danish district heating

Denmark is one of the European countries with the most developed district heating networks, supplying 64% of Danish households [74]. The heat generation for the Danish DH system already includes 52% from renewable energy sources [75]. Figure 2 shows the percentage distribution of fuel mix for district heating production in 2016 in Denmark [75]. Current Danish energy targets are that only renewable energy sources should be used by 2050. With the base load demand being gradually converted to CO_2-neutral energy by using biomass-fuelled plants, heat pumps and geothermal energy, the main goal to be achieved is to avoid the need for peak load boilers, which mainly use natural gas. In addition, 68.9% of all heat is produced in cogeneration with electricity (CHP) [74], so the interaction between the sectors is profound. Extending the heat

storage potential within the DH system is thus essential and it would further increase the importance of the role of DH in any future flexible energy system.
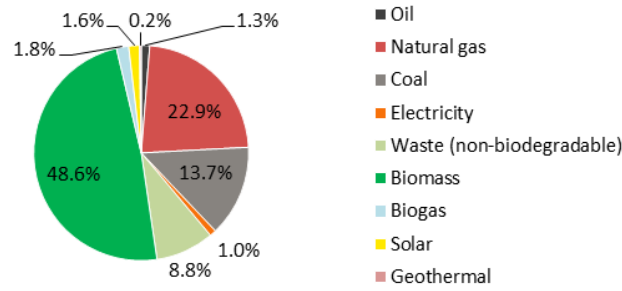
Figure 2: Percentage distribution of fuel mix for district heating production in Denmark (2016)

The Danish district heating is considered a natural monopoly and it has therefore been regulated on the non-profit principle. Although the heat price varies in different areas, the costs that can be included in the heating price are defined by law. According to this, the consumer pays a heat price that should cover all costs pertaining to the heat supply, i.e. fuel costs, facility of heat production, DH network, buildings, operation and maintenance (O&M). It is not allowed for the heat supply company to make a profit, but they should be financially sustainable, so depreciation of assets and financing costs are also including in the determination of heat price. This means that the heat price paid by the consumers is influenced by many parameters, including investment, O&M and the efficiency of the production facility, investment, O&M and heat loss in the DH network, fuel prices, taxes and VAT, subsidies, electricity price (relevant for plants that both use and produce electricity) [74]. Regarding the ownership of the DH production plants, there are different structures of ownership in Denmark. Large energy companies typically own and operate the largest plants, while smaller plants are owned by municipalities or cooperatives. According to the non-profit principle, the structure of the co-operative provides an efficient heat supply at the lowest possible cost to the end customer. The payment for heating by customers is based on private contracts between them and the respective heating supply company. The heat price is fixed for the whole year and comprises a fixed charge per installation or capacity and a variable part based on the actual district heating use.

District heating in the Greater Copenhagen area (i.e. Copenhagen metropolitan area) is currently produced by different plants owned by three companies: 3 waste incineration plants and 1 geothermal plant (these 4 energy sources being politically prioritized), 3 CHP plants, 2 heat accumulators, 4 large peak load boilers and approximately 30 peak load units, which function as a reserve for the base load units – typically if they fail during winter. It is supplied through interconnected transmission and distribution networks. A cooperative between district heating companies has been established (Varmelast.dk), which is responsible for planning the heat production for the supply of Greater Copenhagen, in order to ensure the most financially efficient district heating production. One of the main tasks of Varmelast.dk is to prepare the day-ahead heating plan, which is based on the district heating forecasts disclosed by the district heating companies and considers fuel prices, O&M costs, energy taxes on heat production, CO_2 quota costs, income from the power market and hydraulic bottlenecks in the network [76]. Varmelast.dk performs a joint optimization of heat and power production and aims to ensure the maximum economic benefit for the entire system. The load dispatch is based on marginal heat production costs, while the heat purchase settlement is based on bilateral contracts between producers and district heating companies. The latter are confidential (i.e. not known by Varmelast.dk) and define how the total benefit is shared. There are 3 scheduled intra-day adjustments of the heating plan every day with updated heat consumption forecasts, capacities and power prices.

2.4 Considering occupants' activities in flexible buildings and household energy use

2.4.1 Influence of occupants on building energy use and flexibility potential

For decades, research has focused on understanding all aspects of energy use in residential buildings to improve energy efficiency, and the stochastic nature of occupants' interaction with the building has been shown to be a key aspect. Occupant behaviour in buildings is a determining parameter for the energy use and indoor environment and it has been found that it is a main reason for discrepancies between the estimated and the actual energy use [77], [78]. The main discrepancies are found because of various occupancy patterns and different occupant behaviour under the same thermal conditions. Regarding the occupancy patterns, there is a clear correlation between them and the energy use of a household; [79] showed that energy conservation depends heavily on the occupancy pattern of the household, such that the energy assessment of a building and the estimation of potential energy conservation should be case specific. Another important parameter is the perception of thermal comfort and how occupants react in order to maintain their comfort. There is a wide range of preferences, as well as different activity and clothing insulation values. A combination of all of them, together with other social drivers, affects how an occupant will act to maintain comfort, thus reflecting on the energy use of the building. Some people would adjust the clothing level, others would open the window, while yet others would adjust the temperature set-points of the system. An indicative example is in [80], where it was found that a thermostat set-point could vary significantly, from below 19ºC to above 25ºC, when considering summer air-conditioning use in residential buildings. Such differences in preferences of the heating and cooling set-points define the whole operation of the HVAC system, and are reflected in the discrepancies found between the estimated and the actual energy use. Other important occupant-related factors that may affect energy use include lighting level preferences, solar shading adjustment, window opening behaviour, domestic hot water consumption, and the use of domestic appliances such as washing machines and dishwashing machines.

The use of the energy flexibility in residential buildings requires occupants to increase the range of what they regard as acceptable and in many cases the active participation of occupants who are prepared to adjust their activities and behaviour and become more flexible. [81] presented a pilot test with smart washing machines combined with dynamic tariffs and showed that the smart appliances were only used with smart configurations for 14% of the time. [16] quantified the flexibility of residential smart appliances, domestic hot water tanks and electric vehicles based on a pilot test in Belgium. It was found that the flexibility potential of these energy loads varied considerably between the hours of the day, and from weekend to weekdays. This indicates that in order to exploit the flexibility potential of building loads, modelling the residential load profiles as realistically as possible is essential. Matching the energy consumption in residential buildings to local distributed energy production is the key to the efficient operation of the system. When planning a DSM strategy whose goal is to shift the operation of certain domestic electric appliances in time, it is essential to know the relationship between occupants' presence, activities and energy use. In new low-energy buildings, knowing the occupants' schedules and activities is important, as heat emitted from occupants and appliances has a large impact on the household's heating requirements [42], [82], [83].

2.4.2 Modelling household electricity load profiles using a large dataset of occupants' activities - A first step to facilitate modelling of energy flexibility in dwellings

There is potential for increased flexibility in the electricity loads in buildings from domestic appliances and possibly the heating system, i.e. heat pumps or electric heating. If the occupants' activities are to be addressed in relation to household electricity loads, creating realistic daily household electricity demand profiles is the basis of flexibility modelling for electricity household loads.

For this purpose, two main input datasets are required; i) the set of appliances in the household and the electricity load of each individual appliance and ii) the time and duration of use of the appliances, or the activity pattern of the occupants [84]. Both incorporate elements of variability, but the second aspect, which is related to the occupants' behavioural patterns, incorporates a far greater degree of unpredictability. Two dataset sources are usually employed for the development of the models: detailed measurements at the building level

[85], [86] and time-use survey data. A time-use survey (TUS) is a statistical survey completed by building occupants, usually by keeping logbooks or diaries, that aims to report the main types of activity an individual engages in during a specific time interval. This method is in principle easier to execute as it interferes less with the everyday life of the participants in the survey and it is less expensive than making high-resolution measurements [87].

Many studies have developed models based on TUS data, which are usually available at the national level. A number of studies focus on occupancy and activity patterns in households [88]–[93]. Indicatively, [88] analysed the United Kingdom's time-use survey 2005 which describes how dependent energy-related social practices in the household take pace in relation to the time of the day, including preparing food, washing, cleaning, washing clothes, watching TV and using a computer. In [89] a stochastic bottom-up model was developed based on the French TUS data of 1998/1999, to predict time-dependent activities in residential buildings. In [90] they developed a method to generate occupancy patterns based on the clustering of household occupancy profiles using the United Kingdom's time-use survey 2000 data. There are also studies that associate TUS data to households' electricity use [84], [87], [94]–[100]. For example, in [94] a model for domestic electricity demand was developed based on the United Kingdom's 2000 TUS data by simulating appliance use. The German TUS was used in [95] to develop a stochastic bottom-up model which generates synthetic electrical load profiles. The Swedish TUS was used in [87] to create load profiles both for household electricity and domestic hot water consumption, and in [96] to model domestic lighting demand. The outcomes of the above studies show that TUS can increase understanding of occupant behaviour and subsequently can be used to improve the realism of building energy use in modelling so as to exploit the potential flexibility. However, the Danish TUS (DTUS) data have scarcely been used by the Danish energy research community. In [93] they performed a detailed analysis on the latest DTUS 2008/09 and profiled domestic energy-related daily activities and the time-related characteristics of the activities. The occupancy data were also modelled and used in an energy flexibility analysis in [101]. Creating realistic daily household electricity demand profiles for Danish households is one objective of the present thesis.

2.5   Building modelling

This section provides a brief overview of the different approaches for building modelling with regard to energy use and thermal comfort and concludes with the simulation tool used in the research presented in this thesis.

2.5.1   Building modelling approaches

There are two main approaches for modelling the building stock: top-down and bottom-up.

Top-down models are based on historical/statistical data and economic theory and do not distinguish energy use due to individual end-uses [102]. These models aim to identify the changes in the building stock and their effect on the overall energy consumption, in order to determine the energy supply requirements. They are mainly divided into econometric and technological models. The econometric models focus on price and income, whereas the technological models focus on the characteristics of the building stock. The main advantage of these models is that they require aggregated data with a lower level of detail. The main limitations are that they cannot model the effects of specific technologies, technological changes or specific end-users.

Bottom-up models are models that calculate the energy use of individual buildings or clusters of buildings by describing the individual elements in great detail, and those results can be extrapolated to a wider region according to the representative weight of the modelled sample [102]. The main advantage of these models is that they can model existing or new technologies in great detail. This makes it possible to determine the end-use contribution and to identify targeted areas for the application of specific strategies. The main limitation is that they require a large amount of input data in great detail. Usually they are either difficult to collect, as is the case for building-related information, or vary stochastically, as is the case for occupant-related information. Models therefore often include many assumptions and are computationally intensive. Bottom-up models can

be classified into categories, depending on their ability to describe physical phenomena (in an engineering approach) and on their dependence on data (using statistical techniques):

- Physics-based models, also known as white-box models, consist of equations describing the physical phenomena and a core calculation engine. They are given specified input variables and they predict the output variables of a specific model [103]. The input data include detailed information on characteristics of building components and energy systems, operation strategies, thermal comfort conditions, number of occupants and their schedules, etc. The level of details of the input data depends on the method used and the complexity of the model. The most significant limitation of the white-box models is the unavailability and uncertainty of input data, especially those regarding occupant behaviour. Nevertheless, it has been shown that the empirical data it is possible to collect, in conjunction with a detailed description of physical phenomena, do make it possible to arrive at a trustworthy estimation of the energy performance of a building [104]. Regarding energy use for heating and cooling, the international standard for the energy performance of buildings ISO13790 [105] lists three options for the calculation of energy requirements: i) simple hourly results, ii) monthly (or seasonal) results, iii) dynamic simulation results. For these, two calculation methods are employed: quasi steady-state and dynamic methods. With *quasi steady-state* methods the heat balance is calculated over a long period of time (e.g. monthly or seasonal), using gain and/or loss correlation factors to consider dynamic effects. These models have lower complexity and provide estimations of energy requirements at a low temporal resolution. With *dynamic* methods, the heat balance is calculated with short time steps (e.g. hourly, or varying appropriately) considering the heat that is stored in and released from the mass of the building. Thermal transmission, ventilation heat flows, thermal storage, solar and internal heat gains, and variable weather conditions can be modelled using this approach.

- Data-driven models, also known as black-box models, use historical data and employ statistical techniques or data-mining approaches, to attribute energy use to specific end-uses. They can be divided into three categories: regression analysis, conditional demand analysis and neural networks [102]. Depending on the models, the selection of variables may or may not have a physical interpretation. These models can be applied from individual homes or from a sample of households to national building stock energy forecasting. The difficulty of acquisition of the required historical data is one of the main limitations, together with the fact that they cannot represent the effect of specific technologies or technological changes.

- Hybrid methods have been developed as a combination of the above categories. They consist of a simplified physical representation in combination with historical and sometimes empirical data [104]. They employ statistical methods to predict the energy use of a building. Grey-box models belong to this category, as they consist of stochastic differential equations, which describe a lumped model of the building heat dynamics in continuous time, coupled with a data-driven part, which is represented by discrete time measurement equations [106]. Grey-box models include more meaningful parameters than black-box models but represent dynamic heat transfer phenomena less accurately than white-box models. Nevertheless, they are often employed for control applications due to their short computation times.

2.5.2 Heat transfer modelling for buildings

There are different approaches in literature for heat transfer modelling in buildings. The authors of [107] classify the models into two categories: the mathematical models and the physical models. Mathematical models are based on a differential equation of a n-node model. There are different methods for solving the equation, including implicit Euler methods, explicit Euler methods, Fourier series methods [107]. In physical models, the methods for calculating transient heat transfer include: *i)* Explicit solution of the heat diffusion equation, by finite difference, finite volume or response function methods. These models are complex, in terms of data requirements and analysis, and have thus increased computational time. *ii)* Model reduction techniques represent the phenomena with fewer sets of equations, but intrinsically this leads to lack of generality because the model is limited to the case from which it was derived. *iii)* Model simplification techniques include resistance–capacitance (RC) network and admittance methods. In principle, these methods are a good compromise between accuracy and simplicity, in terms of data requirements and computational time. Grey-box models, which were presented in the previous section, use model simplification

techniques. An electrical analogy is usually employed to represent heat transfer in a room/building: one or more temperature nodes represent the conducting wall in a building, a resistor represents heat transfer, for example the wall can be linked to the ambient air temperature node by a resistor, and the thermal inertia of the wall is represented by the capacitance. The number of nodes used in a model affects its accuracy, data requirements and computational time. Oversimplified models, for example a two-node model may behave poorly, in cases of buildings with high thermal mass and well insulated envelope [108].

2.5.3   Simulation tools for building energy modelling

Numerous simulation tools have been developed over the years using the above approaches. Since this work was based on storage in the thermal mass of the building, it was essential that the thermal mass of the building was considered. In 1996 [109] reviewed 16 computational methods for building loads that take into account the thermal mass. These methods are simplified, easy to use and require less detailed input information and can be calculated either with the use of computer or even by hand calculations. Nowadays, the energy calculations have evolved to sophisticated models, commercially available complex tools, which require a large amount of inputs, but are able to provide simulation results with great accuracy. Some broadly used examples are ESP-r, TRNSYS, BSim, IESVE, IDA ICE, Modelica, EnergyPlus, COMSOL. On the basis of the desired accuracy output and the availability of input information the appropriate tool can be chosen.

In the present work the simulations were performed with the dynamic building performance simulation software IDA Indoor Climate and Energy, version 4.7 [110]. It is a dynamic whole-building simulation tool based on symbolic equations stated in Neutral Modelling Format (NMF) that has undergone validation tests [111]–[114]. The building, systems, controls, network airflow, etc. are simulated in an integrated way and the time-step varies dynamically during runtime to automatically adapt to the nature of the problem. The wall model used by this software is a finite difference model with multi-layered components. Each layer represents one material and is discretized into several nodes. In this way, it is able to capture nonlinear effects in the thermal dynamics of the building that alternative models, such as RC- networks, usually oversimplify [115].

Chapter 3   Physically available energy flexibility that uses the thermal mass of buildings

This chapter is based on Paper I, Paper IV, Paper V, Paper VI and Paper VIII and addresses the 1st objective of the thesis.

This chapter evaluates the physically available energy flexibility in the structural thermal mass of buildings. The results are evaluated in terms of energy and thermal comfort. Different scenarios are investigated, varying the boundary conditions and building design characteristics, while focusing on the thermal response of the concrete elements. The limitations of the approach are discussed. The findings would enable an aggregator/system operator to choose a suitable portfolio of buildings for participation in grid services that increase flexibility in an energy supply system.

The work refers to Danish case studies. The framework of this thesis was the local energy district of Nordhavn, Copenhagen, Denmark, which consists mainly of newly built low-energy residential buildings. The investigations described in Sections 3.1, 3.2 and 3.3 were therefore based on simulation models of low-energy buildings designed according to the Danish Building Regulation 2015 [11], [12]. Details of the building models, methods and results can be found in the respective publications.

3.1   Evaluation of heating energy demand and energy flexibility

This section investigates the flexibility potential of low-energy buildings in terms of the heating energy that can be added to or withheld from such buildings for a certain period of time within a pre-defined range of indoor temperatures. The evaluation was carried out at the building level.

The findings of this study have been published in Energy and Buildings, Elsevier:
Foteinaki, K., Li, R., Heller, A. and Rode, C. (2018) 'Heating system energy flexibility of low-energy residential buildings', Energy and Buildings.

3.1.1   Method

3.1.1.1   Building models

Building regulations are becoming progressively stricter in minimizing heat loss and increasing the efficiency of heating, cooling and ventilation systems in buildings. The Danish Building Regulation 2015 (BR15) [11] introduced[1] a new generation of buildings that will participate in the energy system. Two building types according to the BR15 standard were selected for the study; a single-family house (Figure 3) and an apartment block (Figure 4), both representing typical Danish buildings of their type.

---

[1] When this study was finished, the new building regulation 2018 (BR18) was published. The only difference in the new regulation is the efficiency of heat recovery of the ventilation system for apartment blocks, which, in the new code is the same as for a single-family house, namely 80%. If the simulations were run according to BR18, the only difference in the results would be the heating demand for the apartment block, which would slightly decrease.

Figure 3: Single-family house model
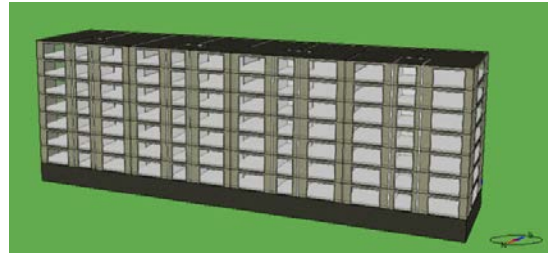
Figure 4: Apartment block model

Table 2 and Table 3 list the properties of the main construction components of the typical single-family house and apartment block, respectively.

Table 2: Properties of main components for single-family house

Components	Thickness [mm]	U-value [W/(m²·K)]	Surface [net m²]	Materials
External wall	448	0.138	109	Aerated concrete (100mm) Insulation class 38 (240mm) Brick (108mm)
Internal load-bearing wall	150	4.082	37	Concrete
Internal non-load-bearing wall	100	1.349	97	Aerated concrete
Roof	567	0.077	149	Plaster board (26mm) Scattered wooden boards (22mm) Insulation class 38 (460mm) Roof tiles (59mm)
Floor	472	0.105	149	Oak planks (22mm) Concrete (100mm) Insulation class 38 (350mm)
Windows	3 pane glazing	0.900	34	-

Table 3: Properties of main components for apartment block

Components	Thickness [mm]	U-value [W/(m²·K)]	Surface [net m²]	Materials
External wall	448	0.138	1726	Aerated concrete (100mm) Insulation class 38 (240mm) Brick (108mm)
Internal load-bearing wall	200	3.704	2779	Concrete
Internal non-load-bearing wall	100	1.349	1921	Aerated concrete
Roof	670	0.092	980	Hollow core concrete (270mm) Insulation class 38 (400mm)
Floor towards ground	470	0.106	980	Concrete (120mm) Insulation class 38 (350mm)
Floor/ceiling decks	407	0.348	6860	Oak planks (14mm) Concrete (80mm) Insulation class 38 (93mm) Concrete (220mm)
Windows	3 pane glazing	0.900	1408	-

The single-family house has a net heated floor area of 149 m² and envelope area per volume 0.998 m²/m³. The effective thermal capacity is calculated 60 MJ/K (see the relevant publication for the detailed calculation) and the heat losses, which are received as output from the simulation tool, are 101 W/K. The ratio of those two leads to a time constant of 165 h. It is divided into two thermal zones: a primarily day-occupied zone, i.e. living

room, kitchen, and a primarily night-occupied zone, i.e. bedrooms. The window area is 22.5% of the heated floor area and are distributed 41% south, 26% north and 33% east/west following the reference single-family house of BR15. The apartment block has a net heated floor area of 6272 m^2 and envelope area per volume 0.265 m^2/m^3. The effective thermal capacity is calculated 2908 MJ/K and the heat losses are 3084 W/K, leading to a time constant of 262 h. The building has 7 floors and an unheated basement, which is assumed to be maintained at about 15°C by heat losses from hot water pipes. Each floor has 8 apartments with the same floor area of 112 m^2 each, and 4 staircases with the same floor area of 21 m^2 each. The window area is 22.5% of the heated floor area and are distributed 52% south, 37% north and 11% east/west. The apartment block was modelled as one thermal zone per apartment and one thermal zone per staircase, using adequate zone multiplication of the zones that show similar thermal behaviour.

In this study only space heating is considered, as the objective of the work is to evaluate the storage capacity of the inherent thermal mass of the building structure. The heat emission system in both buildings is low temperature water radiators dimensioned according to the standard DS 418 [116] for indoor temperature 20°C and outdoor temperature -12°C, using an over-dimensioning factor of 15%. The supply water temperature to the system is 45°C. Mechanical ventilation is installed in the buildings with constant air volume of 0.3 l/s per m^2 of heated floor area, using heat recovery of 80% efficiency for the single-family house and 67% for the apartment block, according to BR15. Minimal infiltration is considered as 1.5 l/s per m^2 of the heated floor area at a pressure differential of 50 Pa and a very low effect of structural thermal bridging. Internal masses are included in the models to represent furniture, with a total area of 26 m^2 in the single-family house and 1120 m^2 in the apartment block. The ground model is calculated in the simulation tool according to the standard ISO 13370 [117]. More detailed information can be found in the relevant publication.

3.1.1.2   Energy flexibility events

Starting from a reference operation of the building, modulations of the temperature set-point of the heating system were performed. The inherent thermal mass was thus activated, being charged after the air temperature set-point is increased and discharged after the air temperature set-point is decreased. In this study the reference operation was a typical thermostatic control with constant air temperature set-point at 22°C, which is a typical desired indoor temperature in Danish households during the heating season. Two types of modulation from the reference operation were considered:

- Increased set-point from 22°C to 24°C for a certain time duration, representing a scenario with more than enough energy from renewable sources in the energy system. In this case, heat supply in buildings can be increased and the additional heat can be stored into the thermal mass (depicted in Figure 5, left). This type of modulation is further referred to as an <u>upward flexibility event</u>.
- Decreased set-point from 22°C to 20°C for a certain time duration, representing a scenario with limited or no energy from renewable sources in the energy system. In this case, heat supply in buildings can be withheld or interrupted, causing heat to be released from the thermal mass into the building (depicted in Figure 5, right). This type of modulation is further referred to as a <u>downward flexibility event</u>.

In all cases, the thermal comfort of occupants should not be compromised. The thermal comfort limits[2] of 22°C ±2 °C were chosen to be within the range of thermal comfort Category II "Normal level of expectations for new buildings" in the heating season, according to the standard EN/DS 15251 [118].

Examples of responses to upward and downward flexibility events are illustrated in Figure 5, together with the main flexibility parameters evaluated in this work, equivalent to those defined in [119].

---

[2] The standard EN/DS 15251 refers to operative temperature. However, the results from the simulations showed that in these buildings, the effect of cold surfaces is very limited, so air and operative temperatures differ very little, i.e. by less than 0.5°C at all times. For the sake of clarity only indoor air temperature is presented in the graphs.
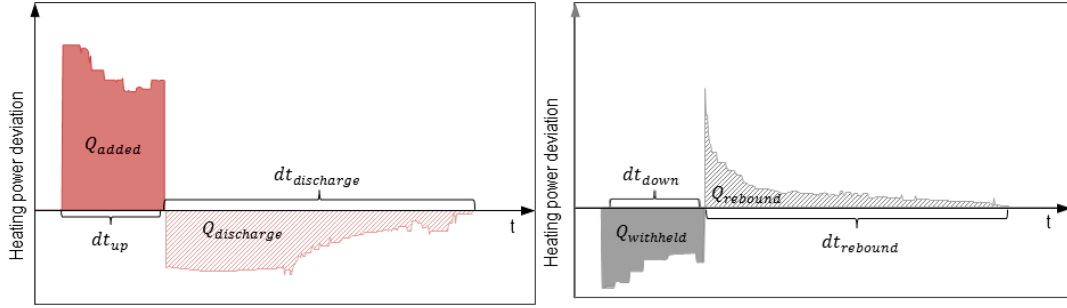
Figure 5: Examples of responses to upward and downward flexibility events and main flexibility parameters

i) Added energy (Q_{added}): the amount of energy that is added to the building during the upward flexibility event. It is given by Equation (1):

$Q_{added} = \int (q_{up} - q_{ref}) dt_{up}$ (1), where:

dt_{up}: the duration of upward flexibility event, when the temperature set-point is increased to 24°C,

q_{up}: the heating power during the upward flexibility event,

q_{ref}: the heating power during the reference operation of the building with the temperature set-point at 22°C.

ii) Discharged energy ($Q_{discharge}$): the amount of energy that is used after being stored in the thermal mass of the building during the upward flexibility event. It is given by Equation (2):

$Q_{discharge} = \int (q_{discharge} - q_{ref}) dt_{discharge}$ (2), where:

$dt_{discharge}$: the duration of time after the end of the upward flexibility event before the heating system returns to normal operation,

$q_{discharge}$: the heating power during the discharging period.

iii) Withheld energy ($Q_{withheld}$): The amount of energy that is withheld from the building during the downward flexibility event. It is given by Equation (3):

$Q_{withheld} = \int (q_{down} - q_{ref}) dt_{down}$ (3), where:

dt_{down}: the duration of downward flexibility event, when the temperature set-point is decreased to 20°C,

q_{down}: the heating power during the downward flexibility event.

iv) Rebound energy ($Q_{rebound}$): the amount of energy that is additionally used by the building in order to return to the initial state after the downward flexibility event. It is given by Equation (4):

$Q_{rebound} = \int (q_{rebound} - q_{ref}) dt_{rebound}$ (4), where:

$dt_{rebound}$: The duration of time after the end of the downward flexibility event before the heating system returns to normal operation,

$q_{rebound}$: the heating power during the rebound effect period.

Both Q [kWh] and q [W] refer to the net energy/heating power of the heat emission system, not the entire heating system, in order to avoid dependencies on the choice of the system, its configuration and the energy carrier.

By definition, the available energy that can be added to or withheld from a building during a specific flexibility event depends on multiple parameters and is inevitably time-dependent. The duration and starting time of the event are main characteristics, thus their impact was assessed:

- Flexibility events with duration 2 hours, 4 hours, 6 hours, 8 hours, 12 hours, 16 hours, and 24 hours.
- Flexibility events with starting time at midnight (00:00), early morning (06:00), midday (12:00) and evening (18:00).

The amount of energy that can be stored in structural thermal mass is particularly sensitive to boundary conditions, so ambient weather conditions were examined in this study including solar radiation and ambient air temperature. Representative examples of days in the heating season in Denmark were chosen as cold, moderate and warm days. The weather data used were from the Danish Meteorological Institute representing the Danish Design Reference Year [120]. Solar radiation was also considered, so both cloudy and clear sky representations of the same days were simulated. Figure 6 shows the ambient air temperature and global solar irradiance on these representative days.
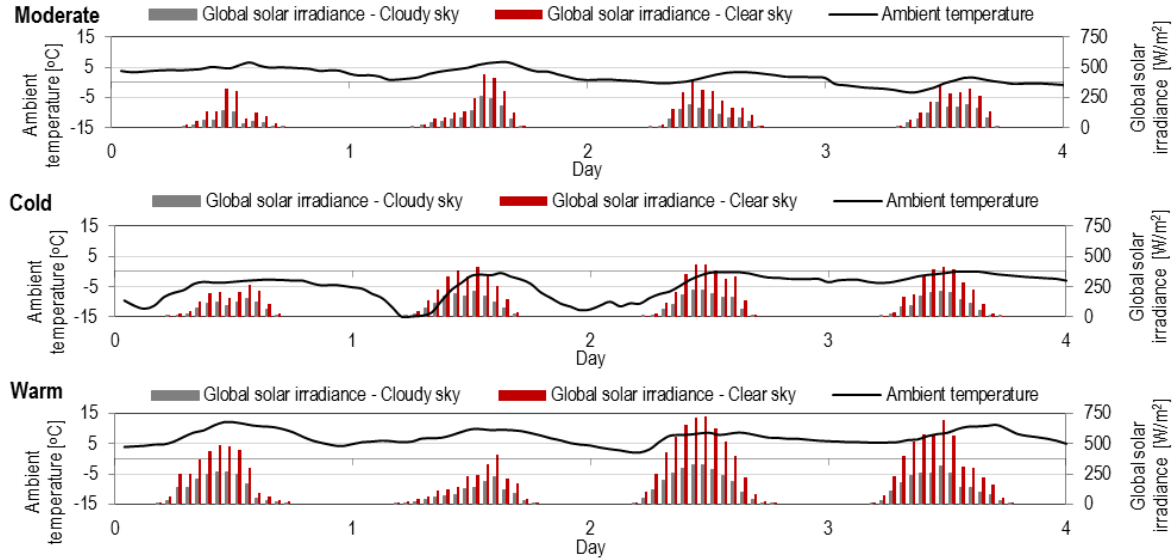
Figure 6: Ambient air temperature and global solar irradiance for representative moderate (top), cold (middle) and warm (bottom) days of the heating season with cloudy and clear sky

Each simulation ran for four virtual days; one day prior to the day when set-point modulation was performed and two days after it. Before each simulation, a dynamic start-up phase of one month was simulated in order to eliminate the effect of initial conditions. The schedules for the internal gains were set according to the standard DS/EN ISO 13790:2008 Table G.8 [105], while the total heat flow rate from internal gains was 5 W/m^2, which was adjusted to meet the average Danish national values [121].The internal heat gains included heat emitted from lighting, equipment and occupants.

The impact of building characteristics, including thermal properties, was examined. Certain design parameters were selected for study, in order to examine the relative impact of each design parameter choice. The range of each parameter used is shown in Table 4. The baseline building case appears with bold font for each parameter.

Table 4: Building design parameter variations

Parameter			Range		
Window U-Value [W/m^{2}K]	1.8	1.5	1.2	**0.9**	0.6
External Wall Insulation Thickness [cm]	16	20	**24**	28	32
External Wall Concrete Thickness[3] [cm]	0[4]	5	**10**	15	20
Internal[5] Wall Concrete Thickness [cm]	5[6]	10	**15**	**20**[7]	25
Windows / Heated Floor Area Ratio [-]	12.5%	17.5%	**22.5%**	27.5%	32.5%

---

[3] Inside of the insulation layer

[4] The external wall with 0 cm concrete represents a wall with thermal insulation on the interior surface.

[5] Internal load-bearing walls are considered in the variation

[6] Buildings with this variation belong to the category of semi-light buildings according to the Danish Building Research Institute (SBi) Guidelines 'Energy Demand for Buildings' [27].

[7] The value for the baseline building case for the Internal Wall Concrete Thickness is 15cm for the single-family house and 20cm for the apartment block.

3.1.2 Results and discussion

3.1.2.1 <u>Heating demand under reference operation</u>

The reference operation of the buildings was with a constant temperature set-point of 22°C during the heating season (November-March). The peak demand for space heating for the single-family house was 2.5 kW (16.8 W/m^2) and the space heating energy use was 21 kWh/m^2 net heated floor area. For the reference operation of the apartment block, the peak demand for space heating was 82 kW (13.1 W/m^2) and the space heating energy use was 12 kWh/m^2 net heated floor area. Figure 7 shows the heat introduced into the house, categorized as heat coming from the heating system, internal gains and solar gains. For the single-family house, 48% of the heating requirements were supplied from the heating system and the other half came from solar and internal heat gains, which contributed 11% and 41% respectively. The apartment block had lower energy use for space heating in comparison to the single-family house, since the ratio of the envelope area per volume was considerably lower. This distribution should be taken into consideration when implementing flexibility events in new buildings. On the one hand, thermal comfort would be less sensitive to any variations in the heat supply, while on the other hand, the influence of uncontrollable factors such as solar and internal gains should be taken into consideration.
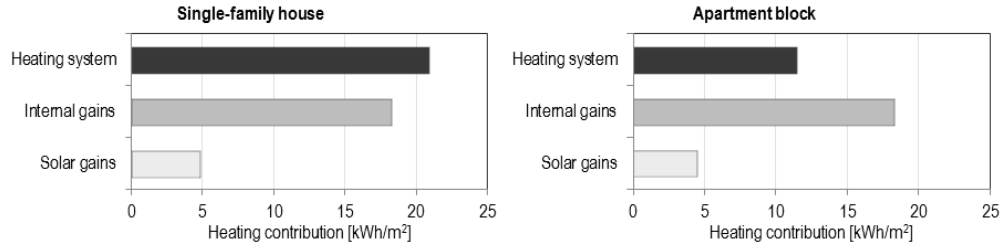
Figure 7: Analysis of heating contribution during reference operation with temperature set-point at 22°C for the single-family house (left) and the apartment block (right)

3.1.2.2 <u>Energy flexibility</u>

3.1.2.2.1 <u>Base case energy flexibility</u>

Two base case flexibility events were implemented, one upward and one downward, both starting at 06:00 with a duration of 8 hours and performed under ambient weather conditions corresponding to moderate winter days in Denmark with a cloudy sky. The colour code used for the figures is as follows: red refers to upward flexibility events, grey to downward flexibility events, and blue to the reference operation. Figure 8 and Figure 9 show results for the single-family house and the apartment block, respectively, with the heating power (top) and indoor air temperature (bottom) during the base case flexibility events. During Day 1, the buildings are under the reference operation and the heating power is depicted with a solid blue curve. In Day 2, the modulations of the base case flexibility events are implemented, with the respective added/withheld heating power being highlighted in the figures, and the resulting effects are over the next 48 hours are apparent.
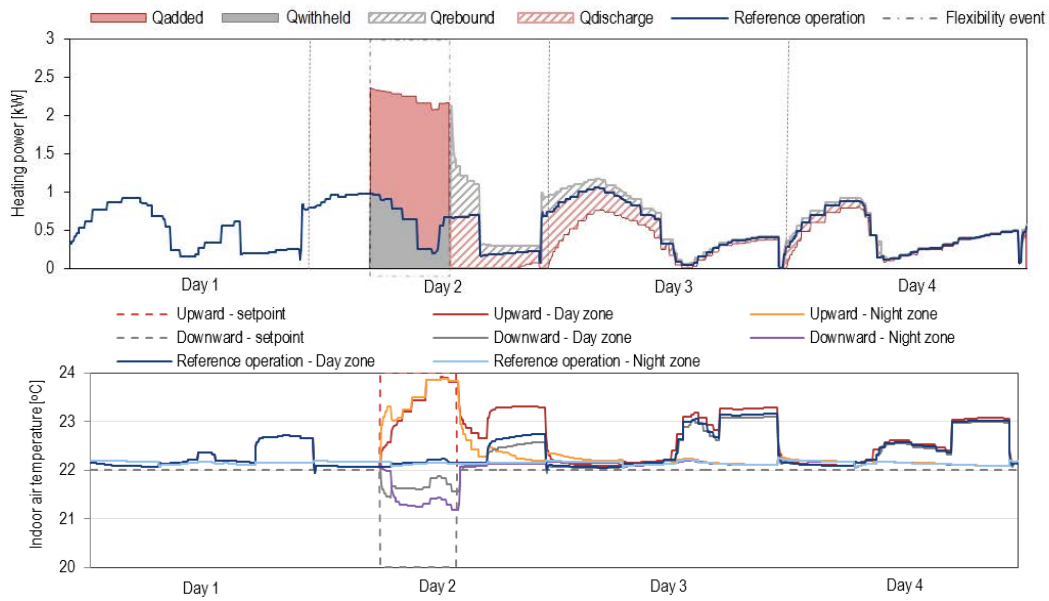
Figure 8: Heating power (top) and indoor air temperature (bottom) during base case flexibility events for the single-family house
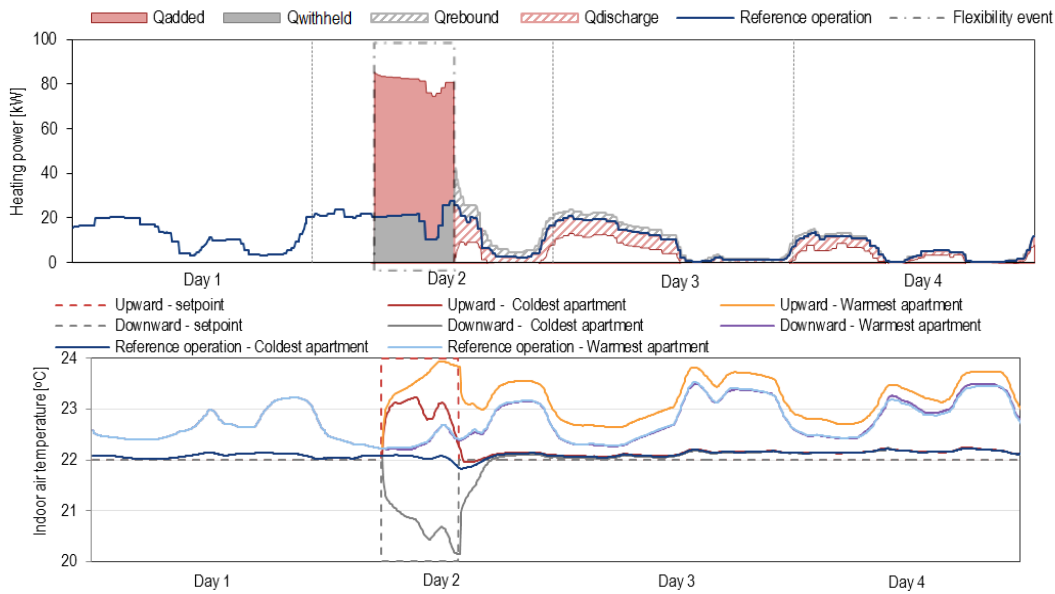
Figure 9: Heating power (top) and indoor air temperature (bottom) during base case flexibility events for the apartment block

For the single-family house, during the upward flexibility event, there was a considerable increase in heating power, which was followed by 10 hours during which the heat supply was terminated. For approximately 40 hours after the event, the energy supply from the heating system was lower than in the reference operation, since energy was being discharged from the thermal mass. For the downward flexibility event, the heat supply was interrupted completely during the event. The event was followed by a peak, which lasted approximately 3 hours. It was expected that withholding would result in a temporary peak load for the heating system. For approximately 20 hours after the event, the energy use was slightly higher than in the reference operation (rebound effect). During the upward event, the set-point of 24°C was reached after approximately 5 hours, in both zones. When decreasing the set-point to 20°C, the temperature decrease was rather slow. Within the 8 hour duration of the event, the temperature dropped to minimum values of 21.5°C and 21.3°C in the day and night zone, respectively. In all cases, the impact of the internal gains was apparent: every day in the evening when internal gains peaked in the day zone, the air temperature increased by almost

1°C, while the energy use was relatively low. It should also be noted that every day, at about midday, energy use decreased due to solar gains, even on a cloudy day.

The thermal behaviour of the apartment block was similar to that of the single-family house. The indoor air temperatures shown were those from the apartments considered as critical, with a middle apartment on the 3rd floor being the warmest and a top corner apartment being the coldest. The two apartments had considerably different thermal environments. The warmest apartment was insignificantly affected by the changes in the set-points, i.e. by changes in the heat supply; the temperature in this apartment was constantly higher than the set-point of 22°C. There were more apartments of the warmer type, so the apartment block was mostly affected by this behaviour. This explains why the peak created due to the rebound effect after the downward flexibility event was relatively small. This thermal behaviour indicates that overheating might be an issue for this type of apartment, especially under milder ambient weather conditions. In the coldest apartment, the temperature decreased at a faster pace compared to the single-family house, dropping almost to 20°C at the end of the downward flexibility event. On the other hand, during the upward flexibility event, the indoor air temperature did not rise higher than to 23.2°C.

The total amount of energy supplied for the four days to the single-family house was 751 Wh/m^2 for the reference operation, 771 Wh/m^2 for the upward flexibility and 751 Wh/m^2 for the downward flexibility. For the apartment block the total energy supplied was 339 Wh/m^2 for the reference operation, 375 Wh/m^2 for the upward flexibility and 324 Wh/m^2 for the downward flexibility. In this case the upward flexibility events led to increased energy use, namely 2.7% for the single-family house and 10.6% for the apartment block, while the downward flexibility events led to the same energy use for the single-family house, but decreased energy use by 4.4% for the apartment block. The apartment block used considerably less energy per square meter than the single-family house, as the ratio of the envelope area per volume of the apartment block (0.265 m^2/m^3) is considerably lower than in the single-family house (0.998 m^2/m^3). The lower energy requirement and heat loss are the reasons why the apartment block performs as an efficient energy storage unit.

The indoor temperature did not change very rapidly. If instead of modulating the set-points, the heat supply had been completely interrupted, the single-family house would have maintained the temperature above 20°C for more than 48 hours, while the apartment block kept the temperature above 20°C for 20 hours in the coldest apartments and for more than 3 days in the other apartments. Either building can therefore remain without any heat supply for a long period of time without jeopardising the thermal comfort of the occupants. These long hours of autonomy allow the system operators to exploit the independence of their operation. Although the low energy requirements limit the energy available for withholding in each building individually, when aggregating many similar types of building, the amount of energy flexibility becomes considerable.

3.1.2.2.2 Energy flexibility of events with various duration, start times, ambient conditions and building design parameters

Figure 10 and Figure 11 show the results of simulations performed for different durations and start times. The graphs show the energy that was either added (Q_{added}) or withheld ($Q_{withheld}$), during the flexibility events, with red being the additional energy and grey being the withheld energy. For the reference events, which are outlined in black, in the single-family house an additional 13 kWh (87 Wh/m^2) were added over 8 hours, while 5 kWh (36 Wh/m^2) were withheld over 8 hours. In the apartment block an additional 492 kWh (78 Wh/m^2) were added over 8 hours, while 156 kWh (25 Wh/m^2) were withheld over 8 hours. A clear asymmetry between the added and the withheld energy should be noted, in both buildings. As previously shown, the heat supply was terminated completely during the downward event, indicating that the amount of available energy to be withheld was determined by the heating requirements of the reference scenario (22°C). Hence, the maximum energy available for withholding is closely related to the heating demand of the buildings during normal operation; this means that for low-energy buildings the potential for withholding is limited. On the other hand, the maximum energy that can be added is limited either by the capacity of the heating system or by the upper thermal comfort limit, in this study 24°C.
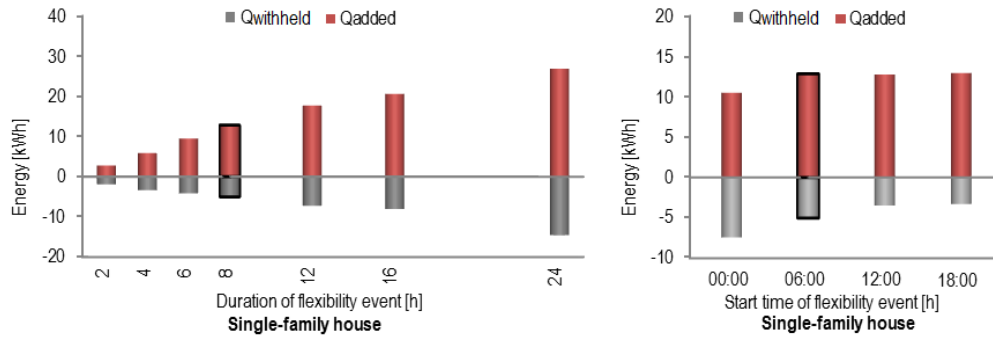
Figure 10: Energy added/withheld during upward/downward flexibility events with different durations (left) and different starting time (right) for the single-family house
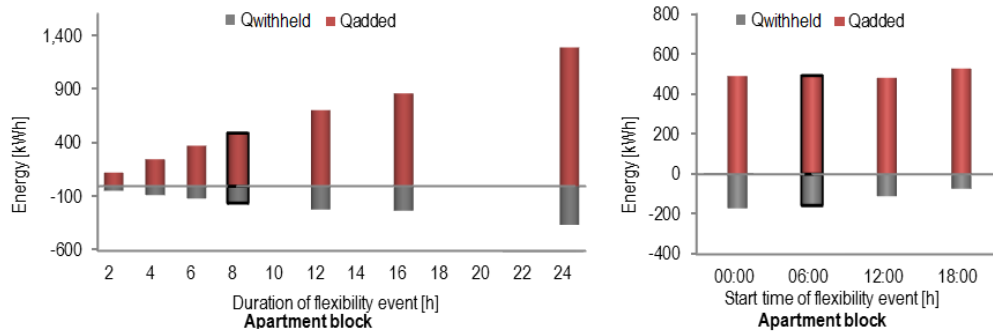
Figure 11: Energy added/withheld during upward/downward flexibility events with different durations (left) and different starting time (right) for the apartment block

Regarding the <u>duration</u> of the events, it can be seen that the increase in the amount of energy added and withheld during the events was almost linearly related to the duration of the events. The reason for this is that when the air temperature had reached 24°C, the surface temperature of the walls was still lower than the air temperature, so heat continued to be absorbed by the wall elements until the end of the event. The <u>start time</u> of the events had a greater influence on the amount of energy that could be withheld than on the amount that could be added. The potential for added energy is almost the same in all cases, apart from the event starting at 00:00 in the single-family house, which was lower by 18%. The reason for this is that during the night the heating demand for space heating of the building (without modulations) is higher than during the day because of lower heat gains. The amount of energy that can be added during an upward flexibility event is limited by the maximum capacity of the space heating system. For both buildings, the potential for withholding is highest at night-time (00:00 and 06:00), and is reduced almost by half in the day time (12:00 and 18:00). During the day, the internal and/or solar gains were substantial, so the heating demand was lower and the potential for withholding was lower.
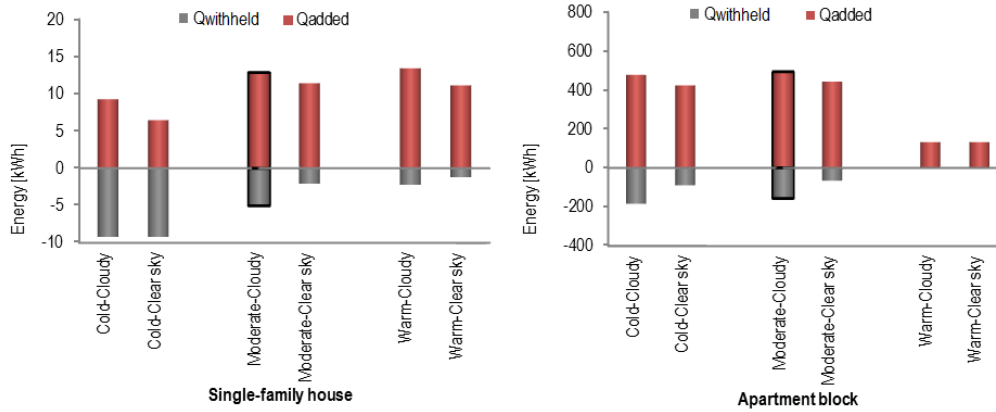
Figure 12: Energy added/withheld during upward/downward flexibility events under different weather conditions for the single-family house (left) and the apartment block (right)

Figure 12 shows the energy flexibility under different <u>weather conditions</u> during the heating season. In all cases with clear sky, with more solar gain, energy flexibility was decreased. For upward flexibility events, solar gains contributed considerably to the increase in the indoor temperature, so the amount that could be added by the heating system was reduced, being limited by the upper limit of thermal comfort. For the downward flexibility events, increased solar gain led to lower energy use in the reference case, so less energy could be withheld compared to the case with cloudy sky. For the warmer days of the heating season the flexibility was low, because heating demand was low. For colder days, since the reference energy requirement in this case was already high in order to meet the heating set-point, the potential for additional heating demand was low, being limited by the capacity of the heating system. On the other hand, since the reference energy requirement was higher, more energy could be withheld.

Figure 13 shows the results of the simulations performed for the different <u>design parameters</u>. Building models were created for every variation. For every building model, its reference operation, i.e. operation without flexibility modulations, was simulated, which was then compared to the upward and downward flexibility events. Every bar represents one variation of the building model: the grey section of the bar shows the energy that was withheld during the downward flexibility event, the red section the energy that was added during the upward flexibility event, while the white patterned section shows the energy use under the reference operation for each duration. The results of the baseline building are outlined in black for each parameter.
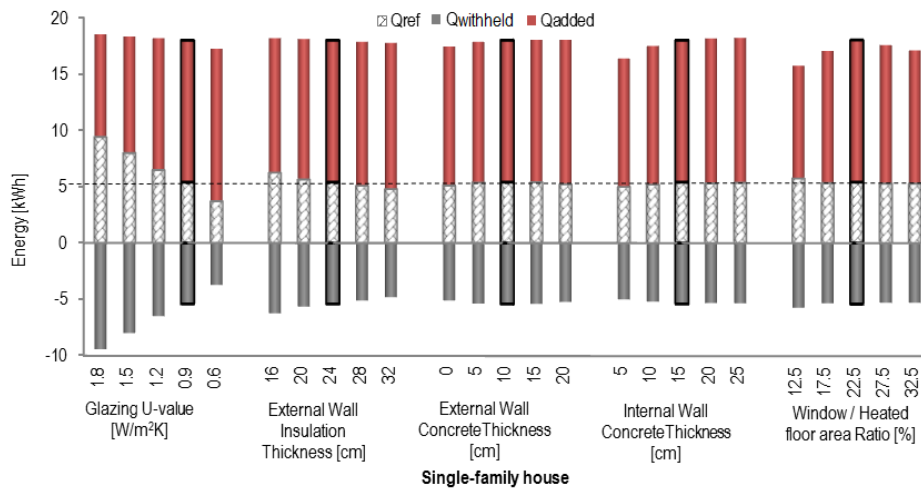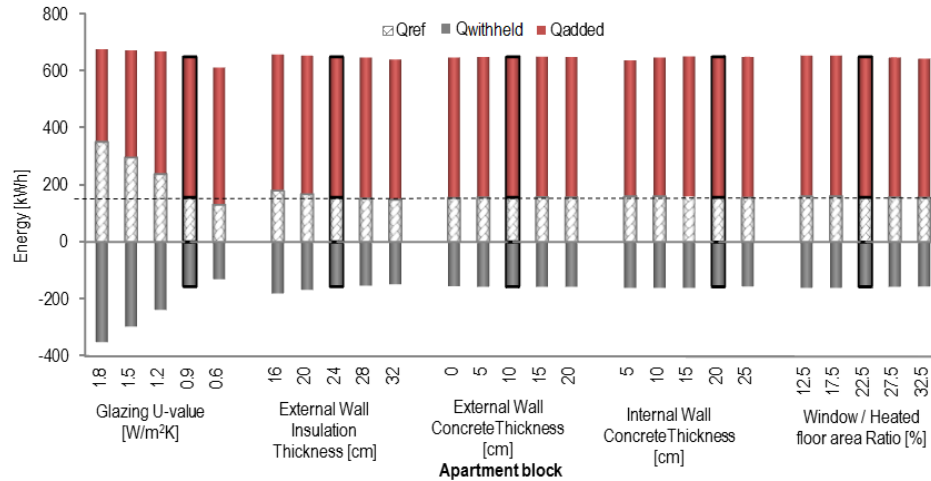
Figure 13: Energy during reference operation and energy added/withheld during upward/downward flexibility events with different geometry characteristics of the single-family house (top) and the apartment block (bottom)

When varying the window U-value or the external wall insulation thickness, the capacity of thermal mass remained unaltered when evaluating the effect of the buildings' heat losses on the flexibility potential. Similar results were obtained for both building types. The upward flexibility decreased as heat losses increased since the heating system has a limited capacity. On the other hand, the downward flexibility increased as heat losses increased, since in buildings with higher losses, the energy use during their reference operation was higher, so there was more energy to be withheld. The magnitude of the effect of the glazing U-value was greater, because among the parameters examined, the heat loss coefficient of the buildings was more affected by the window U-value than by the changes made in the other design parameters.

In order to evaluate the effect of the thermal capacity, the external and internal wall concrete thicknesses were examined. There was no considerable change (less than 5% between variations) in energy flexibility when the thickness of the external wall was changed. Considering the concrete as an element of thermal mass rather than as a structural element, it appears that no benefit is gained by adding concrete thickness greater than 10 cm for the external walls and 15 cm for the internal walls. The contribution of the thermal capacity of the internal walls was shown to be higher than that of the external walls. This finding was expected, since the internal walls are exposed to the indoor air on both sides, while the external walls are only exposed on one side. More importantly, the material of the internal load-bearing walls is concrete, whereas for the external walls it is aerated concrete, which has a lower thermal capacity. The relative effect of the thermal capacity of walls in the apartment block appeared smaller compared to the effect in the single-family house, since there is already a large amount of concrete in the ceiling decks of the apartment block.

The effect of window/heated floor area ratio was complicated as three main elements changed simultaneously: thermal capacity, heat loss and solar gain.

The time constant of all the building models was calculated and the added or withheld energy during the base case upward (red) or downward (grey) flexibility events are plotted in Figure 14.
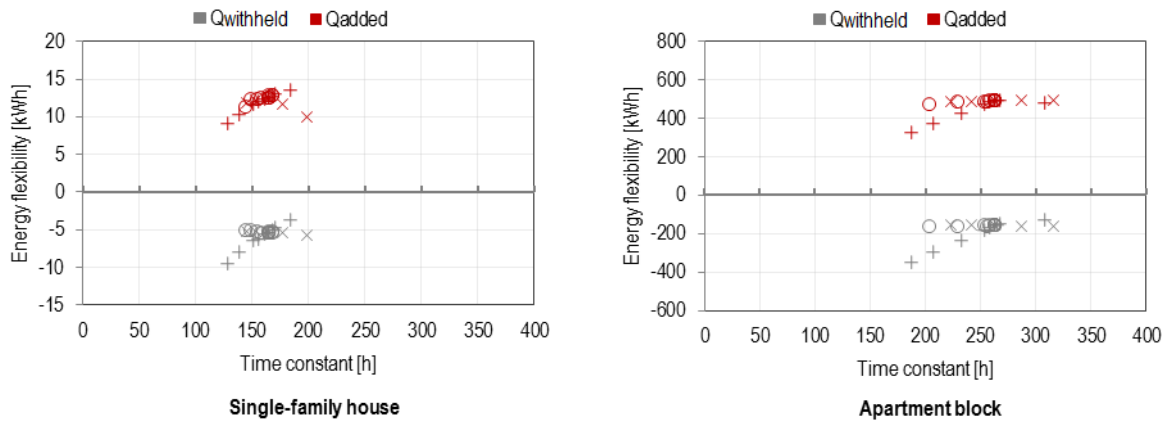
Figure 14: Correlation between energy flexibility potential and time constant for all building variations examined for the single-family house (left) and the apartment block (right). Buildings' variations concerning heat loss effect are marked as +, those concerning thermal capacity effect are marked as ○, those concerning the combination of the previous two and the solar gains are marked as ×

On average, the time constant of the single-family house was shorter, compared to the respective of the apartment block. This is attributed mainly to the ratio of the envelope area per volume of the apartment block (0.265 m^2/m^3) being considerably lower than that of the single-family house (0.998 m^2/m^3). A broader range of results for the time constant was observed for the apartment block, even though the changes in the building design parameters were the same. In addition, in the apartment block two trends were observed: one formed from the variations concerning heat loss (marked as + in the figure) and the other from those concerning the thermal mass effect (marked as ○ in the figure), with the distinction between them being evident. In the single-family house, the behaviour was similar for the downward flexibility potential. However, for the upward flexibility potential a correlation can be observed, which was in this case disturbed only by the solar gains (marked as × in the figure). Although the time constant of the buildings appears not to be enough as an indicator with regards to energy flexibility, it can however indicate the range of the potential. With the building design parameters examined, it was shown that the characteristic to be prioritized when aiming for energy flexibility is the minimization of heat loss. Once this is ensured, it would be beneficial to increase the thermal capacity of the building as well, especially that of the internal walls.

The obtained results are for the investigated type of buildings and should be very carefully extended to other building types. For all variations examined, the buildings remained in the category of heavy buildings, apart from the variation with 5 cm internal walls for the single-family house, which is in the category of semi-light buildings according to the Danish Building Research Institute (SBi) Guidelines 'Energy Demand for Buildings' [121]. In addition, there might be other design parameters which could impact the energy flexibility potential, e.g. different zoning of the buildings, orientation, interior design, shading, etc, as could the heat emission system [44], [45].

3.1.3   Main findings

This study showed that there is a physical potential for flexible heating operation of low-energy buildings using the thermal mass of the buildings as storage. When there is surplus production of energy from renewable sources in the energy system, the buildings can act as storage units that absorb thermal energy in the structural thermal mass (upward flexibility event). On the other hand, in cases of limited or no availability of energy from renewable sources in the energy system, the heat supply to the buildings can be either reduced or interrupted completely for several hours (downward flexibility event). The potential for storage in the thermal mass is higher than for withholding. Although for individual buildings the amount of energy that can be withheld is limited, if aggregated to a neighbourhood or district level, the amount of energy that can be withheld could be considerable.

- The energy flexibility potential depends strongly on the boundary conditions, namely the ambient temperature, solar radiation and internal heat gains. The potential for withholding increased on cold days, while the potential for storing additional energy was highest during days with moderate ambient temperature in the heating season. Increased solar gains led to decreased energy flexibility potential.
- The amount of energy added/withheld during a flexibility event was proportional to the duration of the event, because the buildings have a large heat capacity.
- The different starting time of the flexibility events mainly affected the potential for withholding, with the highest amount of energy available for withholding during the night.
- Heat losses to the ambient govern the potential for flexibility, while the concrete thickness of the walls was not a determinant factor by itself. The contribution of the thermal capacity of the internal walls was shown to be higher than that of the external walls.

3.2 Evaluation of indoor thermal comfort

This section investigates the flexibility potential of low-energy buildings with regards to the rate of temperature decrease, reflecting occupant's thermal comfort. Flexibility can be interpreted here as the ability to adapt to constraints on the heating supply schedule without compromising the occupant comfort. The evaluation was carried out at the apartment level.

The findings of this study have been published in the proceedings of the 15th IBPSA (2017):

Zilio, E., Foteinaki, K., Gianniou, P. and Rode, C. (2017) 'Impact of Weather and Occupancy on Energy Flexibility Potential of a Low-energy Building', in 15th IBPSA Conference. San Francisco, CA, USA, pp. 1493–1502.s

and

Sarran, L., Foteinaki, K., Gianniou, P. and Rode, C. (2017) 'Impact of Building Design Parameters on Thermal Energy Flexibility in a Low-Energy Building in 15th IBPSA Conference. San Francisco, CA, USA, pp. 239–248.

3.2.1 Method

In this study the focus was on occupant thermal comfort at the apartment level, with a different thermal zone for each room in the model. The apartment modelled belongs to a multi-family low-energy building, which was built in 2016 and is located in the Nordhavn district of Copenhagen, Denmark. Details of the building model can be found in the respective publications. Two rooms were used for the assessment, the living room, facing south, and one bedroom, facing north. The indicator used for assessment represents the duration of the thermal comfort period, defined as the number of hours that the operative temperature was maintained above the minimum acceptable temperature for the occupants (Equation (5)), in this work 20°C, after the heat supply had been cut off (Figure 15).

$$\text{Ind} = \min\{t | T(t) = 20°C\} \quad (5)$$
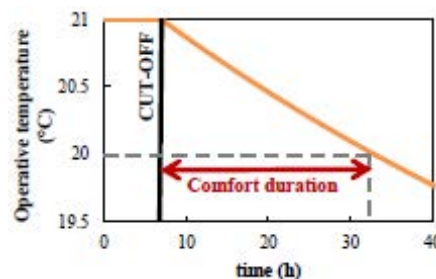
Figure 15: Example of duration of thermal comfort period after the heat supply has been cut off

This indicator gives a concrete indication of the possibilities that the building offers in terms of heat retention and could be used by the grid operator to know how long the building can be independent of the

heating network – keeping in mind the assumptions regarding influential factors, such as the heating set-point, occupants and ambient conditions.

In order to assess the influence of the weather conditions on heat retention, two weather parameters were varied: the outdoor temperature and solar radiation. Three representative temperatures were selected: 5°C, 0°C and -12°C, respectively the highest, the average and the lowest design temperature in January of a representative Danish year. The selected temperatures were kept constant during the simulation period. The second parameter considered was solar radiation. Three typical conditions for the Danish winter were selected with large, limited and no direct solar radiation. The influence of occupancy was also investigated, simulating two, three and four occupants and two typical occupancy schedules for working and retired occupants. For every variation, a single parameter was changed and the rest remained the same as in the reference case, i.e. limited solar radiation, outdoor temperature at 0 °C and three occupants following the schedule for working people.

3.2.2 Results and discussion

For the reference case examined, the rooms maintained the temperature above 20 °C after the heat supply had been cut off for 72 h in the living room and 45 h in the bedroom. The results regarding the outdoor weather and occupancy showed considerable influence on the thermal retention (Figure 16 and Figure 17).
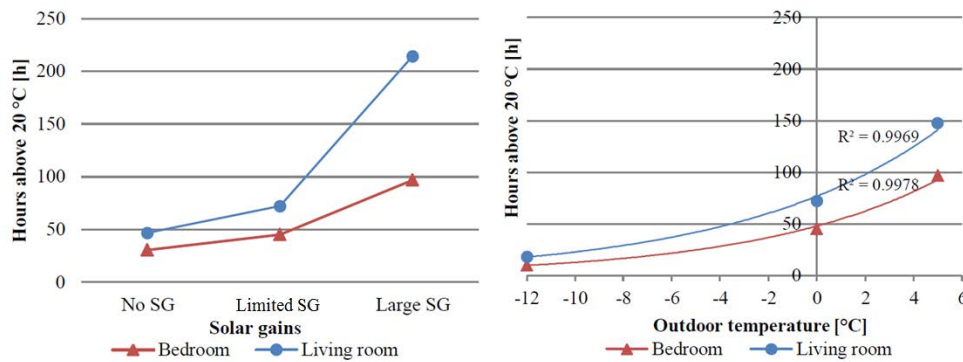
Figure 16: Duration of thermal comfort period after the heat supply has been cut off: Parameter variation results for outdoor weather conditions
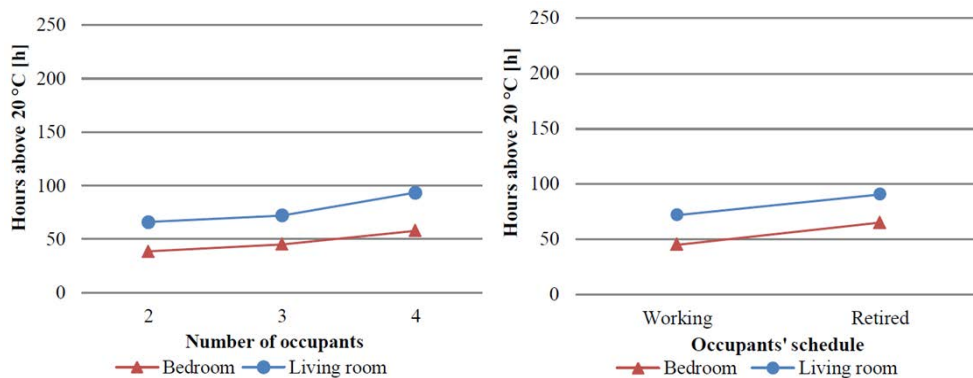
Figure 17: Duration of thermal comfort period after the heat supply has been cut off: Parameter variation results for number of occupants and occupancy schedule

Solar gains and outdoor temperature had considerable influence on the temperature decrease. The duration of the comfort period in the living room can be multiplied by 3 from a case with no solar gains to a case with large solar gains profile, and by 4 when outdoor temperature is 0°C instead of -12°C. The effect of solar radiation on the thermal retention of the building differed from its effect on the energy that could be added. Increased solar gains decreased the energy flexibility potential, but led to an increased number of hours of comfort after the heat supply had been cut off.

There was an increase in the duration of the comfort period by a factor of 1.4 if four occupants were present instead of two occupants. For the two different occupancy schedules, the duration of the comfort period was longer, by a factor of 1.4 for retired people, who are assumed to spend more time in the apartment.

3.2.3 Main findings

This study contributed to the evaluation of thermal comfort in terms of indoor temperature after the heat supply in a low-energy building has been cut off, showing the long period that an apartment can remain thermally comfortable without any heat supply and emphasizing the significance of internal and solar heat gains, as well as ambient temperature.

- Increased solar gains led to decreased energy flexibility potential, but increased the duration of the thermal comfort period after the heat supply had been cut off.
- Lower outdoor temperatures reduced the duration of the thermal comfort period after the heat supply had been cut off.
- The more occupants and the longer time they spend in the apartment, the longer the duration of the thermal comfort period after the heat supply had been cut off.

3.3 Thermal response of concrete elements based on simulations

This section evaluates the effect of the thermal mass of different concrete components on energy flexibility. The surface temperatures and heat fluxes from the concrete walls and ceiling were analysed to obtain the thermal response of the thermal mass of the building during a flexibility event.

The findings of this study have been published in the proceedings of the 9th IAQVEC (2016): Foteinaki, K., Heller, A. and Rode, C. (2016) 'Modeling energy flexibility of low energy buildings utilizing thermal mass', in 9th International Conference on Indoor Air Quality Ventilation & Energy Conservation In Buildings (IAQVEC). Songdo, Incheon. Republic of Korea.

3.3.1 Method

The apartment modelled in this study was part of a multi-family low-energy building, which was built in 2016 and is located in the Nordhavn district of Copenhagen, Denmark. Details of the building model can be found in the respective publications.

The focus of this study was on the thermal mass of the building. Since the thermal behaviour of a building depends on complicated mechanisms and is affected by a number of factors, it was chosen to exclude the impact of the exogenous parameters that were previously examined, i.e. the daily operation of the building, users' patterns and ambient weather conditions. A synthetic weather file was created with stable ambient conditions. Using the Design Reference Year data for Denmark (DRY, 2013), an average day of the heating season for Denmark was estimated, having a constant temperature of 3^0C temperature. Solar radiation and internal gains from occupants, equipment and lighting were excluded, as they could contribute an amount of energy that was added uncontrollably into a building, which would not allow for the thermal mass to be isolated.

The main scenario examined was divided into three periods; the steady state conditions, the pre-heating period and the cool down period after the heat supply had been cut off. Initially, the model was simulated for 5 days to ensure steady state conditions inside the zone and within the walls (days #1 - #5), during which the temperature set-point was set to 20°C. Operative temperature above 20^0C was considered as minimal comfort temperature. On day #6, the operative temperature set-point was increased to 22^0C for 4 hours, as a pre-heating period in order for the thermal mass to absorb heat. Then, the heat supply was cut off and the apartment was left to cool down for the next 4 days (until day #10). During the cooling down process, the focus was on the first day of this cooling period, observing the thermal response of the apartment.

One of the key parameters investigated was the duration of the time that the apartment would need to be pre-heated before such a stop, in order for thermal comfort to be maintained. Simulations were performed for different pre-heating periods of 2 hours and 6 hours.

3.3.2 Results and discussion

Figure 18 (left) shows the operative temperature and the surface temperatures of the ceiling, floor, one of the external walls and one of the internal walls. During the steady state conditions, the operative temperature was maintained at 20°C. During the 4-hour pre-heating period, the temperature was allowed to increase until 22°C, although it only reached 20.6 °C, due to the slow response of the floor heating system. Since the operative temperature increase was small, the surface temperature rise of the ceiling, internal and external wall was minor. The floor surface had the highest surface temperature at all times and achieved a distinct temperature increase during the pre-heating period, as expected due to the floor heating system.

Figure 18 (right) depicts the surface heat fluxes for the ceiling, external and internal wall. Negative values indicate that heat was being absorbed in the walls, while positive values indicate that heat was being released from the walls to the room. The ceiling and the internal wall behaved similarly, absorbing heat during the pre-heating hours and emitting it back to the room, shortly after the cooling down phase began. Although the external wall absorbed heat within the pre-heating hours, heat was never released back into the apartment.
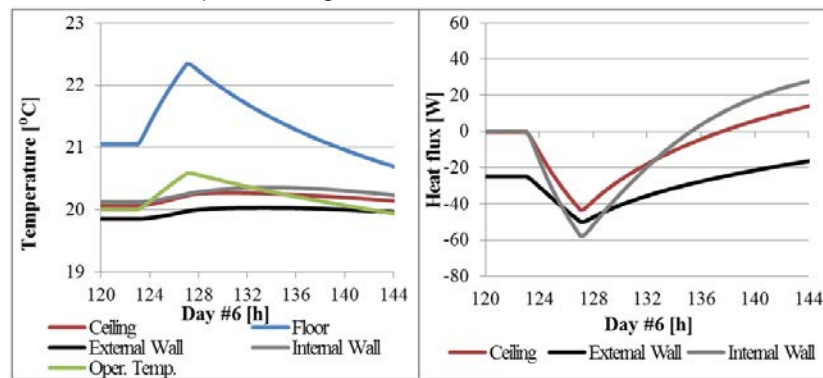
Figure 18: Surface temperatures during day #6 (left). Surface heat fluxes during day #6 (right) (Hours counted since day #1).

Under the steady state conditions, the heating system ran uninterrupted, contributing 1.15 kWh for a duration of 2h, as is depicted in the energy balance in Figure 19 (left). During the first two hours after the heat supply had been cut off the internal walls, including the floor and ceiling, released 0.81 kWh. This accounted for 61% of the demand, namely heat losses from the windows, external walls and thermal bridges, mechanical ventilation and infiltration.
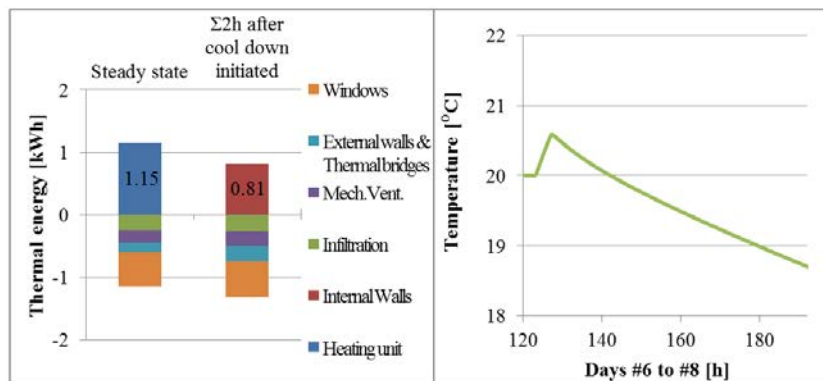
Figure 19. Energy balance for a duration of 2h (left). Operative temperature during days #6-#8 (right) (Hours counted since day #1).

While the apartment cooled down over the following days (Figure 19 (right)), the operative temperature remained above 20 °C for 15 hours after the heat had been cut off. This indicates that the heat flows released would be sufficient for to contribute to load shifting.

Table 5 shows the results of the thermal response of the apartment in different pre-heating periods. The different pre-heating periods had a considerable effect on the number of hours that the operative temperature was maintained above 20°C, being approximately 8 h, 15 h and 21 h for the different pre-heating periods.

Table 5. Thermal response of the apartment for different pre-heating periods

	Pre-heating duration		
	2 h	4 h	6 h
Max operative temperature difference during pre-heating [^{0}C]	0.3	0.6	0.8
No. of hours operative temperature above 20^{0}C [h]	8.3	15.1	21.2
Energy recovered from thermal mass during above hours [kWh]	3.79	7.04	10.1

It was observed that the heat recovered from the thermal mass came from the internal walls, including the ceiling and the floor. The capacity of the thermal mass of the internal walls should therefore be considered as one of the main contributors to the load shifting potential of the apartment. Nevertheless, the external envelope is of equal importance for the load shifting potential of the apartment, since it governs the losses to the ambient. It should be thus investigated in terms of its effect on total heat loss, rather than of its thermal mass.

3.3.3 Main findings

For the chosen apartment of a low-energy building in Copenhagen the thermal mass can be used as short-term thermal energy storage, allowing heat load shifting for several hours, without any contribution from internal or solar gains. This potential increases with longer pre-heating periods.

- The internal walls recovered the part of the heat that was absorbed during the pre-heating period, contributing to the heating requirement of the apartment for several hours.
- The heat that was absorbed in the external walls during the pre-heating period was not released back into the apartment, but was gradually lost to the ambient by heat conduction. However, the external walls affect the potential for load shifting because they determine heat loss to the ambient.

3.4 Thermal response of concrete elements based on in-wall measurements

In the previous sections, the effect of the thermal mass of different building components, i.e. internal and external walls, on energy flexibility was examined using simulation models. This section analyses the dynamic thermal response of a low-energy building using measurement data, to support the simulation studies described in the previous sections. To the knowledge of the author, no recent full-scale monitoring has been performed to document in detail the thermal behaviour of the building mass. A custom-made set of measurements with temperature sensors inside the concrete walls and ceilings, at different depths from the surface to the middle of the concrete layer, makes possible an analysis of the dynamic thermal response of the thermal mass of the building, which can indicate which part of the thermal mass actively participates in heat exchange with the indoor environment and can thus facilitate load shifting strategies.

The findings of this study have been accepted for the 13th REHVA World Congress CLIMA (2019):
Foteinaki, K., Li, R., Heller, A., Christensen, M. H. and Rode, C. (2019) 'Dynamic thermal response of low-energy residential buildings based on in-wall measurements', in 13th REHVA World Congress CLIMA 2019. Bucharest, Romania.

3.4.1 Method

3.4.1.1 Case study building

The case study building is a multi-family apartment block that was completed in 2017 and is located in the Nordhavn district of Copenhagen, Denmark. The building has 72 apartments and 11 town house units. 19 apartments and 1 town house unit agreed to participate in the EnergyLab Nordhavn project [10], monitoring the energy use, indoor environment and temperatures inside the concrete elements. In the present analysis, one apartment has been chosen in order to analyse in depth the thermal response of concrete elements.
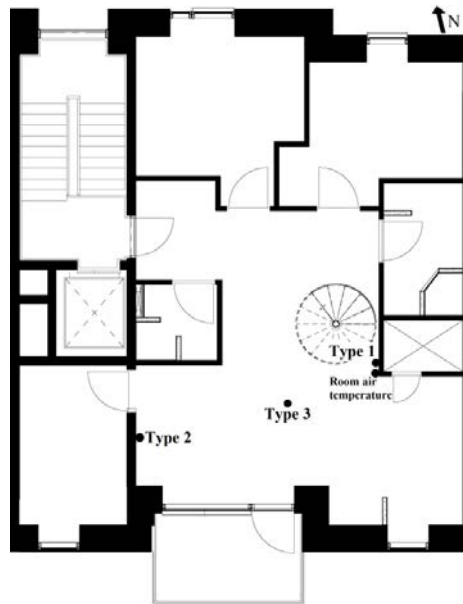
Figure 20: Apartment floor plan and installed sensors [122]

The apartment has an area of 147 m^2 and height 2.7 m. It is on the top floor (5th floor) of the building and has a loft. It has facades to the south and north, while on the east and west sides there are adjacent apartments. Figure 20 shows the floor plan of the apartment (excluding the loft). Table 6 lists the properties of the main building components. The building is connected to the district heating system and the heat emission system in the apartment is floor heating. There is CAV mechanical ventilation and heat recovery from exhaust air with 85% efficiency. Fresh air is supplied in the living room and bedrooms and it is exhausted from the kitchen, bathroom and toilet.

Table 6: Properties of main building components

Components	Thickness [mm]	U-value [W/(m^2·K)]	Materials
External wall	580	0.122	Concrete (180 mm) Insulation class 38 (300 mm) Concrete (70 mm) Air gap (5 mm) Aluminium plates (25 mm)
Internal load-bearing wall	200	3.70	Concrete (200 mm)
Internal non-load-bearing wall	100	1.35	Aerated concrete (100 mm)
Floor/ceiling decks	407	0.34	Oak planks (14 mm) Concrete (80 mm) Insulation class 38 (93 mm) Hollow core concrete (220 mm)
Windows	3 pane glazing	0.72	g-value=0.5, frame fraction 15%, window frame U-value=0.85

3.4.1.2 Monitoring system

The apartment is equipped with sensors measuring air temperature, CO_2 concentration and relative humidity. There is a home management system, which includes control of the heating system via control panels with integrated room air temperature sensors placed in each room. In addition, for research purposes, there are custom-made concrete blocks of size (200 x 60 x 200/100 mm) with built-in sensors that measure

the temperature at different depths. The concrete blocks were prepared in the laboratory of the Technical University of Denmark (DTU), with three integrated temperature sensors, at the surface and at two depths into the material. The sensors used are PT 1000 (DIN EN 60751, CLASS DIN B). The sensors' heads are in direct contact with the concrete that surrounds them, while the sensor cables are covered with a flexible plastic pipe that leads out of the concrete block, to protect them when the sensor block was cast into the concrete wall and ceiling elements. Figure 21 depicts the production process of the concrete blocks. These concrete blocks were subsequently cast into walls and ceilings during the production process. Three different types of setup were created as illustrated in Figure 21.

- Type 1: Sensors were placed in the internal non-load-bearing wall made of 100 mm of aerated concrete, at a height above the floor of 1.1 m and at three depths: 0 mm, 25 mm and 50 mm from the internal surface.
- Type 2: Sensors were placed in the internal load-bearing wall made of 200 mm concrete, at the same height of 1.1 m and at three depths: 0 mm, 50 mm and 100 mm from the internal surface of the living room. Three more sensors were placed in the surface layer at heights 0.1 m, 0.6 m and 1.7 m.
- Type 3: Sensors were placed in the ceiling, in the layer that consisted of 220 mm concrete, at three depths: 0 mm, 55 mm and 110 mm from the lower surface. On top of the concrete there is thermal insulation.

The sensors, listed in Table 7, were placed in elements facing the large open space (which includes the living room and kitchen, further referred to as the living room), as depicted in Figure 20. All measurement data were received by a KNX system and were transferred to a central data management system at DTU. The time resolution of the data was 1 min. Ambient weather data were obtained from the Climate Station at DTU [123] for the months of the analysis.
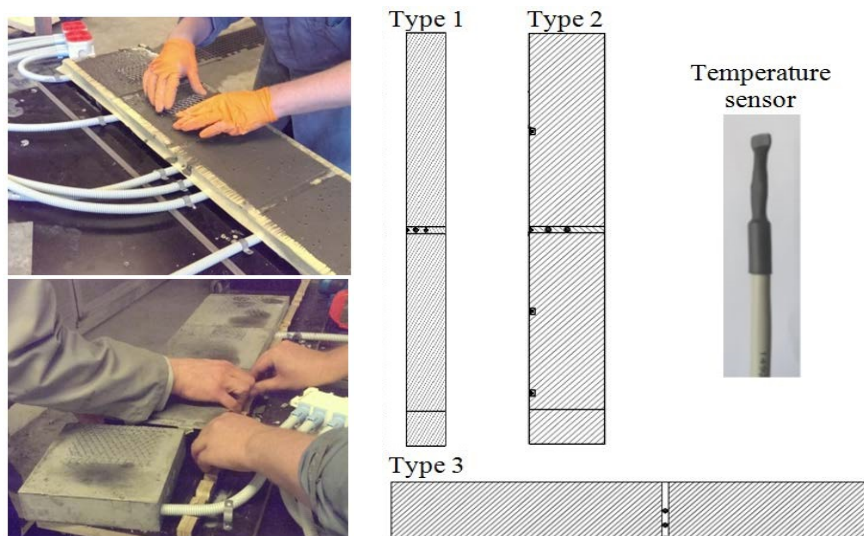
Figure 21: Production process of concrete blocks with integrated temperature sensors (left). Placement of temperature sensors in walls (Type 1 and Type 2) and ceiling (Type 3) (right)

Table 7: Temperature sensors in walls and ceiling

Sensor	Element	Depth	Height
T1-0 mm	Wall	Surface	1.1 m
T1-25 mm	Wall	25mm	1.1 m
T1-50 mm	Wall	50mm	1.1 m
T2-0 mm-1.1 m height	Wall	Surface	1.1 m
T2-50 mm	Wall	50mm	1.1 m
T2-100 mm	Wall	100mm	1.1 m
T2-0 mm -0.1 m height	Wall	Surface	0.1 m
T2-0mm -0.6 m height	Wall	Surface	0.6 m
T2-0mm -1.7 m height	Wall	Surface	1.7 m
T3-0 mm	Ceiling	Surface	3.5 m
T3-55 mm	Ceiling	55mm	3.5 m
T3-110 mm	Ceiling	110mm	3.5 m

3.4.1.3 Data analysis

The analysis was performed for one winter month, February, and one summer month, July. The space heating energy use, CO_2 concentration and relative humidity are reported here. The main goal of the analysis was to determine the dynamic thermal response of the apartment. Room air temperature is therefore discussed in relation to solar gains and the resulting heating patterns. In-depth analysis of temperature from the different nodes inside the concrete elements at different heights and depths was performed. The nodes inside each concrete element were examined in relation to the room air temperature to which the elements were exposed. The data shown are from the living room. For each month, two days were chosen to provide more detail in the analysis of the thermal response. The temperature fluctuations of all nodes in the concrete elements were normalized, in order to evaluate what percentage of the room air temperature fluctuation was achieved at different depths in the concrete (Equation 6), and to evaluate the delay in thermal response (Equation 7):

- $$T_{norm1} = \frac{T_{node} - T_{node(min)}}{T_{room(max)} - T_{room(min)}} \qquad (6)$$
- $$T_{norm2} = \frac{T_{node} - T_{node(min)}}{T_{node(max)} - T_{node(min)}} \qquad (7)$$

3.4.2 Results and discussion

The month of February 2018 had an average ambient temperature of -1 °C. Figure 22 (a) shows the ambient air temperature and the global irradiance for the whole month. The energy use for this month was 1252 kWh (8.5 kWh/m^2). Both the relative humidity and the CO_2 concentration were within the acceptable ranges according to EN/DS 15251 [118]; on average, the relative humidity was 30 % and the CO_2 concentration was 700 ppm. Figure 22 (b) shows the heating power for the whole apartment, as well as the air temperature set-point and the air temperature in the living room. During the month, there were periods with different heating patterns and thermal behaviour.

- At the beginning of the month, there was increased heating use, despite the fact that the temperature set-point in the living room was either 21°C or the heating was turned off. This was due to unusually high set-points in other rooms of the apartment, which affected the air temperature in the living room. During the first three days of the month, there were minimal solar gains, while from the 4th-9th there were considerable solar gains, which resulted in even higher air temperatures at midday, reaching up to 28 °C. Such temperatures are considered very high, especially for the month of February. Nevertheless, the system was controlled entirely by the occupants based on their preferences, so extreme behaviours can be expected.

- From the 10th - 13th, the set-points in the apartment were drastically decreased, while the set-point in the living room was maintained constant at 21°C. During these days, the heating was turned off and there were very low solar gains. It took 4 days for the air temperature to decrease to 21°C.
- With the set-point maintained at 21°C in the period 14th – 24th, a regular heating pattern was followed; the heating system was activated during the night, ran for 4.75 h on average and was subsequently turned off for two days. During this period, the solar gains were average for the season, and affected the air temperature, which increased every midday.
- Towards the end of the month, the temperature set-points of other rooms were increased again and the thermal behaviour resembled what had occurred at the beginning of the month.

The above variations in the temperature set-points and respective heating patterns caused considerable changes in the room air temperature, which makes it possible to examine the thermal changes inside the concrete elements.

Figure 22 (c) shows the temperatures inside the internal non-load-bearing wall (Type 1 sensors) and the room air temperature. All three sensors indicated higher temperatures than the room air temperature. The one in the middle of the wall had the highest temperature, while the other two had almost the same temperature. The other side of the wall is the utility room, so it is most likely that hot pipes traversing that room were heating it up. At the beginning of the month, when the room air temperature was also very high, this effect was not observed, but instead all the layers of the wall had an almost uniform temperature.

Figure 22 (d) shows the temperatures inside the internal load-bearing wall (Type 2 sensors) and the room air temperature of the living room and the adjacent room. The temperatures inside the internal load-bearing wall changed as expected, given that the adjacent room on the other side of the wall had a lower air temperature. They were mostly lower than the room air temperature, with the surface temperature being slightly closer to the room air temperature, followed by the temperatures at 50 mm and 100 mm depth in the concrete. Exceptions were the start of large temperature changes (increase or decrease), when due to the delayed response of the different layers, the temperatures overlapped with each other. The delay of the thermal response in different elements and depths is analysed in detail below.

Figure 22 (e) shows the temperatures inside the ceiling (Type 3 sensors) and the room air temperature. The thermal changes inside the ceiling differed from those in the walls. The three layers of the ceiling had almost the same temperature, with only negligible differences. The response to the room air temperature fluctuations was slow, and daily fluctuations could be only marginally observed, while the temperature curve responded smoothly and cumulatively to the air temperature changes. This may be because this element is exposed to room air temperature fluctuations from only one side, as there is thermal insulation above it, while the walls consist of concrete or aerated concrete and are exposed to room air temperature fluctuations from both sides. Additionally, the ceiling is not directly exposed to solar radiation, while walls may be.

Figure 22 (f) shows the surface temperature of the concrete elements and the room air temperature. The surface temperature of the internal non-load-bearing wall was the highest, for the reasons previously explained. The temperatures on the surface of the internal load-bearing wall at the different heights, 0.1 m, 0.6 m and 1.7 m were almost the same, validating the expectation that floor heating creates a uniform thermal environment with minimal vertical thermal gradients. However, the surface temperature at 1.1 m height was often higher than at the other heights, which indicate that there had been direct solar radiation at this height. The surface temperature of the ceiling was sometimes higher and sometimes lower than that of the other surfaces, due to its slower thermal response. However, during the period with a regular heating pattern (14th – 24th), the temperature of the ceiling was very similar to those of the load-bearing internal wall. These results confirm the findings in the previous Section 3.3, where a similar apartment was simulated and the thermal behaviour of different concrete elements was evaluated.
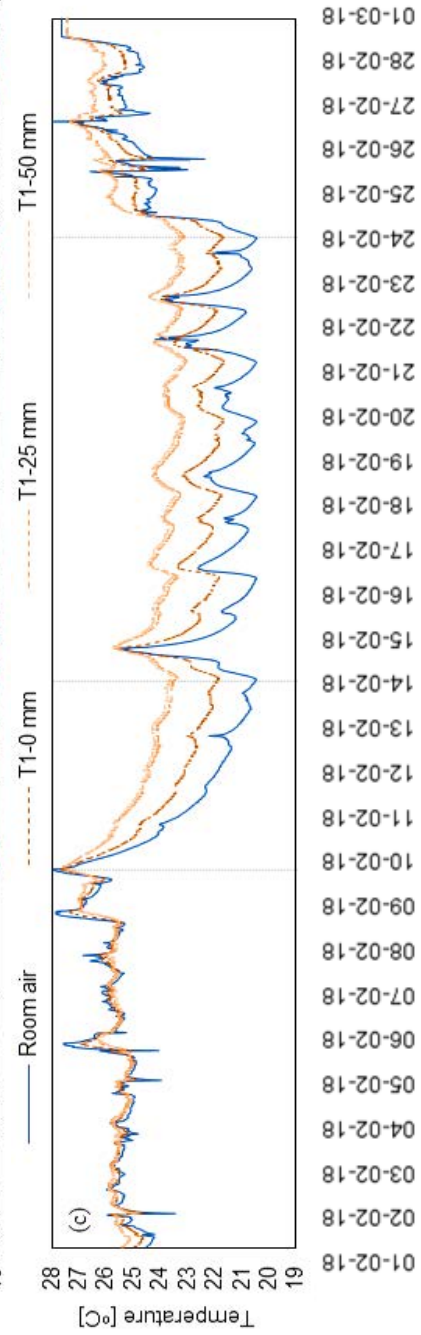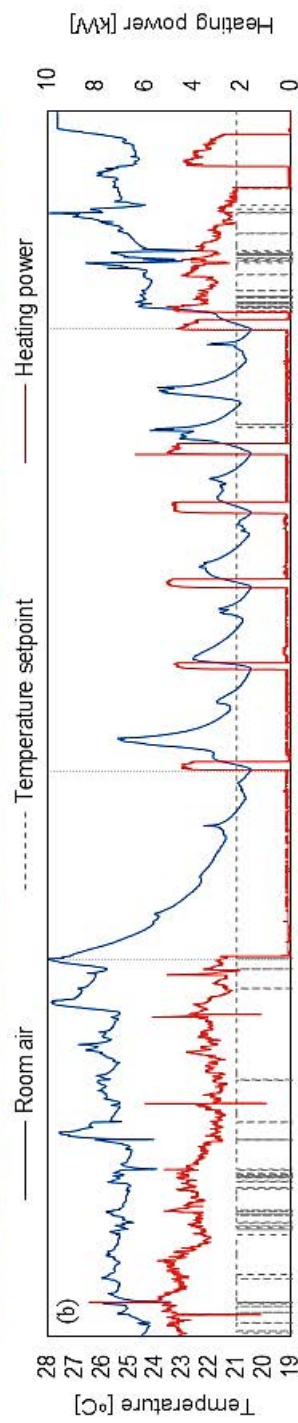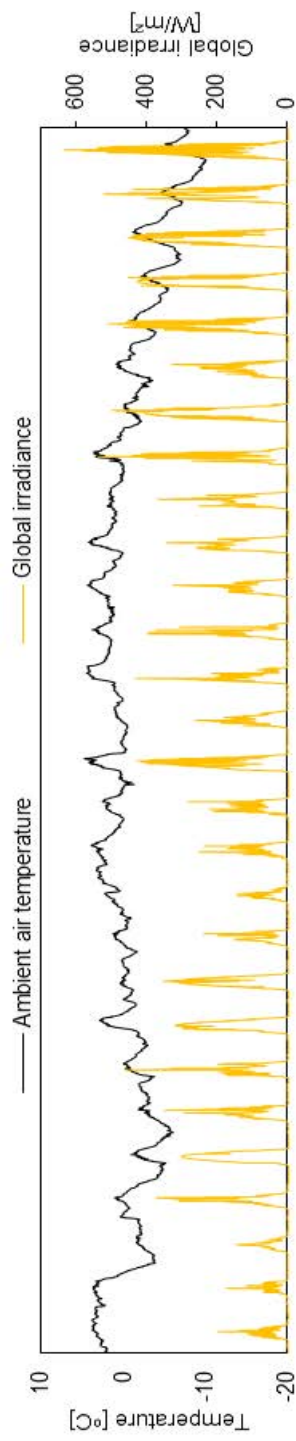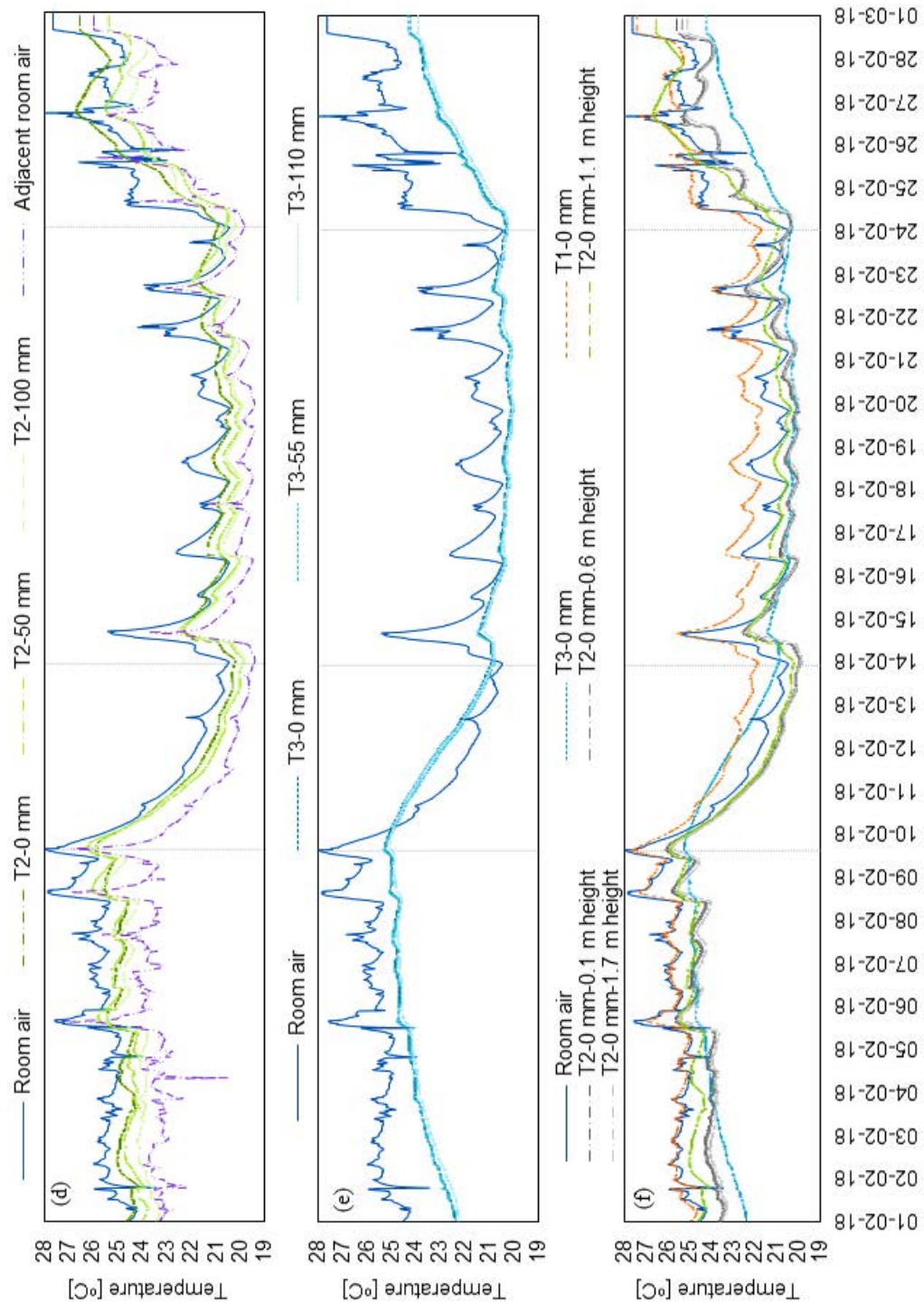
Figure 22: Analysis of thermal response during February 2018: (a) Ambient air temperature and global irradiance. (b) Space heating power, temperature set-point and room air temperature. (c) Temperature inside the non-load-bearing internal wall at 0 mm, 25 mm and 50 mm depth and the room air temperature. (d) Temperature inside the load-bearing internal wall at 0 mm, 50 mm and 100 mm depth and the room air temperature. (e) Temperature inside the ceiling at 0 mm, 55 mm and 110 mm depth and the room air temperature. (f) Surface temperature of the concrete elements and the room air temperature.

In order to improve the understanding of the thermal response of the different layers of the concrete elements, two days were chosen, 18th – 19th February, for more detailed analysis. The temperature fluctuations of each node (i.e. each layer in each element) were normalized against the maximum fluctuation of the room air temperature for those two days. The temperature fluctuation that was achieved at the different depths of the concrete elements was thus quantified as a percentage of the room temperature fluctuation. These data are shown in Figure 23 (a).
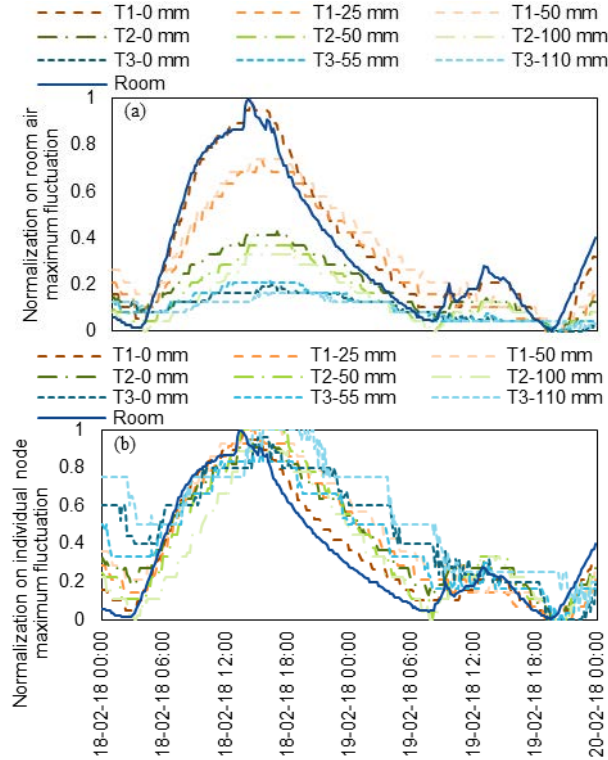
Figure 23: Temperature fluctuations of all nodes between 18th–19th February. (a) Normalized against room air temperature maximum fluctuation. (b) Normalized against individual node maximum temperature fluctuation.

For the two days analysed, the maximum room air temperature fluctuation was 2°C. Comparing the temperature fluctuations achieved in the concrete elements to that of the room air temperature, the highest percentages were achieved in the non-load-bearing internal wall, followed by the load-bearing internal wall and lastly the ceiling. The surface node of the non-load-bearing internal wall experienced almost the same fluctuations as the room air temperature. The other two layers of this wall achieved a temperature increase that was as high as 74% of the room air temperature. The layers of the load-bearing internal wall achieved 43%, 37% and 33% for the surface, 50 mm and 100 mm node respectively. The layers of the ceiling achieved on average 19% of the room air temperature fluctuations. The room air temperature increase during the second day, which was 0.4°C, affected temperatures inside the concrete of the ceiling only marginally.

The temperature fluctuations of each node were normalized against the maximum temperature fluctuation of this node for those two days, such that the temperature fluctuation for each node varied between 0 and 1. The timing of the fluctuations can then be evaluated, quantifying the delay of the thermal response in different elements and at different depths. This is shown in Figure 23 (b). A delay of the thermal response in different elements and at different depths may be seen. During the temperature increase of the first day, the maximum delay was 2 h for the node that was 100 mm deep in the internal load-bearing wall. The delay in the non-load-bearing wall was negligible. The effect was more pronounced during the temperature decrease.

In the measurements made in July 2018, the average ambient temperature was 20.4°C. Figure 24 shows the ambient air temperature and the global irradiance for the whole month, together with the room air temperature. Both the relative humidity and the CO_2 concentration were within acceptable ranges (EN/DS 15251 [118]), with the relative humidity being 50% and the CO_2 concentration 470 ppm on average. The room

air temperature throughout the month indicates a problem of overheating in low-energy buildings, as the average temperature was 26°C and reached a maximum of 30.1°C. The changes in the temperatures inside the concrete elements were similar to what had been observed in February. Details of those results can be found in the relevant paper.
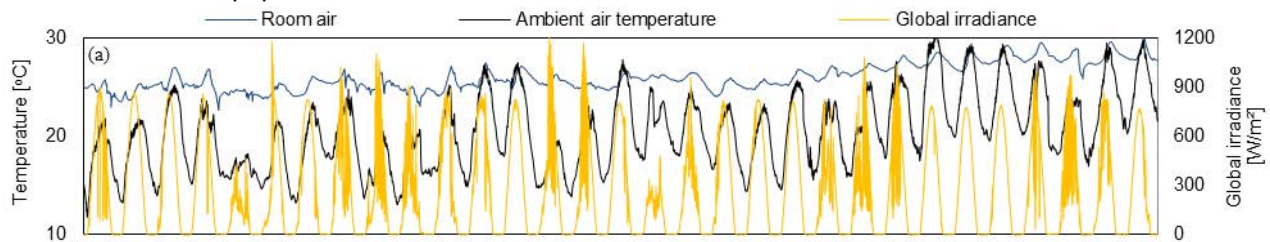
Figure 24: Room air temperature, ambient air temperature and global irradiance during July 2018

Both in February and July, the temperature fluctuations at all different depths and in all the elements indicate that the concrete elements were effectively activated by the room air temperature fluctuations. Following the assumption that was discussed by [124], in order for the thickness of a concrete element to be considered effective, more than 10% of the room air temperature fluctuations should be achieved. According to this, all layers examined may be regarded as effective, namely more than half of the concrete mass exposed to the room air temperature is effective and can actively facilitate load shifting strategies.

The conclusions of this study were based on measurements monitored while the heating system in the apartments was controlled by the occupants. The analysis clearly illustrates the importance of occupant behaviour on energy use for space heating. Further investigations are being performed during the heating season 2019, with the heating temperature set-points in the apartments being remotely controlled.

3.4.3   Main findings

This study used an analysis of measurements in an apartment to confirm that all the internal concrete layers examined may be considered effective, i.e. the internal concrete elements do contribute to the physically available heat storage potential of the building.

- Comparing the temperature fluctuations achieved in the concrete elements to that of the room air temperature (defined as 100%), the highest percentages/dynamics were achieved in the non-load-bearing internal wall (100 mm aerated concrete), i.e. 87% on average, followed by the load-bearing internal wall (200 mm concrete) with 41%, and lastly by the ceiling (220 mm hollow core concrete) with 30%. The layers of the ceiling were less responsive to air temperature fluctuations than those of the internal walls, supporting the findings of the simulation study in Section 3.3.
- The phenomenon of delay in the thermal response of the concrete elements was observed.
- A considerable effect of solar gain on indoor air temperature was observed both during winter and summer months. A problem of overheating was observed in July.
- With the contribution of solar gains and the low heat losses, in order for the apartment to maintain a temperature of 21 °C, it was sufficient that the heating system was turned on for 4.75 h every other day.
- During the month of February there were periods with very different heating temperature set-points and respective heating patterns, due to occupant preferences.

Chapter 4 Energy flexible buildings in relation to the local energy system

This chapter is based on Paper II and Paper VII and addresses the 2ⁿᵈ objective of the thesis.

According to the definition of energy flexible buildings, provided in 2.1.1, the ability of the building to be operated flexibly depends on the local grid requirements [15]. The aspect that this chapter handles is the response of a building to potential load control strategies determined by the flexibility requirements of the local heat supply grid. The framework of this thesis was the Nordhavn energy district in Copenhagen, Denmark, which is connected to the local district heating network. The main investigations were performed with the most common type of building in Nordhavn, low-energy residential buildings, connected to the district heating. The requirements of the local district heating system were considered in the form of signals to the building to dictate the operation of the heating system. The flexibility potential of a building was investigated and is shown in Section 4.1. In order to demonstrate the difference between the district heating grid requirements and the electricity grid requirements, the flexible operation of a heat pump installed in a grid-connected detached house in Denmark was investigated and is presented in Section 4.2. The limitations of these approaches are discussed. Detailed information on models, methods and results can be found in the respective publications.

4.1 Flexible operation of the heating system of a building connected to the district heating system

The findings of this study have been reported in a paper submitted to a peer-reviewed journal:
Foteinaki, K., Li, R., Péan, T., Rode, C. and Salom, J. (2018) Evaluation of energy flexibility of low-energy residential buildings connected to district heating.

4.1.1 Method

This section explains the methodology for achieving flexible operation of the heating system of a building connected to the district heating system. The charging and discharging of the storage medium, i.e. structural thermal mass, is achieved by modulating the indoor air temperature set-point. When increasing the set-point, the heat load in a building is increased and the additional heat is stored in the thermal mass. When decreasing the set-point, the heat load in a building is reduced or interrupted completely, causing heat to be released from the thermal mass of the building to the internal zones.

Initially in this work, a reference operation of the building was defined, with thermostatic control with constant air temperature set-point at 22°C, which is a typical desired indoor temperature in Danish households during the heating season [125]. Different signals then triggered an increase or decrease of the air temperature set-point in order to charge or discharge the thermal mass, respectively. At all times, the thermal comfort of occupants should not to be compromised. The limits of comfortable conditions were chosen to be 20 – 24 °C, in accordance with the thermal comfort Category II "Normal level of expectations for new buildings" for heating season according to the standard EN/DS 15251[118].

4.1.1.1 Data from district heating system

Two sets of data were used as an indication of the district heating requirement; the heat load of Greater Copenhagen and the respective marginal heat production cost. The marginal heat production cost is the cost to produce one additional unit of heat for DH. The cost was used only as a signal, instead of using heat price on the demand side, to reflect the potential for cost reductions in a dynamic pricing scheme. The marginal heat production cost was chosen to be used as signal, as it represents the variation of production costs and the effects of the market on the heat production are reflected adequately, as shown in [66]. In [126] it was shown that although the gap in magnitude between the marginal cost and the heat price is large, the marginal heat

cost can adequately reflect the increase of variable heat production cost with increased heat demand. The data sets were provided by the DH utility company of Copenhagen, HOFOR A/S [127].

Figure 25 (left) illustrates a heat map graph of the heat load, having on the x-axis the days of the heating season and on the y-axis the time of the day. Marginal heat production cost data are shown in the same format in Figure 25 (right).
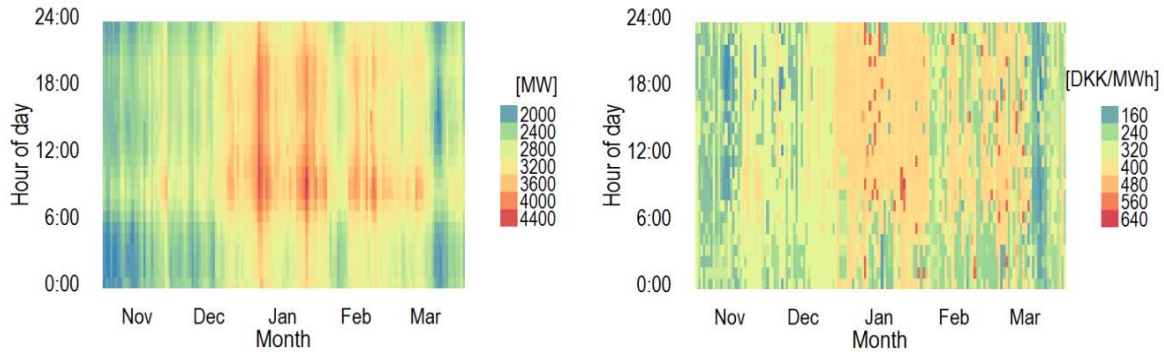
Figure 25: Heat map graph of heat load (left) and marginal heat production cost (right) in Greater Copenhagen during a heating season

The graphs indicate a correlation between the heat production cost and the heat load, but only to a certain extent, since there are many parameters that affect the cost, as detailed in Section 2.3.2. A clear diurnal pattern of heat load can be seen. A similar pattern may be seen for the marginal heat production cost, but it is not as clear as it is for heat load.

4.1.1.2 Implementation

Two indirect load control strategies were studied, assuming first the non-existence and second the existence of a communication platform between the building and the supplier:

i)   Assuming no communication platform between the building and the heat supplier, a constant strategy was implemented with one or two flexibility events every day during the whole heating season. This could be achieved with indirect control by giving monetary incentives to the occupants, for example fixed contract with time-of-use tariffs. The occupants set lower temperatures when the heat cost is high and vice versa. In this case, fixed schedules for temperature set-points were used. They were determined based on the average daily profiles of the heat load of the area and the marginal heat production cost, according to which it was, on average, favourable for the system to use heat during the night, both to flatten the heat load curve of Greater Copenhagen and to use heat with a lower production cost. Figure 26 shows scenarios with the scheduled temperature set-points.
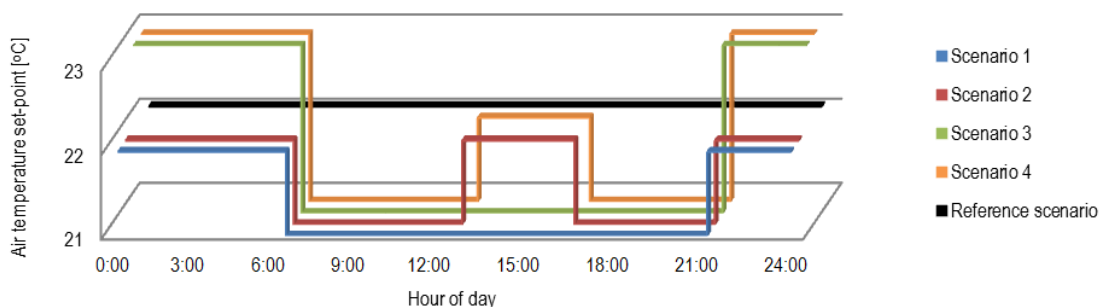
Figure 26: Scenarios for fixed schedules for temperature set-points in the temperature range 21-23 ºC

ii)   Assuming a communication platform between the building and the heat supplier, a signal is sent to the building from the supplier to communicate the need for load adjustment and the home management system modulates the temperature set-points according to this signal. In this case, the signal was the hourly marginal heat production cost. The aim of this strategy was to shift the energy use towards the hours when heat costs

are low. Thresholds for the marginal heat production costs were therefore set according to which the building modulates the temperature set-points. When the signal was lower than the low cost threshold (C_{low}), the set-point was increased, in order to store heat in the thermal mass of the building. Likewise, when the signal was higher than the high cost threshold (C_{high}), the set-point was decreased so as to discharge the stored heat. When the signal was between the two thresholds, an interpolation of the set-point was used according to Equation 8. In addition, a dead-band of 0.5°C was used to prevent the controller from being activated by small temperature deviations.

$$T_{setpoint,i} = \begin{cases} T_{setpoint,min} \text{ ,} & C_i > C_{high} \\ T_{setpoint,max} \text{ ,} & C_i < C_{low} \\ \frac{T_{setpoint,max} - T_{setpoint,min}}{C_{high} - C_{low}} \cdot \left(C_{high} - C_i\right) + T_{setpoint,min} \text{ ,} & C_{high} \geq C_i \geq C_{low} \end{cases} \tag{8}$$

The marginal heat production cost has large seasonal variations and considerable differences between the months of the heating season [66]. In the present work, the percentile distribution of marginal cost for each month was used and the thresholds referred to the respective percentiles for each month individually. The 25% or 50% percentiles of the monthly cost distribution were used as C_{low}, and the 50% or 75% percentile of the monthly cost distribution were used as C_{high}. As in the previous strategy, scenarios without and with pre-heating of the building were studied.

Table 8 shows the scenarios examined with the minimum and maximum temperature set-point for each scenario, and the low and high cost thresholds defined as percentiles of the monthly marginal cost.

Table 8: Scenarios for dynamic modulations for temperature set-points with the respective cost thresholds

		$T_{setpoint, min}$	$T_{setpoint, max}$	C_{low}	C_{high}
Scenario 5	No pre-heating	21 °C	22 °C	-	50%
Scenario 6	No pre-heating	21 °C	22 °C	-	75%
Scenario 7	Pre-heating	21 °C	23 °C	25%	75%
Scenario 8	Pre-heating	21 °C	23 °C	50%	75%
Scenario 9	Pre-heating	21 °C	23 °C	25%	50%
Scenario 10	Pre-heating	21 °C	23 °C	50%	50%

The building model used was the apartment block described in Section 3.1. More detailed information can be found in the respective publication. The ambient weather conditions used in this study were weather data collected from the DTU Climate Station [123] for the year corresponding to the heat load and marginal heat production cost data. The internal heat gains included heat emitted from lighting, equipment and occupants. The schedules for the internal gains were set according to the standard DS/EN ISO 13790:2008 Table G.8 [105], while the total heat flow rate from internal gains was adjusted to 5 W/m^2 in order to correspond to the average Danish national values [121].

4.1.1.3   Performance evaluation

For the scenarios examined, the following parameters were evaluated:
i)   The total energy used for space heating of the building for the whole heating season.
ii) The total cost for production of the heat that was used in the building for space heating.
iii) The indoor operative temperature, as an indicator of thermal comfort [118]. For the sake of clarity, the operative temperature of the critical apartment is presented, which is a top-corner apartment and was chosen because of its higher exposure to ambient conditions.
iv) The energy used for space heating of the building between 6:00-9:00, namely the morning peak load hours for the DH system [128].
v)   The potential for flexible operation, based on two flexibility indicators, equivalent to the one defined in [129]:

   a) Evaluation of total energy use during high load hours versus during low load hours according to Equation (9):

$$F_1 = \frac{E_{low\ load} - E_{high\ load}}{E_{low\ load} + E_{high\ load}} \qquad (9)$$

where: $E_{high\ load}$, the total space heating energy use during high load hours, between 6:00–21:00, $E_{low\ load}$, the total space heating energy used during low load hours, between 21:00-6:00 (next morning). The indicator ranges between -1 and 1, with the optimal operation being when $F_1 = 1$, namely energy was used only during low load hours.

b) Evaluation of total energy use during high production cost hours versus during low production cost hours, according to Equation (10):

$$F_2 = \frac{E_{low\ cost} - E_{high\ cost}}{E_{low\ cost} + E_{high\ cost}} \qquad (10)$$

where: $E_{high\ cost}$, the total space heating energy use during high production cost hours, when the cost was higher than the median value of costs of each month, $E_{low\ cost}$, the total space heating energy use during low production cost hours, when the cost was lower than the median value of costs of each month. The indicator ranges between -1 and 1, with the optimal operation being when $F_2 = 1$, namely energy is used only during low production cost hours.

4.1.2 Results and discussion

During the reference operation of the building, namely when the building was controlled with a constant temperature set-point of 22°C, the energy use for space heating was 12 kWh/(year·m^2 net heated floor area) and the peak demand was 82 kW (13.1 W/m^2). Details of the energy performance, the thermal behaviour and the physically available energy flexibility of this building can be found in Section 3.1.

The scenarios were implemented for the entire heating season and were evaluated based on parameters *i*, *ii* and *iii* in Section 4.1.1.3. Details of those results can be found in the respective publication. Based on those, some of the implemented scenarios were selected for further evaluation using average load and temperature profiles, as well as the parameters *iv* and *v*. Table 9 shows the average performance and flexibility potential across the heating season from the implementation of the selected scenarios.

Table 9: Average performance and flexibility potential in different scenarios during the heating season

Scenarios	Difference from reference operation				F1	F2
	Cost [%]	Energy use in morning [%]	Average temperature [°C]	Total energy [%]		
Reference	–	–	–	–	-0.20	0.08
Scenario 1	-15.5%	-74.0%	-0.6	-10.8%	0.53	0.30
Scenario 2	-14.0%	-80.6%	-0.4	-11.0%	0.23	0.22
Scenario 3	-6.0%	-83.0%	0.0	2.1%	0.79	0.36
Scenario 4	-5.8%	-86.5%	0.1	1.4%	0.67	0.34
Scenario 5	-12.2%	-40.6%	-0.3	-6.0%	0.02	0.40
Scenario 6	-10.7%	-40.7%	-0.2	-5.1%	-0.01	0.36
Scenario 9	-12.2%	-42.7%	-0.3	0.3%	0.06	0.52

- Scenario 1 yielded the highest cost decrease of 15.5%, and an energy decrease of 10.8%. However, this was at the expense of lower indoor temperatures, which were reduced by 0.6 °C compared to the mean temperature of the reference operation.
- Scenario 3 achieved the highest indicator of load shifting during night time, namely 0.79. Cost was decreased by 6%, but energy use was moderately increased by 2.1%. The mean indoor temperature was the same as that of the reference operation, but with more fluctuations during the day.
- Scenario 4 achieved the highest decrease in energy use during morning peak hours: 86.5%. Cost was decreased by 5.8%, with only small differences in the total energy use and mean indoor temperature.
- Scenario 9 achieved the highest indicator of load shifting during periods with lower heat production cost, namely 0.52. Cost was decreased by 12.2%, with almost the same energy use as the reference scenario. The mean indoor temperature was slightly lower than that of the reference operation and fluctuated within a wider temperature range.

Figure 27 (left) illustrates the average daily heat load patterns for the different scenarios together with that of Greater Copenhagen (right axis) and Figure 27 (right) illustrates the average daily profile of indoor temperatures in the different scenarios and in the reference operation.
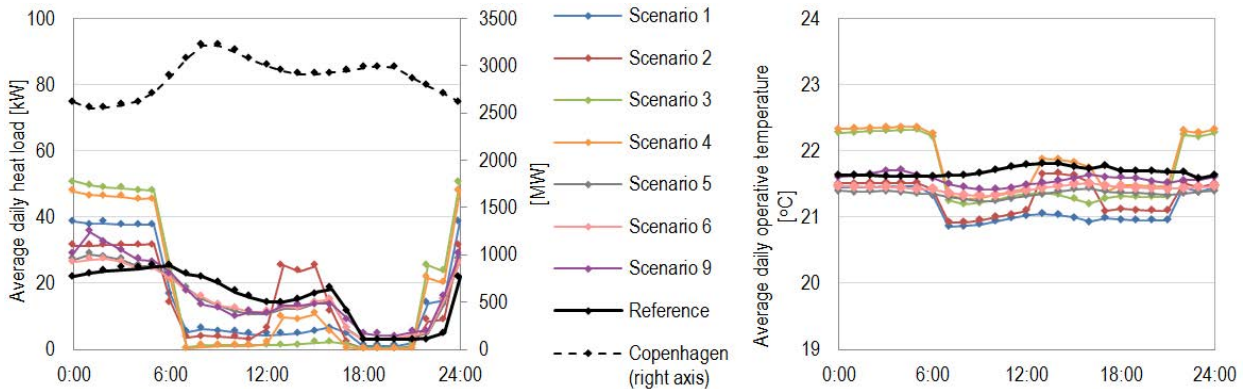
Figure 27: Left: Average daily heat load of the building in different scenarios and reference operation (left axis); average daily heat load in Greater Copenhagen (right axis). Right: Average daily operative temperature in different scenarios and reference operation

For all scenarios, the maximum load was increased compared to the reference operation. The scenarios with pre-heating of the building resulted in higher peak loads, while the scenarios which only decreased the set-point showed a behaviour closer to that of the reference operation. The occurrence of new building peak loads was a result that was anticipated, but it is arguable whether it undermines the implementation of those strategies. In terms of the building itself, the new peaks were within the installed capacity of the heating system, so no additional investment would be required. This means that for the building it is not problematic. Regarding the DH system, the time when the new peaks occur is critical. For all scenarios the highest heating use occurred during the night period, i.e. 21:00 -6:00, with new peaks been created at the transition between the day set-point and the night set-point. This means that the new peaks occurred at hours when the overall load of the system is low, and on average the marginal heat production cost is low. The new peaks may therefore not pose challenges to the system; however this would depend on the scale of the implementation. In all cases, load shifting from day to night was achieved, so the daily load pattern of the building contributed to smoothing the load of the Greater Copenhagen area, which was indeed one of the goals.

The morning peak in the heat load of Greater Copenhagen, which occurs between 6:00-9:00 could be mitigated by reducing the space heating demand in this type of building during this period. All scenarios examined had lower energy use during this period, but the scenarios with fixed schedules for set-points achieved higher reductions. The evening peak in the heat load of Greater Copenhagen, which occurs around 19:00, cannot be mitigated with these scenarios in this type of buildings, since the space heating demand for the reference operation was already minimal due to the internal heat gains during these hours.

Regarding the average daily profile of indoor temperatures, the scenarios with the fixed temperature schedules presented a clear pattern, with Scenarios 1 and 2 being constantly below the temperatures of the reference operation, while Scenarios 3 and 4 fluctuated both above and below those of reference operation. In scenarios with dynamic signals the average daily pattern appeared to be smooth, with small fluctuations during the day. However, on an hour-to-hour evaluation across the heating season, there were stronger fluctuations and these scenarios covered a broader spectrum of temperatures.

Figure 28 shows the performance of the scenarios according to the two flexibility indicators described in Section 0.
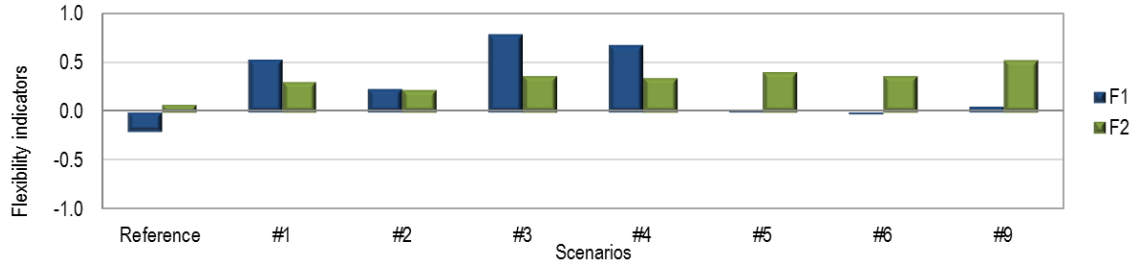
Figure 28: Flexibility indicators in different scenarios and reference operation

It can be seen that for all scenarios, both indicators improved compared to reference operation of the building. F_1 for the reference operation was -0.20, i.e. there was higher energy use during the high load hours than during low load hours. The scenarios with fixed schedules for set-points achieved higher values for F_1. The highest value of F_1 was achieved for Scenario 3 (0.79) followed by Scenario 4 (0.67), which were the scenarios with pre-heating during the night. The scenarios with dynamic response to the cost signal improved the indicator compared to the reference operation, but only slightly. Regarding F_2, during reference operation of the building it was almost 0, which means that there was equal energy use during high and low production cost period. The scenarios with dynamic response to the cost signal achieved higher values, with Scenario 9 being the highest with 0.52.

Choosing which of the scenarios to implement is a multifactorial decision. First and foremost, it depends on the services that energy flexible buildings should provide to the energy system. It may be the minimization of energy use during specific hours, the reduction of cost, the alleviation of local congestion problems, or the smoothing of the overall heat load. Such results may come at the expense of a wider indoor temperature range and/or more fluctuations in the indoor temperature during the day. The level of acceptance of thermal comfort changes may also affect the choice of strategy. In some cases, higher total energy use was observed, but this may be considered acceptable, as costs would still be less and probably it is less carbon intensive.

The signals used in this study had a considerable influence on the obtained results. Different signals can be used to trigger the flexibility of a building, such as CO_2 emissions or preferably the actual heat prices. To date, in Denmark the heat price paid by customers is constant across the year and fixed by individual contracts, so there is no incentive for individual customers to participate in such strategies or to decrease their energy use during peak hours. However, dynamic heat pricing is being studied and it was the scope of this work to identify if there is potential for this type of building to be operated flexibly. By using different signals, the quantification of the results and metrics may be different, but the thermal response of the building is anticipated to be similar. Further work on managed demand response in buildings connected to DH is needed, and the value of energy flexibility will depend on the specific DH market structure.

In this study, the approach that was followed was an indirect load control assuming that all the occupants participated in the control strategy. Reality would probably be different, as in indirect load control occupants would have the choice not to participate, i.e. not to adjust their set-points. This would result in effects of a different magnitude than those simulated in this study. The percentage of occupants who participate in the control system is an important parameter when planning to implement flexibility strategies in residential buildings. Another important parameter, especially if using thermal mass as storage to facilitate flexibility, is the thermal comfort acceptability range of occupants, which can vary significantly, as was also pointed out by [72]. In the present study, this may be more critical since many of the proposed scenarios require set-points to be changed in a way that is opposite to typical night set-back schedules. Nevertheless, for occupants to be willing to accept changes in thermal comfort if their buildings should be operated flexibly, they will have to be properly informed and motivated. Since monetary incentives attract the most attention and more powerfully motivate participation [72], [53], it should be further investigated how the benefits achieved for the system at the production side could be reflected in the prices that the occupants pay.

In addition to their decision whether to participate in flexibility strategies, occupants of residential buildings have an impact on the flexibility potential through their behaviour, in terms of occupancy patterns and thermal comfort preferences. The schedule and intensity of the occupants' patterns affect the internal gains in the

45

building considerably, especially in low-energy buildings, and thus the heating requirement. Thermal comfort preference, i.e. temperature set-point, has a considerable effect on heating demand and thus on the potential for flexible operation. In this study, a deterministic occupancy pattern assumed by standards was used and a constant reference set-point of 22°C, which is a typical desired indoor temperature in Danish households during the heating season. However, these may both be different in reality, so more representative or stochastic models of occupant behaviour would improve the validity of the results [87], [101], [130], [131].

An important factor that must be further investigated is the effect of the implementation of those scenarios at the district or city level. In the scenarios implemented, new peak loads were created in the building, at the beginning of low production cost or low system load periods. In order to avoid disturbances in the system, a smoother ramp in the heating set-point control in the building could be set and/or the heat supplier could send signals, which are slightly shifted in time to different categories of consumers. The specific design of the district heating system in the area, as well as hydraulic constraints should also be considered.

4.1.3   Main findings

This study showed that there is a potential in low-energy residential buildings for them to be operated flexibly, using the thermal mass of the buildings for short-term energy storage, in order to be able to offer flexibility services to the district heating system:

- The requirements of the DH system were addressed by using rule based scheduling of the building's heating system based on the demand of the district heating system and cost-based scheduling corresponding to the marginal heat production cost.
- Highly effective heat load shifting was achieved (between 40% and 87%) to avoid the DH system peak load hours.
- Cost reductions of up to 15% were achieved.
- The total energy use either increased by up to 2% or decreased by up to 11%. Increased energy use may be considered acceptable as part of load shifting strategies, if it costs less to be produced and can be beneficial for the environment if it comes from renewable energy sources.
- New peaks in the heating load of the building were created.
- The magnitude of the achieved benefits is dependent on whether the changes in energy use are acceptable and on the thermal comfort required by the occupants of the building.

4.2   Flexible operation of a building equipped with heat pump

This section evaluates the flexibility potential of a refurbished detached house in Denmark, by means of intelligent scheduling of a heat pump. The optimization of the operation of the system was based on a price-signal, in order to reflect the electricity grid requirements. The scheduling of the heat pump was conducted through the coupling of a dynamic building simulation tool with an optimization tool.

The findings of this study have been published in the proceedings of the 15th IBPSA (2017):
Gianniou, P., Foteinaki, K., Heller, A. and Rode, C. (2017), 'Intelligent Scheduling of a Grid-Connected Heat Pump in a Danish Detached House', Department of Civil Engineering, DTU , Kgs . Lyngby, Denmark, in 15th IBPSA Conference. San Francisco, CA, USA, pp. 95–102.

4.2.1   Method

A price-based control strategy for a heat pump was implemented to permit the exploitation of dynamic electricity prices and thus control of the energy load according to the requirements of the grid. The scheduling of the heat pump comprised two parts: the control of the system, and its optimization. A building model of a typical refurbished Danish detached house was used. The building area was 153m^2 and was equipped with an air-to-water heat pump of 13 kW with a COP equal to 3.5, with low-temperature water radiators. The details of the building model can be found in the respective publication.

The reference temperature set-point was set to 20°C. The operation of the heat pump was forced to increase the temperature set-point by up to 3°C during low-tariff hours. Low electricity prices were defined as the ones that were lower than the average electricity price in that specific month. In this way, altering the temperature set-point would cause heat to be stored into the thermal mass during low price periods and to be released back to the room when prices were higher.

The optimization was defined as minimization of the operating cost of the heat pump. This cost depended on the variable electricity prices and on the consumption of the heat pump. The cost-optimal control of the heat pump on a 3-day horizon was selected so that any phenomena of cumulative heat storage into the thermal mass could be observed. Due to increased computation time, it was decided not to investigate a longer period. The optimization problem of the intelligent scheduling of the heat pump according to the price signal was formulated as shown in Equation 11 and Equation 12:

$$\text{Minimize } C_{HP} \qquad (11)$$
$$C_{HP} = p_{el} \cdot W \qquad (12)$$

where C_{HP} is the operating cost of the heat pump, p_{el} is the total electricity price and W is the energy consumption of the heat pump.

The optimization of the system operation was conducted through the boiler schedule, adjusting the part load operation of the heat pump during the day. The optimization was conducted with the use of the open-source software MOBO. MOBO is a generic freeware designed to handle single-objective and multi-objective optimization problems with continuous or discrete variables. Four optimization algorithms and different solver settings were tested. The algorithm and solver settings that achieved the biggest cost reduction were selected and implemented in the building model. These results were compared to the ones of the reference case with normal operation of the heat pump.

Three climate cases were selected out of the entire simulation period; i) the coldest 3-day period of the heating season with a mean ambient temperature of -4°C; ii) the warmest 3-day period of the heating season, with a mean ambient temperature of 11°C; iii) an intermediate period when the average ambient temperature was 3°C. The prices for electricity were set in the model through a profile reflecting real electricity prices in 2015 according to the Nordic electricity market Nord Pool for East Denmark. During this period, wind power generation accounted for 74% of the total electricity production, which explains the low electricity prices that triggered the price signal. These prices reflect the total electricity prices consisting of variable el-spot prices, which account for 32% of the total price in Denmark, while the remaining 68% are fixed taxes for local network, grid and system tariffs, public service obligation tariff and further subscriptions to electrical companies based on the Association of Danish Energy Companies (2015). The total electricity prices were used in the model so that they correspond to what electricity customers have to pay. The same price-signal was used for all three cases of weather data to ensure comparability. Figure 29 shows the electricity spot prices during this 3-day period. The negative prices indicate a surplus of wind power generation during these days.
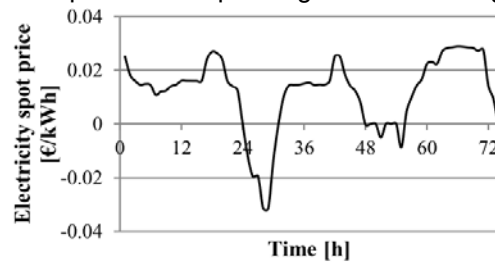
Figure 29: Electricity spot prices over 3 days

4.2.2 Results and discussion

The cost-optimal solution refers to the minimum cost (€) that each optimization algorithm achieved, which means the total operating cost of the heat pump operated to heat the building for the examined 3 days. Figure 30 shows the power consumption for the reference and optimized case for each of the weather cases.
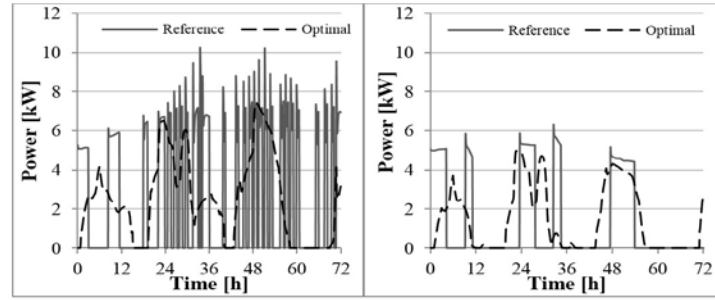
Figure 30: Power results for the optimized scheduling of the heat pump and the reference operation for cold (left) and intermediate (right) weather data
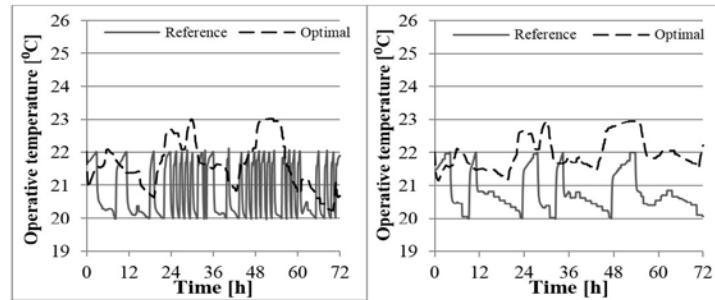
Figure 31: Operative temperature results for the optimized scheduling of the heat pump and the reference operation for cold (left) and intermediate (right) weather data

For the cold weather, when using the thermostat as in the reference case, the heat pump turned on and off in very small intervals, in order to cover the high demand, which resulted in high power peaks. On the other hand, for the optimal case, the power consumption presented a considerably smoother pattern, which was fully in line with the price signal. Taking the highest peak in power, there was a reduction of 27% (2.75 kW). There were small parts of the load that were shifted in time, but this schedule achieved considerable peak shaving. For the intermediate climate case, the power consumption pattern was similar to that of the reference and optimal cases. The timing of the peaks was almost the same, but peak shaving of 21% (1.32 kW) was achieved in the optimal case. The same simulations were performed for three warm days of the heating season, but it was found that the energy demand was almost zero, which left no room for optimization.

Table 10: Total energy consumption and operating cost of the heat pump for 3 days

Weather	Total energy consumption (kWh)		Total operating cost (€)	
	Reference	Optimal	Reference	Optimal
Cold	191	180	2.998	1.742
Intermediate	92	104	0.979	0.761
Warm	0	0	0	0

The results regarding the total energy consumption and operating costs are shown in Table 10. For the cold climate, there was an energy consumption reduction of 6% in the optimal case, while for the intermediate climate there was a 13% increase in the optimal case. This indicates that when implementing a DSM strategy, i.e. peak shaving, this might result in increased consumption overall. As far as cost reduction was concerned, in the cold weather case, optimally scheduling the heat pump resulted in a 42% decrease in the total operating cost of the heat pump for the 3-day period. In the intermediate case, the cost reduction was 22% compared to reference operation of the heat pump.

Figure 31 shows the operative temperature for the reference and optimized cases. The optimal cases had higher operative temperature than the respective reference cases, since the set-point was increased to 23°C when the electricity prices were low. There is a clear correlation between the power consumption pattern and the operative temperature pattern. This explains why the temperature of the reference case of the cold climate showed frequent fluctuations, whereas the temperature of the optimal case for the cold climate and both cases of the intermediate climate showed a smooth pattern.

It should be noted that the electricity prices according to which the optimal scheduling of the heat pump was conducted in the three weather cases were found to be low compared to the average monthly price, which resulted in an increased heating set-point most of the time.

4.2.3 Main findings

Optimal scheduling of the heat pump was achieved using a dynamic electricity price signal. There was a different approach for the building connected to a DH system and the building supplied by heat pump, mainly due to the different requirements of each system.

- The optimized scheduling of the heat pump led to power peak reduction of up to 27% and cost reduction up to 42% for a 3-day horizon with very high wind production.
- Warm weather days in the heating season could not be considered for optimal scheduling of the heat pump, since the very low heating demand left no room for optimization.
- The optimal scheduling of the heat pump maintained good thermal comfort of the occupants in terms of operative temperature.

Chapter 5   Modelling household electricity load profiles - A first step to facilitate modelling of energy flexibility in dwellings

This chapter is based on Paper III and addresses the 3rd objective of the thesis.

There is potential for increased flexibility in the electricity loads in buildings from domestic appliances and possibly the heating system, i.e. electric heating and heat pumps, as shown in 4.2. If the occupants' activities are to be addressed in relation to household electricity loads, creating realistic daily household electricity demand profiles is the basis of flexibility modelling for electricity household loads

The aim of this chapter was to link occupant energy-related activities to electricity demand, in order to obtain a realistic daily electricity load profile for Danish households using information collected from the occupants, i.e. Danish time-use survey (DTUS) data. The approach was to combine appliance ownership and power data with data on occupant activities from the DTUS. The limitations of the approach are discussed. Detailed information on the models, methods and results can be found in the respective publication. The objective of the models created in this work was to obtain a realistic daily electricity demand profile. A description of the detailed shape of the load profile was the purpose of this work, as it is of great interest for various applications, including DSM modelling and tariff planning.

5.1.1   Method

5.1.1.1   Data for model development

Table 12 summarizes the datasets used for the development of the models. The main input dataset for the development of the models was the Danish time-use survey (DTUS) conducted in 2008-2009.

Table 11: Datasets for model development

Dataset	Description	Measurement period	Location of households	Number of participants	Data resolution
DTUS 2008/09	Danish time-use survey	03/2008-03/2009	Denmark	9640 individuals from 4679 households	10-min
Nordhavn_Appl	Measurements on electricity use of individual appliances	18/01/2018 18/04/2018	Nordhavn, Copenhagen	17 apartments	1-min

The study includes data about the time-use of activities performed throughout the day by a representative sample of the Danish population. Specifically, 9640 individuals from 4679 households participated in this survey, by responding to a questionnaire, filling out a diary and an expenditure booklet [132], [133]. The time resolution of the diary was 10 min, namely the day was divided into 144 time intervals, starting at 4:00 and ending at 3:50 in the morning. Bonke and Fallesen 2010 [133] provide more detailed descriptions of the DTUS, the methods and the responses. Barthelmes et al. 2018 [93] used the DTUS data to create profiles of occupant daily activities during different seasons and weekdays/weekends, and to identify the time-related characteristics of the activities, i.e. starting times, ending times and durations. The DTUS pre-coded 35 activities, which were then reported by the participants. In [93] these activities were consolidated into the 10 energy- and occupancy-related activities shown in Table 12, focusing on activities taking place inside the

domestic environment. The rest of the activities were categorized as "Not at home". The same clustering of activities was also used in the present work.

Table 12: Activity clustering [93]

No.	New clusters	Activities included in the DTUS 2008/09
1	Sleeping	Sleeping
2	Toilette	Toilette
3	Eating	Eating
4	Cooking/washing dishes	Cooking/washing dishes
5	Cleaning/washing clothes	Cleaning/washing clothes
6	Practical work	Other work, do-it-yourself work, garden work
7	Family care/free time	Child care, reading with children, family care, reading, hobby, social gathering, phone conversations
8	Relaxing/TV/IT	TV/radio/music, IT, relaxing
9	Not at home	Work, lunch break, transportation as part of work, transport to and from work education, education, transport to and from education, shopping, errands, visiting public offices, pick up/bring children, association activities, voluntary work and similar, exercise/sport, entertainment/culture, restaurant/café
10	Other	Other

The dataset "Nordhavn_ Appl" was collected in the framework of the EnergyLab Nordhavn project [10] and includes measurements at the individual appliance level. The measurements were performed in 17 apartments and included six main appliances: oven, hob, microwave oven, dishwasher, washing machine and tumble dryer. The measurements were used to calibrate the average power used during the operation of each of the appliances used in the models.

5.1.1.2   Data for model comparison

Table 13 lists the data sets that were used for validation and comparison with the models. The models' comparison was performed in terms of the total electricity use in the households. The available measurement datasets are characterized by the diversity of the participating households. The dataset "Esbjerg_Tot" was collected by SydEnergi, the largest electricity utility company in southern Denmark, and was analysed in [134]. The dataset "Korngården_Tot" was analysed in detail in [135]. The dataset "Nordhavn_Tot" was collected in the framework of the EnergyLab Nordhavn project [10]. The only data available on an individual appliance level were those from "Nordhavn" that were used for the calibration of the models' appliance parameters. The "Nordhavn_Tot" dataset was used for validation, while the datasets "Korngården_Tot" and "Esbjerg_Tot" were used for a qualitative comparison.

Table 13: Datasets for model validation/comparison

Dataset	Description	Measurement period	Geographical location	Number of households	Data resolution
Nordhavn_Tot	Measurements on total electricity use of the household	18/01/2018 – 18/04/2018	Nordhavn, Copenhagen	17 apartments	1-min
Korngården_Tot	Measurements on total electricity use of the household	05/2016 – 05/2017	Copenhagen metropolitan area	61 apartments	1-hour
Esbjerg_Tot	Measurements on total electricity use of the household	10-16/01/2011	Esbjerg	32,241 single-family houses and apartments	1-hour

The measurement period, the geographical location of the households and the socio-economic characteristics of the occupants in the participating households varied considerably and this should be considered when analysing the data:

- The dataset of "Nordhavn_Tot" is a relatively limited sample of measurements in apartments in the district of Nordhavn in the city of Copenhagen, Denmark.
- The dataset of "Esbjerg_Tot" is a large dataset and comprises measurements both in apartments and single-family houses of the city of Esbjerg, which is a city on the West coast of Denmark. The measurement period was limited to one week.
- The dataset of "Korngården_Tot" consists of measurements in apartments in the outskirts of Copenhagen. The apartment block is part of a social housing association.

Information on the number of the residents in the measured apartments/single-family houses was not available for any of the datasets.

5.1.1.3   Modelling

Two modelling approaches were used to construct the mean electricity load profile of a household. Each one used the results generated by analysing the DTUS 2008/09 data [93] as inputs and converted those to electricity load profiles. The occupant activities model used in each approach is described in Section 5.1.1.3.1. Section 5.1.1.3.2 describes the conversion of the activities to electricity consumption. In both models, each activity was mapped with a set of appliances. In both models, separate profiles for weekdays and weekends were created.

5.1.1.3.1   Occupant activities model

Two models were developed.

- In Model 1, the electricity profile was a simple conversion model of the occupant activity profiles. The activity profiles were determined from the DTUS 2008/2009 data as the percentage of respondents who performed an activity at each 10-min time interval. The percentage of each activity was used directly as the probability of a certain activity and associated use of appliances [93]. Figure 32 presents the activities profiles separately for weekdays (left) and weekends (right).
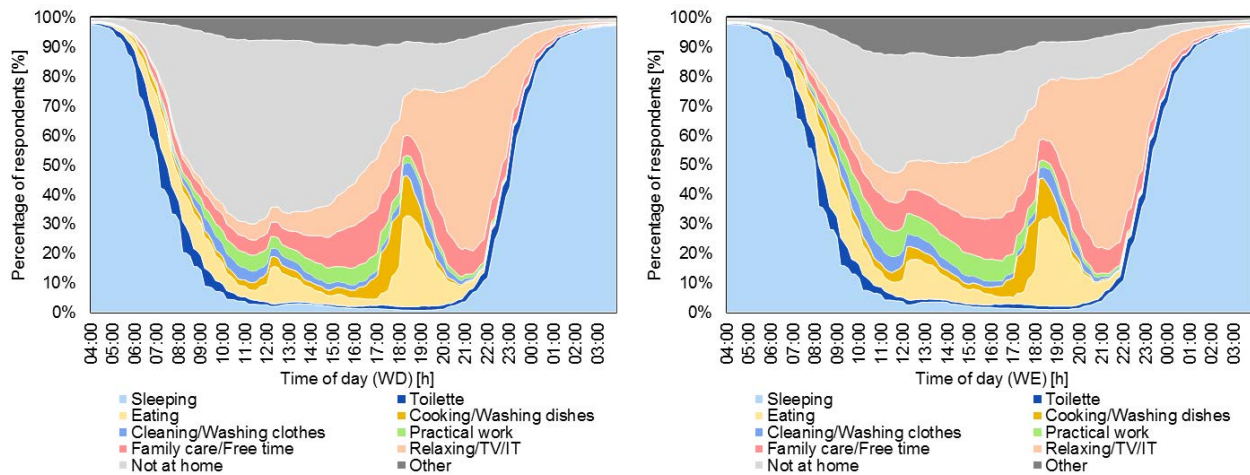
Figure 32: Occupant activities profile during weekdays (left) and weekends (right)

- In Model 2, an activity profile was generated based on the probability of starting an activity and the duration of each activity. Similar to Model 1, each activity was associated with the use of certain appliances. The probability of starting an activity depended on the time of day and the duration of the activities were given as a probability density. The inputs of Model 2 were thus the time-related characteristics of the activities: starting times and duration. Figure 33 shows the number of activities started during weekdays (left) and weekends (right). They were based on [93], but were reconstructed with 10 min resolution, in order to be consistent with the resolution of all the input data in the model. Figure 34 shows the survival functions, namely the probability that an activity continued longer than time t after it was initiated.
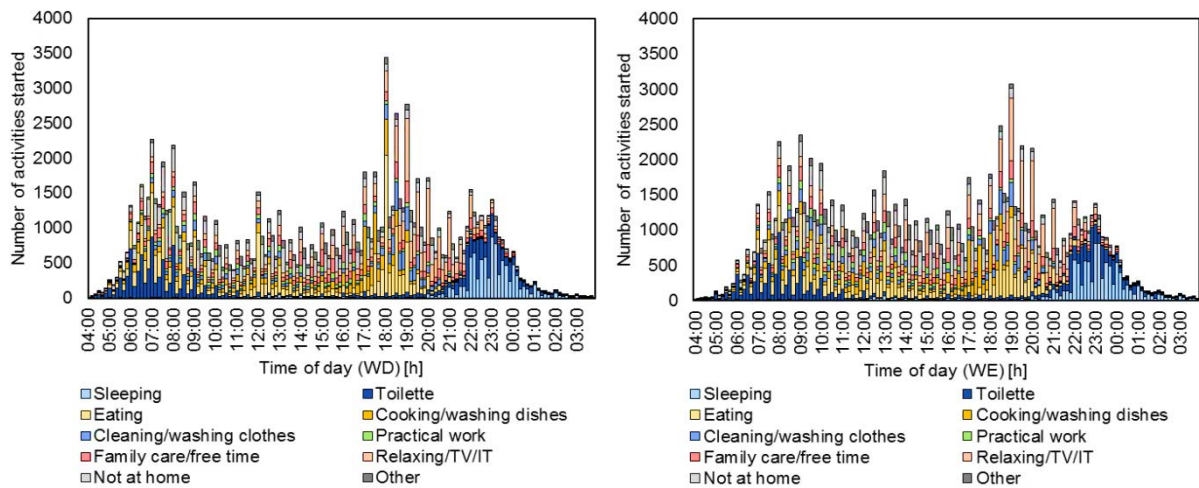
Figure 33: Number of activities started during weekdays (left) and weekends (right)
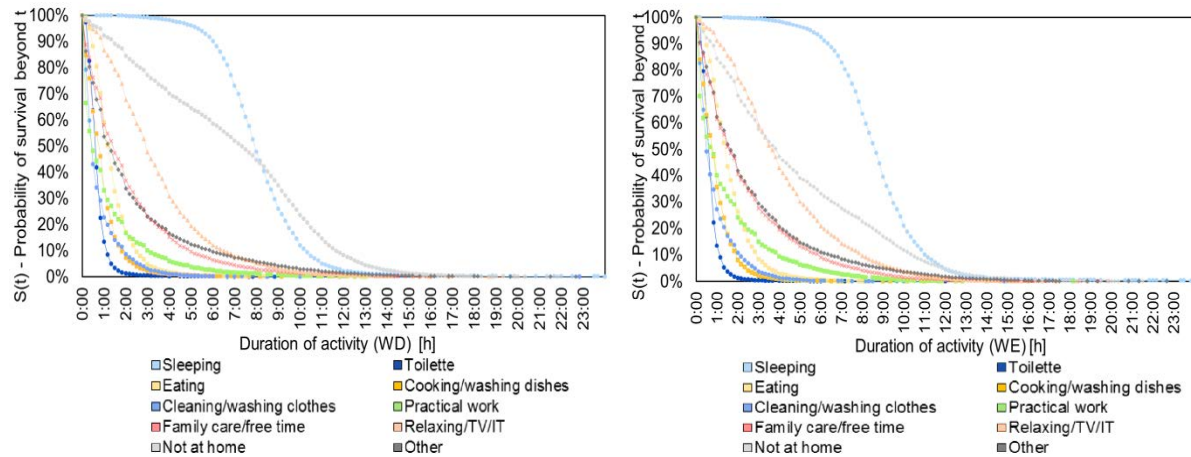
Figure 34: Survival functions during weekdays (left) and weekends (right)
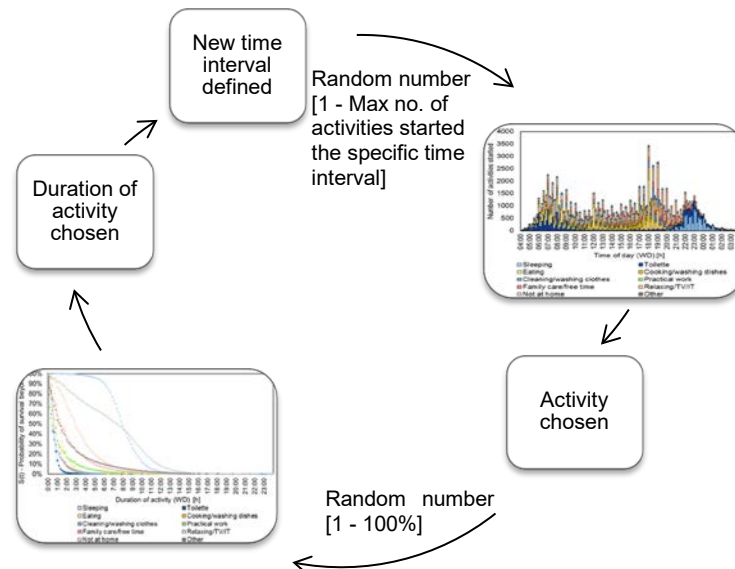
Figure 35: Structure for constructing occupant activities profiles model for Model 2

Figure 35 outlines the structure for constructing occupant activities profiles for Model 2. In each time interval of the day, a specific number of activities were started according to the DTUS 2008/09 data, which is shown in each bar in Figure 33. For a specific time interval, the model drew a random number between 1 and

the maximum number of activities started in this time interval. The activity to be started was selected by comparing the random number to the respective bar of the graph. The survival curve of the specific activity (Figure 34) was then used to select the duration of the activity by drawing a new random number (between 1% and 100%) and resulted in the duration for which this activity should last. After this, a new time interval was defined and the process was repeated. Aggregating the daily profiles thus created, a mean occupant activities profile for Model 2 was obtained.

For both models, the output resolution was 10 min. However, since the resolution in the measurement datasets was 1 h, the comparisons were performed with 1 h averages of the models' output.

5.1.1.3.2   Conversion of activities to electricity consumption

The electricity consumption in this model considered non-thermal applications. The activities associated with <u>electric appliances</u>, i.e. electricity use, were Activity 4: Cooking/Washing dishes, Activity 5: Cleaning/Washing clothes and Activity 8: Relaxing/TV/IT. The electricity load of each activity for each time interval was calculated from the electricity use of a combination of the appliances associated with this activity. When the appliances were not in use, their stand-by power consumption was considered. For each activity there is great variability in the number and type of appliances with which it can be associated. Assumptions were therefore made for the set of appliances used in the model, based on the data of appliance ownership at the national level [136]. An average constant power load was assumed for each activity during each 10 min interval, determined by the different combinations of appliances that are used simultaneously. Details of the combinations can be found in Table 14. For each activity, an average of all the combinations in Table 14 was used. The cold appliances were modelled as a constant power load, not related to occupant activities. In reality, they operate on a cyclic load with thermostatic control, but on a daily basis they can be adequately represented by their average power use. The appliances associated with the Activities 4, 5 and 8 and the cold appliances are the most common ones found in a Danish household, but not all of them. In the "Nordhavn_ Appl" dataset there are measurements for specific appliances, namely oven, hob, microwave oven, dishwasher, washing machine and tumble dryer. These data were used to calibrate the average electricity use of these appliances in the models. For the rest of the appliances, data from [136] and [137] were used.

Table 14: Combinations of appliances used in Activity 4 (Cooking / washing dishes), Activity 5 (Cleaning / washing clothes), Activity 8 (Relaxing / TV / IT) and Cold appliances and the respective power

Activity 4 - Cooking/washing dishes				Average power	Activity 8 - Relaxing/TV/IT			Average power
Hob	+ Hood			805 W	TV			111 W
Oven	+ Hood			1103 W	TV	+	DVD or Video	151 W
Hob	+ Hood	+	Kettle	2565 W	TV	+	PC or Laptop	213 W
Oven	+ Hood	+	Micro oven	2139 W	Stereo system			106 W
Dishwasher				422 W	Stereo system	+	PC or Laptop	207 W
All the above				5121 W	PC or Laptop			101 W
Activity 5 - Cleaning/washing clothes				**Average power**	**Cold appliances**			**Average power**
Washing machine				299 W	Fridge	+	Upright freezer	40 W
Washing machine	+	Dryer		1357 W	Fridge	+	Chest freezer	45 W
Washing machine	+	Vacuum cleaner		1303 W	Fridge & freezer			48 W
Dryer				1058 W	Fridge & freezer	+	Upright freezer	63 W
Dryer	+	Vacuum cleaner		2061 W	Fridge & freezer	+	Chest freezer	69 W
Vacuum cleaner				1003 W				
All the above				2361 W				

Electricity use for <u>lighting</u> was modelled as daylight-dependent and occupancy-dependent and was based on the model developed by Widen et.al 2009 [87], [96], according to which the lighting power was given by Equation (13):

$$P(t) = \begin{cases} P_{min} \frac{L(t)}{L_{max}} + P_{max}\left(1 - \frac{L(t)}{L_{max}}\right), & L \le L_{max} \\ P_{min}, & L > L_{max} \end{cases} \qquad (13)$$

A maximum threshold of illuminance was predefined. When the illuminance in the household was higher than the threshold, the lighting power was equal to a minimum lighting power. When the illuminance was lower than the threshold, the lighting power varied depending on the ratio of the actual illuminance and the maximum threshold. This calculation was valid when the occupant was at home and awake, otherwise the lighting power was assumed to be zero Watts. In the present work, the illuminance threshold (L_{max}) was set to 500 lux, as recommended in EN/DS 15251 [118]. The illuminance level $L(t)$ was obtained from conversion of irradiance data from the year 2008 [123] to illuminance. The conversion used the total diffuse radiation from surfaces, considering the diffuse radiation from windows and reflection from surfaces of the direct radiation from windows [138]. The data of the conversion model of irradiance-illuminance were of 1 hour resolution and were generated with IDA ICE simulation software [110] for a vertical, south-facing, triple-glazed window with a transmittance of 0.74. The P_{min} and P_{max} were defined as one bulb being switched on, and one third of all the installed bulbs being switched on, respectively. Details of the parameters used can be found in Table 15.

Table 15: Input data for lighting model [136], [139]

Type of bulbs	Percentage of ownership	Average power per bulb
Low energy bulbs	33%	11 W
Incandescent lamps	33%	40 W
Fluorescent strip lamps	12%	20 W
Halogen bulbs	23%	20 W

5.1.2 Results and discussion

Ideally, the load profiles generated by the models should be compared to measurements performed in the same households as where the DTUS were carried out. However, this was not possible, since such measurement data did not exist. Instead, the modelled profiles were compared to the average measured electricity profiles of the three datasets. The data of "Nordhavn" was used for the validation as the information on electric appliances from there was used for model calibration. The other two datasets were used for qualitative comparison, evaluating how the models performed, as there were no data available for calibration.

Figure 36 presents the average daily electricity load profile for weekdays and weekends.
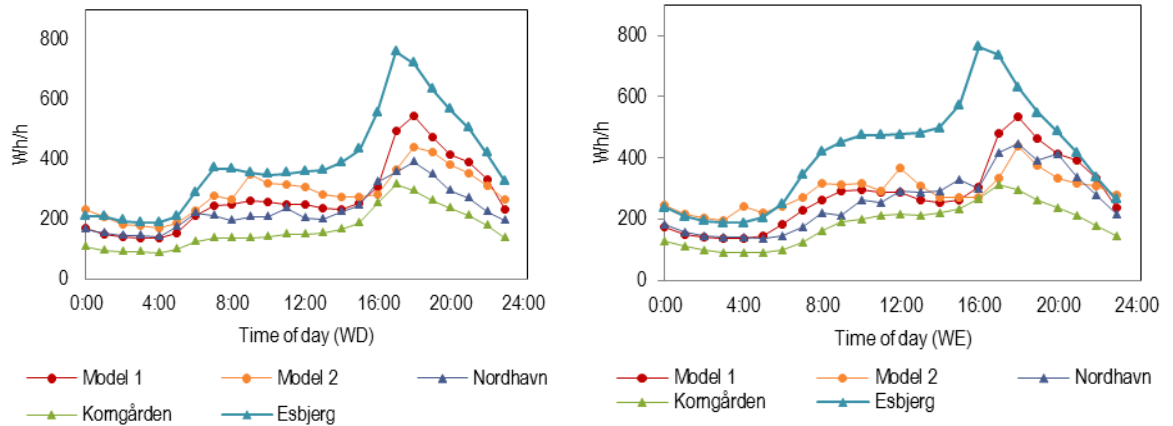
Figure 36: Average daily electricity load profile for weekdays (left) and weekends (right)

Overall the profiles followed a similar pattern. The lowest level of electricity use was during the night, followed by a morning increase during breakfast time. This level was, in general, maintained during the day until the late-afternoon, when the electricity use started to increase, reaching its highest peak in the evening. Subsequently, electricity use decreased towards the night level. During a weekend day, the morning increase in electricity use was shifted later in time and the consumption was higher during the day. Both in weekdays and weekends, the profiles had different magnitudes. Compared to "Esbjerg_Tot", "Nordhavn_Tot" and "Korngården_Tot" both had lower consumption, as expected since the datasets were from apartments only, which in general have lower consumption than single-family houses [140]. "Korngården_Tot", particularly,

were data from social housing apartments, which presumably have a lower level of equipment and thus lower electricity consumption. "Esbjerg_Tot", on the other hand, had an almost equal sample of apartments and single-family houses, and thus higher consumption. In other words, the correspondence between measured and modelled data should be interpreted in context. The three datasets of electricity use were measured in buildings different from the larger DTUS sample that was used for the modelling, which had a considerable impact on the estimated consumption.

Regarding Model 1, although there were differences in scale between the measured and modelled profiles, the overall pattern was adequately represented. There was good correspondence of peaks and valleys during the day, both in terms of timing and magnitude, and the difference between a weekday and a weekend was captured as well. During the weekend, the profile of Model 1 was similar to that of "Nordhavn_Tot". In Model 2 there were some discrepancies between the measured and modelled data. An increase in consumption at 9:00 on a weekday and 12:00 on a weekend day were observed, which were not present in the measured profiles. Additionally, the evening peak was lower in magnitude compared to the other profiles, particularly at weekends.

Table 16 presents Pearson correlation coefficients and mean relative error between model and measurements, calculated for each model during weekdays and weekends, based on the 1-hour average load profiles. The Pearson correlation coefficient is a measure of how well a linear function describes the correlation between the modelled and measured profiles. A perfect match between modelled and measured load profiles would result in a Pearson correlation coefficient of 1. The mean relative error is the mean of the absolute relative difference between the modelled and measured load profiles.

Table 16: Correlation coefficient and mean relative error based on 1-hour average load profiles for Model 1 and Model 2 (WD = weekday, WE = Weekend)

	Pearson Correlation Coefficient		Mean Relative Error	
Model 1	WD	WE	WD	WE
Nordhavn_Tot	0.95	0.95	18.4	14.5
Korngården_Tot	0.95	0.90	64.9	51.5
Esbjerg_Tot	0.97	0.93	29.3	30.9
Model 2				
Nordhavn_Tot	0.85	0.83	29.5	31.5
Korngården_Tot	0.84	0.80	85.7	73.3
Esbjerg_Tot	0.88	0.82	20.8	26.1

The correlation with Model 1 was above 0.95 for weekdays and above 0.90 for weekends, indicating that Model 1 was able to capture the shape of the load profile very well. The correlation with Model 2 was lower, yet still above 0.80. The magnitude of the mean relative errors was expected, as they reflect also the differences in scale of the load, which depends on the typology of measured households in each dataset. The errors of Model 1 were overall lower compared to those of Model 2.

The timing of peak loads is an important parameter, especially for demand side management, so it was specifically evaluated. Figure 37 shows the average daily electricity load profile normalized against the individual maximum of each load profile, for weekdays and weekends.

During weekdays, the evening peaks occurred at different hours displaced by one hour for the different measured datasets. The peak was at 18:00 in the "Nordhavn_Tot" dataset and the two models. "Korngården_Tot" and "Esbjerg_Tot" peaked at 17:00, indicating differences in behavioural patterns between the datasets, possibly related to the occupation of the population of the latter two being more labour intensive than the average of Denmark [141]. There was a closer correspondence in the timing of the patterns in the weekdays compared to the weekends. Model 1 clearly captured the diurnal pattern in a weekday, while Model 2 presented discrepancies. The electricity use was higher in the period 7:00-13:00, with a peak at 9:00 which was as high as approximately 65% of the main evening peak. The similarities in measured and modelled

patterns during the weekend were not as clear as for the weekday, yet the general patterns were still observed.
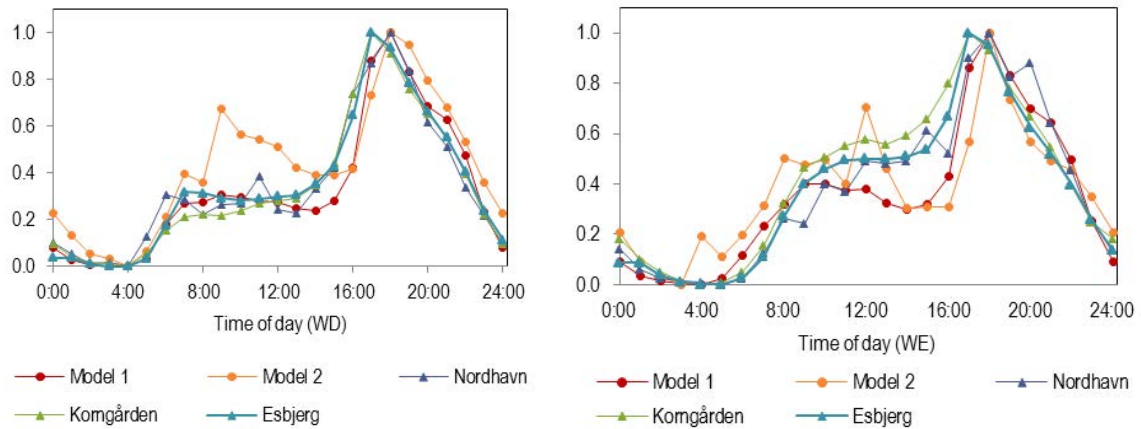
Figure 37: Average daily electricity load profile normalized against the individual maximum and minimum of each load profile for weekdays (left) and weekends (right)

Overall, Model 2 produced a less reliable profile of the electricity load compared to Model 1. There could be different sources of error in the process. Firstly, Figure 33, which shows the number of activities started every 10-min of the day, shows a pattern for the initiation of the activities. Four peaks can be observed: morning peak (06:00-09:00), midday peak (12:00), evening peak (17:00-20:00) and bedtime peak (22:00-23:00). This pattern was not taken into consideration in Model 2, since the start of the activities were selected based on the probabilities created by the maximum number of activities started in the specific time step. In addition, the responses recorded in diaries were not always well-reported, as the participants of the survey were solely responsible for filling in the diaries. Indicatively, in the graphs with the activities started, which were reported with 10-min resolution, it can be seen that the respondents tended to report the start of the activities primarily at the full or half of every hour. This created a variable profile of the probability of starting an activity, which was reflected in the electricity load profile.

5.1.3 Main findings

Using information collected from occupants, i.e. Danish time-use survey (DTUS) data, about the timing of household activities and data on appliance ownership and power rating, it was possible to model domestic electricity profiles, which can then be used for flexibility modelling in dwellings.

- The model links occupant energy-related activities to electricity demand, i.e. Danish time-use survey data are combined with appliance ownership and appliance power ratings.
- Two modelling approaches were implemented to model the occupant energy-related activities: in the first, the occupant activity profiles from the DTUS were used directly, while in the second, the probabilities of starting time and duration of the occupant activities were used to reconstruct a pattern of occupant activities.
- The modelled daily profile of electricity use was compared with three measured datasets of varying sizes and from different parts of Denmark and it was shown that the detailed shape of the load profile was captured and there were high correlations between the modelled and measured profiles.
- A realistic daily electricity load profile for Danish households was obtained.

Chapter 6 Conclusions

This research was performed as part of the "EnergyLab Nordhavn – New urban energy infrastructure" project, which is a smart city research and demonstration project based in the newly developed Nordhavn district of Copenhagen, Denmark. The main hypothesis of this thesis was that:

> *"Low-energy residential buildings can be induced to operate as energy flexible elements in a district energy system."*

The thesis was divided into three main objectives, the findings of which collectively address the hypothesis. The objectives were pursued by modelling and data analysis of low-energy residential buildings and their heating systems in Denmark and specifically in the Nordhavn development.

The *first objective* was to investigate the <u>physical potential for flexible heating operation</u> of low-energy buildings, using only the inherent structural thermal mass of the buildings as storage, while maintaining thermal comfort. A dynamic model that can adequately capture transient phenomena was used. When there is surplus production of energy from renewable sources in the system, the heating set-point in the building can be increased, so that the building absorbs thermal energy in the structural thermal mass (upward flexibility event). On the other hand, when there is limited or no availability of energy from renewable sources in the energy system, the heating set-point in the building can be decreased, so that the heat supply to the buildings can be reduced or interrupted for a certain period of time, causing heat to be released to indoor air from the thermal mass of the building (downward flexibility event). An evaluation of the physically available flexibility potential was performed in terms of i) the heating energy that can be added to or withheld from the buildings for a certain period of time, ii) the number of hours that the building can remain without any heat supply without jeopardising the thermal comfort for the occupants. It was shown that buildings can remain without heat supply for many hours without jeopardising the thermal comfort of the occupants. These long hours of autonomy allow the system operators to exploit the independence of their operation. During flexibility events under moderate weather conditions of the Danish heating season, starting at 06:00 and lasting for 8 hours, the heating energy added to a low-energy apartment block was 76 Wh/m^2 and the energy withheld was 25 Wh/m^2. The low energy requirements of the buildings limit the energy that is available for withholding in each building individually, but if aggregated to a neighbourhood or district level, the amount of energy available for withholding could become considerable. When there is surplus production of energy in the system, the buildings can act as heat storage units that absorb considerable quantities of thermal energy in the structural thermal mass. The amount of energy added or withheld during a flexibility event was found to be almost proportional to the duration of the event, which indicates that the buildings have large heat capacity. Changing the time of the day that the flexibility events started mainly affected the potential for withholding, with the highest amount of energy available for withholding being during the night.

The findings showed that the physically available flexibility potential can be affected by a number of factors, including the characteristics of the building, the ambient conditions and the occupants. Focusing on the <u>thermal mass</u> of different concrete elements, it was shown that the contribution of the thermal capacity of the internal walls was higher than that of the external walls. Measurements from a custom-made set of temperature sensors cast inside the concrete walls and ceilings, at different depths from the surface to the middle of the concrete layer, confirmed that all the internal concrete layers examined could contribute to the physically available heat storage potential of the building. It was shown that the design characteristics of the building that determine its rate of heat loss to the ambient have a larger effect on the available energy flexibility. The high dependence of flexibility potential on <u>boundary conditions</u>, namely ambient temperature and solar radiation, was demonstrated, and their effect on energy was different from their the effect on thermal comfort. The amount of energy available for withholding increased during cold days, while lower temperatures

reduced the number of hours of thermal comfort after the heat supply had been interrupted. Increased solar gains led to decreased energy flexibility potential, but increased the number of hours of thermal comfort after the heat supply had been interrupted. An effect of the number of occupants and their occupancy pattern was shown: thermal comfort becomes less sensitive to any variations in the heat supply, the more occupants there are and the longer time they spend in the apartment.

Having demonstrated the physically available flexibility potential, the *second objective* was to investigate the operational flexibility potential of low-energy buildings in relation to an energy grid. In the context of the project "EnergyLab Nordhavn" and due to the very limited literature on the topic, the focus of this work was to show how the heating system of a low-energy building could be operated to meet the flexibility requirements of a given district heating grid. The market structure for heat is not as developed and transparent as it is for electricity, and it is not yet sufficiently mature to permit managed demand response. In Denmark, the heat price paid by customers is still constant across the year and fixed by individual contracts. However, dynamic heat pricing is under research and it was the scope of the present work to propose a methodology for exploiting the flexibility potential of buildings connected to the district heating grid. The requirements of the DH system were addressed based on data that were provided by the district heating utility company of Copenhagen, HOFOR A/S. The demand of the district heating system was used for rule base scheduling and the marginal heat production cost was used for cost-based scheduling of the building's heating system. One of the main achievements of this work was that it was shown that low-energy residential buildings can be operated flexibly, using the thermal mass of the buildings as short-term energy storage, so as to be able to offer flexibility services to the district heating network. Highly effective heat load shifting was achieved (between 40% and 87%) to avoid the district heating system's peak load hours, while a cost decrease of up to 15% was achieved in all the scenarios examined. These results may be obtained at the expense of adverse effects, as increasing the flexibility of the heating system operation may result in increased total energy use and new peaks in the heating load of the building. Nevertheless, higher energy use may be considered acceptable, if it costs less to be produced and can be beneficial for the environment, e.g. if it can then originate from renewable sources. The magnitude of the benefits that can be achieved depends on whether the changes in energy use are acceptable and on the level of thermal comfort required by the occupants. Providing flexibility services to the district heating system and extending its heat storage potential is essential and it would further increase the importance of the role of district heating in the flexible energy systems of the future that allow the integration of a larger proportion of energy from renewable sources.

The *third objective* of the work was to address the occupants' activities, as they play an important role for the successful implementation of flexibility strategies in residential buildings. In residential buildings there is a potential for flexible electricity loads caused by the use of domestic appliances. The occupant energy-related activities were therefore addressed in relation to household electricity loads. A model was created that links occupant energy-related activities to electricity demand. Using information collected from a large group of Danes, i.e. Danish time-use survey (DTUS) data, about the timing of household activities, in combination with statistical data on appliance ownership and power rating, a realistic daily electricity load profile for Danish households was derived, which can be used in energy flexibility modelling of dwellings. Depending on the available resources and the level of accuracy required, the parameter estimation process in the model could be adjusted to become more area- and grid-specific.

Based on the findings of this research, the structural thermal mass of low-energy buildings with its inherent thermal capacity could be added to the portfolio of solutions that provide storage in the energy system, as it was shown that low-energy buildings can be operated to provide flexibility services to the district heating energy system. The thermal behaviour of low-energy buildings, their physical and operational potential for energy flexibility, taking into consideration the relation of the building with the energy system and the occupants' activities, are considered to be a step forward in the use of low-energy buildings in future energy systems.

Chapter 7 Future research

Based on the findings of the present work and taking into account the assumptions and simplifications that had to be made, the following topics are considered worthwhile for future research:

- Use of the thermal mass of buildings in combination with other thermal storage systems at the building and district level, with appropriate prioritization strategies. In order to increase the thermal storage potential of buildings, the integration of phase change materials in the structural thermal mass of the building should be considered.

- In this work, the flexibility strategies proposed were modelled in one building. It is important to further investigate the effect of the implementation of those strategies at the district or city level. In order to avoid disturbances in the system, a smoother ramp in the temperature set-point control in the building could be adopted and/or the heat supplier could send signals that are slightly shifted in time to different categories of consumers. The specific design of the district heating system in the area and hydraulic constraints should also be considered.

- Development of flexibility strategies for domestic electricity loads, both for traditional and new loads, e.g. heat pumps, domestic appliances, electric vehicles, using the electricity load profiles developed in this work.

- The various influences that occupants have on flexibility strategies in residential buildings must be further studied. In buildings without intelligent management system, occupant thermal comfort and the range of acceptability must be pre-defined if buildings are to be operated flexibly. In buildings with intelligent management system, boundaries of occupant acceptance can be determined or predicted using historical data. Finding ways to encourage occupants to adopt flexible behaviour or to accept flexible system operation is essential. In addition, a user-friendly home management system which can provide efficient communication between the energy grid and occupants should be developed.

- Development of appropriate market structures that encourage the integration of flexibility services in the energy market. Thereafter, depending on the services that the buildings are to offer to the local energy system, appropriate control signals should be identified for the implementation of flexibility strategies in residential buildings.

References

[1] Edenhofer, O., R. Pichs-Madruga, Y. Sokona, E. Farahani, S. Kadner, K. Seyboth, A. Adler, S. B. I. Baum, P. Eickemeier, J. S. B. Kriemann, S. Schlömer, C. von Stechow, T. Zwickel, and J. C. Minx, *Climate Change 2014: Mitigation of Climate Change. Contribution of Working Group III to the Fifth Assessment Report of the Intergovernmental Panel on Climate Change*. Cambridge, United Kingdom and New York, NY, USA: Cambridge University Press, 2014.

[2] European Commission, "European Council 23-24/10/2014 - Conclusions on 2030 Climate and Energy Policy Framework," Brussels, Belgium, 2014.

[3] Danish Energy Agency, "Energiscenarier frem mod 2020, 2035 og 2050 - Energy scenarios towards 2020, 2035 and 2050," Copenhagen, Denmark (in Danish), 2014.

[4] H. Hermanns, H. Wiechmann, and E. E. Baden-w, "Future Design Challenges for Electric Energy Supply," 2009.

[5] P. Denholm and M. Hand, "Grid flexibility and storage required to achieve very high penetration of variable renewable electricity," *Energy Policy*, vol. 39, no. 3, pp. 1817–1830, 2011.

[6] P. D. Lund, J. Lindgren, J. Mikkola, and J. Salpakari, "Review of energy system flexibility measures to enable high levels of variable renewable electricity," *Renew. Sustain. Energy Rev.*, vol. 45, pp. 785–807, 2015.

[7] A. H. Mohsenian-Rad, V. W. S. Wong, J. Jatskevich, R. Schober, and A. Leon-Garcia, "Autonomous demand-side management based on game-theoretic energy consumption scheduling for the future smart grid," *IEEE Trans. Smart Grid*, vol. 1, no. 3, pp. 320–331, 2010.

[8] C. W. Gellings, "The concept of demand-side management for electric utilities," *Proc. IEEE*, vol. 73, no. 10, pp. 1468–1470, 1985.

[9] European Commission, "EU Reference Scenario 2016 - Energy, transport and GHG emissions - Trends to 2050," *Energy, transport and GHG emissions - Trends to 2050*, 2016. [Online]. Available: https://ec.europa.eu/energy/sites/ener/files/documents/ref2016_report_final-web.pdf.

[10] EnergyLab Nordhavn, "EnergyLab Nordhavn – New Urban Energy Infrastructures," 2018. [Online]. Available: http://energylabnordhavn.weebly.com/.

[11] Danish Transport and Construction Agency, "Danish Building Regulations 2015," 2015.

[12] Ministry of Transport Building and Housing, "Executive order on building regulations 2018 (BR18)," 2018. [Online]. Available: http://bygningsreglementet.dk/~/media/Br/BR-English/BR18_Executive_order_on_building_regulations_2018.pdf.

[13] Danish Energy Agency, Danish Board of District Heating, and State of Green, "District heating - Danish experiences," 2015.

[14] Ecorys and Copenhagen Resources Institute, "Resource efficiency in the building sector. Sustainable Buildings and Climate Initiative.," no. May, 2014.

[15] S. Ø. Jensen, A. Marszal-Pomianowska, R. Lollini, W. Pasut, A. Knotzer, P. Engelmann, A. Stafford, and G. Reynders, "IEA EBC Annex 67 Energy Flexible Buildings," *Energy Build.*, vol. 155, pp. 25–34, 2017.

[16] R. D'hulst, W. Labeeuw, B. Beusen, S. Claessens, G. Deconinck, and K. Vanthournout, "Demand response flexibility and flexibility potential of residential smart appliances: Experiences from large pilot test in Belgium," *Appl. Energy*, vol. 155, pp. 79–90, 2015.

[17] E. Mckenna, M. Mcmanus, S. Cooper, and M. Thomson, "Economic and environmental impact of lead-acid batteries in grid-connected domestic PV systems," *Appl. Energy*, vol. 104, pp. 239–249, 2013.

[18] M. Thomann and F. Popescu, "Estimating the effect of domestic load and renewable supply variability on battery capacity requirements for decentralized micro- grids," *Procedia - Procedia Comput. Sci.*, vol. 32, pp. 715–722, 2014.

[19] International Energy Agency (IEA), "Technology roadmap: Electric and plug-in hybrid electric vehicles," *Int. Energy Agency, Tech. Rep*, no. June, p. 52, 2011.

[20] K. O. Aduda, T. Labeodan, W. Zeiler, and G. Boxem, "Demand side flexibility coordination in office buildings: A framework and case study application," *Sustain. Cities Soc.*, vol. 29, pp. 139–158, 2017.

[21] S. O'Connell and S. Riverso, "Flexibility analysis for smart grid demand side services incorporating 2nd life EV batteries," in *2016 IEEE PES Innovative Smart Grid Technologies Conference Europe (ISGT-Europe)*, 2017.

[22] J. Heier, C. Bales, and V. Martin, "Combining thermal energy storage with buildings – a review,"

Renew. Sustain. Energy Rev., vol. 42, pp. 1305–1325, 2015.

[23] G. Masy, E. Georges, C. Verhelst, and V. Lemort, "Smart grid energy flexible buildings through the use of heat pumps and building thermal mass as energy storage in the Belgian context," *Sci. Technol. Built Environ.*, vol. 4731, pp. 800–811, 2015.

[24] F. Kuznik, D. David, K. Johannes, J. Roux, F. Kuznik, D. David, K. Johannes, and J. A. Roux, *A review on phase change materials integrated in building walls To cite this version : HAL Id : hal-00541875 A review on Phase Change Materials Integrated in Building Walls*. 2014.

[25] A. Arteconi, N. J. Hewitt, and F. Polonara, "Domestic demand-side management (DSM): Role of heat pumps and thermal energy storage (TES) systems," *Appl. Therm. Eng.*, vol. 51, no. 1–2, pp. 155–165, 2013.

[26] S. Stinner, K. Huchtemann, and D. Müller, "Quantifying the operational flexibility of building energy systems with thermal energy storages," *Appl. Energy*, vol. 181, pp. 140–154, 2016.

[27] A. De Gracia and L. F. Cabeza, "Phase change materials and thermal energy storage for buildings," *Energy Build.*, vol. 103, pp. 414–419, 2015.

[28] P. D. Lund, "Sizing and applicability considerations of solar combisystems," *Sol. Energy*, vol. 78, no. 1, pp. 59–71, 2005.

[29] A. Arteconi, N. J. Hewitt, and F. Polonara, "State of the art of thermal storage for demand-side management," *Appl. Energy*, vol. 93, pp. 371–389, 2012.

[30] H. Johra and P. Heiselberg, "Influence of internal thermal mass on the indoor thermal dynamics and integration of phase change materials in furniture for building energy storage: A review," *Renew. Sustain. Energy Rev.*, vol. 69, pp. 19–32, 2017.

[31] Y. Li and P. Xu, "Thermal Mass Design in Buildings – Heavy or Light?," *Int. J. Vent.*, vol. 5, no. 1, pp. 143–150, 2006.

[32] J. A. Orosa and A. C. Oliveira, "A field study on building inertia and its effects on indoor thermal environment," *Renew. Energy*, vol. 37, no. 1, pp. 89–96, 2012.

[33] T. Moffiet, D. Alterman, S. H. K. Colyvas, A. Page, and B. Moghtaderi, "A statistical study on the combined effects of wall thermal mass and thermal resistance on internal air temperatures," *J. Build. Phys.*, vol. 38, no. 5, pp. 419–443, 2014.

[34] L.-S. Wang, P. Ma, E. Hu, D. Giza-Sisson, G. Mueller, and N. Guo, "A study of building envelope and thermal mass requirements for achieving thermal autonomy in an office building," *Energy Build.*, vol. 78, pp. 79–88, 2014.

[35] B. Givoni, "Effectiveness of mass and night ventilation in lowering the indoor daytime temperatures. Part I: 1993 experimental periods," *Energy Build.*, vol. 28, no. 4, pp. 25–32, 1998.

[36] N. Artmann, H. Manz, and P. Heiselberg, "Climatic potential for passive cooling of buildings by night-time ventilation in Europe," *Appl. Energy*, vol. 84, no. 2, pp. 187–201, 2007.

[37] P. Blondeau, M. Spérandio, and F. Allard, "Night ventilation for building cooling in summer," *Sol. Energy*, vol. 61, no. 5, pp. 327–335, 1997.

[38] D. M. Burch, D. F. Krintz, and R. S. Spain, "The effect of Wall Mass on Winter Heating Loads and Indoor Comfort – An experimental study," *ASHRAE Trans.*, vol. 90, no. 2, 1984.

[39] L. A. Bellamy and D. W. Mackenzie, "Thermal performance of buildings with heavy walls," *BRANZ Study Report No.108*. pp. 1–45, 2001.

[40] B. Österlind, "Effektbegränsning av fjärrvärme: Försök med centraliserad styrning av abonnenternas effektuttag," Byggforskningsrådet, ISBN 91-50-3714, 1982.

[41] K. Foteinaki, A. Heller, and C. Rode, "Modeling energy flexibility of low energy buildings utilizing thermal mass," in *Proceedings of IAQVEC*, 2016.

[42] K. Foteinaki, R. Li, A. Heller, and C. Rode, "Heating system energy flexibility of low-energy residential buildings," *Energy Build.*, vol. 180, pp. 95–108, 2018.

[43] J. Kensby, A. Trüschel, and J.-O. Dalenbäck, "Potential of residential buildings as thermal energy storage in district heating systems – Results from a pilot test," *Appl. Energy*, vol. 137, pp. 773–781, 2015.

[44] J. Le Dréau and P. Heiselberg, "Energy flexibility of residential buildings using short term heat storage in the thermal mass," *Energy*, vol. 111, pp. 991–1002, 2016.

[45] G. Reynders, T. Nuytten, and D. Saelens, "Potential of structural thermal mass for demand-side management in dwellings," *Build. Environ.*, vol. 64, pp. 187–199, 2013.

[46] G. Reynders, J. Diriken, and D. Saelens, "Generic characterization method for energy flexibility: Applied to structural thermal storage in residential buildings," *Appl. Energy*, vol. 198, pp. 192–202, 2017.

[47] H. Wolisz, H. Harb, and P. Matthes, "Dynamic simulation of thermal capacity and charging/discharging

performance for sensible heat storage in building wall mass," in *Proceedings of IBPSA*, 2013.

[48]   H. Wolisz, P. Block, R. Streblow, and D. Müller, "Dynamic activation of structural thermal mass in a multizonal building with due regard to thermal comfort," *14th Int. Conf. IBPSA - Build. Simul. 2015, BS 2015, Conf. Proc.*, pp. 1291–1297, 2015.

[49]   D. Six, J. Desmedt, J. V. A. N. Bael, and D. Vanhoudt, "Exploring the Flexibility Potential of Residential Heat Pumps," *21st Int. Conf. Electr. Distrib.*, no. 0442, pp. 6–9, 2011.

[50]   B. Favre and B. Peuportier, "Application of dynamic programming to study load shifting in buildings," *Energy Build.*, vol. 82, pp. 57–64, 2014.

[51]   S. Kärkkäinen, K. Sipilä, L. Pirvola, J. Esterinen, E. Eriksson, and S. Soikkeli, "Demand side management of the district heating systems." Research Notes 2247, Espoo, p. 95, 2003.

[52]   S. Karjalainen, "Thermal comfort and use of thermostats in Finnish homes and offices," *Build. Environ.*, vol. 44, no. 6, pp. 1237–1245, Jun. 2009.

[53]   R. Li, G. Dane, C. Finck, and W. Zeiler, "Are building users prepared for energy flexible buildings?—A large-scale survey in the Netherlands," *Appl. Energy*, vol. 203, pp. 623–634, 2017.

[54]   C. Evens and S. Kärkkäinen, "Pricing models and mechanisms for the promotion of demand side integration," p. 58, 2009.

[55]   H. Lund, A. N. Andersen, P. A. Østergaard, B. V. Mathiesen, and D. Connolly, "From electricity smart grids to smart energy systems - A market operation based approach and understanding," *Energy*, vol. 42, no. 1, pp. 96–102, 2012.

[56]   H. Lund, P. A. Østergaard, D. Connolly, I. Ridjan, B. V. Mathiesen, F. Hvelplund, J. Z. Thellufsen, and P. Sorknæs, "Energy Storage and Smart Energy Systems," *Int. J. Sustain. Energy Plan. Manag.*, vol. 11, pp. 3–14, 2016.

[57]   M. Münster, P. E. Morthorst, H. V. Larsen, L. Bregnbæk, J. Werling, H. H. Lindboe, and H. Ravn, "The role of district heating in the future Danish energy system," *Energy*, vol. 48, no. 1, pp. 47–55, 2012.

[58]   T. Nuytten, B. Claessens, K. Paredis, J. Van Bael, and D. Six, "Flexibility of a combined heat and power system with thermal energy storage for district heating," *Appl. Energy*, vol. 104, pp. 583–591, 2013.

[59]   H. Cai, C. Ziras, S. You, R. Li, K. Honoré, and H. W. Bindner, "Demand side management in urban district heating networks," *Appl. Energy*, vol. 230, no. November, pp. 506–518, 2018.

[60]   N. J. Hewitt, "Heat pumps and energy storage - The challenges of implementation," *Appl. Energy*, vol. 89, no. 1, pp. 37–44, 2012.

[61]   D. Patteeuw, G. Reynders, K. Bruninx, C. Protopapadaki, E. Delarue, W. D'haeseleer, D. Saelens, and L. Helsen, "CO2-abatement cost of residential heat pumps with active demand response: Demand- and supply-side effects," *Appl. Energy*, vol. 156, pp. 490–501, 2015.

[62]   L. Schibuola, M. Scarpa, and C. Tambani, "Demand response management by means of heat pumps controlled via real time pricing," *Energy Build.*, vol. 90, pp. 15–28, 2015.

[63]   T. Q. Péan, J. Salom, and J. Ortiz, "Potential and optimization of a price-based control strategy for improving energy flexibility in Mediterranean buildings," *Energy Procedia*, vol. 122, pp. 463–468, 2017.

[64]   E. Nyholm, S. Puranik, É. Mata, M. Odenberger, and F. Johnsson, "Demand response potential of electrical space heating in Swedish single-family dwellings," *Build. Environ.*, vol. 96, pp. 270–282, 2016.

[65]   M. Åberg, L. Fälting, and A. Forssell, "Is Swedish district heating operating on an integrated market? - Differences in pricing, price convergence, and marketing strategy between public and private district heating companies," *Energy Policy*, vol. 90, pp. 222–232, 2016.

[66]   H. Li, Q. Sun, Q. Zhang, and F. Wallin, "A review of the pricing mechanisms for district heating systems," *Renew. Sustain. Energy Rev.*, vol. 42, pp. 56–65, 2015.

[67]   J. Song, F. Wallin, and H. Li, "District heating cost fluctuation caused by price model shift," *Appl. Energy*, vol. 194, pp. 715–724, 2017.

[68]   F. Wernstedt, P. Davidsson, and C. Johansson, "Demand side management in district heating systems," *Proc. 6th Int. Jt. Conf. Auton. agents multiagent Syst. - AAMAS '07*, vol. 5, p. 1, 2007.

[69]   C. Johansson, F. Wernstedt, and P. Davidsson, "Deployment of Agent Based Load Control in District Heating Systems," *First Int. Work. Agent Technol. Energy Syst. (ATES 2010)*, pp. 75–82, 2010.

[70]   D. Basciotti and R.-R. Schmidt, "Demand side management in district heating networks: Simulation Case Study on Load Shifting," *Euro Heat Power*, vol. 10, pp. 43–46, 2013.

[71]   D. F. Dominković, P. Gianniou, M. Münster, A. Heller, and C. Rode, "Utilizing thermal building mass for storage in district heating systems: Combined building level simulations and system level optimization," *Energy*, vol. 153, pp. 949–966, 2018.

[72]   T. Sweetnam, C. Spataru, M. Barrett, and E. Carter, "Domestic demand-side response on district

heating networks," *Build. Res. Inf.*, vol. 0, no. 0, pp. 1–14, 2018.

[73]   J. Van Deventer, J. Gustafsson, and J. Delsing, "Controlling district heating load through prices," *2011 IEEE Int. Syst. Conf. SysCon 2011 - Proc.*, pp. 461–465, 2011.

[74]   Danish Energy Agency, "Regulation and planning of district heating in Denmark." Danish Ministry of Energy, Utilities and Climate and COWI A/S, p. 27, 2015.

[75]   Energistyrelsen, "Energistatistik 2016, Data, tabeller, statistikker og kort," Copenhagen, 2017.

[76]   "Varmelast.dk," 2018. [Online]. Available: http://varmelast.dk/en.

[77]   Y. Zhang, X. Bai, F. P. Mills, and J. C. V. Pezzey, "Rethinking the role of occupant behavior in building energy performance: A review," *Energy Build.*, vol. 172, pp. 279–294, 2018.

[78]   I. EBCP, "Final Report Annex 53. Total energy use in buildings Analysis and evaluation methods," 2016.

[79]   E. Marshall, J. K. Steinberger, V. Dupont, and T. J. Foxon, "Combining Energy Efficiency Measure Approaches and Occupancy Patterns in Building Modelling in the UK Residential Context," *Energy Build.*, vol. 111, pp. 98–108, 2015.

[80]   A. Al-Mumin, O. Khattab, and G. Sridhar, "Occupants' behavior and activity patterns influencing the energy consumption in the Kuwaiti residences," *Energy Build.*, vol. 35, no. 6, pp. 549–559, 2003.

[81]   C. B. A. Kobus, E. A. M. Klaassen, R. Mugge, and J. P. L. Schoormans, "A real-life assessment on the effect of smart appliances for shifting households' electricity demand," *Appl. Energy*, vol. 147, pp. 335–343, 2015.

[82]   F. Karlsson, P. Rohdin, and M. L. Persson, "Measured and predicted energy demand of a low energy building: Important aspects when using building energy simulation," *Build. Serv. Eng. Res. Technol.*, vol. 28, no. 3, pp. 223–235, 2007.

[83]   C. Isaksson and F. Karlsson, "Indoor climate in low-energy houses-an interdisciplinary investigation," *Build. Environ.*, vol. 41, no. 12, pp. 1678–1690, 2006.

[84]   J. Widén and E. Wäckelgård, "A high-resolution stochastic model of domestic activity patterns and electricity demand," *Appl. Energy*, vol. 87, no. 6, pp. 1880–1892, 2010.

[85]   S. Firth, K. Lomas, A. Wright, and R. Wall, "Identifying trends in the use of domestic appliances from household electricity consumption measurements," *Energy Build.*, vol. 40, no. 5, pp. 926–936, 2008.

[86]   A. Marszal-Pomianowska, P. Heiselberg, and O. Kalyanova Larsen, "Household electricity demand profiles - A high-resolution load model to facilitate modelling of energy flexible buildings," *Energy*, vol. 103, pp. 487–501, 2016.

[87]   J. Widén, M. Lundh, I. Vassileva, E. Dahlquist, K. Ellegård, and E. Wäckelgård, "Constructing load profiles for household electricity and hot water from time-use data-Modelling approach and validation," *Energy Build.*, vol. 41, no. 7, pp. 753–768, 2009.

[88]   J. Torriti, "Understanding the timing of energy demand through time use data: Time of the day dependence of social practices," *Energy Res. Soc. Sci.*, vol. 25, pp. 37–47, 2017.

[89]   U. Wilke, F. Haldi, J. L. Scartezzini, and D. Robinson, "A bottom-up stochastic model to predict building occupants' time-dependent activities," *Build. Environ.*, vol. 60, pp. 254–264, 2013.

[90]   G. Buttitta, W. Turner, and D. Finn, "Clustering of Household Occupancy Profiles for Archetype Building Models," *Energy Procedia*, vol. 111, no. September 2016, pp. 161–170, 2017.

[91]   I. Richardson, M. Thomson, and D. Infield, "A high-resolution domestic building occupancy model for energy demand simulations," *Energy Build.*, vol. 40, no. 8, pp. 1560–1566, 2008.

[92]   D. Aerts, J. Minnen, I. Glorieux, I. Wouters, and F. Descamps, "A method for the identification and modelling of realistic domestic occupancy sequences for building energy demand simulations and peer comparison," *Build. Environ.*, vol. 75, pp. 67–78, 2014.

[93]   V. M. Barthelmes, R. Li, R. K. Andersen, W. Bahnfleth, S. P. Corgnati, and C. Rode, "Profiling Occupant Behaviour in Danish Dwellings using Time Use Survey Data," *Energy Build.*, vol. 177, pp. 329–340, 2018.

[94]   I. Richardson, M. Thomson, D. Infield, and C. Clifford, "Domestic electricity use: A high-resolution energy demand model," *Energy Build.*, vol. 42, no. 10, pp. 1878–1887, 2010.

[95]   D. Fischer, A. Härtl, and B. Wille-Haussmann, "Model for electric load profiles with high time resolution for German households," *Energy Build.*, vol. 92, pp. 170–179, 2015.

[96]   J. Widén, A. M. Nilsson, and E. Wäckelgård, "A combined Markov-chain and bottom-up approach to modelling of domestic lighting demand," *Energy Build.*, vol. 41, no. 10, pp. 1001–1012, 2009.

[97]   A. Capasso, W. Grattieri, R. Lamedica, and A. Prudenzi, "Bottom-up approach to residential load modeling," *IEEE Trans. Power Syst.*, vol. 9, no. 2, pp. 957–964, 1994.

[98]   Y. S. Chiou, K. M. Carley, C. I. Davidson, and M. P. Johnson, "A high spatial resolution residential energy model based on American Time Use Survey data and the bootstrap sampling method," *Energy*

Build., vol. 43, no. 12, pp. 3528–3538, 2011.

[99] B. Yu, J. Zhang, and A. Fujiwara, "A household time-use and energy-consumption model with multiple behavioral interactions and zero consumption," *Environ. Plan. B Plan. Des.*, vol. 40, no. 2, pp. 330–349, 2013.

[100] M. Jalas and J. K. Juntunen, "Energy intensive lifestyles: Time use, the activity patterns of consumers, and related energy demands in Finland," *Ecol. Econ.*, vol. 113, pp. 51–59, 2015.

[101] A. Wang, R. Li, and S. You, "Development of a data driven approach to explore the energy flexibility potential of building clusters," *Appl. Energy*, 2018.

[102] L. Swan and V. Ugursal, "Modeling of end-use energy consumption in the residential sector: A review of modeling techniques," *Renew. Sustain. Energy Rev.*, no. 13, pp. 1819–1835, 2009.

[103] ASHRAE, *ASHRAE Handbook: Fundamentals*. 2013.

[104] M. Kavgic, A. Mavrogianni, D. Mumovic, a. Summerfield, Z. Stevanovic, and M. Djurovic-Petrovic, "A review of bottom-up building stock models for energy consumption in the residential sector," *Build. Environ.*, vol. 45, no. 7, pp. 1683–1697, 2010.

[105] DS/EN ISO 13790, "Energy performance of buildings – Calculation of energy use for space heating and cooling," *Dansk Stand.*, p. 178, 2008.

[106] P. Bacher and H. Madsen, "Identifying suitable models for the heat dynamics of buildings," *Energy Build.*, vol. 43, no. 7, pp. 1511–1522, 2011.

[107] J. H. Kämpf and D. Robinson, "A simplified thermal model to support analysis of urban resource flows," *Energy Build.*, vol. 39, no. 4, pp. 445–453, 2007.

[108] A. Tindale, "Third-order lumped-parameter simulation method," *Build. Serv. Eng. Res. Technol.*, vol. 14, no. 3, pp. 87–97, Aug. 1993.

[109] C. A. Balaras, "The role of thermal mass on the cooling load of buildings . An overview of computational methods," *Energy Build.*, vol. 24, pp. 1–10, 1996.

[110] EQUA Simulation AB, "IDA Indoor Climate and Energy - A new generation building performance simulation software," *IDA Indoor Climate and Energy*, 2018. [Online]. Available: https://www.equa.se/en/ida-ice.

[111] EQUA Simulation AB, "Validation of IDA Indoor Climate and Energy 4 . 0 with respect to CEN Standards EN 15255-2007 and EN 15265-2007," Solna, Sweden, 2010.

[112] EQUA Simulation AB, "Validation of IDA Indoor Climate and Energy 4.0 build 4 with respect to ANSI/ASHRAE Standard 140-2004," Solna, Sweden, 2010.

[113] S. Kropf and G. Zweifel, "Validation of the Building Simulation Program IDA-ICE According to CEN 13791 „ Thermal Performance of Buildings - Calculation of Internal Temperatures of a Room in Summer Without Mechanical Cooling - General Criteria and Validation Procedures "," 2001.

[114] P. Loutzenhiser, H. Manz, and G. Maxwell, "International Energy Agency's SHC Task 34 - ECBCS Annex 43 Project C: Empirical Validations of Shading / Daylighting / Load I nteractions in Building Interactions Energy Simulation Tools," 2007.

[115] A. Thavlov and H. W. Bindner, "A Heat Dynamic Model for Intelligent Heating of Buildings," *Int. J. Green Energy*, vol. 12, no. 3, pp. 240–247, Mar. 2015.

[116] DS 418, "Beregning af bygningers varmetab - Calculation of heat loss from buildings," *Dansk Stand.*, 2011.

[117] DS/EN ISO 13370, "Thermal performance of buildings – Heat transfer via the ground – Calculation methods," *Dansk Stand.*, vol. 2. udgave, 2008.

[118] EN/DS 15251, "Indoor environmental input parameters for design and assessment of energy performance of buildings addressing indoor air quality, thermal environment, lighting and acoustics," *Dansk Stand.*, p. 54, 2007.

[119] D. Fischer, T. Wolf, J. Wapler, R. Hollinger, and H. Madani, "Model-based flexibility assessment of a residential heat pump pool," *Energy*, vol. 118, pp. 853–864, 2017.

[120] P. G. Wang, M. Scharling, K. P. Nielsen, K. B. Wittchen, and C. Kern-Hansen, "Technical Report 13-19 2001 – 2010 Danish Design Reference Year - Reference Climate Dataset for Technical Dimensioning in Building , Construction and other Sectors," Copenhagen, 2013.

[121] S. Aggerholm and K. Grau, "Bygningers energibehov - Beregningsvejledning - SBi-anvisning 213," Aalborg, 2014.

[122] ARKITEMA ARCHITECTS, "Architectural drawings." Århus, Denmark, 2015.

[123] Technical University of Denmark - Department of Civil Engineering, "DTU Climate Station-Climate Data," 2018. [Online]. Available: http://climatestationdata.byg.dtu.dk.

[124] J. Babiak, M. Minarova, and B. W. Olesen, "What is the effective thickness of a thermally activated concrete slab?," in *Proceedings of CILIMA*, 2007.

[125] T. S. Larsen, R. L. Jensen, and O. Daniels, "Målinger og Analyse af Indeklima og Energiforbrug i Komforthusene," Department of Civil Engineering, Aalborg University, 2012.

[126] Q. Sun, H. Li, F. Wallin, and Q. Zhang, "Marginal costs for district heating," *Energy Procedia*, vol. 104, pp. 323–328, 2016.

[127] HOFOR A/S, "Greater Copenhagen Utility," 2018. [Online]. Available: https://www.hofor.dk.

[128] C. Sandersen and K. Honoré, "District heating flexibility – short term heat storage in buildings," EnergyLab Nordhavn Deliverables, 2018.

[129] J. Le Dréau and P. Heiselberg, "Energy flexibility of residential buildings using short term heat storage in the thermal mass," *Energy*, vol. 111, pp. 991–1002, 2016.

[130] R. Li, F. Wei, Y. Zhao, and W. Zeiler, "Implementing Occupant Behaviour in the Simulation of Building Energy Performance and Energy Flexibility: Development of Co-Simulation Framework and Case Study," *Proc. Build. Simul. 2017*, pp. 1339–1346, 2017.

[131] J. Widén, A. Molin, and K. Ellegård, "Models of domestic occupancy, activities and energy use based on time-use data: Deterministic and stochastic approaches with application to various building-related simulations," *J. Build. Perform. Simul.*, vol. 5, no. 1, pp. 27–44, 2012.

[132] J. Bonke, "Tax-reforms, normal and actual working hours and welfare in the beginning of the 20th's Denmark," *Electron. Int. J. Time Use Res.*, vol. 13, no. 1, pp. 91–108, 2016.

[133] J. Bonke and P. Fallesen, "The impact of incentives and interview methods on response quantity and quality in diary-and booklet-based surveys," *Surv. Res. Methods*, vol. 4, no. 2, pp. 91–101, 2010.

[134] A. Tureczek, P. Nielsen, and H. Madsen, "Electricity Consumption Clustering Using Smart Meter Data," *Energies*, vol. 11, no. 4, p. 859, 2018.

[135] J. K. Kristensen, "Energy management and its influence on building energy performance and indoor environment," Technical University of Denmark, 2017.

[136] Danish Energy Agency, "Elmodelbolig Statistics," 2018. [Online]. Available: http://statistic.electric-demand.dk/. [Accessed: 11-Jun-2018].

[137] I. Richardson and M. Thomson, "Domestic Electricity Demand Model – Simulation Example," 2010. [Online]. Available: https://dspace.lboro.ac.uk/2134/5786.

[138] K. Johnsen and K. Grau, "tsbi3: Computer Program for Thermal Simulation of Buildings. User's Guide." p. The Danish Building Research Institute, Denmark, 1994.

[139] European Commission, "End-use metering campaign in 400 households of the European Community." p. Project EURECO-SAVE PROGRAMME Contract N° 4.1031, 2002.

[140] Energistyrelsen, "Energistatistik 2010," 2010. [Online]. Available: http://www.b14cms.dk/users/klimakompasset.dk/www/files/pdf/Energistatistik_2010.pdf. [Accessed: 15-Oct-2015].

[141] Statistics Denmark, "Living conditions/Education and knowledge/Labour, income and wealth," 2018. [Online]. Available: http://www.statistikbanken.dk. [Accessed: 10-Jun-2018].

Appendix - Published and submitted papers

PAPER I: Foteinaki, K., Li, R., Heller, A. and Rode, C. (2018) 'Heating system energy flexibility of low-energy residential buildings', *Energy and Buildings*. Elsevier B.V. doi: 10.1016/j.enbuild.2018.09.030.

Heating system energy flexibility of low-energy residential buildings

Kyriaki Foteinaki[a],*, Rongling Li[a], Alfred Heller[b], Carsten Rode[a]

[a] Department of Civil Engineering, Technical University of Denmark, Nils Koppels Allé Building 402, 2800 Kgs. Lyngby, Denmark

[b] NIRAS, Østre Havnegade 12, 9000 Aalborg, Danmark

* Corresponding author, e-mail: kyfote@byg.dtu.dk

Abstract

Energy flexibility is proposed as a cost-effective solution facilitating secure operation of the energy system while integrating large share of renewables. With strict building regulations in Denmark, newly built buildings are low-energy buildings. In order to identify the role of low-energy buildings in the energy system, we investigated the physical potential for flexibility and analysed the thermal storage capacity existing inherently in the structural mass. Two building types were studied: single-family house and apartment block. The aim is to quantify the energy that can be added to or curtailed from each building during a time period without compromising thermal comfort. Different scenarios (starting time and duration), building design characteristics and boundary conditions were studied. The findings showed that low-energy buildings are highly robust and can remain autonomous for several hours. Although for individual buildings the available energy for curtailment is limited, if many buildings are aggregated energy flexibility becomes significant. The potential for storage in the thermal mass is considerable. The analysis presented high dependence of flexibility potential on boundary conditions (ambient temperature, solar radiation, internal gains) and underlined the importance of envelope insulation. Heat losses govern the potential for flexibility, while the walls' thermal mass has a secondary influence.

Keywords

Energy flexibility, Building thermal mass, Thermal energy storage, Low-energy building, Demand response

1 Introduction

It is anticipated that the share of renewable energy will constantly grow in the energy system. According to the European Council's climate and energy agreement from 2014, one of the three key targets for the year 2030 is that at least 27% of the European energy supply must derive from renewable energy sources (RES) [1]. Some countries have set even stricter energy frameworks; for example, Denmark aims to achieve an energy supply independent from fossil fuels by 2050 [2]. The fluctuating energy production from RES is the main challenge of power grid controllability and stability, hence

stressing the need for balancing strategies. Among others, flexible energy systems have been proposed as a cost-effective solution that would facilitate a secure operation of the energy system while integrating a large share of renewables. Methods for reducing peak loads and shifting demand have attracted great attention, such as developing appropriate markets and introducing new end use technologies for energy storage in the system [3]. Towards this direction, the building sector has great potential, as firstly buildings constitute 40% of the primary energy use in most European countries, and secondly the already existing large thermal mass in buildings can be utilized for thermal energy storage facilitating load shifting. The concept of energy flexibility of a building is not new, but has recently gained attention and was defined by IEA Energy in Buildings and Communities Program (EBC) Annex 67 "Energy Flexible Buildings" as "the ability to manage its demand and generation according to local climate conditions, user needs and grid requirements" [4]. Hence, energy flexible buildings will be able to respond to load control strategies determined by the requirements of the respective energy network [4].

Buildings consist of different types of shiftable loads requiring different control approaches, i.e. space heating and cooling, domestic hot water, charging of electric vehicles, etc. A number of studies have been performed on energy flexibility in buildings targeting one or more of the aforementioned loads of a building. Indicatively, [5] modelled household load profiles in order to investigate the flexibility potential of domestic appliances, while [6] quantified the demand response flexibility of residential smart appliances, domestic hot water buffers and electric vehicles based on a pilot test in Belgium. The heat loads in a building can be exploited by utilizing different thermal energy storage technologies available, reviewed by [7]. Those most broadly used are the inherent thermal mass of the building structure ([8],[9]), with or without the integration of phase changing materials [10],[11], and additional units such as hot water tanks ([12],[13]).

In this study the structural thermal mass of buildings will be utilized as storage medium. The thermal mass is readily available in every building, requiring one extra investment, i.e. appropriate controllers of the heating system. In existing residential buildings most often such controllers are missing. Commercial buildings and new residential buildings frequently have the heating system connected to a building/home management system, which would have to be reprogrammed to be used for flexibility measures responding to an external signal. The characteristics of each building are decisive for the characterization of the flexibility potential [14]. In principle, the parameters that generically define the operation, energy needs and performance of a building will also set the framework and boundaries for the flexibility potential. The functional typology as well as the construction age and building type are among the most important parameters to be considered [14–16]. The functional typology, i.e. residential, commercial, etc., defines the type and intensity of loads available for flexibility and the occupancy profiles in general [17]. The construction age of the building,

or renovation if relevant, defines first and foremost the properties of the thermal envelope and the installed systems [14],[16],[18].

Research so far was mainly focused on typical examples of the building stock, namely old or moderately aged buildings, as cases studies to assess the flexibility potential such as [8],[19],[20],[21],[22]. In order for the concept of energy flexibility to be used on the energy system scale and across sectors, a portfolio with different potentials and dynamics should be available including building categories offering different options of services. Regarding the new generation of buildings, there are few studies that have studied and contrasted the potential of older to newer buildings [14–16], as well as [23] which studied a refurbished apartment of multi-family Mediterranean nZEB building, and [9] which studied a low-energy single-family house in France.

According to the Danish Building Regulation 2015 (BR15), for the new generation of buildings in Denmark "the total demand of the building for energy supply for heating, ventilation, cooling and domestic hot water must not exceed 30.0 kWh/m² per year plus 1000 kWh per year divided by the heated floor area" [24]. These buildings are well-insulated, airtight and may be heavy-weight, thus have large thermal storage capacity. In this study we analyse the thermal storage capacity of buildings which exists inherently in their structural mass. Two building types of different scales are studied, a single-family house and a multi-family apartment block. The aim is to quantify the energy that can be added to or curtailed from each building at a specific time period, namely the flexibility potential, under different scenarios in order to identify the role of low-energy buildings in the future energy system. The objective is to quantify the physically available energy flexibility of this type of buildings. The economic feasibility of the utilization of this flexibility is out of the scope of this study. Emphasis is given on building design characteristics and boundary conditions. This information could be provided to an aggregator/system operator enabling them to choose a suitable portfolio of buildings to participate in grid services facilitating flexibility in the operation of the energy system.

The structure of this paper is organized as follows. Section 2 explains the approach and presents the scenarios examined. Then the simulation models of the buildings are detailed, the boundary conditions are presented, followed by the building design parameter variations. In Section 3 the results of the simulations are presented and analysed, along with discussion of the outcomes. The main conclusions are summarized in the final section.

2   Methodology

2.1   Energy flexibility events

In this section, the methodology for the evaluation of using structural thermal mass as storage medium is explained. Starting from a reference operation of the building, modulations of the temperature set-point of the heating system are performed. The inherent thermal mass is thus activated, either being charged after the air temperature set-point is increased, or being discharged after the air temperature set-point is decreased. In this study the reference operation is a typical thermostatic control with constant air temperature set-point at 22°C, which is a typical desired indoor temperature in Danish households during the heating season. Two types of modulation from the reference operation are considered:

- Increased set-point to 24°C for a certain time duration, representing a scenario with abundance of renewable energy production in the energy system. In this case, heat supply in buildings can be increased and the additional heat introduced can be stored into the thermal mass (depicted in Figure 1, left). This type of modulation is further referred to as an upward flexibility event.

- Decreased set-point to 20°C for a certain time duration, representing a scenario with limited or no availability of renewable energy production in the energy system. In this case, heat supply in buildings can be curtailed or interrupted, imposing heat to be released from the thermal mass into the building (depicted in Figure 1, right). This type of modulation is further referred to as a downward flexibility event.

In all cases, thermal comfort of occupants ought not to be compromised. The limits of comfortable conditions[1] of 22°C ±2 °C are chosen to be within the range of thermal comfort Category II "Normal level of expectations for new buildings" for heating season according to the standard EN/DS 15251 [25].

In related studies found in literature, the quantification of the flexibility potential is based on the response of a building to a signal from a specific energy system [9], [26]. The quantification is demonstrated during the operation of the building, using indicators such as energy, cost, CO_2 emissions, etc., under specific system boundary conditions. In those cases, generalization and comparability of the results is limited. [20], [14] and [16] proposed and used a generic characterization method of the thermal response of the building, mostly relevant for the design phase of a building, and this is the approach also used in this work. Exemplary responses to upward and downward flexibility events are illustrated in Figure 1, together with the main flexibility parameters evaluated in this work, equivalent to those defined in [27].

---

[1] The standard EN/DS 15251 refers to operative temperature. However, the results from the simulations showed that in these buildings, the effect of cold surfaces is very limited, so air and operative temperatures have small differences, i.e. less than 0.5°C at all times. For the sake of clarity only indoor air temperature is presented in the graphs.
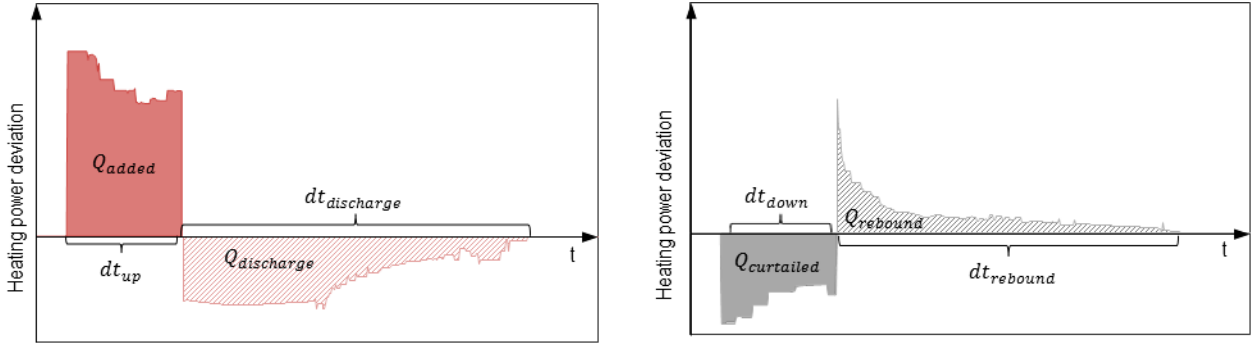
Figure 1: Exemplary responses to upward and downward flexibility events and main flexibility parameters

i) Added energy (Q_{added}): the amount of energy that is added to the building during the upward flexibility event. It is given by Equation (1): $Q_{added} = \int (q_{up} - q_{ref})dt_{up}$ (1), where:

dt_{up}: the duration of upward flexibility event, when the temperature set-point is increased to 24°C,

q_{up}: the heating power during the upward flexibility event,

q_{ref}: the heating power during the reference operation of the building with the temperature set-point at 22°C.

ii) Discharged energy ($Q_{discharge}$): the amount of energy that is utilized after being stored in the thermal mass of the building during the upward flexibility event. It is given by Equation (2):

$Q_{discharge} = \int (q_{discharge} - q_{ref}) dt_{discharge}$ (2), where:

$dt_{discharge}$: the duration of time after the end of the upward flexibility event before the heating system returns to normal operation,

$q_{discharge}$: the heating power during the discharging period.

iii) Curtailed energy ($Q_{curtailed}$): The amount of energy that is curtailed from the building during the downward flexibility event. It is given by Equation (3): $Q_{curtailed} = \int (q_{down} - q_{ref})dt_{down}$ (3), where:

dt_{down}: the duration of downward flexibility event, when the temperature set-point is decreased to 20°C,

q_{down}: the heating power during the downward flexibility event.

iv) Rebound energy ($Q_{rebound}$): the amount of energy that is additionally utilized by the building in order to return to the initial state after the downward flexibility event. It is given by Equation (4):

$Q_{rebound} = \int (q_{rebound} - q_{ref})dt_{rebound}$ (4), where:

$dt_{rebound}$: The duration of time after the end of the downward flexibility event before the heating system returns to normal operation,

$q_{rebound}$: the heating power during the rebound effect period.

Both Q [kWh] and q [W] refer to the net energy/heating power of the heat emission system, not the entire heating system, in order to avoid dependencies on the choice of the system, its configuration and the energy carrier.

By definition, the available energy that can be added to or curtailed from a building during a specific flexibility event depends on multiple parameters and is inevitably time-dependent. As the storage medium is the structural mass of the building, the characteristics of the building are of vital importance, including thermal properties, which are presented in Section 2.4. The quantification is determined during a specific flexibility event. The duration and starting time of the event are main characteristics, thus their impact is assessed. In this study, the following flexibility events are investigated:

- Flexibility events with duration 2 hours, 4 hours, 6 hours, 8 hours, 12 hours, 16 hours, and 24 hours.

- Flexibility events with starting time at midnight (00:00), early morning (06:00), midday (12:00) and evening (18:00).

Structural thermal mass, in contrast to other storage media, is particularly sensitive to boundary conditions. Ambient weather conditions are examined in this study (Section 2.3) including solar radiation and ambient air temperature.

2.2 Building models

The building regulations become progressively stricter on minimizing heat losses and increasing efficiency of heating, cooling and ventilation systems in buildings. The Danish Building Regulation 2015 (BR15) [24] introduced the new generation of buildings that will participate in the energy system. Two building types according to the BR15 standard are chosen to be studied; a single-family house (Figure 2) and an apartment block (Figure 3), both representing typical Danish buildings of its type. The design, construction and materials chosen are in accordance with BR15, the Danish Building Research Institute (SBi) Guidelines 'Energy Demand for Buildings' [28] and some details are supplemented by TABULA Webtool [18]. Both building types are heavy-weight and well insulated.
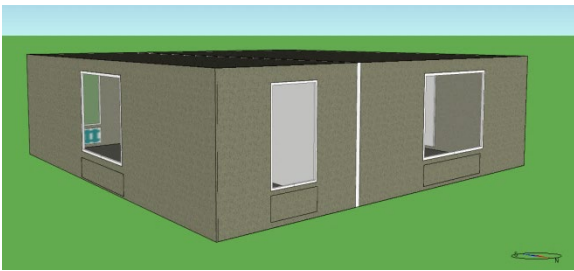
Figure 2: Single-family house model   **Figure 3: Apartment block model**
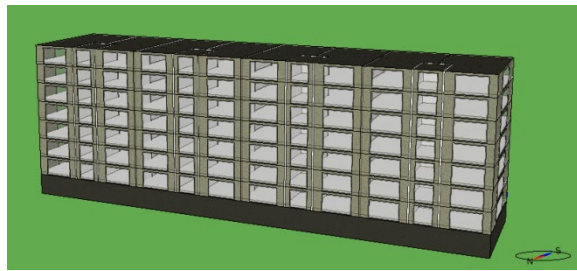
Table 1 and Table 2 present the properties of the main construction components of the single-family house and apartment block, respectively. The properties of the materials used are shown in Table 3.

Table 1: Properties of main components for single-family house

Components	Thickness [mm]	U-value [W/(m²·K)]	Surface [net m²]	Materials
External wall	448	0.138	109	Aerated concrete (100mm) Insulation class 38 (240mm) Brick (108mm)
Internal load-bearing wall	150	4.082	37	Concrete
Internal non-bearing wall	100	1.349	97	Aerated concrete
Roof	567	0.077	149	Plaster board (26mm) Scattered wooden boards (22mm) Insulation class 38 (460mm) Roof tiles (59mm)
Floor	472	0.105	149	Oak planks (22mm) Concrete (100mm) Insulation class 38 (350mm)
Windows	3 pane glazing	0.900	34	-

Table 2: Properties of main components for apartment block

Components	Thickness [mm]	U-value [W/(m²·K)]	Surface [net m²]	Materials
External wall	448	0.138	1726	Aerated concrete (100mm) Insulation class 38 (240mm) Brick (108mm)
Internal load-bearing wall	200	3.704	2779	Concrete
Internal non-bearing wall	100	1.349	1921	Aerated concrete
Roof	670	0.092	980	Hollow core concrete (270mm) Insulation class 38 (400mm)
Floor towards ground	470	0.106	980	Concrete (120mm) Insulation class 38 (350mm)
Floor/ceiling decks	407	0.348	6860	Oak planks (14mm) Concrete (80mm) Insulation class 38 (93mm) Concrete (220mm)
Windows	3 pane glazing	0.900	1408	-

Table 3: Material properties

Material properties	Thermal conductivity [W/(m·K)]	Density [kg/m³]	Specific heat [J/(kg·K)]
Aerated concrete	0.175	650	900
Concrete	2.000	2300	900
Brick	0.730	1800	840
Insulation class 38	0.038	20	750
Gypsum board	0.220	970	1090
Oak planks	0.170	750	2000
Roof tiles	0.840	1900	800
Hollow core concrete (40% hollow core)	1.600	1380	900
Furniture	0.130	1000	1300

The single-family house has a net heated floor area of 149 m^2 and envelope area per volume 0.998 m^2/m^3. The effective thermal capacity is calculated 60 MJ/K (see Appendix for the detailed calculation) and the heat losses, which are received as output from the simulation tool, are 101 W/K. The ratio of those two leads to a time constant of 165 hours. The single-family house model is divided into two thermal zones: a primarily day-occupied zone, i.e. living room, kitchen, and a primarily night-occupied zone, i.e. bedrooms. The windows comprise 22.5% of the heated floor area and are distributed 41% south, 26% north and 33% east/west following the reference single-family house of BR15.

The apartment block has a net heated floor area of 6272 m^2 and envelope area per volume 0.265 m^2/m^3. The effective thermal capacity is calculated 2908 MJ/K and the heat losses are 3084 W/K, leading to a time constant of 262 hours. The building has 7 floors and an unheated basement, which is assumed to be around 15°C, maintained from heat losses of hot water pipes. Each floor has 8 apartments with the same floor area of 112 m^2 each, and 4 staircases with the same floor area of 21 m^2 each. The windows comprise 22.5% of the heated floor area and are distributed 52% south, 37% north and 11% east/west. The apartment block was modelled as one thermal zone per apartment and one thermal zone per staircase, using adequate zone multiplication of the zones that present similar thermal behaviour.

In this study only space heating is considered, as the objective of the work is to evaluate the storage capacity of the inherent thermal mass of the building structure. The heat emission system in both buildings is low temperature water radiators dimensioned according to the standard DS 418 [29] for indoor temperature 20°C and outdoor temperature -12°C, using an over-dimensioning factor of 15%. The maximum heating power of the radiators is 21 W/m^2 heated floor area for the single-family house and 14 W/m^2 heated floor area for the apartment block, both controlled with proportional controller. The supply water temperature to the system is 45 °C. Mechanical ventilation is installed in the buildings with constant air volume of 0.3 l/s per m^2 of heated floor area, using heat recovery of 80% efficiency for the single-family house and 67% for the apartment block[2], according to BR15. Minimal infiltration is considered as 1.5 l/s per m^2 of the heated floor area at a pressure differential of 50 Pa. A very low effect of structural thermal bridging is considered, about 0.02 W/K per m^2 envelope. Internal masses are included in the models to represent furniture, with a total area of 26 m^2 in the single-family house and 1120 m^2 in the apartment block. The furniture is assumed to have the properties shown in Table 3 with thickness of 10 mm and convective heat transfer coefficient of 6 W/m^{2}K. The ground model is calculated in the simulation tool according to the standard ISO 13370 [30].

---

[2] When this study was finished, the new building regulation 2018 (BR18) was published. The only difference in the new regulation is the efficiency of heat recovery of the ventilation system for apartment blocks, which, in the new code, is the same as the single-family house, namely 80%. If the simulations were run according to BR18, the only difference in the results would be the heating demand for the apartment block, which would slightly decrease.

The simulations are performed with the building performance simulation software IDA Indoor Climate and Energy, version 4.7 [31]. It is a dynamic whole-building simulation tool based on symbolic equations stated in Neutral Modeling Format (NMF) and has undergone several validation tests [32–36]. The building, systems, controls, network airflow, etc. are simulated in an integrated way and the time-step varies dynamically during runtime to automatically adapt to the nature of the problem.

2.3   Boundary conditions

The performance of the structural thermal mass as a storage medium is highly dependent on boundary conditions. Regarding the ambient weather conditions, in this study representative days of the heating season in Denmark are chosen for cold, moderate and warm days. The weather data used are from the Danish Meteorological Institute representing the Danish Design Reference Year [37]. Solar radiation is also considered, so simulations run both with cloudy and clear sky. Figure 4 presents the ambient air temperature and global solar irradiance used in the simulations for cold, moderate and warm days with cloudy and clear sky. Each simulation runs for four days; one day prior to the day when set-point modulation is performed and two days after that. Before each simulation, a dynamic start-up phase of one month is simulated in order to eliminate the effect of initial conditions.
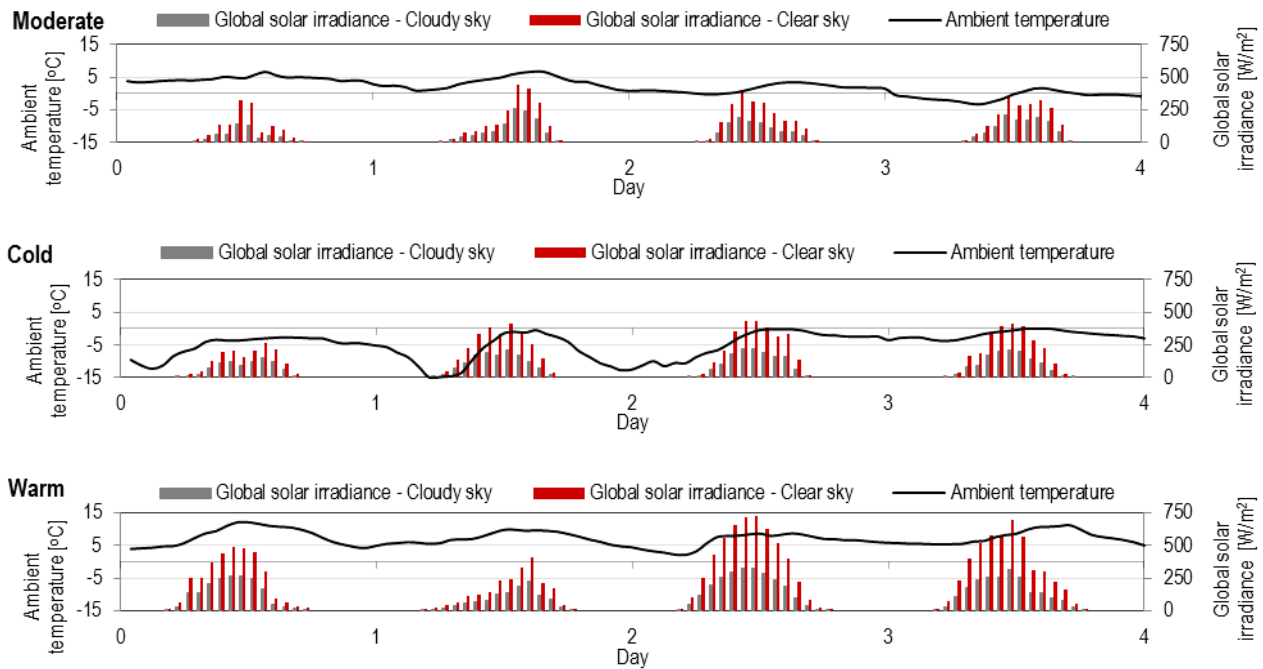
Figure 4: Ambient air temperature and global solar irradiance for representative moderate (top), cold (middle) and warm (bottom) days of the heating season with cloudy and clear sky

The schedules for the internal gains are set according to the standard DS/EN ISO 13790:2008 Table G.8 [38], which are different for primarily day or night occupied zones. The internal heat gains include heat emitted from lighting, equipment

and occupants. In the single-family house there are two thermal zones, each with the respective schedule for internal gains, while in the apartment block, which is modelled as one thermal zone per apartment, two components of internal gains are used in the same zone, one for each schedule. Figure 5 shows the ratio of internal gains compared to the maximum internal gains for every hour of the day. The total heat flow rate from internal gains is 5 W/m^2, which is lower than the one indicated by the standard [38], but it is adjusted in order to meet the average Danish national values [28].
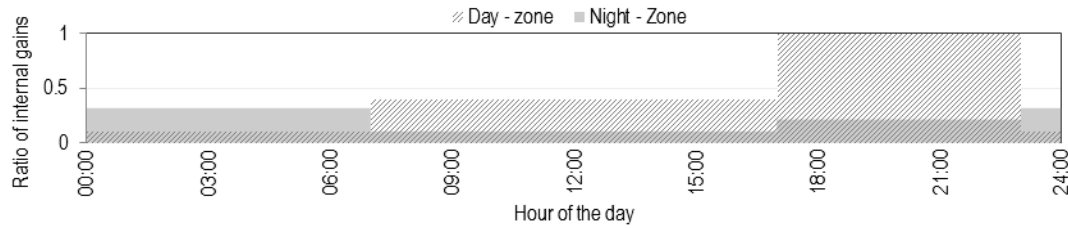
Figure 5: Schedules for internal gains in the primarily day-occupied and night-occupied zone

2.4 Building design parameter variations

Since the storage medium is the structural thermal mass, the design parameters of external and internal walls are influential parameters in the quantification of the indicator, as also underlined by [9],[14],[20],[39]. Certain parameters are chosen to be studied, in order to examine the relative impact of each design parameter choice. The range of each parameter used is presented in Table 4. The baseline building case is presented with bold font for each parameter.

Table 4: Building design parameter variations

Parameter	Range				
Window U-Value [W/m²K]	1.8	1.5	1.2	**0.9**	0.6
External Wall Insulation Thickness [cm]	16	20	**24**	28	32
External Wall Concrete Thickness[3] [cm]	0[4]	5	**10**	15	20
Internal[5] Wall Concrete Thickness [cm]	5[6]	10	**15**	**20**[7]	25
Windows / Heated Floor Area Ratio [-]	12.5%	17.5%	**22.5%**	27.5%	32.5%

The aim of the parameter study is to examine two properties of the thermal mass: the heat losses to the ambient and the thermal capacity of the thermal mass, in order to contrast their contribution to the amount of energy that can be added to or curtailed from the buildings during flexibility events. To examine the effect of the heat losses, the window U-value and the

---

[3] Inside of the insulation layer

[4] The external wall with 0 cm concrete represents a wall with thermal insulation on the interior surface.

[5] Internal load-bearing walls are considered in the variation

[6] Buildings with this variation belong to the category of semi-light buildings according to the Danish Building Research Institute (SBi) Guidelines 'Energy Demand for Buildings' [27].

[7] The value for the baseline building case for the Internal Wall Concrete Thickness is 15cm for the single-family house and 20cm for the apartment block.

external wall insulation thickness are studied while keeping the thermal capacity of thermal mass unaltered. To study the effect of the thermal capacity, the external wall concrete thickness is adjusted, with the insulation thickness being adjusted accordingly to ensure that the heat losses to the ambient remained unaltered. Similarly, the effect of the thermal capacity of internal thermal mass is studied with variations of the internal load-bearing wall concrete thickness. When changing the window to heated floor area ratio, the effect is rather complicated as both the capacity of thermal mass and the heat losses change, while simultaneously the solar gains are affected.

3   Results and Discussion

In this section, the results of the simulations are presented and discussed. In Section 3.1, the operation of the buildings is presented under reference conditions with the temperature set-point constantly at 22°C, in order to briefly demonstrate the energy performance of this type of buildings and provide a better insight of the respective thermal behaviour. In Section 3.2.1 the results for the chosen base case flexibility events implemented to the buildings are presented, one upward and one downward, and the thermal behaviour of the buildings is analysed. Flexibility events with different duration and start time are presented in Section 3.2.2. The analysis of the impact of dynamic boundary conditions is detailed in Section 3.3. In Section 3.4, the influence of building design parameters on energy flexibility is presented.

3.1   Heating demand under reference operation

This section presents the reference operation of the buildings with constant temperature set-point at 22°C during the heating season (November-March). The peak demand for space heating for the single-family house was 2.5 kW (16.8 W/m^2) and the space heating energy use was 21 kWh/m^2 net heated floor area. Figure 6 presents the heat introduced into the house, categorized into heat coming from the heating system, internal gains (occupants, equipment and lighting) and solar gains. For the single-family house 48% of the heating needs were supplied from the heating system. The other half came from solar and internal heat gains, which contributed with 11% and 41% respectively. This distribution should be taken into consideration when implementing flexibility events to new buildings. On the one hand, the thermal comfort would be less sensitive to any variations in the heat supply, while on the other hand, the influence of uncontrollable factors such as solar and internal gains should be taken into consideration.
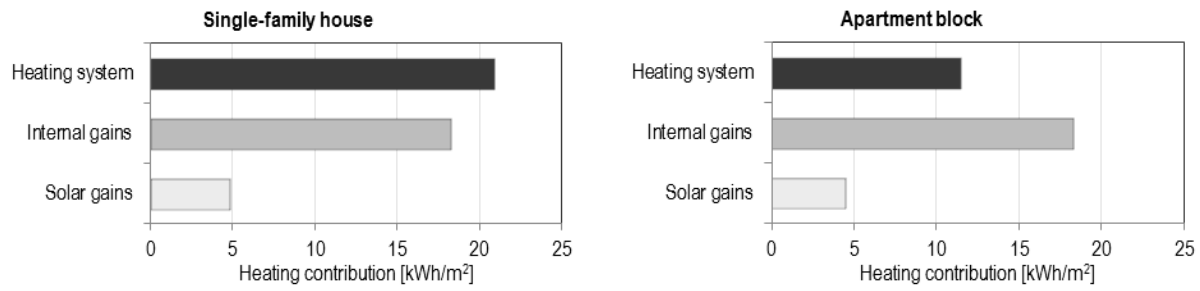
Figure 6: Analysis of heating contribution during reference operation with temperature set-point at 22°C for the single-family house (left) and the apartment block (right)

For the reference operation of the apartment block, the peak demand for space heating was 82 kW (13.1 W/m^2) and the space heating energy use was 12 kWh/m^2 net heated floor area. The apartment block had lower energy use for space heating in comparison to the single-family house, since the ratio of the envelope area per volume is significantly lower. As depicted in Figure 6, the heat sources in the apartment block had partly different contributions compared to those of the single-family house. The internal gains in the apartment were of the same schedule and intensity as in the single-family house, but the percentage contribution was higher, covering a total of 53% of the building space heating needs. The solar gains were marginally lower in the apartment than in the single-family house, but the percentage contribution was a little higher (13%). Thereby, the contribution of the heating system was limited to 34% of the total heating needs of the apartment.

3.2   Energy flexibility

3.2.1   Base case energy flexibility

In this section, two base case flexibility events are presented, one upward and one downward. The implemented events started at 06:00, had duration of 8 hours and were performed under ambient weather conditions of moderate winter days in Denmark with cloudy sky as depicted in Figure 4 (top). Consistent colour code is used for the figures as follows: red refers to upward flexibility events, grey to downward flexibility events, and blue to the reference operation. Figure 7 and Figure 8 present results of the single-family house and the apartment block, respectively, with the heating power (top) and indoor air temperature (bottom) during the base case flexibility events. During Day 1, the buildings are under the reference operation and the heating power is depicted with a solid blue curve. In Day 2, the modulations of the base case flexibility events are implemented, with the respective added/curtailed heating power being highlighted in the figures, and the effects are observed onwards.
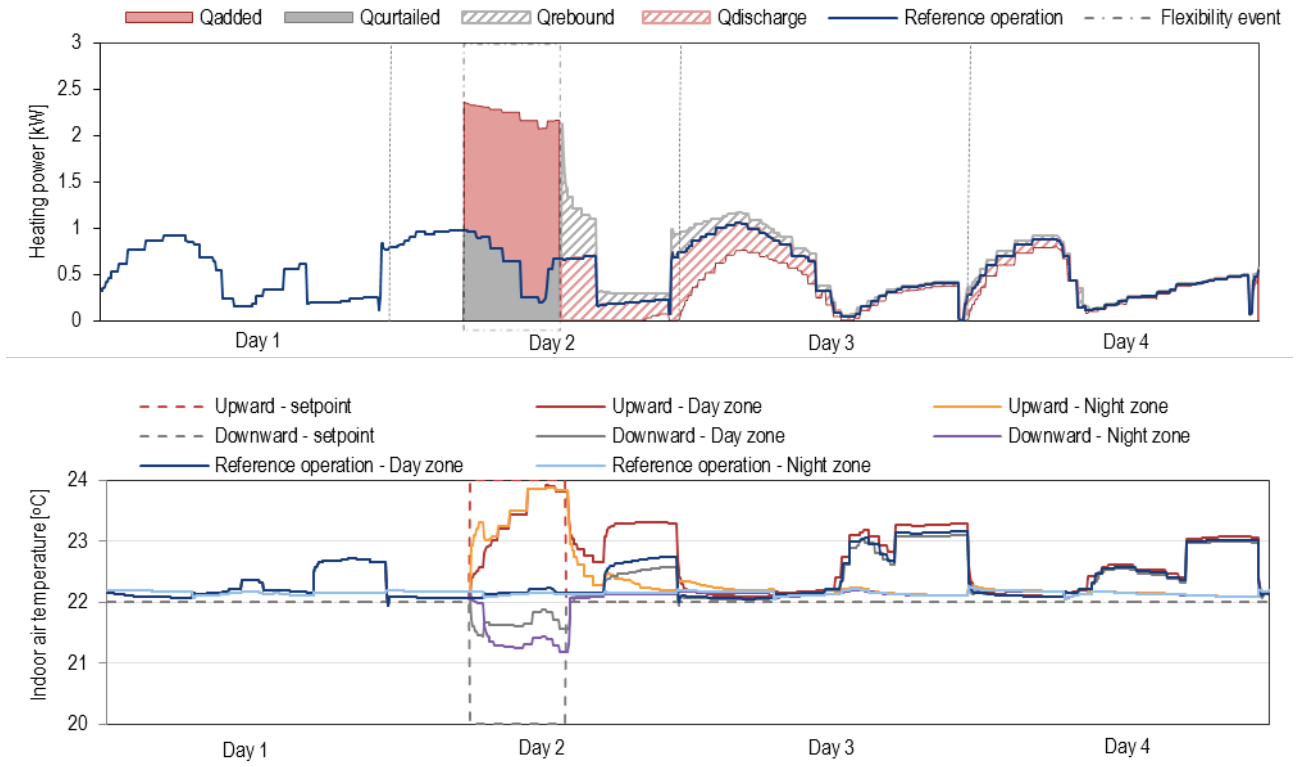
Figure 7: Heating power (top) and indoor air temperature (bottom) during base case flexibility events for the single-family house

For the single-family house, during the upward flexibility event, there was a considerable increase in heating power, which was followed by 10 hours during which the heat supply was eliminated. For approximately 40 hours after the event, the energy supply from the heating system was lower than the one of the reference operation, since energy was discharged from the thermal mass. For the downward flexibility event, the heat supply was interrupted completely during the event. The event was followed by a peak, which lasted approximately 3 hours. It was expected that utilization of flexibility results in increased peaks for the heating system. Although it was not the focus of this study, implications on the heating system, such as the new heating peaks created, should be taken into consideration when utilizing the flexibility [40]. For approximately 20 hours after the event, the energy use was slightly higher than the one of the reference operation (rebound effect). The bottom graph of Figure 7 shows the indoor air temperatures of the two zones. The temperature set-points are presented with the dashed lines. Regarding the upward event, the set-point of 24°C was reached after approximately 5 hours in both zones. When decreasing the set-point to 20°C, the temperature decrease was rather slow. Within the 8 hour duration of the event, the temperature dropped to minima of 21.5°C and 21.3°C in the day and night zone, respectively. In all cases, the impact of the internal gains was apparent; every day in the evening when internal gains peaked in the day zone, the air temperature increased by almost 1°C, while the energy use was relatively low. It can be also noticed that every day around midday the energy use decreased due to the existence of solar gains, even on a cloudy day.
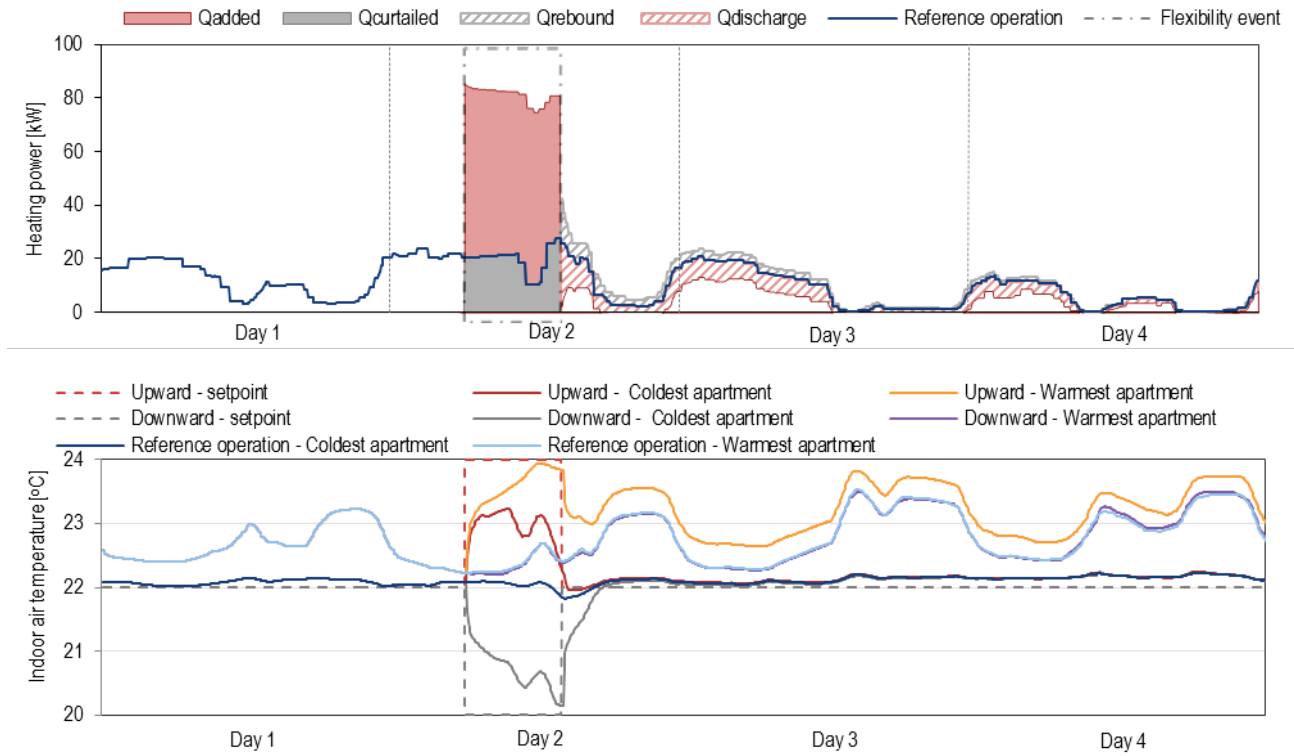
Figure 8: Heating power (top) and indoor air temperature (bottom) during base case flexibility events for the apartment block

Regarding the apartment block (Figure 8), the thermal behaviour was similar to the one of the single-family house. The indoor air temperatures depicted were those from the apartments considered as critical, with a middle apartment on the 3rd floor being the warmest and a top corner apartment being the coldest. The two apartments have considerably different thermal environments. The warmest apartment was insignificantly affected by the changes in the set-points, thereby any potential changes in the heat supply. It can be also noticed that the temperature in this apartment was constantly higher than the set-point of 22°C. In the apartment block there are more apartments of the warmer type, so the apartment block is mostly affected by this behaviour. This explains why the peak created due to the rebound effect after the downward flexibility event was relatively small. This thermal behaviour indicates that overheating might be an issue for this type of apartments, especially under milder ambient weather conditions. In the coldest apartment, the temperature decreased at a faster pace compared to the single-family house, dropping close to 20°C at the end of the downward flexibility event. On the other hand, during the upward flexibility event, the indoor air temperature did not manage to increase higher than 23.2°C. An important diversity between the thermal behaviour of the two apartments is noted. Since the same modulation was implemented for the entire apartment block, the thermal comfort of all apartments needed to be considered. Another approach could be to apply different flexibility modulations in different types of apartments, which could lead to higher potential for flexibility, but this was not implemented in this study.

The total amount of energy supplied for the four days to the single-family house was 751 Wh/m² for the reference operation, 771 Wh/m² for the upward flexibility and 751 Wh/m² for the downward flexibility. For the apartment block the total energy supplied was 339 Wh/m² for the reference operation, 375 Wh/m² for the upward flexibility and 324 Wh/m² for the downward flexibility. In this case the upward flexibility events led to increased energy use, namely 2.7% for the single-family house and 10.6% for the apartment block, while the downward flexibility events led to the same energy use for the single-family house, but decreased energy use by 4.4% for the apartment block. The apartment block used considerably less energy per square meter than the single-family house, as the ratio of the envelope area per volume of the apartment block (0.265 m²/m³) is considerably lower than the one for the single-family house (0.998 m²/m³). The small energy needs together with the small heat loss are the reasons why the apartment block performs as an efficient energy storage body.

Summing the energy that was additionally introduced (Q_{added}) or curtailed ($Q_{curtailed}$), during the flexibility events the results are presented with a bar in Figure 9, with red being the additional energy and grey being the curtailed energy.
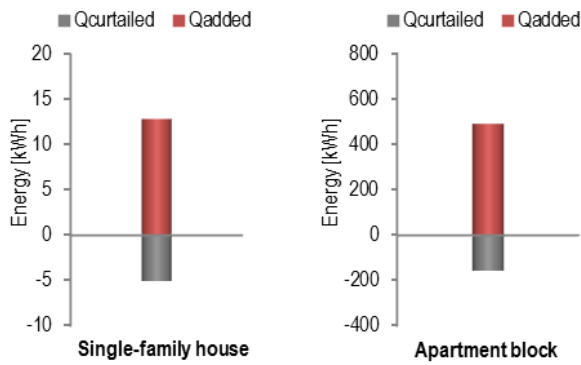
Figure 9: Energy added/curtailed during upward/downward flexibility events for the single-family house (left) and the apartment block (right)

In the single-family house (Figure 9, left) 13 kWh (87 Wh/m²) were additionally added during 8 hours, while 5 kWh (36 Wh/m²) were curtailed during 8 hours. In the apartment block (Figure 9, right) 492 kWh (78 Wh/m²) were additionally added during 8 hours, while 156 kWh (25 Wh/m²) were curtailed during 8 hours. A clear asymmetry between the added and the curtailed energy is noticed in both buildings. As previously shown, the heat supply was eliminated during the downward event. This means that the amount of available energy to be curtailed is determined by the heating need of the reference scenario (22°C). Hence, the maximum energy available for curtailment is highly related to the heating demand of the buildings during normal operation; thereby, for low-energy buildings the potential for curtailment is limited. On the other hand, the maximum energy that can be added is limited either by the capacity of the heating system or by the upper thermal comfort limit, in this study 24°C.

As already mentioned, the low heating demand restricts the potential for curtailment, hence downward energy flexibility. However, the indoor temperature does not change fast. If instead of modulating the set-points, the heat supply

is completely interrupted, the single-family house maintains the temperature above 20°C for more than 48 hours, while the apartment block keeps the temperature above 20°C for 20 hours in the coldest apartments and more than 3 days in the rest of the apartments. The buildings are, thereby, robust and can be independent for a long period of time without jeopardising the thermal comfort of the occupants. These long hours of autonomy allow the system operators to exploit the independence of their operation. Although the low energy needs limit the energy available for curtailment in each building individually, aggregating similar type of buildings to a large number, the amount of energy becomes considerable. The potential for upward flexibility appeared greater, enabling the energy system to use these buildings as heat sinks if needed or implementing preheating to the buildings if their autonomy needs to be prolonged. The different thermal behaviour with regards to energy flexible operation of this category of buildings in comparison to other categories of buildings broadens the portfolio of options for system operators when flexibility is needed in the system.

3.2.2 Energy flexibility of events with various duration and start time

The duration and start time of the flexibility event are parameters that are to be decided according to the system's needs every time that a flexibility event is to be implemented. Simulations were performed first varying the duration of the flexibility events between 2, 4, 6, 8, 12, 16 and 24 hours (each of them starting at 06:00), and then varying the starting time, with events starting at 00:00, 06:00, 12:00 and 18:00 (with a duration of 8 hours each of them). The rest of the boundary conditions remained as the base case flexibility events. Figure 10 and Figure 11 present the results of the simulations performed for the single-family house and the apartment block, respectively. The base case flexibility events are outlined with black colour.
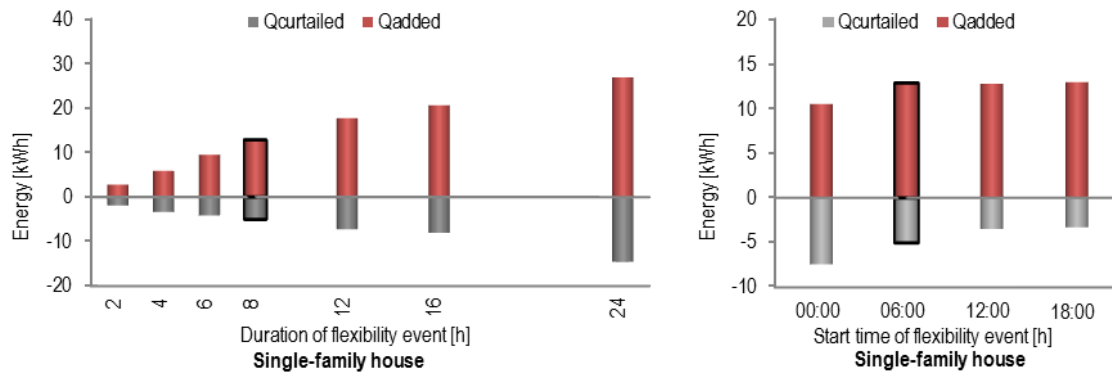
Figure 10: Energy added/curtailed during upward/downward flexibility events with different durations (left) and different starting time (right) for the single-family house
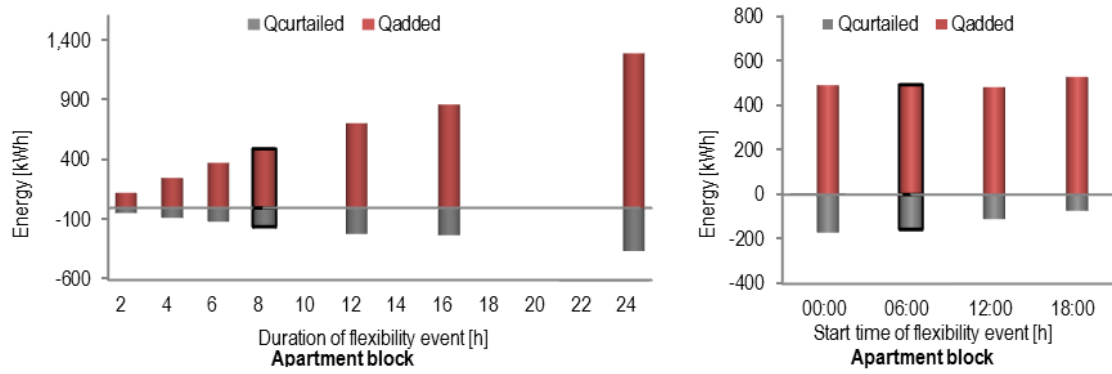
Figure 11: Energy added/curtailed during upward/downward flexibility events with different durations (left) and different starting time (right) for the apartment block

Regarding the duration of the events, it can be seen that the increase of the amount of energy added and curtailed during the events was almost linear to the duration of the events. This is explained as, when the air temperature had reached 24°C, the surface temperature of the walls was still lower than the air temperature, so heat continued being absorbed by the wall elements until the end of the event, as depicted in Figure 12 for the base case flexibility event in the single-family house.
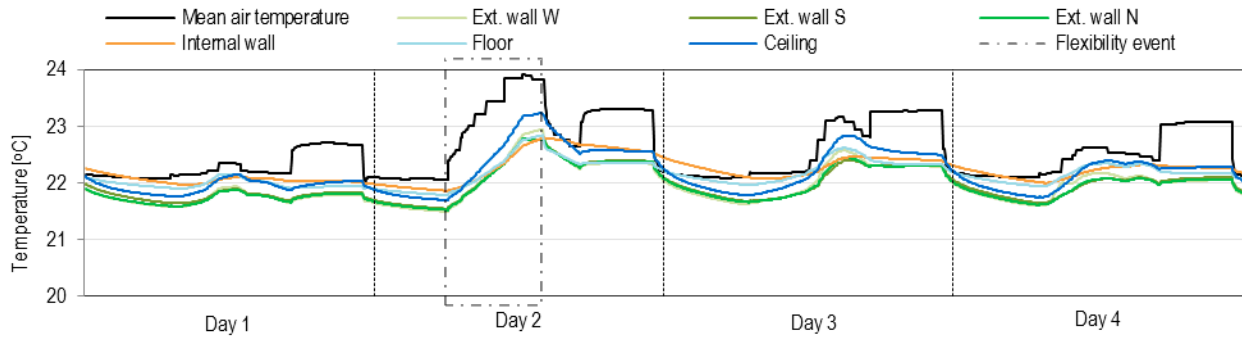
Figure 12: Indoor air and wall surface temperatures during the 8-hour event for the single-family house (day zone)

For the single-family house the potential for upward flexibility varied between 20 Wh/m^2 for a 2-hour event and 180 Wh/m^2 for a 24-hour event, while the potential for downward flexibility varied between 13 Wh/m^2 for a 2-hour event and 98 Wh/m^2 for a 24-hour event. Similarly for the apartment block, the potential for upward flexibility varied between 20 Wh/m^2 for a 2-hour event and 206 Wh/m^2 for a 24-hour event, while for the downward event the flexibility potential varied between 7 Wh/m^2 for a 2-hour event and 57 Wh/m^2 for a 24-hour event.

Regarding the start time of the events, the influence is more evident for the available energy to be curtailed rather than added. The potential for added energy is almost the same in all cases, apart from the event starting at 00:00 in the single-family house, which was lower by 18%. The reason for this is that during the night the heating demand for space heating of the building (without modulations) is higher than during the day because of lower heat gains. Thereby, the energy that can be added during the upward flexibility event is less, due to the limited capacity of the space heating system. For both

buildings, the potential for curtailment is highest at night-time (00:00 and 06:00), while it decreases almost by half during day time (12:00 and 18:00). During the day, the internal and/or solar gains were substantial, thus the heating demand was lower, hence the potential for curtailment was lower.

Similar modulations were performed by [14] and [16]. The former simulated available capacities for the Belgian building stock under static and dynamic boundary conditions. When comparing for the upward modulation of 2°C for 2 hours, using dynamic boundary conditions for a renovated single-family house, it was found that the available capacity was 43 Wh/m^2. For the same modulation to a passive single-family house studied by [16], the capacity found was around 25 Wh/m^2. In this study, for the upward modulation of 2 hours shown in Figure 10, the capacity found was 3 kWh or 20 Wh/m^2. The deviations can be attributed to the differences in boundary conditions and thermal properties of the buildings.

3.3 Influence of boundary conditions

Boundary conditions are crucial parameters in this study. The ambient weather conditions, although uncontrollable, should be considered before implementing a flexibility event. Figure 13 presents the energy flexibility under different weather conditions during the heating season as presented in Section 2.3, namely cold, moderate and warm ambient air temperature with cloudy or clear sky. The base case flexibility events are outlined with black colour. The start time and duration are those of the base case flexibility events, namely started at 06:00 and lasted for 8 hours.
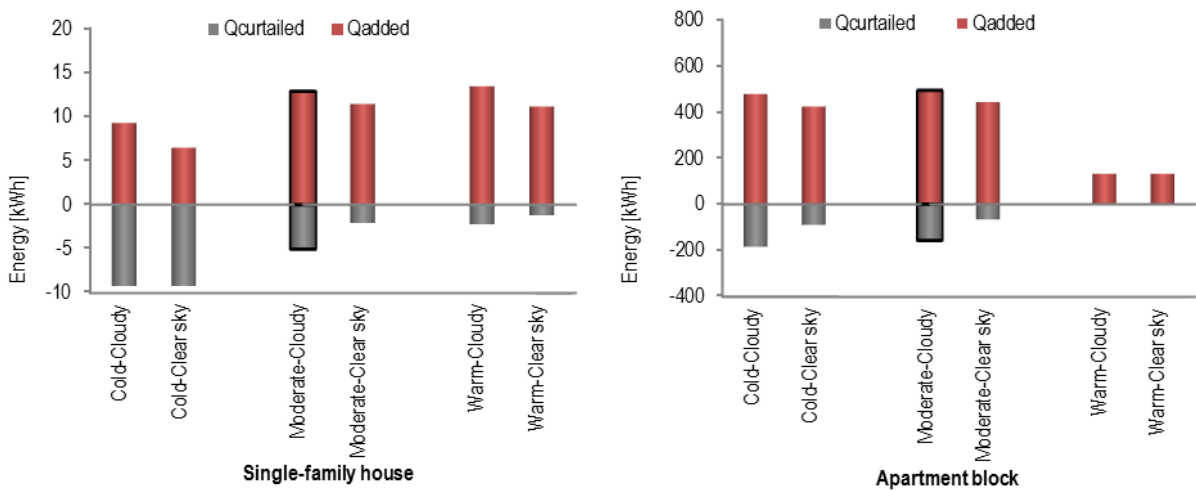
Figure 13: Energy added/curtailed during upward/downward flexibility events under different weather conditions for the single-family house (left) and the apartment block (right)

In all cases with clear sky, thus more solar gains, the flexibility was decreased. For the flexibility upwards, the decrease was on average 15 Wh/m^2 for the single-family house and 6 Wh/m^2 for the apartment block. This is attributed to the fact that solar gains contributed significantly to the increase of the indoor temperature, so the contribution of the heating system was decreased. Therefore, the additional energy was lower compared to the cases with cloudy sky, hence the potential for

additional energy was limited by the upper limit of thermal comfort. For the flexibility downwards, the decrease was on average 9 Wh/m² for the single-family house and 10 Wh/m² for the apartment block. This is attributed to the higher solar gains that lead to lower energy use of the reference case, thus lower amount of energy to be curtailed compared to the case with cloudy sky.

The ambient air temperature is also a determinant parameter for the energy flexibility. For warmer days of the heating season the flexibility was low as heating demand was low. For the single-family house the decrease was only marginal (1 Wh/m²) for the upward events, while it was 12 Wh/m² for the downward events. For the apartment block, in warm days, both the upward and downward flexibility decreased drastically. For colder days, the upward flexibility was decreased by 3 Wh/m² for the apartment block and 28 Wh/m² for the single-family house. Since the reference energy need in this case was already high in order to meet the heating set-point, the potential for additional heating demand was low, being limited by the capacity of the heating system. On the other hand, since the reference energy need was higher, there was higher potential for curtailment, thus the flexibility potential downward was increased, only by 4 Wh/m² for the apartment block, while by 38 Wh/m² for the single-family house.

Along with the ambient weather, internal heat gains are also important boundary conditions, as it became apparent from the analysis of the results. Both the intensity and the schedule of internal heat gains significantly affect the heating profile of the buildings and consequently the potential for flexibility. Similar observations were also underlined by the passive house studied in [16]. In the present study, the occupant behaviour was modelled deterministically. Future research should include models with stochastic occupancy and occupant behaviour [41–44] in order to improve the realism of energy flexibility quantification. Furthermore, research is required to what extent occupants would be willing to accept the influences on thermal comfort if their buildings should be operated flexibly. This may be more critical when using thermal mass as means to facilitate flexibility, than if flexibility is provided by components of the DHW systems of buildings. In order to achieve a flexible energy system, informed and motivated occupants are essential [45].

3.4   Influence of building design parameters

To study the impacts of design parameters on energy flexibility, building models were created for every variation shown in Table 4. For every building model, its reference operation, i.e. operation without flexibility modulations, was simulated. This reference operation was then compared to the upward and downward flexibility events, which every time started at 06:00 and lasted for 8 hours. Figure 14 presents the energy use of these three operation modes. Every bar represents one variation of the building model. The grey section of the bar shows the energy that was curtailed during the downward flexibility event, the red section of the bar shows the energy that was added during the upward flexibility event,

while the white patterned section of the bar shows the energy use under the reference operation for the respective duration. The results of the baseline building are outlined with black colour for each parameter.
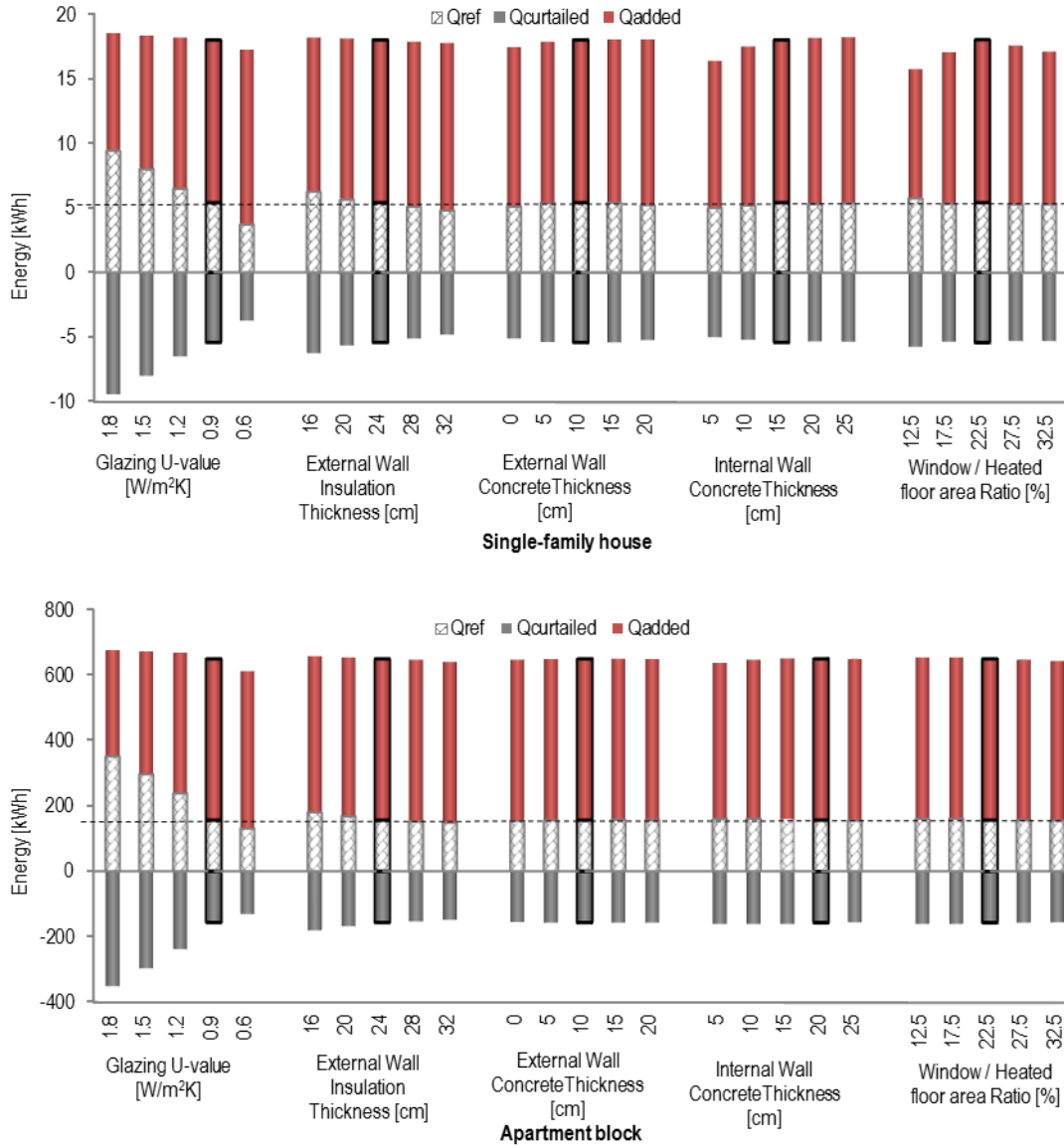
Figure 14: Energy during reference operation and energy added/curtailed during upward/downward flexibility events with different geometry characteristics of the single-family house (top) and the apartment block (bottom)

As explained in Section 2.4, when varying the window U-value or the external wall insulation thickness, the capacity of thermal mass remained unaltered to evaluate the effect of the buildings' heat losses on the flexibility potential. Similar results were obtained for both building types. The upward flexibility decreased as heat losses increased since the heating system has a limited capacity. For the variation with the highest losses, the potential for upward flexibility decreased by 28% for the single-family house and by 34% for the apartment block. On the other hand, the downward flexibility increased as heat losses increased; for the variation with the highest losses, the increase was 75% for the single-family house and

125% for the apartment block. The reason for this is that for the buildings with higher losses, the energy use during their reference operation was higher, so there was more energy to be curtailed during the downward flexibility event. The magnitude of the effect was greater for the glazing U-value, because among the parameters examined, the heat loss coefficient of the buildings was affected mostly by the window U-value.

In order to evaluate the effect of the thermal capacity, the external and internal wall concrete thicknesses were examined. There was no significant change (less than 5% between variations) in energy flexibility when the thickness of the external wall was changed, since the thermal capacity of walls is limited by the penetration depth inside the concrete. Considering the concrete as thermal mass element rather than structural element, it appears that there is no benefit gained by adding concrete thickness greater than 10 cm for the external walls and 15 cm for the internal walls, which is in line with the outcome of [46]. Nevertheless, the contribution of the thermal capacity of the internal walls was shown to be higher than that of the external walls. This finding was indeed expected, since the internal walls are exposed to the indoor air on both sides, while the external walls are only exposed on one side. Also, the material of the internal load-bearing walls is concrete, whereas for the external walls it is aerated concrete, which has smaller thermal capacity. For the single-family house, the variation with 5 cm internal walls resulted in 10% lower potential for upward flexibility and 8% lower potential for downward flexibility. The relative effect of thermal capacity of walls in the apartment block appeared smaller compared to the effect in the single-family house, since there is a large amount of concrete in the ceiling decks of the apartment block. For the baseline single-family house, the shares in the total effective thermal mass of external walls, internal walls, floor and roof are 10%, 28%, 55% and 7% respectively. For the baseline apartment block the shares of external walls, internal walls, floor, roof and floor/ceiling decks are 2%, 20%, 4%, 4% and 70% respectively.

The obtained results are for the investigated type of buildings and should be very carefully assessed in order to be extended to other building types. For all variations examined, the buildings remained in the category of heavy buildings, apart from the variation with 5 cm internal walls for single-family house, which is in the category of semi-light buildings according to the Danish Building Research Institute (SBi) Guidelines 'Energy Demand for Buildings' [28].

The effect of window/heated floor area ratio was complicated as three main elements changed simultaneously: thermal capacity, heat losses and solar gains. For the single-family house, when the ratio either increased or decreased from the baseline building, the upward flexibility potential decreased. The change in downward flexibility was not significant. For the apartment block the behaviour was different, as the effect of the different elements seemed to counterbalance each other and the potential remained unaltered for all variations.

The time constant of all the building models was calculated and the added or curtailed energy during the base case upward (red) or downward (grey) flexibility events are plotted in Figure 15.
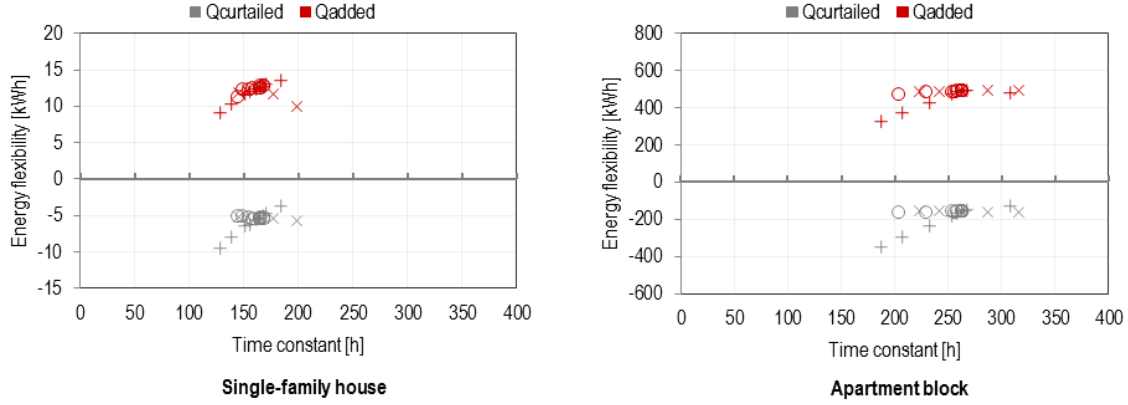
Figure 15: Correlation between flexibility potential and time constant for all variations examined for the single-family house (left) and the apartment block (right). Buildings' variations concerning heat loss effect are marked as + , those concerning thermal capacity effect are marked as ○ , those concerning the combination of the previous two and the solar gains are marked as × .

On average, the time constant of the single-family house was shorter, compared to the respective of the apartment block. This is attributed mainly to the ratio of the envelope area per volume of the apartment block (0.265 m^2/m^3) being considerably lower than the one for the single-family house (0.998 m^2/m^3). In the apartment block, a broader range of results for the time constant was observed, although the changes in the building design parameters were the same. Furthermore, in the apartment block there were two clear trends observed, one formed from the variations concerning heat losses (marked as + in the figure) and the other from those concerning the thermal mass effect (marked as ○ in the figure), with the distinction between them being evident. In the single-family house, the behaviour was similar for the downward flexibility potential. However, for the upward flexibility potential a correlation can be observed, which was in this case disturbed only by the solar gains (marked as × in the figure). Although the time constant of the buildings appears not to be enough as an indicator with regards to energy flexibility from building thermal mass and heating systems, it can however indicate the range of the potential.

With the building design parameters examined, it was shown that the characteristic to be prioritized when aiming for energy flexibility is the minimization of heat losses. Once this is ensured, it would be beneficial to increase the thermal capacity of the building as well, especially that of the internal walls. The effect of the glazing area did not present a clear trend, hence no direct guideline can be suggested from the obtained results. However, there might be other design parameters important for investigation. For example, different zoning of the buildings, i.e. different sizes of apartments, orientation, uses, interior design, shading, etc., would also impact the thermal behaviour of the buildings. Furthermore, in

this study only sensible heat storage has been considered. The integration of phase changing materials in the structural thermal mass of the building could also be considered, as reviewed by [10].

4 Conclusions

We investigated flexibility potential for new buildings, considering the heating energy that can be added to or curtailed from the buildings for a certain period of time without compromising thermal comfort for the occupants. Two building types were modelled in the building performance simulation software IDA ICE: a single-family house and an apartment block. Both are well-insulated heavy-weight buildings following the Danish Building Regulation 2015. A scenario for reference operation of the buildings with constant heating temperature set-point at 22°C was initially simulated. Two deviations from this reference were considered with increased set-point to 24°C or decreased set-point to 20°C for a period of time. The first case (upward flexibility event) represented a scenario with abundance of renewable energy production in the energy system, when the heat supply in a building can be increased, in order for thermal energy to be stored in the thermal mass. The second (downward flexibility event) represented a scenario with limited/no availability of renewable energy in the energy system, when the heat supply in buildings needs to be curtailed or completely interrupted.

During flexibility events under moderate weather conditions of the Danish heating season, starting at 06:00 and lasting for 8 hours, the heating energy added to the single-family house was 87 Wh/m^2 and the energy curtailed was 36 Wh/m^2; while the heating energy added to the apartment block was 76 Wh/m^2 and the energy curtailed was 25 Wh/m^2. In all cases examined, clear asymmetries between the amount of added and curtailed energy were noticed. Although for individual buildings, the amount of energy to be curtailed is limited, if aggregated to a neighbourhood or district level, the amount of energy available for curtailment becomes significant. At the same time, in cases of abundant production of renewable energy in the system, the buildings can act as storage media absorbing considerable quantities of thermal energy in the structural thermal mass. Furthermore, the findings show that low-energy buildings are highly robust and can remain autonomous for several hours maintaining thermal comfort.

It was shown that the amount of energy added/curtailed during the event was proportional to the duration of the event, which indicates that the buildings have large heat capacity. The different starting time of the flexibility events mainly affected the potential for curtailment, with the highest available energy to be curtailed being during the night. The analysis presented high dependence of flexibility potential on boundary conditions, namely ambient temperature, solar radiation and internal gains. The potential for curtailment increased during cold days, while the potential for storing additional energy was highest during days with moderate ambient temperature for the heating season. Increased solar gains led to decreased

flexibility potential. From the different building design parameters examined, it shown that heat losses to the ambient govern the potential for flexibility, while the concrete thickness of the walls was not a determinant factor by itself. The contribution of the thermal capacity of the internal walls was shown to be higher than that of the external walls.

This work provided a deep insight into thermal behaviour of low-energy buildings and their physical potential for energy flexibility. The results can be extended with aggregation studies creating a category of such buildings that can be added to the portfolio of solutions for storage in the energy system, thus facilitating higher penetration of renewable energy. Feasibility studies need to be performed to assess the active participation of buildings in the energy market, as appropriate business models for flexibility services are yet to be developed. Finally, further studies will be needed on occupants' thermal comfort, acceptability and behavioural response.

Acknowledgements

Appendix

The total heat capacity is given by Equation (A.1) [47], as the sum of the capacity of the individual building components: $Total\ heat\ capacity = \sum \rho \cdot C_p \cdot A \cdot d$, (A.1), where:

ρ , the density of the material [kg/m³],

C_p, the specific heat capacity of the material [J/(kg·K)],

A , the surface area of the material [m²],

d , the depth [m] of the layer of the material considered. Only materials on the inner side of the insulation layer were considered.

If the depth of the material was higher than the penetration depth of the material, then the penetration depth was used for d. The penetration depth is calculated according to Equation (A.2): $d = \sqrt{\frac{a \cdot t}{\pi}}$ (A.2) [47], where:

t , the duration of the period [s], in this work considered as one day,

α , the thermal diffusivity, [m²/s].

The methodology corresponds to the simplified calculation of the heat capacity of the standard EN ISO 13786 [48], but in this work the thermal diffusivity is calculated for each material, instead of using the conventional value mentioned in the standard.

References

[1]   European Commission, European Council 23-24/10/2014 - Conclusions on 2030 Climate and Energy Policy Framework, Brussels, Belgium, 2014.

[2]   Danish Energy Agency, Danish climate policies, (2017). https://ens.dk/en/our-responsibilities/energy-climate-politics/danish-climate-policies (accessed November 19, 2017).

[3]   P. Denholm, M. Hand, Grid flexibility and storage required to achieve very high penetration of variable renewable electricity, Energy Policy. 39 (2011) 1817–1830. doi:10.1016/j.enpol.2011.01.019.

[4]   S.Ø. Jensen, A. Marszal-Pomianowska, R. Lollini, W. Pasut, A. Knotzer, P. Engelmann, A. Stafford, G. Reynders, IEA EBC Annex 67 Energy Flexible Buildings, Energy Build. 155 (2017) 25–34. doi:10.1016/j.enbuild.2017.08.044.

[5]   A. Marszal-Pomianowska, P. Heiselberg, O. Kalyanova Larsen, Household electricity demand profiles - A high-resolution load model to facilitate modelling of energy flexible buildings, Energy. 103 (2016) 487–501. doi:10.1016/j.energy.2016.02.159.

[6]   R. D'hulst, W. Labeeuw, B. Beusen, S. Claessens, G. Deconinck, K. Vanthournout, Demand response flexibility and flexibility potential of residential smart appliances: Experiences from large pilot test in Belgium, Appl. Energy. 155 (2015) 79–90. doi:10.1016/j.apenergy.2015.05.101.

[7]   J. Heier, C. Bales, V. Martin, Combining thermal energy storage with buildings – a review, Renew. Sustain. Energy Rev. 42 (2015) 1305–1325. doi:10.1016/j.rser.2014.11.031.

[8]   H. Wolisz, H. Harb, P. Matthes, Dynamic simulation of thermal capacity and charging/discharging performance for sensible heat storage in building wall mass, in: 13th Conf. Int. Build. Perform. Simul. Assoc., Chambery, France, 2013: pp. 2716–2723.

[9]   B. Favre, B. Peuportier, Application of dynamic programming to study load shifting in buildings, Energy Build. 82 (2014) 57–64. doi:10.1016/j.enbuild.2014.07.018.

[10]   H. Johra, P. Heiselberg, Influence of internal thermal mass on the indoor thermal dynamics and integration of phase change materials in furniture for building energy storage: A review, Renew. Sustain. Energy Rev. 69

(2017) 19–32. doi:10.1016/j.rser.2016.11.145.

[11]   C. Finck, R. Li, R. Kramer, W. Zeiler, Quantifying demand flexibility of power-to-heat and thermal energy

storage in the control of building heating systems, Appl. Energy. 209 (2018) 409–425.

doi:10.1016/j.apenergy.2017.11.036.

[12]   A. Arteconi, N.J. Hewitt, F. Polonara, Domestic demand-side management (DSM): Role of heat pumps and

thermal energy storage (TES) systems, Appl. Therm. Eng. 51 (2013) 155–165.

doi:10.1016/j.applthermaleng.2012.09.023.

[13]   S. Stinner, K. Huchtemann, D. Müller, Quantifying the operational flexibility of building energy systems with

thermal energy storages, Appl. Energy. 181 (2016) 140–154. doi:10.1016/j.apenergy.2016.08.055.

[14]   G. Reynders, J. Diriken, D. Saelens, Generic characterization method for energy flexibility: Applied to structural

thermal storage in residential buildings, Appl. Energy. 198 (2017) 192–202. doi:10.1016/j.apenergy.2017.04.061.

[15]   G. Masy, E. Georges, C. Verhelst, V. Lemort, Smart grid energy flexible buildings through the use of heat pumps

and building thermal mass as energy storage in the Belgian context, Sci. Technol. Built Environ. 4731 (2015)

800–811. doi:10.1080/23744731.2015.1035590.

[16]   J. Le Dréau, P. Heiselberg, Energy flexibility of residential buildings using short term heat storage in the thermal

mass, Energy. 111 (2016) 991–1002. doi:10.1016/j.energy.2016.05.076.

[17]   K.O. Aduda, T. Labeodan, W. Zeiler, G. Boxem, Demand side flexibility coordination in office buildings: A

framework and case study application, Sustain. Cities Soc. 29 (2017) 139–158. doi:10.1016/j.scs.2016.12.008.

[18]   TABULA WebTool, (2017). http://webtool.building-typology.eu (accessed October 11, 2017).

[19]   H. Wolisz, P. Block, R. Streblow, D. Müller, Dynamic activation of structural thermal mass in a multizonal

building with due regard to thermal comfort, 14th Int. Conf. IBPSA - Build. Simul. 2015, BS 2015, Conf. Proc.

(2015) 1291–1297.

[20]   G. Reynders, T. Nuytten, D. Saelens, Potential of structural thermal mass for demand-side management in

dwellings, Build. Environ. 64 (2013) 187–199. doi:10.1016/j.buildenv.2013.03.010.

[21]   J. Kensby, A. Trüschel, J.-O. Dalenbäck, Potential of residential buildings as thermal energy storage in district

heating systems – Results from a pilot test, Appl. Energy. 137 (2015) 773–781.

doi:10.1016/j.apenergy.2014.07.026.

[22]   D. Six, J. Desmedt, J.V.A.N. Bael, D. Vanhoudt, Exploring the Flexibility Potential of Residential Heat Pumps,

21st Int. Conf. Electr. Distrib. (2011) 6–9.

[23] T. Péan, J. Ortiz, J. Salom, Impact of Demand-Side Management on Thermal Comfort and Energy Costs in a Residential nZEB, Buildings. 7 (2017) 37. doi:10.3390/buildings7020037.

[24] The Danish Transport and Construction Agency, Danish Building Regulations 2015, (2015).

[25] EN/DS 15251, Indoor environmental input parameters for design and assessment of energy performance of buildings addressing indoor air quality, thermal environment, lighting and acoustics, Dansk Stand. (2007) 54.

[26] F. Oldewurtel, D. Sturzenegger, G. Andersson, M. Morari, R.S. Smith, Towards a standardized building assessment for demand response, Proc. IEEE Conf. Decis. Control. (2013) 7083–7088. doi:10.1109/CDC.2013.6761012.

[27] D. Fischer, T. Wolf, J. Wapler, R. Hollinger, H. Madani, Model-based flexibility assessment of a residential heat pump pool, Energy. 118 (2017) 853–864. doi:10.1016/j.energy.2016.10.111.

[28] S. Aggerholm, K. Grau, Bygningers energibehov - Beregningsvejledning - SBi-anvisning 213, Aalborg, 2014.

[29] DS 418, Beregning af bygningers varmetab - Calculation of heat loss from buildings, Dansk Stand. (2011).

[30] DS/EN ISO 13370, Thermal performance of buildings – Heat transfer via the ground – Calculation methods, Dansk Stand. 2. udgave (2008).

[31] EQUA Simulation AB, IDA Indoor Climate and Energy - A new generation building performance simulation software, IDA Indoor Clim. Energy. (2017). https://www.equa.se/en/ida-ice.

[32] EQUA Simulation AB, Validation of IDA Indoor Climate and Energy 4 . 0 with respect to CEN Standards EN 15255-2007 and EN 15265-2007, Solna, Sweden, 2010.

[33] EQUA Simulation AB, Validation of IDA Indoor Climate and Energy 4.0 build 4 with respect to ANSI/ASHRAE Standard 140-2004, Solna, Sweden, 2010.

[34] S. Kropf, G. Zweifel, Validation of the Building Simulation Program IDA-ICE According to CEN 13791 „ Thermal Performance of Buildings - Calculation of Internal Temperatures of a Room in Summer Without Mechanical Cooling - General Criteria and Validation Procedures ", 2001.

[35] P. Loutzenhiser, H. Manz, G. Maxwell, International Energy Agency's SHC Task 34 - ECBCS Annex 43 Project C: Empirical Validations of Shading / Daylighting / Load I nteractions in Building Interactions Energy Simulation Tools, 2007.

[36] S. Moosberger, Test of IDA Indoor Climate and Energy version 4.0 according to CIBSE TM33, Luzern, 2007.

[37] P.G. Wang, M. Scharling, K.P. Nielsen, K.B. Wittchen, C. Kern-Hansen, Technical Report 13-19 2001 – 2010 Danish Design Reference Year - Reference Climate Dataset for Technical Dimensioning in Building ,

Construction and other Sectors, Copenhagen, 2013.

[38]   DS/EN ISO 13790, Energy performance of buildings – Calculation of energy use for space heating and cooling, Dansk Stand. (2008) 178.

[39]   L.-S. Wang, P. Ma, E. Hu, D. Giza-Sisson, G. Mueller, N. Guo, A study of building envelope and thermal mass requirements for achieving thermal autonomy in an office building, Energy Build. 78 (2014) 79–88. doi:10.1016/j.enbuild.2014.04.015.

[40]   E. Georges, B. Cornélusse, D. Ernst, V. Lemort, S. Mathieu, Residential heat pump as flexible load for direct control service with parametrized duration and rebound effect, Appl. Energy. 187 (2017) 140–153. doi:10.1016/j.apenergy.2016.11.012.

[41]   J. Widén, M. Lundh, I. Vassileva, E. Dahlquist, K. Ellegård, E. Wäckelgård, Constructing load profiles for household electricity and hot water from time-use data-Modelling approach and validation, Energy Build. 41 (2009) 753–768. doi:10.1016/j.enbuild.2009.02.013.

[42]   J. Widén, A. Molin, K. Ellegård, Models of domestic occupancy, activities and energy use based on time-use data: Deterministic and stochastic approaches with application to various building-related simulations, J. Build. Perform. Simul. 5 (2012) 27–44. doi:10.1080/19401493.2010.532569.

[43]   A. Wang, R. Li, S. You, Development of a data driven approach to explore the energy flexibility potential of building clusters, Appl. Energy. (2018). (under review).

[44]   R. Li, F. Wei, Y. Zhao, W. Zeiler, Implementing Occupant Behaviour in the Simulation of Building Energy Performance and Energy Flexibility: Development of Co-Simulation Framework and Case Study, Proc. Build. Simul. 2017. (2017) 1339–1346.

[45]   R. Li, G. Dane, C. Finck, W. Zeiler, Are building users prepared for energy flexible buildings?—A large-scale survey in the Netherlands, Appl. Energy. 203 (2017) 623–634. doi:10.1016/j.apenergy.2017.06.067.

[46]   P. Ma, L.-S. Wang, Effective heat capacity of interior planar thermal mass (iPTM) subject to periodic heating and cooling, Energy Build. 47 (2012) 44–52. doi:10.1016/j.enbuild.2011.11.020.

[47]   H.E. Hansen, P. Kjerulf-Jensen, B.O. Stampe, Varme- og klimateknik : Grundbog, DANVAK, 1988.

[48]   DN/EN ISO 13786, Thermal performance of building components – Dynamic thermal characteristics – Calculation methods, Dansk Stand. (2008).

PAPER II: <u>Foteinaki, K.,</u> Li, R., Péan, T., Rode, C. and Salom, J. (2018) 'Evaluation of energy flexibility of low-energy residential buildings connected to district heating'. S*ubmitted to the peer-reviewed journal Energy and Buildings, Elsevier (December 2018)*

Evaluation of energy flexibility of low-energy residential buildings connected to district heating

Kyriaki Foteinaki[a,*], Rongling Li[a], Thibault Péan[b,c], Carsten Rode[a], Jaume Salom[b]

[a] Department of Civil Engineering, Technical University of Denmark, Brovej, Building 118, 2800 Kgs. Lyngby, Denmark
[b] Catalonia Institute for Energy Research (IREC), Jardins de les Dones de Negre 1, 08930 Sant Adrià de Besòs (Barcelona), Spain
[c] Universitat Politècnica de Catalunya (UPC), C/Pau Gargallo 5, 08028 Barcelona, Spain
* Corresponding author, e-mail: kyfote@byg.dtu.dk

Abstract

Energy flexibility is a cost-effective solution to facilitate secure operation of the energy system while integrating large share of renewables. Thermal energy infrastructure is a great asset for flexibility in systems with widely developed district heating networks. The aim of the present work is to investigate the potential for low-energy residential buildings to be operated flexibly, according to the needs of district heating system. An apartment block is studied, utilizing the storage capacity of thermal mass as storage medium. Two sets of data are utilized: heat load of Greater Copenhagen and dynamic heat production cost which is used as a price signal for the scheduling of the heating use in the building. Scenarios with different control signals are determined in order to achieve load shifting. The findings show that pre-heating is highly effective for load shifting and peak load reduction. Heat load shifting is achieved in all scenarios between 40% and 87%. Although with load shifting higher energy use may occur, it occurs mostly at times when the city heat load is lower and heat production is less expensive and less carbon-intensive. Indoor temperature has a wider range and/or more fluctuations, yet remains within acceptable limits.

Keywords

Energy flexibility, Building thermal mass, Heating demand

1. Introduction

A high penetration of renewable energy has already been achieved in many countries and it is anticipated to increase in the near future. Integrating a larger share of renewable sources in the energy system challenges the controllability and stability of the system due to the fluctuating production. The stochastic nature of the production side stresses the need for flexibility at the demand side. Methods for reducing peak loads and shifting demand have attracted great attention, developing the framework for appropriate markets and introducing new control strategies and end use technologies for energy storage in the system [1]. Initially, the focus was on the electricity sector, though gradually a multi-carrier energy system came into perspective, and nowadays integration of sectors is strongly encouraged. Lund et al. 2012 [2] explains the need for the electricity grids to be seen as part of integrated smart energy systems and underlines the importance of including flexible Combined Heat and Power (CHP) production for the stability of the grid. Lund et al. 2016 [3], uses an integrated cross-sector approach to identify optimum storage solutions to integrate larger shares of renewable energy, as opposed to focusing on individual sub-sectors. Münster et al. 2012 [4] underlined the importance of district heating system (DH), concluding that DH can contribute to the security of supply and sustainability of future energy systems cost-effectively.

One very important element of DH networks is the potential for short-term heat storage, facilitating the optimization of the CHP cogeneration according to the electricity sector without compromising the heating sector [5,6]. By use of heat storage, when there is sufficient electricity production in the system from intermittent renewable energy, for example wind turbines, CHP can decrease their production since heat can be supplied from the storage. Respectively, the CHP plant can increase the production when there is higher demand for electricity. In that case, if the heat production is higher than the heat demand, the storage can be charged; conversely, if the heat production is lower than the heat demand, the heat storage can be discharged. This provides flexibility to the energy system, which is a significant aspect for the integration of larger share of intermittent renewables, which is crucial for the optimal operation of the system both economically and environmentally. Thereby, the thermal energy infrastructure, with the existing energy storage and the potential for extension, is considered a great asset for flexibility.

The building sector with the already existing large mass of the building stock appears to have potential for short-term thermal energy storage. There are different possibilities for short-term thermal energy storage in the buildings, including utilization of the thermal mass of buildings, use of phase changing materials and domestic hot water storage tanks [7]. The two latter may require new investments. Although domestic hot water storage tanks are common in Danish households, especially in apartment blocks, they are not necessarily available in every building; instantaneous heat exchangers are also used to supply domestic hot water from the DH network. Phase changing materials is an emerging technology but research is still needed and applications in buildings are rare [7–9]. On the other hand, the thermal mass of the building stock is available and can be used as short-term thermal energy storage with limited investment cost for control installations. The use of the thermal mass of buildings has been studied by many researchers already and it is shown that it can be utilized as short term thermal energy storage. Most often, case study buildings connected to the electricity grid have been used, with integrated heat pumps [10–14] or with electrical space heating systems [15]. There are fewer studies that have worked with buildings which are connected to the district heating grid. Compared to the electricity system, the available information and expertise on demand shifting for DH is limited. An important impediment to this is that the market structure for heat is not as developed and transparent as it is for electricity, so it is not mature yet to facilitate demand response. For instance, time-varying tariffs are not applied. Åberg et al. 2016 [16] discussed the Swedish experience: although this country has liberalized the district heating pricing the past two decades, the district heating market has not evolved yet to an integrated market. Li et al. [17] reviewed existing heat pricing models and methods and Song et al. [18] conducted a survey to capture the current structure of DH price models in Sweden, in an effort to improve DH market and heat pricing transparency. Yet, both studies [17,18] underlined that market transparency needs to be improved in order to effectively implement demand shifting strategies in the DH system.

Nevertheless, important benefits are anticipated from demand response in the DH system. For the system, reduction of heat production costs by reducing the start-ups and avoiding the use of peak load boilers, handling capacity issues in the existing network, thus reducing network investment costs by more efficient use of the existing pipes and installations, running CHP plants at the most efficient states and being able to adjust the cogeneration to benefit from high potential of renewables in the electricity system, thus increasing the revenue of the CHP plant from electricity sales. In addition, environmental benefits are achieved by substituting the carbon-intensive peak load boilers and facilitating the production from renewables in the system. However, in order for the consumer to have a benefit from participating in demand response, monetary incentives need to be offered. Li et al. 2015 [17] suggests that engaging consumers on the demand side is equally important with renovating DH supply and distribution system, in order to achieve energy savings and CO_2 emissions reduction and suggests the development of real-time pricing mechanism in the DH sector.

Previous work on demand response in buildings connected to DH was focused on the load shape rather than heat pricing. Wernstedt et al. [19] implemented a multi-agent system to control a DH network with 14 buildings in order to achieve peak shaving without reducing the quality of services, emphasizing the importance of taking many small local decisions to impact the overall system performance. In continuation, Johansson et al. [20] describes the results from the implementation of the load control based on the multi-agent system in three DH systems in Sweden. It was shown that the system achieved reduction of peak loads up to 20% of the total load. Basciotti and Schmidt [21] simulated an optimization algorithm, utilizing the thermal capacity of buildings with a certain flexibility in the time of reaching the set-point. The results estimated peak reduction up to 35% with about 2% increased heat use for the considered DH network. Dominković et al. [22] implemented an optimization model of case study energy system in a Danish city, focusing on the impact of storage in the building thermal mass on the energy supply of DH. They showed that the building thermal mass was used as intra-day storage and that it facilitated effective utilization of larger share of solar thermal heating energy. Evaluating the potential of individual buildings with field studies, Kensby et al. [23] presented results from 5 case studies of multifamily residential buildings, which were tested for their potential to act as thermal energy storage by adjusting the signals of the supply temperature to the radiator system, and showed that heavy concrete buildings can tolerate changes in heat deliveries without significant deterioration of indoor climate. Sweetnam et al. [24] performed a field study in 28 households connected to a DH network in England, implementing load shifting, which improved the load factor (ratio of mean to maximum demand) from 0.29 to 0.44, with consequent increased energy use of approximately 3%. To the knowledge of the authors, there are only a few studies performing demand response based on dynamic pricing. In [25] they summarized the results of three case study buildings where demand response demonstrations were carried out and propose DH tariff structures that encourage the utilization of DSM; they recommend that the tariffs in DH should reflect the suppliers' marginal heat production costs, are understandable by the customers and consider legal constraints. Deventer et al. 2011 [26] proposed and simulated an implementation of demand response,

with a sensor network exchanging information between the heat supplier and the building substation. The indoor temperature set-point was modulated according to variable pricing for heating in order to reduce the energy use during peak load hours. The study showed energy use reduction of 20% while the indoor temperature was reduced by 1°C with an outdoor temperature of -15°C.

1.1 Danish district heating

Denmark is one of the European countries with the most developed district heating networks, supplying 64% of Danish households [27]. The heat generation for the Danish DH system has already integrated 52% renewable energy [28]. Figure 1 presents the percentage distribution of fuel mix for district heating production in 2016 in Denmark [28].
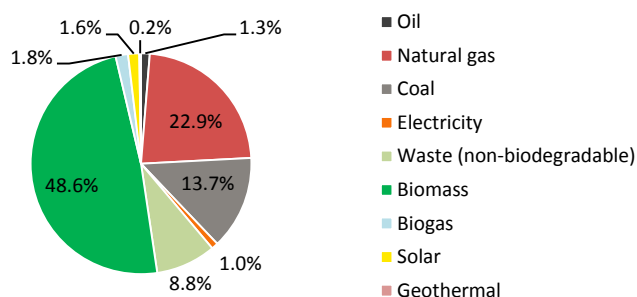
Figure 1: Percentage distribution of fuel mix for district heating production in Denmark (2016)

According to the Danish energy targets it shall be based only on renewables by 2050. With the base load demand being gradually converted to CO_2-neutral energy by using biomass-fuelled plants, heat pumps and geothermal energy, the main goal to be achieved is to avoid the utilization of peak load boilers, which mainly use natural gas. In addition, 68.9% of all heat is produced in cogeneration with electricity (CHP) [27], therefore the interaction between the sectors is profound. Thereby, extending the heat storage potential within the DH system is essential and it would further increase the importance of the role of DH in the future flexible energy system.

The Danish district heating is considered a natural monopoly and it has been therefore regulated by a non-profit principle. Although the heat price paid by the consumers varies in different areas, the costs that can be included in the heating price are defined by law. According to this, the consumer pays a heat price that should cover all costs pertaining to the heat supply, as it is not permissible for the heat supply company to make profit, but they should be financially sustainable. Thereby, the heat price paid by the consumers are influenced by many parameters, including investment, operation and maintenance (O&M) and efficiency of the production facility, investment, O&M and heat loss in the DH network, fuel prices, taxes and VAT, subsidies, electricity price (relevant for plants that use/produce electricity) [27]. Regarding the ownership of the DH production plants, there are different structures of ownerships in Denmark. Large energy companies typically own and operate the largest plants, while smaller plants are owned by municipalities or cooperatives. Along with the non-profit principle, the structure of the cooperative provides an efficient heat supply at the lowest possible price for the end customer. The payment for heating by the customers is fixed for the whole year and it is based on private contracts between them and the respective heating supply company.

DH in Greater Copenhagen area (i.e. Copenhagen metropolitan area) is produced by different plants owned by three companies: 3 waste incineration plants and 1 geothermal plant (these 4 energy sources being politically prioritized), 3 CHP plants, 2 heat accumulators, 4 large peak load boilers and approximately 30 peak load units, which function as a reserve for the base load units – typically if they fail during winter. It is supplied through interconnected transmission and distribution networks. A cooperative between the DH companies has been established (Varmelast.dk). One of the main tasks of Varmelast.dk is to prepare the day-ahead heating plan, which is based on the DH forecasts disclosed by the DH companies and considers fuel prices, operating and maintenance costs, energy taxes on heat production, CO_2 quota costs, income from the power market and hydraulic bottlenecks in the network [29]. Varmelast.dk performs a joint optimization of heat and power production and aims to ensure the maximum economic benefit for the entire system. The load dispatch is based on marginal heat production costs, while the heat price is defined in bilateral contracts between suppliers and buyers. The heat price contracts are confidential, i.e. not known by Varmelast.dk and define how the total benefit is shared. There are 3 scheduled intra-day adjustments of the heating plan every day with updated heat consumption forecasts, capacities and power prices.

The present work is part of the "EnergyLab Nordhavn – New urban energy infrastructure" project, which is a smart

city research project based in the Nordhavn district, Copenhagen. Nordhavn is a new development area in Copenhagen, in which the majority of the building stock is being built from 2014 and onwards. The buildings are built according to the strict energy performance requirements of the Danish Building Regulations (BR15 [30] / BR18 [31]), thus it is defined as an area for low-energy buildings by the City of Copenhagen development plan. After economic evaluation of the available options [32], district heating was chosen for heat supply in the area. Low-energy buildings are well-insulated, airtight and may be heavy-weight with a concrete core, thus have large thermal storage capacity. To the best knowledge of the authors, this category of buildings has not been utilized yet as a potential storage medium in the DH system. A multifamily residential apartment block in Nordhavn, Denmark, is studied in the present work. The physically available thermal storage capacity existing inherently in the structural mass has been analyzed in [33] and the findings showed that low-energy buildings are highly robust and can remain autonomous for several hours. This study evaluates the feasibility of the utilization of this flexibility potential. It investigates the benefits in the DH from the exploitation of these buildings if operated flexibly. Two sets of data from the district heating system are utilized as indication for the district heating needs: the hourly heat load of Greater Copenhagen and the respective marginal heat production cost. Scenarios with different control signals are determined based on the given data, which drive the operation of the heating system of the building. The aim is to demonstrate the potential of the building for flexible operation, in order to shift heat load in time, avoiding peak load periods and utilizing heat during periods that heat production is less expensive. The implemented scenarios are evaluated based on the effect on heat cost, energy use, thermal comfort and load shifting potential.

The structure of this paper is organized as follows. Section 2 analyses the available data from the district heating system in Copenhagen and narrates the approach. Then, the parameters of the simulations performed are presented, including the building model and the boundary conditions. Section 3 presents and analyses the results of the simulation studies and Section 4 discusses the outcomes. The main conclusions are summarized in Section 5.

2. Methodology

This section explains the methodology for the evaluation of using structural thermal mass as storage medium in the DH. The charging and discharging of the storage medium, i.e. structural thermal mass, is achieved by modulating the indoor air temperature set-point. When increasing the set-point, the heat load in a building is increased and the additional heat is stored into the thermal mass. When decreasing the set-point, the heat load in a building is curtailed or interrupted, imposing heat to be released from the thermal mass of the building to the internal zones.

Initially in this work, a reference operation of the building was defined, with thermostatic control with constant air temperature set-point at 22°C, which is a typical desired indoor temperature in Danish households during the heating season [34]. Then, different signals triggered an increase or decrease of the air temperature set-point in order to charge or discharge the thermal mass. At all times, thermal comfort of occupants ought not to be compromised. The limits of comfortable conditions were chosen to be between of 20 – 24 °C, in accordance with the thermal comfort Category II "Normal level of expectations for new buildings" for heating season according to the standard EN/DS 15251[35].

2.1 Data from district heating system

Given the complication of the heat market in Denmark and the heat pricing mechanism, which is not transparent enough, choosing a signal to represent the needs of DH is not straightforward. As previously explained, the DH price paid by the customers is based on individual contracts and is constant throughout the year, thereby, different signals had to be chosen. Two sets of data were used as indication of the district heating needs; the heat load of Greater Copenhagen and the respective marginal heat production cost. The marginal heat production cost was chosen to be used as signal, as the variation of production costs is represented and the effects of the market on the heat production are reflected adequately, as shown by Li et al.2015 [17]. Sun et al.2016 [36] showed that although the gap in magnitude between the marginal cost and the heat price is large, the marginal heat cost can adequately reflect the increase of variable heat production cost with increased heat demand. The data sets were provided to us by the DH utility company of Copenhagen, HOFOR A/S [37].

The marginal heat production cost is the cost to produce one additional unit of heat through DH. Since the DH system consists of several production plants, the marginal heat production cost of the DH system is equal to the marginal cost of the production plant with the highest operational costs. There are different factors affecting the marginal cost pricing method as reviewed by [17] and respective methods and tools developed to calculate the marginal heat cost. One of the critical factors is the allocation of joint costs of CHP plants. In Denmark, where the regulated heating supply co-exists

with the liberalized electricity supply, there are two ways of allocating the costs. In small-scale CHP units, for which making profit in the electricity market is not allowed, the cost of fuel is allocated to heat and afterwards the income from selling the electricity is deducted from the total heat cost. This method has been used by Sjödin and Henning 2004 [38], after discussing different methods of allocation, and later adopted by [39] and [36]. In larger CHP plants, for which making profit in the electricity market is allowed, negotiations between the heating and electricity side define the sharing of the costs. We cannot disclose details for the calculation of the marginal heat production cost used in the present work, as it was performed with a tool developed and used by HOFOR A/S [37], and it is the company's confidential information. The basic components that were included in this calculation are heat demand, fuel costs, emission taxes, variable operation and maintenance costs of the plants, income from electricity sell and subsidies. The cost was used only as a signal, instead of using heat price on demand side, to reflect the potential of savings under a dynamic pricing scheme. Figure 2 presents the hourly data for the heat load (top) and the marginal heat production cost (bottom) in Greater Copenhagen calculated for a representative year.
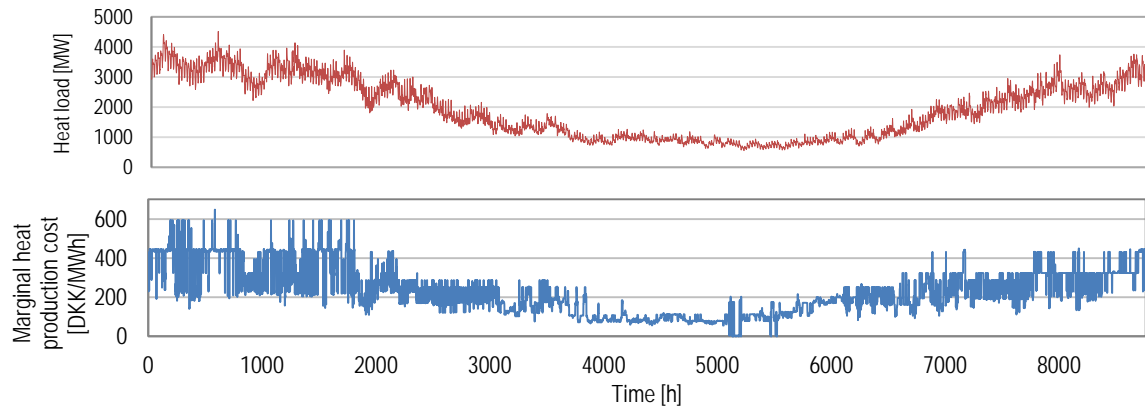
Figure 2: Hourly data for heat load (top) and marginal heat production cost (bottom) in Greater Copenhagen

The graphs show a seasonal pattern, having high heat load and high marginal heat production cost during the heating season, which both become lower in the intermediate season and lowest during summer. Analyzing the given data during the heating season, in order to identify potential patterns, Figure 3 (left) illustrates a heat map graph of the heat load, having on the x-axis the days of the heating season and on the y-axis the time of the day. Each time step is displayed with a small rectangle, which is colored based on the heat load value in that time step. This format shows both diurnal and seasonal patterns. In this study, heating season is the period November-March. Marginal heat production cost data are presented in the same format in Figure 3 (right).
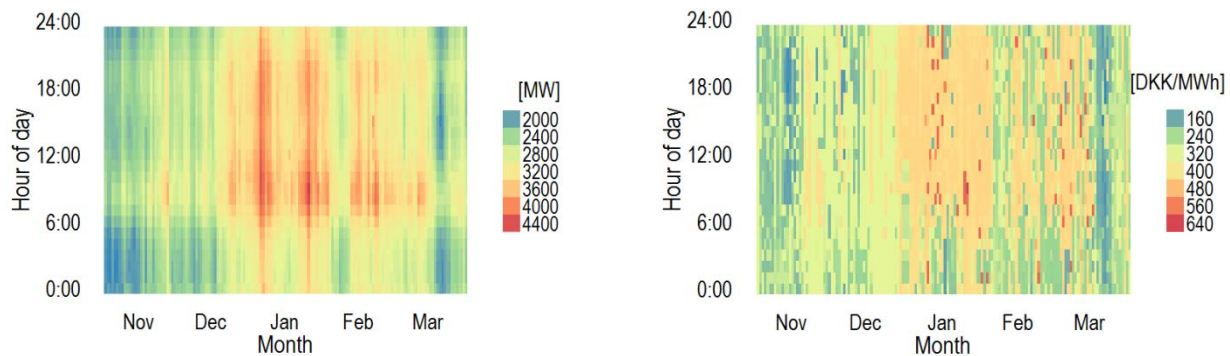
Figure 3: Heat map graph of heat load (left) and marginal heat production cost (right) in Greater Copenhagen during heating season

The graphs indicate a correlation between the heat production cost and the heat load, but only up to a certain extent, since there are many parameters that affect the cost, as previously explained. A clear diurnal pattern of heat load can be seen. A similar pattern is observed for the marginal heat production cost, but it is not as clear as it is for heat load.

2.2 Implementation

There are two main different approaches to implement demand response in the building sector: direct and indirect load

control [25], [40]. In the direct load control, the supplier controls directly the loads of the consumers and has the right to perform load modulations in order to facilitate the operation of the system. The indirect load control refers to ways of motivating consumers to participate in demand response, by adjusting the timing and/or the magnitude of their energy use [41]. Most often indirect control is realized based on costs; the supplier provides variable tariff schemes that will motivate the consumers to benefit from low-cost periods and avoid high-cost periods. The dynamics of the tariff scheme may vary, including time-of-year (seasonal) pricing, time-of-use pricing (daily or weekly variations), critical-peak pricing and real-time pricing. The consumers are informed about the prices one day or some hours in advance and decide whether or not to participate in this demand response activity. More demand response types can be found in literature [42], and different methods could also be combined. In our approach, indirect control was chosen assuming participation of all occupants of the examined building. Two indirect load control strategies were studied, assuming first the non-existence and second the existence of a communication platform between the building and the supplier:

- Assuming no communication platform between the building and the heat supplier, a constant strategy was implemented with one or two flexibility events every day during the whole heating season. This could be achieved with indirect control by giving monetary incentives to the occupants, for example fixed contract with time-of-use tariffs. The occupants set lower temperatures when the heat cost is high and vice versa. In this case, fixed schedules for temperature set-points were used (Section 2.2.1), determined based on average daily profiles of the heat load of the area and the marginal heat production cost.

- Assuming a communication platform between the building and the heat supplier, a signal is sent to the building from the supplier to communicate the need for load adjustment and the home management system modulates the temperature set-points according to this signal. In this case, the signal was the hourly marginal heat production cost (Section 2.2.2).

2.2.1   Fixed schedules for temperature set-points

Based on the average daily profiles of heat load and marginal heat production cost, it is, on average, favorable for the system to utilize heat during night time, in order both to flatten the heat load curve of Greater Copenhagen and to use heat with lower production cost. Figure 4 shows scenarios with scheduled temperature set-points. Scenario 1 allowed for lower indoor temperature during the day. Scenario 2 was more conservative in terms of thermal comfort, with the set-point being lower for shorter period, i.e. in the morning and afternoon. Scenario 3 had the same pattern as Scenario 1, but with higher temperature during night, in order to pre-heat the building before the lower temperature set-point period starts. Scenario 4 was similar to scenario 2, but with night pre-heating of the building. Two sets of modulations were performed, one with temperature range 21-23 °C and another one with 20-24 °C, in order to evaluate the potential with different ranges of thermal comfort. These scenarios were opposite from typical night setback. Night setback increases morning peak load, while in this study we aim to reduce the morning and evening peak loads.
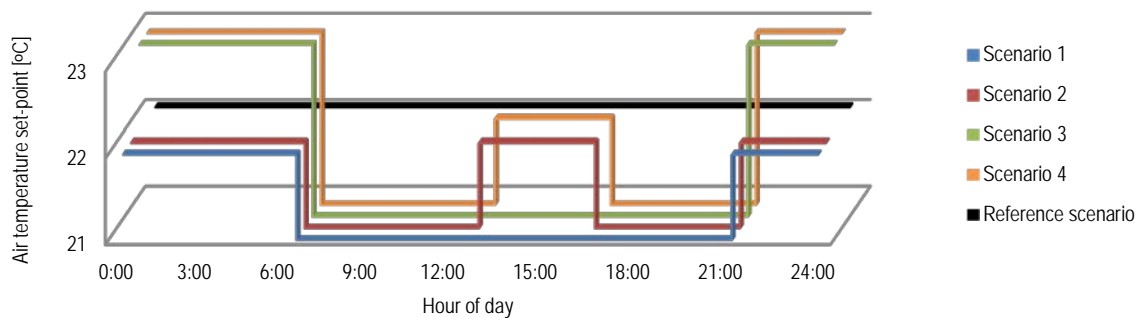
Figure 4: Scenarios for fixed schedules for temperature set-points with temperature range 21-23 °C

2.2.2   Dynamic temperature set-points

The aim of this strategy was to shift the energy use towards the hours when heat costs are low. Therefore, thresholds for the marginal heat production costs were set, according to which the building modulates the temperature set-points. When the signal was lower than the low cost threshold (C_{low}), the set-point was increased, in order to store heat in the thermal mass of the building. Likewise, when the signal was higher than the high cost threshold (C_{high}), the set-point was decreased to discharge the stored heat. When the signal was between the two thresholds, an interpolation for the set-point

was used given in Eq. 1. In addition, a deadband of 0.5 ºC was used to prevent the controller from activating for small temperature deviations.

$$T_{setpoint,i} = \begin{cases} T_{setpoint,min} \, , & C_i > C_{high} \\ T_{setpoint,max} \, , & C_i < C_{low} \\ \frac{T_{setpoint,max} - T_{setpoint,min}}{C_{high} - C_{low}} \cdot (C_{high} - C_i) + T_{setpoint,min} \, , & C_{high} \geq C_i \geq C_{low} \end{cases}$$
Eq. (1)

The marginal heat production cost has large seasonal variations and significant differences between the months of the heating season [17]. In the present work, the percentile distribution of marginal cost for each month was used and the thresholds referred to the respective percentiles of each month individually. Similar to the previous strategy, scenarios without and with pre-heating of the building were studied. Table 1 presents the scenarios examined with the minimum and maximum temperature set-point for each scenario, as well as low and high cost thresholds defined as percentiles of the monthly marginal cost. For scenarios without pre-heating (Scenarios 5-6), C_{low} was not needed, since the set-point was either decreased or maintained. In scenarios with different thresholds, the 25% or 50% percentile of the monthly cost distribution were used as C_{low}, and the 50% or 75% percentile of the monthly cost distribution were used as C_{high} (Scenarios 7-10). The temperature range used in these scenarios is 21-23 ºC, since the set-points were generally modulated more times per day than these of the fixed schedules, so ±2 ºC was not considered appropriate.

Table 1: Scenarios for dynamic modulations for temperature set-points with the respective cost thresholds

		$T_{setpoint, min}$	$T_{setpoint, max}$	C_{low}	C_{high}
Scenario 5	No pre-heating	21 ºC	22 ºC	-	50%
Scenario 6	No pre-heating	21 ºC	22 ºC	-	75%
Scenario 7	Pre-heating	21 ºC	23 ºC	25%	75%
Scenario 8	Pre-heating	21 ºC	23 ºC	50%	75%
Scenario 9	Pre-heating	21 ºC	23 ºC	25%	50%
Scenario 10	Pre-heating	21 ºC	23 ºC	50%	50%

2.2.3 Performance evaluation

For the scenarios examined, the following parameters were evaluated.

i. The total energy used for space heating of the building for the whole heating season, given by Equation (1):

$$E_{tot} = \sum_1^{heating\ season} E_i \tag{2}$$

where: E_i , the space heating energy use for every hour.

ii. The total production cost of the heat that was used in the building for space heating. It is given by Equation (2):

$$MHPC_{tot} = \sum_1^{heating\ season} E_i \cdot MHPC_i \tag{3}$$

where: $MHPC_i$, the marginal heat production cost of every hour.

iii. The indoor operative temperature, as an indicator of thermal comfort [35]. For the sake of clarity, the operative temperature of the critical apartment is presented, which is a top-corner apartment and was chosen because of its higher exposure to ambient conditions.

iv. The energy used for space heating of the building between 6:00-9:00, namely the morning peak load hours [43].

v. The potential for flexible operation, based on two flexibility indicators, equivalent to the one defined in [44]:

a) Evaluation of total energy use during high load hours versus during low load hours according to Equation (3):

$$F_1 = \frac{E_{low\ load} - E_{high\ load}}{E_{low\ load} + E_{high\ load}} \tag{4}$$

where: $E_{high\ load}$, the total space heating energy use during high load hours, between 6:00–21:00,

$E_{low\ load}$, the total space heating energy used during low load hours, between 21:00-6:00 (next morning). The indicator ranges between -1 and 1, with the optimal operation being when $F_1 = 1$, namely energy was used only during low load hours.

b) Evaluation of total energy use during high production cost hours versus during low production cost hours, according to Equation (4):

$$F_2 = \frac{E_{low\ cost} - E_{high\ cost}}{E_{low\ cost} + E_{high\ cost}} \tag{5}$$

where: $E_{high\ cost}$, the total space heating energy use during high production cost hours, when the cost was

higher than the median value of costs of each month, $E_{low\ cost}$, the total space heating energy use during low production cost hours, when the cost was lower than the median value of costs of each month. The indicator ranges between -1 and 1, with the optimal operation being when $F_2 = 1$, namely energy is used only during low production cost hours.

The scenarios were implemented for the entire heating season and were evaluated based on parameters *i*, *ii* and *iii*. A selection of the implemented scenarios was further evaluated using average load and temperature profiles and parameters *iv* and *v*. Evaluation of the scenarios was also performed for a cold day in Denmark with average ambient temperature of -8ºC and daily solar irradiance of 2.2 kWh/m²/day.

2.3 Building model

The building type studied was a multifamily apartment block (Figure 5), designed according to the Danish Building Regulation 2015 (BR15) [30]. It represents a typical Danish building of this type, it is heavy-weight and well insulated, as according to BR15, "the total demand of the building for energy supply for heating, ventilation, cooling and domestic hot water must not exceed 30.0 kWh/m² per year plus 1000 kWh per year divided by the heated floor area". The design, construction and materials chosen were in accordance with BR15 and Danish Building Research Institute (SBi) Guidelines 'Energy Demand for Buildings' [45]. Some details were supplemented by TABULA Webtool [46].
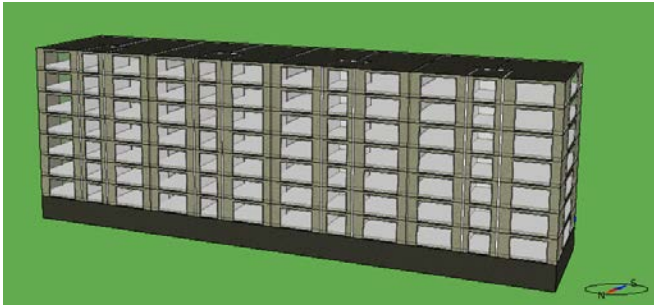
Figure 5: Apartment block model

The building has a net heated floor area of 6272 m² and envelope area per volume 0.265 m²/m³. It consists of 7 floors and an unheated basement. Each floor has 8 apartments with the same floor area of 112 m² each, and 4 staircases with the same floor area of 21 m² each. The windows comprise 22.5% of the heated floor area and are distributed 52% south, 37% north and 11% east/west. The apartment block is modelled as one thermal zone per apartment and one thermal zone per staircase, using adequate zone multiplication of the zones that present similar thermal behavior. The building is connected to the DH grid. In this study only space heating was investigated, as the objective of the work was to evaluate the storage of the building structure itself. The heat emission system is low temperature water radiators of maximum heating power 14 W/m² heated floor area and the supply water temperature to the system is 45°C. There is mechanical ventilation in the building with constant air volume of 0.3 l/s per m² of heated floor area with heat recovery of 67% efficiency[1], according to BR15. Detailed information of the building model can be found in [33]. The simulations were performed with the building performance simulation software IDA Indoor Climate and Energy, version 4.7 [47]. It is a dynamic whole-building simulation tool based on symbolic equations stated in Neutral Modeling Format (NMF) that has undergone validation tests [48–51]. The building, systems, controls, network airflow, etc. are simulated in an integrated way and the time-step varies dynamically during runtime to automatically adapt to the nature of the problem.

2.3.1   Boundary conditions

The boundary conditions contribute significantly to the performance of structural thermal mass as storage medium. The ambient weather conditions used in this study were weather data collected from the DTU Climate Station [52] for the year corresponding to the heat load and marginal heat production cost data. Figure 6 presents indicatively the ambient air temperature and global solar irradiance.

---

[1] When this study was finished, the new building regulation 2018 (BR18) was published. The only difference in the new regulation is the efficiency of heat recovery of the ventilation system for apartment blocks, which, in the new code, is 80%. If the simulations were run according to BR18, the only difference in the results would be the heating demand for the apartment block, which would slightly decrease.
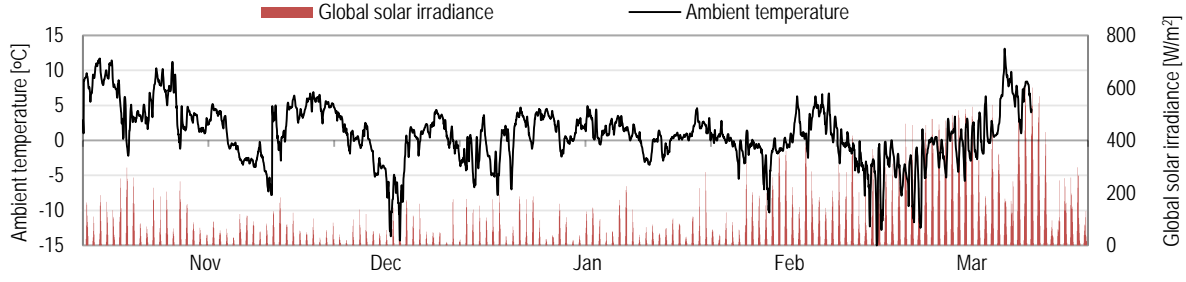
Figure 6: Ambient air temperature and global solar irradiance for the heating season
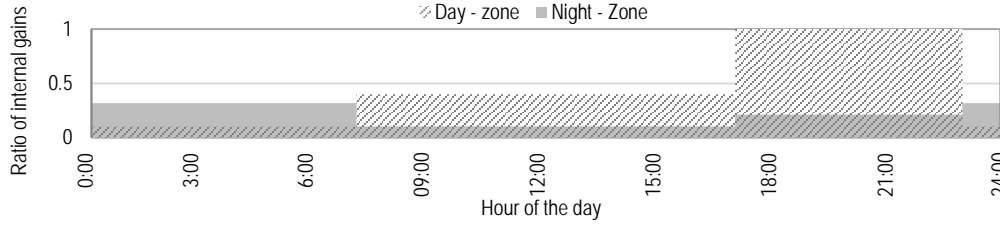
Figure 7: Schedules for internal gains according to DS/EN ISO 13790:2008

The internal heat gains included heat emitted from lighting, equipment and occupants. The schedules for the internal gains were set according to the standard DS/EN ISO 13790:2008 Table G.8 [53], which were different for primarily day or night occupied zones. Since in the model there was one thermal zone per apartment, two components of internal gains were used in the same zone, one for each schedule. Figure 7 shows the ratio of internal gains compared to the maximum internal gains for every hour of the day. The total heat flow rate from internal gains was 5 W/m², which was lower than the one indicated by the standard [53], but it was adjusted in order to meet the average Danish national values [45].

3. Results

During the reference operation of the building, namely when the building was controlled with constant temperature set-point at 22ºC, the energy use for space heating was 12 kWh/(year·m² net heated floor area) and the peak demand was 82 kW (13.1 W/m²). Details on the energy performance, the thermal behavior and the physically available energy flexibility of this building can be found in [33].

This section presents the results of the flexibility potential when the building was operated during the entire heating season. Firstly, an example of the control operation is presented for one week of February, in order to demonstrate the operation of the two different strategies implemented, namely fixed set-point modulations (e.g. Scenario 3) and dynamic set-point modulations reacting to the signal (e.g. Scenario 9). Figure 8 (top) depicts the heat load of Greater Copenhagen and Figure 8 (middle) the marginal heat production cost, as well as C_{low} and C_{high} for Scenario 9. Figure 8 (bottom) shows the respective set-points according to Scenario 3 and Scenario 9.
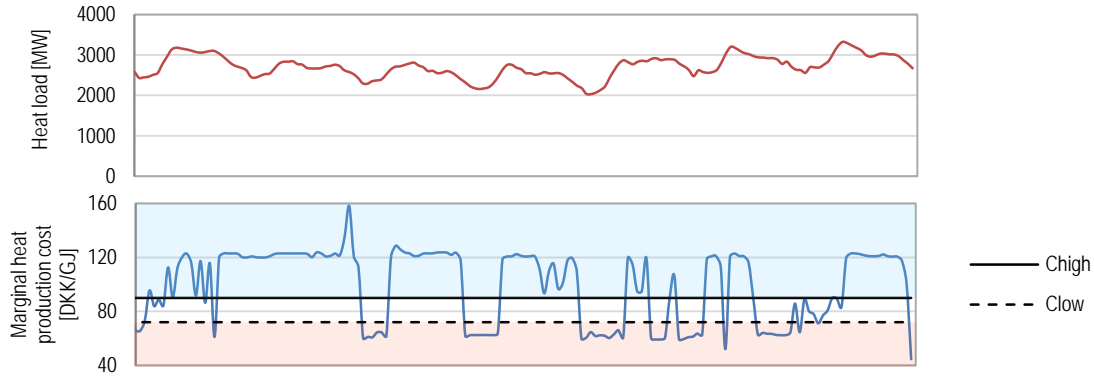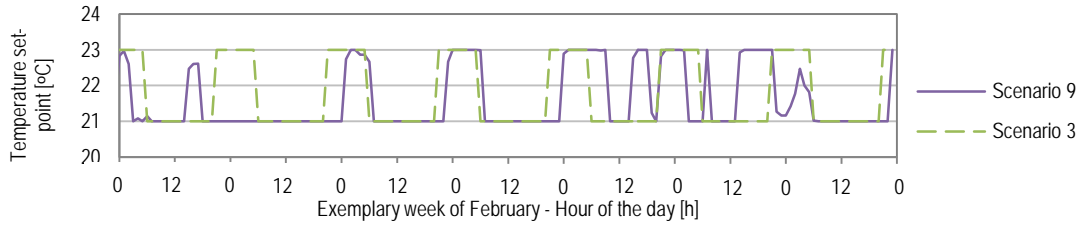
Figure 8: Exemplary week of February. Top: Heat load in Greater Copenhagen., Middle: Marginal heat production cost, C_{high} and C_{low} for Scenario 9. Bottom: Temperature set-points according to Scenario 3 and Scenario 9

In Scenario 3, the set-point was modulated at fixed hours, thereby it roughly followed inversely the heat load pattern by increasing the demand at night, when the heat load on the district heating system is usually lower. Scenario 9 reacted inversely to the cost signal, aiming to utilize heat when it costs less to be produced. There was a correlation in the patterns of the marginal heat production cost and the heat load, which was reflected in the operation of the control set-points of Scenarios 3 and 9, but only to a certain extent. For instance, in this exemplary week, during the second day the set-point of Scenario 9 remained unaltered, while in the fifth and sixth day it was modulated more often than that of Scenario 3.

3.1 Effects of fixed schedules for temperature set-points

This subsection presents the results for the scenarios that control the temperature with fixed set-point schedules. Figure 9 presents the difference between the reference operation of the building and each scenario examined. The top figure shows the cost of heat used in the building during the heating season, while the middle figure shows the total energy use during the heating season. The bottom figure shows box plots of the operative temperature in the critical apartment across the heating season, for the reference operation and the scenarios examined.
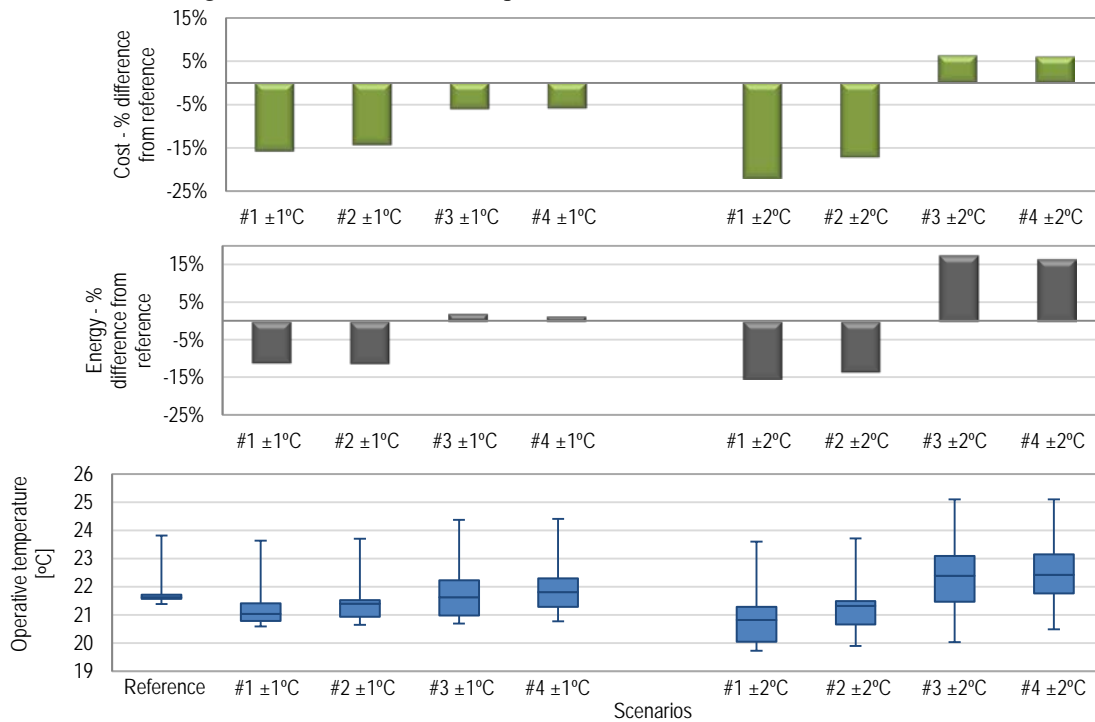
Figure 9: Effects of fixed schedules. Top: Percentage difference of cost between the reference operation and each scenario. Middle: Percentage difference of energy use between the reference operation and each scenario. Bottom: Box plots of operative temperature in the critical apartment during the heating season for the reference operation and each scenario.

For Scenarios 1 and 2, using the ±1ºC modulation schemes, the cost was lower by 15.5% and 14% respectively for the two scenarios compared to the reference operation of the building, while the total energy use was lower by 11%. This difference is attributed to the lower operative temperatures throughout the heating season. The mean value of the operative temperatures was lower by 0.6 ºC for Scenario 1 and by 0.3 ºC for Scenario 2. Scenarios 3 and 4, which pre-heat the building during the night, presented a different behavior. The cost was decreased by 6%, while the total energy use was marginally increased by 2% and 1.5 %, respectively. The mean operative temperature was almost the same as in

the reference operation, but temperature was fluctuating within a wider range. Thereby, although using marginally higher energy, the cost was decreased with small thermal comfort variations.

When the same schedules were implemented but with ±2 ºC, the differences were apparent. For the two scenarios without pre-heating of the building, both the cost and the energy use decrease were higher, but at the expense of lower operative temperatures, which dropped below 20 ºC. For the scenarios with pre-heating of the building during the night, there was higher cost and total energy use compared to the reference operation, which is attributed to the overall higher operative temperatures. Furthermore, the temperature fluctuations were strong, which in many cases are associated with thermal discomfort. Therefore, those strategies with set-point modulations of ±2 ºC are not recommended for a control strategy of daily fixed schedules throughout the heating season in a low-energy building, but they can be possibly used for occasional events with other control strategies.

3.2 Effects of dynamic temperature set-points

This subsection presents the results for the scenarios that control the temperature according to the signal of marginal heat production cost. Figure 10 presents the difference between the reference operation of the building and each scenario examined. The top figure shows the cost of heat used in the building during the heating season, while the middle figure shows the total energy use during the heating season. The bottom figure shows box plots of the operative temperature in the critical apartment across the heating season, for the reference operation and the scenarios examined.
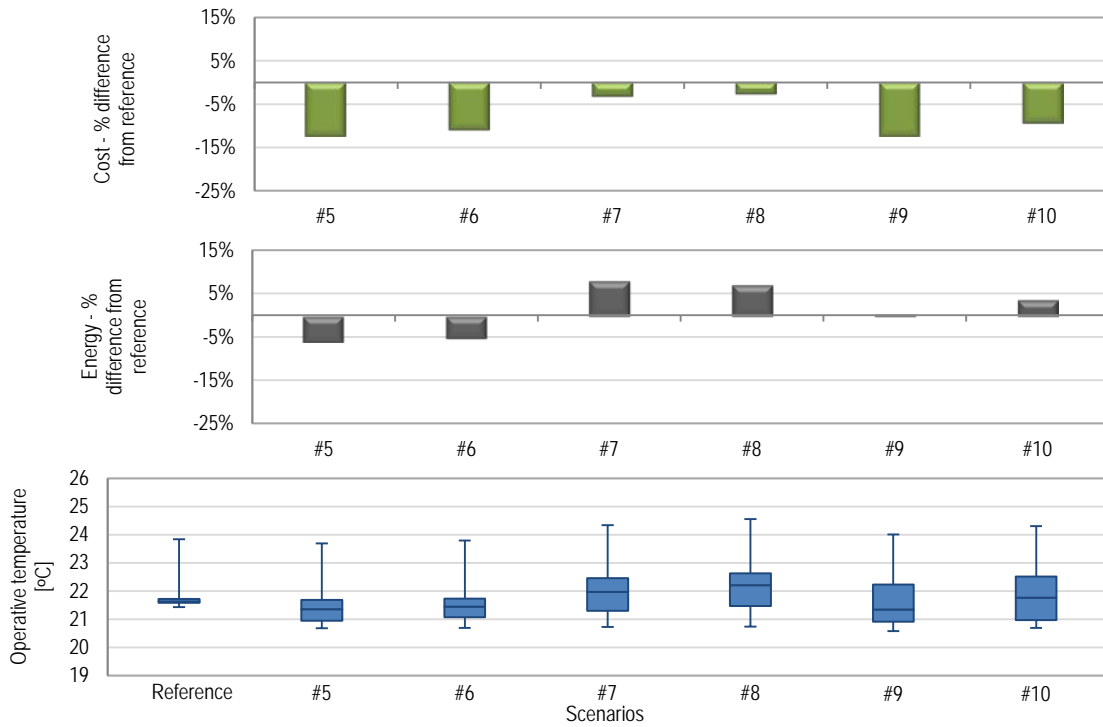
Figure 10: Effects of dynamic signal. Top: Percentage difference of cost between the reference operation and each scenario. Middle: Percentage difference of energy use between the reference operation and each scenario. Bottom: Box plots of operative temperature in the critical apartment during the heating season for the reference operation and each scenario.

All scenarios implemented achieved cost reduction between 3% and 12%, while the effect on energy use and operative temperatures varied among the different scenarios. Scenarios 5 and 6, which allowed only decrease of temperature set-point, not increase, behaved similarly to Scenarios 1 and 2, but the effects were at a slightly lower magnitude. In Scenarios 5 and 6 cost was reduced by 12% and 11%, and energy by 6% and 5%. The median temperature was lower by 0.3 ºC and 0.2 ºC respectively, while there were marginally wider temperature ranges. Scenarios 7 and 8 set the high cost threshold higher than the other scenarios, so the temperature set-point is decreased less often. As a result, overall higher temperatures occurred compared to the other dynamic scenarios and the reference operation; thereby, higher total energy was used. Although cost was still decreased, the magnitude of the decrease was lower than any other dynamic scenario. Scenario 9 set the low cost threshold at the 25% percentile, so the temperature set-point was increased less often. There was a significant decrease of cost by 12%, while the energy use was almost the same as the reference operation. The mean operative temperature was moderately lower and the temperature fluctuated within a wider range. Scenario 10 set both the high and the low thresholds approximately at the median value of the costs, such that the temperature set-point is

frequently modulated. This led to a wide temperature range and higher energy use by 3.5%. Nevertheless, the costs were still lower by 9%.

3.3 New heating profiles and energy flexibility

Based on the evaluation of the performance of scenarios so far, half of the scenarios were selected, in order to further investigate the effects of their implementation. Scenarios 1-4, which modulate the temperature by ±1°C, were selected for the fixed schedules. From the scenarios with dynamic signals, Scenarios 5, 6 and 9 were selected, since higher cost decrease was achieved. The average daily heat load patterns were calculated for the different scenarios and are depicted in Figure 11 (left), together with that of Greater Copenhagen (right axis). Figure 11 (right) presents the average daily profile of indoor temperatures in the different scenarios and the reference operation.
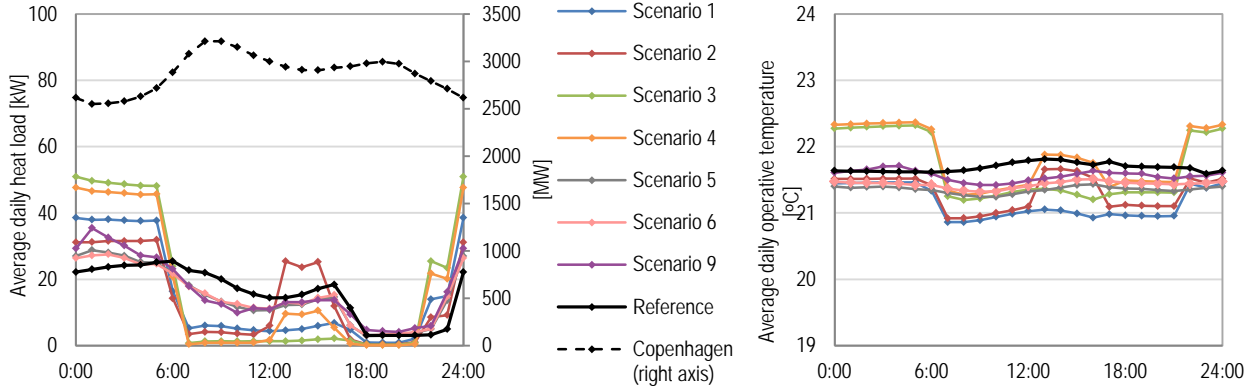
Figure 11: Left: Average daily heat load of the building in different scenarios and reference operation (left axis); average daily heat load in Greater Copenhagen (right axis). Right: Average daily operative temperature in different scenarios and reference operation

For all scenarios implemented, the maximum load was increased compared to the reference operation. The scenarios with pre-heating of the building presented higher peak loads, which was expected since the temperature increase that needed to be achieved, i.e. from 21 °C to 23 °C, was higher, hence the peak load was higher. The scenarios which only decreased the set-point presented a behavior closer to that of the reference operation. The occurrence of new peak loads was a result that was anticipated, but it is under discussion whether it undermines the implementation of those strategies. In terms of the building itself, the new peaks were within the installed capacity of the heating system, so no additional investment would be required. Therefore, technically for the building it is not problematic. Regarding the DH system, the time when the new peaks occur is essential. For all scenarios the highest heating use occurred during the night period, i.e. 21:00 -6:00, with new peaks been created at the transition between the day set-point to the night set-point. This means that the new peaks occurred at hours when the overall load of the system is low, and on average the marginal heat production cost is low. Thereby, the new peaks may not pose challenges to the system; however this would depend on the scale of the implementation. In all cases, load shifting from day to night was achieved, so the daily load pattern of the building acted towards smoothing the load of the Greater Copenhagen, which was indeed one of the targets.

The morning peak in the heat load of Greater Copenhagen which occurs between 6:00-9:00 could be mitigated by lowering the space heating demand in this type of buildings during this period. All scenarios examined had lower energy use during this period, but the scenarios with fixed schedules for set-points achieved higher reductions. The highest reductions in the morning energy use were achieved in Scenarios 4 and 3 by 86.5% and 83% respectively. For the scenarios with dynamic response to the cost signal the reductions were around 41%. The evening peak in the heat load of Greater Copenhagen, which occurs around 19:00, cannot be mitigated with these scenarios in this type of buildings, since the space heating demand for the reference operation was already minimal due to the internal heat gains during these hours.

Regarding the average daily profile of indoor temperatures, the scenarios with the fixed temperature schedules presented a clear pattern, with Scenarios 1 and 2 being constantly below the temperatures of the reference operation, while Scenarios 3 and 4 fluctuated higher and lower than those of the reference. In scenarios with dynamic signals the average daily pattern appeared to be smooth, with small fluctuations during the day. Although in Figure 10 it was shown that the indoor temperatures in these scenarios covered a broader spectrum of temperatures, when they were averaged on a daily basis they levelled out to smooth profiles.

Figure 12 presents the performance of the implemented scenarios according to the two flexibility indicators described

in Section 2.2.3. Flexibility indicator F_1 (blue bars), evaluates the total energy use during high load versus low load hours. The optimal operation is when the flexibility indicator is equal to 1, namely energy is used only during low load hours. Flexibility indicator F_2 (green bars), evaluates the total energy use during high production cost versus low production cost hours. The optimal operation is when the flexibility indicator is equal to is 1, namely energy is used only during low production cost hours.
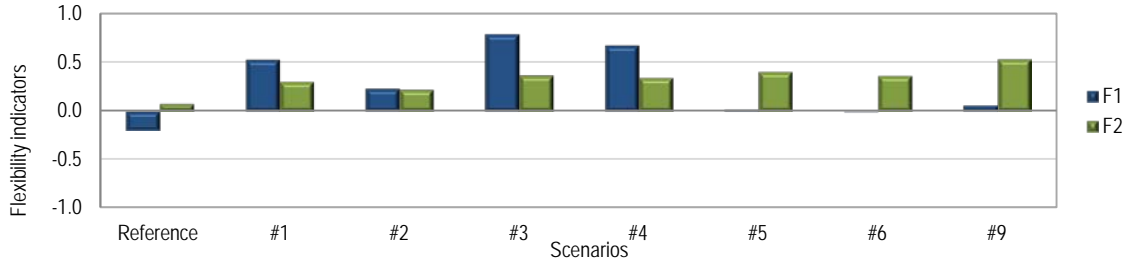
Figure 12: Flexibility indicators in different scenarios and reference operation

It can be seen that for all scenarios, both indicators improved compared to the reference operation of the building. F_1 for the reference operation was -0.20, namely there was higher energy use during the high load hours than during low load hours. The scenarios with fixed schedules for set-points achieved higher values for F_1. The highest value of F_1 was achieved for Scenario 3 (0.79) followed by Scenario 4 (0.67), which were the scenarios with pre-heating during night. The scenarios with dynamic response to the cost signal, improved the indicator compared to the reference operation, but only to a lower degree. Regarding F_2, during reference operation of the building it was almost 0, which means that there was equal energy use during high and low production cost period. The scenarios with dynamic response to the cost signal achieved higher values, with Scenario 9 being the highest with 0.52.

Table 2 shows the average performance and flexibility potential from the implementation of the selected scenarios.

Table 2: Average performance and flexibility potential in different scenarios during the heating season

Scenarios	Difference from reference operation				F1	F2
	Cost [%]	Energy use in morning [%]	Average temperature [ºC]	Total energy [%]		
Reference	–	–	–	–	-0.20	0.08
Scenario 1	-15.5%	-74.0%	-0.6	-10.8%	0.53	0.30
Scenario 2	-14.0%	-80.6%	-0.4	-11.0%	0.23	0.22
Scenario 3	-6.0%	-83.0%	0.0	2.1%	0.79	0.36
Scenario 4	-5.8%	-86.5%	0.1	1.4%	0.67	0.34
Scenario 5	-12.2%	-40.6%	-0.3	-6.0%	0.02	0.40
Scenario 6	-10.7%	-40.7%	-0.2	-5.1%	-0.01	0.36
Scenario 9	-12.2%	-42.7%	-0.3	0.3%	0.06	0.52

- Scenario 1 presented the highest cost decrease of 15.5%, as well as energy decrease of 10.8%. However, this was at the expense of lower indoor temperature, which was reduced by 0.6 ºC compared to the mean temperature of the reference operation.
- Scenario 3 achieved the highest indicator of load shifting during night time, namely 0.79. Cost was decreased by 6%, but energy use was moderately increased by 2.1%. The mean indoor temperature was the same as that of the reference operation, but with more fluctuations during the day.
- Scenario 4 achieved the highest decrease in energy use during morning peak hours by 86.5%. Cost was decreased by 5.8%, with only small differences in the total energy use and mean indoor temperature.
- Scenario 9 achieved the highest indicator of load shifting during periods with lower heat production cost, namely 0.52. Cost was decreased by 12.2%, with almost the same energy use as the reference scenario. The mean indoor temperature slightly lower than that of the reference operation and fluctuated within a wider temperature range.

The study was performed across the entire heating season; however, the weather is expected to have significant influence among the various scenarios. Indicatively, Table 3 presents the average performance evaluation and flexibility potential of the selected scenarios during a cold day of the heating season.

Table 3: Average performance and flexibility potential in different scenarios during a cold day

Scenarios	Difference from reference operation				F1	F2
	Cost [%]	Energy use in morning [%]	Average temperature [ºC]	Total energy [%]		

Reference	−	−	−	−	0.03	-0.77
Scenario 1	-4.4 %	-75.1 %	-0.5 °C	-0.1 %	0.80	-0.55
Scenario 2	-8.0 %	-79.5 %	-0.2 °C	-2.9 %	0.57	-0.60
Scenario 3	28.1 %	-80.9 %	0.1 °C	36.6 %	0.88	-0.51
Scenario 4	14.7 %	-80.9 %	0.3 °C	21.7 %	0.87	-0.51
Scenario 5	-41.7 %	-69.7 %	-0.7 °C	-18.2 %	0.63	0.24
Scenario 6	-35.7 %	-72.7 %	-0.7 °C	-9.2 %	0.41	0.08
Scenario 9	-40.4 %	-79.2 %	-0.7 °C	0.0 %	0.82	0.65

For the scenarios with fixed schedules, during a very cold day the potential for cost reduction was lower and F_2 was considerably lower than the average of the heating season. Scenarios 3 and 4 that pre-heated the building during the night resulted in higher costs and considerably higher energy use. The scenarios with dynamic response to the cost signal, achieved considerable cost reduction, but at the expense of lower indoor temperatures.

4. Discussion

Choosing which of the scenarios to implement is a multifactorial decision. First and foremost, it depends on the services that energy flexible buildings should provide to the energy system. It may be the minimization of energy use during specific hours, the reduction of cost, the alleviation of local congestion problems, or the smoothing of the overall heat load. Furthermore, the aforementioned results may come at the expense of a wider temperature range and/or more fluctuations in the indoor temperature during the day. The level of acceptance of thermal comfort changes may as well affect the choice of the strategy to be implemented. In some cases higher total energy was observed, but this may be considered acceptable, as it is still costs less and it is probably less carbon intensive.

The signals used in this study have a significant influence on the obtained results. Different signals can be used to trigger the flexibility of a building, such as CO_2 emissions or preferably the actual heat prices. To date, in Denmark the heat price paid by the customers is constant across the year and fixed by individual contracts, so there is no incentive for the individual customers to participate in similar strategies and decrease their energy use during peak hours. However, dynamic heat pricing is under research and it was the scope of this work to identify if there is potential for this type of building to be operated flexibly. By using different signals, the quantification of the results and metrics may be different, but the thermal response of the building is anticipated to be similar. Further work towards demand response in building connected to DH is needed and it will heavily depend on the specific DH market structure.

In this study, the approach that was followed was an indirect load control assuming that all occupants of the building participated in the control strategy. Reality would probably be different, as in the indirect load control occupants would have the choice not to participate, i.e. adjust their set-points. This would result in effects of a different magnitude than those simulated in this study. The percentage of occupants who participate in the control scheme is an important parameter when planning to implement flexibility strategies in residential buildings. Another important parameter, especially if using thermal mass as storage to facilitate flexibility, is the thermal comfort acceptability range of occupants which can vary significantly, as it was also pointed out by [24], who performed a field study on a sample of 28 homes in England deploying heating system demand-shifting with a focus on occupants' thermal comfort. In the present study, this may be more critical since many of the proposed scenarios suggest opposite set-points to typical night set-back schedules. Nevertheless, for occupants to be willing to accept the changes on thermal comfort if their buildings should be operated flexibly, they need to be properly informed and motivated. Since monetary incentives are those, which mostly attract attention and motivate participation [24], [41], it should be further investigated how the benefits achieved for the system at the production side could be reflected to the prices that the occupants pay.

In addition to their decision whether to participate in flexibility strategies or not, occupants of residential buildings have an impact on the flexibility potential with their behavior, in terms of occupancy patterns and thermal comfort preferences. The schedule and intensity of the occupants' patterns affect significantly the internal gains in the building, especially in low-energy buildings, and thus the demand that the heating system should cover. Furthermore, the thermal comfort preference, i.e. temperature set-point, affects significantly the heating demand; thereby, the potential for flexible operation. In this study, a deterministic occupancy pattern from standards was used and a reference set-point of 22 °C constantly, which is a typical desired indoor temperature in Danish households during the heating season. However, those may be different in reality, thus more representative or stochastic models for occupants' behavior would improve the realism of the obtained results [54–57].

An important parameter to be further investigated is the effect of the implementation of those scenarios on the district

or city level. In the scenarios implemented, new peak loads were created in the building, at the beginning of low production cost or low system load periods. In order to avoid disturbances in the system, a smoother ramp in the heating set-point control in the building could be set and/or the heat supplier could send signals which are slightly shifted in time to different categories of consumers. The specific design of the district heating system in the area, as well as hydraulic constraints should be considered as well.

5.   Conclusions

This paper modelled the potential for a low-energy residential building to be operated flexibly, according to the needs of the district heating system. The structural thermal mass was used as storage medium to facilitate the flexible operation of the building, which was achieved by modulating the indoor air temperature set-point. Different control strategies were implemented, determined based on the marginal heat production cost and the heat load of Greater Copenhagen. The different control signals triggered an increase or decrease of the air temperature set-point, in order to charge or discharge the thermal mass. Based on the average daily profiles of heat load and marginal heat production cost, it was, on average, favorable for the system to utilize heat during night time, as the total heat load in the area is low and base load boilers are normally used. Thus, heat costs less to be produced, and it is less carbon-intensive. With all scenarios implemented, load shifting was achieved between 40% and 87%. In most scenarios, the total energy use either increased by up to 2% or decreased by up to 18% and there were also reduced costs, except scenario 3 and 4 on the cold winter day.   This is due to higher heat loss from the building on the extremely cold day. Higher energy use may be considered acceptable, as it costs less to be produced and can be beneficial for the environment if it comes from renewable sources. With pre-heating at night, a significant energy reduction in the morning was reached, which was up to 86.5%. With the implemented strategies, new peaks in the heating load of the building were created. However, since they occurred during low load hours and were within the installed capacity of the building heating system, they are not considered as an impediment to the proposed strategies. The thermal environment was changed, as a wider temperature range and/or more frequent fluctuations in the indoor temperature occurred. The choice of the best performing scenario is not straightforward, as it would depend on the services that the building is to offer to the district heating system. Some scenarios indicated higher potential for cost reduction, or achieved greater load shifting. The magnitude of the achieved benefits is associated with the acceptable changes in the energy use and in the thermal comfort set by the occupants of the building.

More control strategies could be investigated, with different boundary conditions and temperature ranges, or using different data to create control signals. However, this study showed that there is potential in low-energy residential buildings to be operated flexibly, utilizing the thermal mass of the buildings as short term energy storage. Further investigations are to be performed in this research topic and real-life demonstrations are taking place within the EnergyLab Nordhavn project.

References

[1]   A.H. Mohsenian-Rad, V.W.S. Wong, J. Jatskevich, R. Schober, A. Leon-Garcia, Autonomous demand-side management based on game-theoretic energy consumption scheduling for the future smart grid, IEEE Trans. Smart Grid. 1 (2010) 320–331. doi:10.1109/TSG.2010.2089069.

[2]   H. Lund, A.N. Andersen, P.A. Østergaard, B.V. Mathiesen, D. Connolly, From electricity smart grids to smart energy systems - A market operation based approach and understanding, Energy. 42 (2012) 96–102. doi:10.1016/j.energy.2012.04.003.

[3]   H. Lund, P.A. Østergaard, D. Connolly, I. Ridjan, B.V. Mathiesen, F. Hvelplund, J.Z. Thellufsen, P. Sorknæs,

Energy Storage and Smart Energy Systems, Int. J. Sustain. Energy Plan. Manag. 11 (2016) 3–14. doi:10.5278/ijsepm.2016.11.2.

[4]   M. Münster, P.E. Morthorst, H. V. Larsen, L. Bregnbæk, J. Werling, H.H. Lindboe, H. Ravn, The role of district heating in the future Danish energy system, Energy. 48 (2012) 47–55. doi:10.1016/j.energy.2012.06.011.

[5]   T. Nuytten, B. Claessens, K. Paredis, J. Van Bael, D. Six, Flexibility of a combined heat and power system with thermal energy storage for district heating, Appl. Energy. 104 (2013) 583–591. doi:10.1016/j.apenergy.2012.11.029.

[6]   H. Cai, C. Ziras, S. You, R. Li, K. Honoré, H.W. Bindner, Demand side management in urban district heating networks, Appl. Energy. 230 (2018) 506–518. doi:10.1016/j.apenergy.2018.08.105.

[7]   J. Heier, C. Bales, V. Martin, Combining thermal energy storage with buildings – a review, Renew. Sustain. Energy Rev. 42 (2015) 1305–1325. doi:10.1016/j.rser.2014.11.031.

[8]   A. Arteconi, N.J. Hewitt, F. Polonara, State of the art of thermal storage for demand-side management, Appl. Energy. 93 (2012) 371–389. doi:10.1016/j.apenergy.2011.12.045.

[9]   H. Johra, P. Heiselberg, Influence of internal thermal mass on the indoor thermal dynamics and integration of phase change materials in furniture for building energy storage: A review, Renew. Sustain. Energy Rev. 69 (2017) 19–32. doi:10.1016/j.rser.2016.11.145.

[10]   N.J. Hewitt, Heat pumps and energy storage - The challenges of implementation, Appl. Energy. 89 (2012) 37–44. doi:10.1016/j.apenergy.2010.12.028.

[11]   G. Reynders, T. Nuytten, D. Saelens, Potential of structural thermal mass for demand-side management in dwellings, Build. Environ. 64 (2013) 187–199. doi:10.1016/j.buildenv.2013.03.010.

[12]   D. Patteeuw, G. Reynders, K. Bruninx, C. Protopapadaki, E. Delarue, W. D'haeseleer, D. Saelens, L. Helsen, CO2-abatement cost of residential heat pumps with active demand response: Demand- and supply-side effects, Appl. Energy. 156 (2015) 490–501. doi:10.1016/j.apenergy.2015.07.038.

[13]   L. Schibuola, M. Scarpa, C. Tambani, Demand response management by means of heat pumps controlled via real time pricing, Energy Build. 90 (2015) 15–28. doi:10.1016/j.enbuild.2014.12.047.

[14]   T.Q. Péan, J. Salom, J. Ortiz, Potential and optimization of a price-based control strategy for improving energy flexibility in Mediterranean buildings, Energy Procedia. 122 (2017) 463–468. doi:10.1016/j.egypro.2017.07.292.

[15]   E. Nyholm, S. Puranik, É. Mata, M. Odenberger, F. Johnsson, Demand response potential of electrical space heating in Swedish single-family dwellings, Build. Environ. 96 (2016) 270–282. doi:10.1016/j.buildenv.2015.11.019.

[16]   M. Åberg, L. Fälting, A. Forssell, Is Swedish district heating operating on an integrated market? - Differences in pricing, price convergence, and marketing strategy between public and private district heating companies, Energy Policy. 90 (2016) 222–232. doi:10.1016/j.enpol.2015.12.030.

[17]   H. Li, Q. Sun, Q. Zhang, F. Wallin, A review of the pricing mechanisms for district heating systems, Renew. Sustain. Energy Rev. 42 (2015) 56–65. doi:10.1016/j.rser.2014.10.003.

[18]   J. Song, F. Wallin, H. Li, District heating cost fluctuation caused by price model shift, Appl. Energy. 194 (2017) 715–724. doi:10.1016/j.apenergy.2016.09.073.

[19]   F. Wernstedt, P. Davidsson, C. Johansson, Demand side management in district heating systems, Proc. 6th Int. Jt. Conf. Auton. Agents Multiagent Syst. - AAMAS '07. 5 (2007) 1. doi:10.1145/1329125.1329454.

[20]   C. Johansson, F. Wernstedt, P. Davidsson, Deployment of Agent Based Load Control in District Heating Systems, First Int. Work. Agent Technol. Energy Syst. (ATES 2010). (2010) 75–82.

[21]   D. Basciotti, R.-R. Schmidt, Demand side management in district heating networks: Simulation Case Study on Load Shifting, Euro Heat Power. 10 (2013) 43–46.

[22]   D.F. Dominković, P. Gianniou, M. Münster, A. Heller, C. Rode, Utilizing thermal building mass for storage in district heating systems: Combined building level simulations and system level optimization, Energy. 153 (2018) 949–966. doi:10.1016/j.energy.2018.04.093.

[23]   J. Kensby, A. Trüschel, J.-O. Dalenbäck, Potential of residential buildings as thermal energy storage in district heating systems – Results from a pilot test, Appl. Energy. 137 (2015) 773–781. doi:10.1016/j.apenergy.2014.07.026.

[24]   T. Sweetnam, C. Spataru, M. Barrett, E. Carter, Domestic demand-side response on district heating networks, Build. Res. Inf. 0 (2018) 1–14. doi:10.1080/09613218.2018.1426314.

[25]   S. Kärkkäinen, K. Sipilä, L. Pirvola, J. Esterinen, E. Eriksson, S. Soikkeli, Demand side management of the

district heating systems, (2003) 104. http://www.vtt.fi/inf/pdf/.

[26] J. Van Deventer, J. Gustafsson, J. Delsing, Controlling district heating load through prices, 2011 IEEE Int. Syst. Conf. SysCon 2011 - Proc. (2011) 461–465. doi:10.1109/SYSCON.2011.5929104.

[27] Danish Energy Agency, Regulation and planning of district heating in Denmark, 2015. http://www.ens.dk/sites/ens.dk/files/climate-co2/Global-Cooperation/Publications/Publications/regulation_and_planning_of_district_heating_in_denmark.pdf.

[28] Energistyrelsen, Energistatistik 2016, Data, tabeller, statistikker og kort, Copenhagen, 2017. https://ens.dk/sites/ens.dk/files/Statistik/estat2016.pdf.

[29] Varmelast.dk, (2018). http://varmelast.dk/en.

[30] Danish Transport and Construction Agency, Danish Building Regulations 2015, 2015. http://historisk.bygningsreglementet.dk/file/591081/br15_english.pdf.

[31] Ministry of Transport Building and Housing, Executive order on building regulations 2018 (BR18), (2018). http://bygningsreglementet.dk/~/media/Br/BR-English/BR18_Executive_order_on_building_regulations_2018.pdf.

[32] Danish Energy Agency, Danish Board of District Heating, State of Green, District heating - Danish experiences, 2015. doi:10.1109/ICEMI.2013.6743020.

[33] K. Foteinaki, R. Li, A. Heller, C. Rode, Heating system energy flexibility of low-energy residential buildings, Energy Build. (2018). doi:10.1016/j.enbuild.2018.09.030.

[34] T.S. Larsen, R.L. Jensen, O. Daniels, Målinger og Analyse af Indeklima og Energiforbrug i Komforthusene, Department of Civil Engineering, Aalborg University, 2012. http://vbn.aau.dk/files/60642088/Komforthusene_M_linger_og_Analyse_af_Indeklima_og_Energiforbrug_i_8_Passivhuse_2008_2011.pdf.

[35] EN/DS 15251, Indoor environmental input parameters for design and assessment of energy performance of buildings addressing indoor air quality, thermal environment, lighting and acoustics, Dansk Stand. (2007) 54.

[36] Q. Sun, H. Li, F. Wallin, Q. Zhang, Marginal costs for district heating, Energy Procedia. 104 (2016) 323–328. doi:10.1016/j.egypro.2016.12.055.

[37] HOFOR A/S, Greater Copenhagen Utility, (2018). https://www.hofor.dk.

[38] J. Sjödin, D. Henning, Calculating the marginal costs of a district-heating utility, Appl. Energy. 78 (2004) 1–18. doi:10.1016/S0306-2619(03)00120-X.

[39] K. Difs, L. Trygg, Pricing district heating by marginal cost, Energy Policy. 37 (2009) 606–616. doi:10.1016/j.enpol.2008.10.003.

[40] S. Karjalainen, Thermal comfort and use of thermostats in Finnish homes and offices, Build. Environ. 44 (2009) 1237–1245. doi:10.1016/j.buildenv.2008.09.002.

[41] R. Li, G. Dane, C. Finck, W. Zeiler, Are building users prepared for energy flexible buildings?—A large-scale survey in the Netherlands, Appl. Energy. 203 (2017) 623–634. doi:10.1016/j.apenergy.2017.06.067.

[42] C. Evens, S. Kärkkäinen, Pricing models and mechanisms for the promotion of demand side integration, (2009) 58. http://www.ece.hut.fi/enete/Pricong_models.pdf.

[43] C. Sandersen, K. Honoré, District heating flexibility – short term heat storage in buildings, EnergyLab Nordhavn Deliverables, 2018. http://www.energylabnordhavn.com/uploads/3/9/5/5/39555879/d5.2c_short_term_heat_storage_in_buildings.pdf.

[44] J. Le Dréau, P. Heiselberg, Energy flexibility of residential buildings using short term heat storage in the thermal mass, Energy. 111 (2016) 991–1002. doi:10.1016/j.energy.2016.05.076.

[45] S. Aggerholm, K. Grau, Bygningers energibehov - Beregningsvejledning - SBi-anvisning 213, Aalborg, 2014.

[46] TABULA WebTool, (2017). http://webtool.building-typology.eu (accessed October 11, 2017).

[47] EQUA Simulation AB, IDA Indoor Climate and Energy - A new generation building performance simulation software, IDA Indoor Clim. Energy. (2018). https://www.equa.se/en/ida-ice.

[48] EQUA Simulation AB, Validation of IDA Indoor Climate and Energy 4 . 0 with respect to CEN Standards EN 15255-2007 and EN 15265-2007, Solna, Sweden, 2010.

[49] EQUA Simulation AB, Validation of IDA Indoor Climate and Energy 4.0 build 4 with respect to ANSI/ASHRAE Standard 140-2004, Solna, Sweden, 2010.

[50] S. Kropf, G. Zweifel, Validation of the Building Simulation Program IDA-ICE According to CEN 13791 „ Thermal Performance of Buildings - Calculation of Internal Temperatures of a Room in Summer Without

Mechanical Cooling - General Criteria and Validation Procedures ", 2001.

[51]   P. Loutzenhiser, H. Manz, G. Maxwell, International Energy Agency's SHC Task 34 - ECBCS Annex 43 Project C: Empirical Validations of Shading / Daylighting / Load I nteractions in Building Interactions Energy Simulation Tools, 2007.

[52]   Technical University of Denmark - Department of Civil Engineering, DTU Climate Station-Climate Data, (2018). http://climatestationdata.byg.dtu.dk.

[53]   DS/EN ISO 13790, Energy performance of buildings – Calculation of energy use for space heating and cooling, Dansk Stand. (2008) 178.

[54]   A. Wang, R. Li, S. You, Development of a data driven approach to explore the energy flexibility potential of building clusters, Appl. Energy. (2018). doi:10.1016/j.apenergy.2018.09.187.

[55]   R. Li, F. Wei, Y. Zhao, W. Zeiler, Implementing Occupant Behaviour in the Simulation of Building Energy Performance and Energy Flexibility: Development of Co-Simulation Framework and Case Study, Proc. Build. Simul. 2017. (2017) 1339–1346.

[56]   J. Widén, A. Molin, K. Ellegård, Models of domestic occupancy, activities and energy use based on time-use data: Deterministic and stochastic approaches with application to various building-related simulations, J. Build. Perform. Simul. 5 (2012) 27–44. doi:10.1080/19401493.2010.532569.

[57]   J. Widén, M. Lundh, I. Vassileva, E. Dahlquist, K. Ellegård, E. Wäckelgård, Constructing load profiles for household electricity and hot water from time-use data-Modelling approach and validation, Energy Build. 41 (2009) 753–768. doi:10.1016/j.enbuild.2009.02.013.

PAPER III: <u>Foteinaki, K.</u>, Li, R., Rode, C. and Andersen, R. K. (2018) 'Modelling household electricity load profiles based on Danish time- use survey data'. *Submitted to the peer-reviewed journal Energy and Buildings, Elsevier (December 2018)*

Modelling household electricity load profiles based on Danish time-use survey data

Kyriaki Foteinaki[a,*], Rongling Li[a], Carsten Rode[a], Rune Korsholm Andersen[b]

[a] Department of Civil Engineering, Technical University of Denmark, Brovej, Building 118, 2800 Kgs. Lyngby, Denmark

[b] International Centre for Indoor Environment and Energy, Department of Civil Engineering, Technical University of Denmark, Nils Koppels Alle, Building 402, 2800 Kgs. Lyngby, Denmark

* Corresponding author, e-mail: kyfote@byg.dtu.dk

Abstract

The relationship among occupants' presence, activities and appliance use is essential for households' energy use. In the present work, we aimed to link occupants' energy-related activities to electricity demand, in order to obtain a representative daily electricity load profile for Danish households using Danish time-use survey (DTUS) data. The approach was to combine appliance ownership and power ratings with occupant activities from the DTUS. Two modelling approaches were implemented: in the first approach, the occupant activities profiles from the DTUS were used directly to determine activities at 10-minute intervals. In the second approach, the probabilities of starting time and duration of the occupant activities were used to determine activities. In both approaches, appliance use was assigned to the energy-related activities. The set of appliances used in each activity was determined from a national database of appliance ownership, and the appliances' power was calibrated using information from apartments in Copenhagen, Denmark. The modelled daily electricity load profile was compared with three measured datasets of varying sizes and from different parts of Denmark. Both approaches captured important qualitative characteristics of the measured load profiles. However, the first approach used a more simple method and resulted in smaller errors than the second approach.

Keywords: Household electricity profile, Time-use survey data, Load modelling, Daily load profiles, Residential building

1. Introduction

Residential buildings were responsible for 27 % of the final energy consumption in the 28 EU member states in 2016 [1]. For decades, research has focused on understanding the aspects of energy use in residential

buildings to improve energy efficiency. Within the wide building energy research, the element of stochasticity of the occupants' interaction with the building is a key aspect. Refs. [2,3] found that it is a determining parameter for the energy use and indoor environment in a building and it is one of the main reasons for discrepancies between the estimated and the actual energy use. Especially, in new low-energy buildings knowing the occupants' schedules and activities is important, as heat emitted from occupants and appliances has a large impact on the household's heating needs [4–6]. Furthermore, the target of low-carbon energy use [7] and the subsequent increasing electricity generation from renewable energy sources have stimulated the implementation of new strategies in the energy system, including demand side management (DSM) and distributed energy production. In order to facilitate the implementation of such low-carbon measures, modelling the residential load profiles as realistically as possible is essential. Matching the energy consumption in residential buildings to local distributed energy production is key for the efficient operation of the system. When planning a DSM strategy aiming to shift the operation of certain domestic electric appliances in time, it is essential to know the relationship between occupants' presence, activities and energy use.

The most common modelling approach has been bottom-up models, namely models that calculate the electricity use of individual buildings or clusters of buildings by describing the individual elements in great detail, and those results can be extrapolated to a wider region according to the representative weight of the modelled sample [8]. Using this approach, modelling the electricity use in a household requires two main input datasets; i) the set of appliances in the household, the electricity load of each individual appliance and the variations in power demand whilst appliances are switched on and ii) the time and duration of use of the appliances, or the activity pattern of the occupants [9]. Both incorporate elements of variability, but the second aspect, which is related to the occupants' behavioural patterns, incorporates a far greater degree of unpredictability.

Two dataset sources are usually employed for the development of the models: detailed measurements at the building level [10,11] and time-use survey data. A time-use survey (TUS) is a statistical survey completed by residents, usually by keeping logbooks or diaries about the time-use of activities an individual engages in during a specific time interval throughout the day. The second method is easier to execute as it interferes less with the everyday life of the participants in the survey and it is less expensive than making high resolution measurements [12].

Many studies have developed models based on TUS data, which are available usually at the national level. A number of studies focus on occupancy and activity patterns in households [13–18]. Indicatively, Torriti 2017 [13] analysed the United Kingdom's time-use survey 2005 discussing how dependent energy-related social

practices in the household take place in relation to the time of the day, including preparing food, washing, cleaning, washing clothes, watching TV and using a computer. Wilke et al. 2013 [14] developed a stochastic bottom-up model and a set of calibration activities to predict residential activities based on time-dependent probabilities of start time and duration of activities using the French TUS data of 1998/1999. Buttitta et al. 2017 [15] developed a method to generate occupancy patterns based on the clustering of household occupancy profiles using the United Kingdom's time-use survey 2000 data. There are also studies that associate TUS data to households' electricity use [9,12,19–25]. Capasso et al. 1994 introduced a bottom-up stochastic model using an Italian time-use survey. They modelled start and duration of activities and attached each individual activity to electric load [22]. Richardson et al. 2010 [19], developed a model for active occupancy and domestic electricity demand. The active occupancy was modelled as a Markov-chain model and the transition probabilities were based on the United Kingdom's 2000 TUS data. Widen et al. 2009a [12] used the Swedish TUS data to create load profiles both for household electricity and domestic hot water consumption with a deterministic conversion model. Widén et al. 2009b [21] modelled domestic lighting demand using non-homogeneous Markov chains to generate synthetic occupancy patterns. Widén and Wäckelgård 2010 [9] extended the method to generate synthetic activity patterns, which were used to create household electricity profiles. Fischer et al. 2015 [20] used the German TUS to develop a stochastic bottom-up model which generates synthetic electrical load profiles, incorporating seasonal occupant behaviour, a distinction of weekend days and a correlation between start time and duration of an activity. The modelling approaches vary in the degree of complexity, in the level of detail used for occupant behaviour modelling and in the level of detail of appliance data used for electricity load modelling. Complicated stochastic models require long computation times and detailed input data, which might not always be available.

Nevertheless, the outcomes of the aforementioned studies show that TUS can increase understanding of occupants' behaviour and could potentially be used to improve the realism of building energy use in modelling. However, the Danish TUS (DTUS) data have scarcely been used by the Danish energy research community. This work was initiated by Barthelmes et al. 2018 [18], who performed a detailed analysis on the latest DTUS 2008/09 and profiled domestic energy-related daily activities, time-related characteristics of the activities, such as starting times, ending times and durations, and occupancy patterns. The occupancy was also modelled and used in an energy flexibility analysis in Ref. [26]. Following this work, the aim of the present paper was to map the selected energy-related activities to electricity demand, in order to obtain electricity load profiles in Danish households. Two modelling approaches were implemented utilizing different sets of input information to model

the occupant activities, as the availability of input data and the expected output may vary for different cases. The first approach used the occupant activities profiles from the DTUS directly to determine the activities at 10 min intervals. Sets of appliances with constant electricity demand were assigned to energy-related activities and the aggregation of those generated the total household electricity load profile. The second approach generated stochastic occupant activities profiles based on the probabilities of time-related characteristics of the activities, i.e. starting time and duration; those were subsequently converted to electricity load profiles. Both approaches followed the fit-for-purpose modelling principle, considering the trade-off between modelling error and input uncertainty. Since various input parameters might not always been known or defined at national level, which was the case in Denmark, high input uncertainties might be introduced. The objective of this work was thus to create models that are less complex, but still generate a daily electricity demand profile that can be representative of large numbers of Danish households. The detailed shape of the load profile was the purpose of this work, as it is of great interest for various applications, including tariff planning, load management as peak clipping and valley filling, and integration of distributed renewable energy production.

The structure of this paper is organized as follows. Section 2 presents the datasets used for constructing the models and those used for comparison. Section 3 explains the modelling approach of each model. In Section 4 the results of the models are presented and compared to the measurement datasets, followed by discussions in Section 5. The main conclusions are summarized in the final Section 6.

2. Data

2.1. Data for model development

Table 1: Datasets for model development.

Dataset	Description	Measurement period	Location of households	Number of participants	Data resolution
DTUS 2008/09	Danish time-use survey	03/2008-03/2009	Denmark	9640 individuals from 4679 households	10-min
Nordhavn_Appl	Measurements on electricity use of individual appliances	18/01/2018 18/04/2018	Nordhavn, Copenhagen	17 apartments	1-min

Table 1 summarizes the datasets used for the development of the models. The main input dataset for the development of the models was the Danish time-use survey (DTUS) conducted in 2008-2009. The study includes data about the time-use of activities performed throughout the day by a representative sample of the

Danish population. Specifically, 9640 individuals from 4679 households participated in this survey, by responding to a questionnaire, filling out a dairy and an expenditure booklet [27,28]. The time resolution of the diary was 10 min, namely the day was divided into 144 time intervals, starting at 4:00 and ending at 3:50 in the morning. Bonke and Fallesen 2010 [28] provide more detailed descriptions of the DTUS, the methods and the responses. Barthelmes et al. 2018 [18] used the DTUS data to create profiles of occupants' daily activities during different seasons and weekdays/weekends, and to identify the time-related characteristics of the activities, i.e. starting times, ending times and durations. The DTUS pre-coded 35 activities which were then reported by the participants. In Ref. [18] these activities were consolidated into the 10 energy- and occupancy-related activities shown in Table 2, focusing on activities taking place inside the domestic environment. The rest of the activities were categorized as "Not at home". The same clustering of activities was also used in the present work. For more information about the basis of this consolidation the reader is referred to Ref. [18]. A similar consolidation into energy-related activities was established by Jaboob [29].

Table 2: Activity clustering [18].

No.	Activity clustering in [18]	Activities included in the DTUS 2008/09
1	Sleeping	Sleeping
2	Toilette	Toilette
3	Eating	Eating
4	Cooking/washing dishes	Cooking/washing dishes
5	Cleaning/washing clothes	Cleaning/washing clothes
6	Practical work	Other work, do-it-yourself work, garden work
7	Family care/free time	Child care, reading with children, family care, reading, hobby, social gathering, phone conversations
8	Relaxing/TV/IT	Television (TV), radio, music, information technology applications (IT), relaxing
9	Not at home	Work, lunch break, transportation as part of work, transport to and from work education, education, transport to and from education, shopping, errands, visiting public offices, pick up/bring children, association activities, voluntary work and similar, exercise/sport, entertainment/culture, restaurant/café
10	Other	Other

The dataset "Nordhavn_ Appl" was collected in the framework of the EnergyLab Nordhavn project [30] and includes measurements at the individual appliance level. The measurements were performed in 17 apartments and included six main appliances: oven, hob, microwave oven, dishwasher, washing machine and tumble dryer. The measurements were used to determine the average power used during the operation of each of the appliances, which is listed in Table 3. For the rest of the appliances considered in the models the average power use was obtained from literature.

Table 3: Average power during operation of each appliance measured in the "Nordhavn_Appl" dataset.

Appliance	Average power [W]
Oven	1220
Hob	910
Microwave oven	1400

Dishwasher	670
Washing machine	410
Dryer	2300

2.2. Data for model comparison

Table 4 lists the datasets that were used for validation and comparison with the models. The "Nordhavn_Tot" dataset was used for validation, as some of the models' appliance parameters were obtained from the individual appliance data from "Nordhavn_Appl" (listed in Table 1). The datasets "Korngården_Tot" and "Esbjerg_Tot" were used for a qualitative comparison. The models' comparison was performed in terms of the total electricity use in the households. The available sets of measurement datasets are characterized by the diversity of the participating households. The dataset "Esbjerg_Tot" was collected by SydEnergi, the largest electricity utility company in southern Denmark, and was analysed in Ref. [31]. The dataset "Korngården_Tot" was analysed in detail in Ref. [32]. The dataset "Nordhavn_Tot" was collected in the framework of the EnergyLab Nordhavn project [30].

Table 4: Datasets for model validation/comparison.

Dataset	Description	Measurement period	Geographical location	Number of households	Data resolution
Nordhavn_Tot	Measurements on total electricity use of the household	18/01/2018 – 18/04/2018	Nordhavn, Copenhagen	17 apartments	1-min
Korngården_Tot	Measurements on total electricity use of the household	05/2016 – 05/2017	Copenhagen metropolitan area	61 apartments	1-hour
Esbjerg_Tot	Measurements on total electricity use of the household	10-16/01/2011	Esbjerg	32,241 single-family houses and apartments	1-hour

The measurement period, the geographical location of the households and the socio-economic characteristics of the occupants in the participating households varied considerably and this should be considered when analysing the data:

- The dataset of "Nordhavn_Tot" is a relatively limited sample of measurements in apartments in the district of Nordhavn in the city of Copenhagen, Denmark.

- The dataset of "Esbjerg_Tot" is a large dataset and comprises measurements both in apartments and single-family houses of the city of Esbjerg, which a city on the West coast of Denmark. The measurement period was limited to one week.

- The dataset of "Korngården_Tot" consists of measurements in apartments in the outskirts of Copenhagen. The apartment block is part of a social housing association.

Information on the number of the residents in the measured apartments/single-family houses was not available for any of the datasets.

3. Method

Two modelling approaches were used to construct the mean electricity load profile of a household. Each one used the results generated by analysing the DTUS 2008/09 data [18] as inputs and converted those to electricity load profiles. The occupant activities model used in each approach is described in Section 3.1. Section 3.2 describes the conversion of the activities to electricity consumption. In both models, each activity was mapped with a set of appliances. Separate profiles for weekdays and weekends were created. The modelling approaches were based on previous studies mentioned in Section 1, but implemented with simplifications adjusting the model complexity, considering the trade-off between modelling error and input uncertainty and computation time. Models with lower level of complexity were created, but still aiming to generate a daily electricity demand profile that can be representative of Danish households. Model 1 followed a deterministic approach, using directly the occupant activities profiles from the DTUS to determine activities. This method can be very detailed, if the available dataset allows it, and can preserve actual sequences of activities making the modelling of individual households more accurate. The main drawbacks of the method are that access to large and detailed input datasets is required and that the modelled profiles inherit the limitations of the input dataset, in terms of type of household and time characteristics. On the other hand, stochastic models, Model 2, have the possibility to generate profiles for an arbitrary number of households of different types, as some applications require longer data series.

3.1. Occupant activities model

Two models were developed. In Model 1, the electricity profile was a simple conversion model of the occupant activities profiles. The activity profiles were determined from the DTUS 2008/2009 data as the percentage of respondents who performed an activity at each 10-min time interval. The percentage of each activity was used directly as the probability of a certain activity and associated use of appliances. Figure 1 shows the activities profiles stemming from Ref. [18], but reconstructed separately for weekdays (left) and weekends (right).
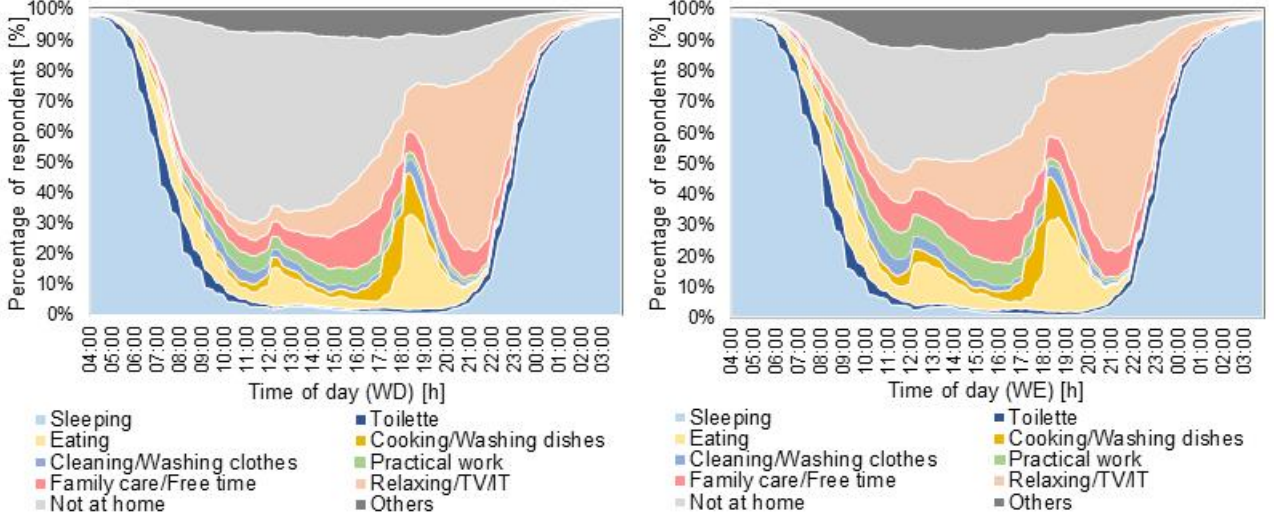
Figure 1: Occupant activities profile during weekdays (left) and weekends (right).

Model 2 generated synthetic occupant activities profiles based on the probabilities of starting an activity and the duration of each activity. Similar to Model 1, each activity was associated with the use of certain appliances. Figure 2 shows the relative frequency of starting each activity, with 10 min resolution, which depended on the time of day and was different for weekdays (left) and weekends (right). The typical duration of an activity was calculated by Ref. [18] using the Kaplan-Meier estimate method [33]. This method calculates the probability of an event to occur after a certain amount of time [34]. To obtain a survival function of each activity, the probability that an activity continued longer than time *t* after it was initiated was calculated using the equation (1):

$$\widehat{S}_t = \prod_{t_i \le t} \left(1 - \frac{d_i}{n_i}\right), \qquad (1)$$

where $\widehat{S}_t$ is the probability of survival at time *t*, d_i is the number of activities terminated at time *t* and n_i the number of activities continued longer than time *t*. Figure 3 shows the survival functions that yield the probability density for the duration of the activities, which was independent of the time of the day but different for weekdays and weekends. The survival functions stem from Ref. [18], but were recalculated to include the variability between weekdays and weekends. The inputs of Model 2 were thus the time-related characteristics of the activities: starting times and duration.
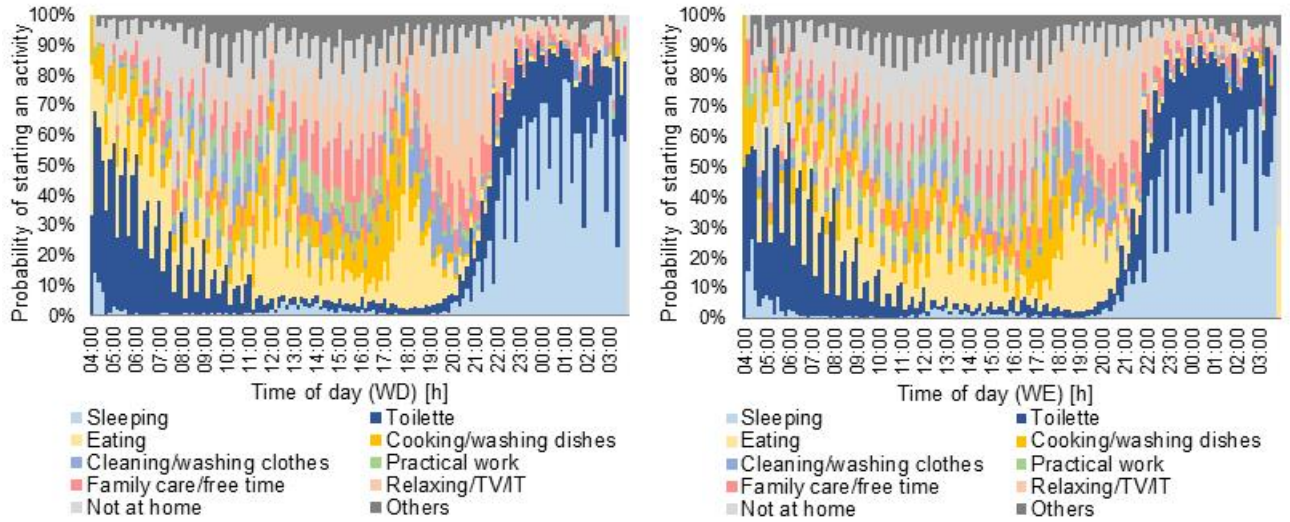
Figure 2: Probability of starting an activity during weekdays (left) and weekends (right).
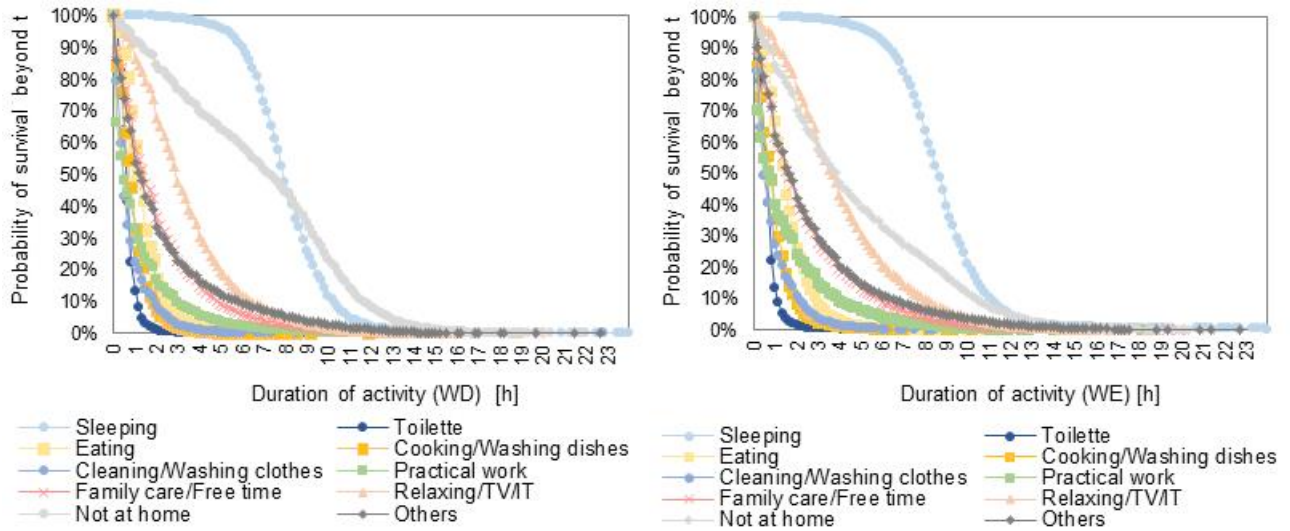
Figure 3: Survival functions during weekdays (left) and weekends (right).

Figure 4 outlines the procedure for generating synthetic occupant activities profiles for Model 2. The model assumed that at every discrete time step *k*, the occupant performed an activity *j*. For the next time step *k+1*, the occupant either continued with the same activity or changed to another activity. At time *t*, the activity *j* to be started was selected by drawing a random number between 0-1 and comparing it to the probability of starting an activity at this time of the day (Figure 2). The probability of starting an activity was independent from the previous activity. The duration of the activity *Δt* was selected by drawing a random number between 0-1 and comparing it to the probability of survival of the specific activity *j* (Figure 3). The new time, *t=t+Δt*, was thus defined and the process was repeated. Aggregating the daily profiles generated, the mean occupant activities profile for Model 2 was obtained. The number of synthetic activity profiles generated with Model 2 was the same

as the number of the respondents in the survey. The convergence of the aggregated profile was tested to ensure that the aggregate profiles are stable with regards to the number of individual activity sequences.
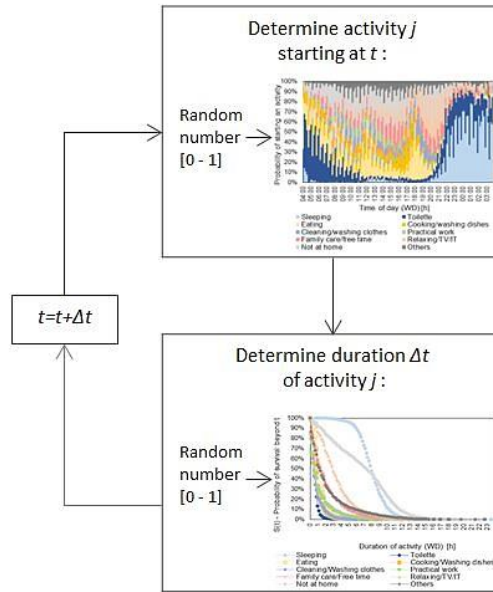
Figure 4: Generation of synthetic activity profiles for Model 2.

For both models, the output resolution was 10 min. However, since the resolution in the measurement datasets was 1 h, the comparisons were performed with 1 h averages of the models' output.

3.2. Conversion of activities to electricity consumption

3.2.1. Electric appliances

The electricity consumption in this model considered non-thermal applications. The activities associated with electricity use were Activity 4: Cooking/Washing dishes, Activity 5: Cleaning/Washing clothes and Activity 8: Relaxing/TV/IT. The electricity load of each activity for each time interval was calculated from the electricity use of a combination of the appliances associated with this activity. When the appliances were not in use, their stand-by power consumption was considered. The appliances associated with the Activities 4, 5 and 8 and the cold appliances are the most common ones found in a Danish household according to national statistics [35], but not all of them. Every household is equipped with a different set of appliances and each of them varies in age and characteristics. In the "Nordhavn_ Appl" dataset there are measurements for specific appliances, namely oven, hob, microwave oven, dishwasher, washing machine and tumble dryer. These data were used to determine the average power load during use of these appliances in the models. For the rest of the appliances, data from Refs. [35] and [36] were used as an average power for each appliance. The detailed input data used

for each individual appliance, namely percentage of ownership, average power load during use and stand-by power, can be found in Table 5.

For each activity there is great variability in the number and type of appliances with which it can be associated. Assumptions were therefore made for the set of appliances used in the model based on the data of appliance ownership at the national level [35]. A constant power load was assumed for each activity during each 10 min interval, determined by different combinations of appliances that are used simultaneously. The combinations used can be found in Table 6. The combinations in Table 6 are determined from Table 5, as in the following example:

$$\text{Washing machine} + \text{Dryer} = 73\% * 410 + 46\% * 2300 = 1357 \; W \qquad (2)$$

For each activity, an average of all the combinations was used. The cold appliances were also modelled as a constant power load, not related to occupants' activities. In reality, they operate on a cyclic load with thermostatic control, but on a daily basis they can be adequately represented by their average power use.

Table 5: Input data for individual appliances. The values marked with * are obtained from measurements of individual appliances in the "Nordhavn_Appl" dataset.

Appliance	Percentage of ownership [35]	Average power during use [35], [36]	Stand-by power [36]
Oven	90%	1220 *W* *	3 *W*
Hob	88%	910 *W* *	1 *W*
Hood	90%	5 *W*	-
Microwave oven	74%	1400 *W* *	2 *W*
Kettle	88%	2000 *W*	1 *W*
Dishwasher	63%	670 *W* *	1 *W*
Vacuum cleaner	88%	1140 *W*	-
Washing machine	73%	410 *W* *	1 *W*
Dryer	46%	2300 *W* *	1 *W*
PC (stationary)	105%	141 *W*	5 *W*
Laptop	108%	50 *W*	3 *W*
LCD TV	52%	170 *W*	3 *W*
Plasma TV	18%	280 *W*	3 *W*
LED TV	7%	88 *W*	3 *W*
CRT TV	301%	100 *W*	15 *W*
Stereo system	106%	100 *W*	9 *W*
DVD-player	100%	34 *W*	2 *W*
Video	132%	34 *W*	2 *W*
Fridge	66%	37 *W*	-
Upright freezer	34%	45 *W*	-
Chest freezer	46%	45 *W*	-
Fridge & freezer	75%	64 *W*	-
Other devices	100%	48.5 *W*	-

Table 6: Combinations of appliances used in Activity 4 (Cooking/washing dishes), Activity 5 (Cleaning/washing clothes), Activity 8 (Relaxing/TV/IT) and Cold appliances and the respective power [W] per household.

Activity 4 - Cooking/washing dishes		Constant power load	Activity 8 - Relaxing/TV/IT	Constant power load
Hob	+ Hood	805 W	TV	111 W

Oven	+ Hood			1103 W	TV	+ DVD or Video	151 W
Hob	+ Hood	+	Kettle	2565 W	TV	+ PC or Laptop	213 W
Oven	+ Hood	+	Micro oven	2139 W	Stereo system		106 W
Dishwasher				422 W	Stereo system	+ PC or Laptop	207 W
All the above				5121 W	PC or Laptop		101 W
Average for Activity 4				*2026 W*	*Average for Activity 8*		*148 W*
Activity 5 - Cleaning/washing clothes		Constant power load			Cold appliances		Constant power load
Washing machine				299 W	Fridge	+ Upright freezer	40 W
Washing machine	+	Dryer		1357 W	Fridge	+ Chest freezer	45 W
Washing machine	+	Vacuum cleaner		1303 W	Fridge & freezer		48 W
Dryer				1058 W	Fridge & freezer	+ Upright freezer	63 W
Dryer	+	Vacuum cleaner		2061 W	Fridge & freezer	+ Chest freezer	69 W
Vacuum cleaner				1003 W			
All the above				2361 W			
Average for Activity 5				*1349 W*	*Average for Cold appliances*		*53 W*

3.2.2. Lighting

Electricity use for lighting was modelled as daylight-dependent and occupancy-dependent and was based on the model developed by Widen et.al 2009 [12,21], according to which the lighting power was given by the equation (3):

$$P(t) = \begin{cases} P_{min}\frac{L(t)}{L_{max}} + P_{max}\left(1 - \frac{L(t)}{L_{max}}\right), & L \leq L_{max} \\ P_{min}, & L > L_{max} \end{cases} \quad (3)$$

A maximum threshold of illuminance, L_{max}, was predefined. When the illuminance $L(t)$ in the household was higher than the threshold, the lighting power $P(t)$ was equal to a minimum lighting power P_{min}. When the illuminance was lower than the threshold, the lighting power varied depending on the ratio of the actual illuminance and the maximum threshold. This calculation was valid when the occupant was at home and awake, otherwise the lighting power was assumed to be zero Watts.

In the present work, the illuminance threshold, L_{max}, was set to 500 lux, as recommended in EN/DS 15251 [37]. The illuminance level $L(t)$ was obtained from conversion of irradiance data from the year 2008 [38] to illuminance. The possible difference when using data from the year 2018 was considered, and it was concluded that the difference in the average consumption is minimal. The conversion used the total diffuse radiation from surfaces, considering the diffuse radiation from windows and reflection from surfaces of the direct radiation from windows [39]. The data of the conversion model of irradiance-illuminance were of 1 hour resolution and were generated with IDA ICE simulation software [40] for a vertical, south-facing, triple-glazed window with a transmittance of 0.74. The P_{min} and P_{max} were defined as one bulb being switched on, and one third of all the installed bulbs being switched on, respectively. Details of the parameters used can be found in Table 7.

Table 7: Input data for lighting model [35,41]**.**

Type of bulbs	Percentage of ownership	Average power per bulb
Low energy bulbs	33%	11 *W*
Incandescent lamps	33%	40 *W*
Fluorescent strip lamps	12%	20 *W*
Halogen bulbs	23%	20 *W*

4. Results

Ideally, the load profiles generated by the models should be compared to measurements performed in the same households as where the DTUS were carried out. However, this was not possible, since such measurement data did not exist. Instead, the modelled profiles were compared to the average measured electricity profiles of the three datasets presented in Section 2.2. The load dataset of "Nordhavn_Tot" was used for the validation as the information on electric appliances from there was used for model calibration. The other two datasets were used for qualitative comparison, evaluating how the models performed, as there were no data available for calibration.

The annual electricity use per household was estimated from the daily load profiles by weighting the total loads for the weekdays, i.e. 261 days, and the weekends, i.e. 104 days. The average annual electricity consumption both for the measured and the modelled loads are shown in Figure 5.
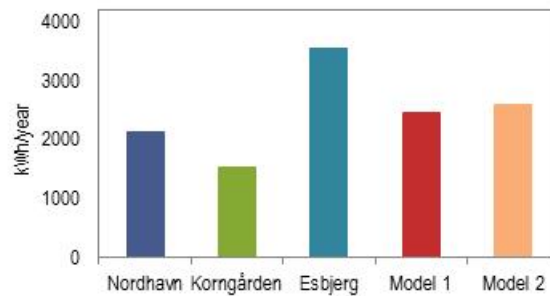
Figure 5: Average annual electricity use.

A considerable variation was observed between the measurements. Compared to "Esbjerg_Tot", "Nordhavn_Tot" and "Korngården_Tot" both had lower consumption, 2135 kWh and 1525 kWh respectively, as expected since the datasets were from apartments only, which in general have lower consumption than single-family houses [42]. "Korngården_Tot", particularly, was data from social housing apartments, which presumably have a lower level of equipment and thus lower electricity consumption. "Esbjerg_Tot", on the other hand, had an almost equal sample of apartments and single-family houses, and thus a higher consumption of 3535 kWh. The correspondence between measured and modelled data should be interpreted in context. The three datasets of electricity use were measured in buildings different to the larger DTUS sample that was used for the modelling. This fact had high impact on the aggregated annual consumption. The annual consumption of the

two models differed by 6%. The difference between "Nordhavn_Tot" and Model 1 and Model 2 was -13% and -17% respectively, with the measured data being the lower. For the evaluation of the correspondence it should be considered that the "Nordhavn_Tot" dataset was measured in apartments exclusively, unlike the DTUS sample, which included other types of housings as well. The difference of Model 1 with the "Korngården_Tot" and "Esbjerg_Tot" dataset was -38% and 44% respectively. According to the "Danish Energy Agency" and "Statistics Denmark", on average, a typical apartment had an electricity consumption of 2443 kWh/year in 2010, while the consumption of a single-family house was 4090 kWh/year [42,43]. There are significant differences on the annual electricity use per household depending on the number of occupants. In Denmark 38% of the households have 1 occupant, 33% 2 occupants, 12% 3 occupants and 17% 4 or more occupants [44]. Due to the calibration of the model with the "Nordhavn_Appl" data, the annual electricity consumption of the models was very close to that of the typical apartment in Denmark, but underestimated that of the single-family houses; yet they provided a reliable estimate of the annual electricity use for the overall geographical region of Denmark.

Figure 6 shows the average daily electricity load profile for weekdays and weekends.
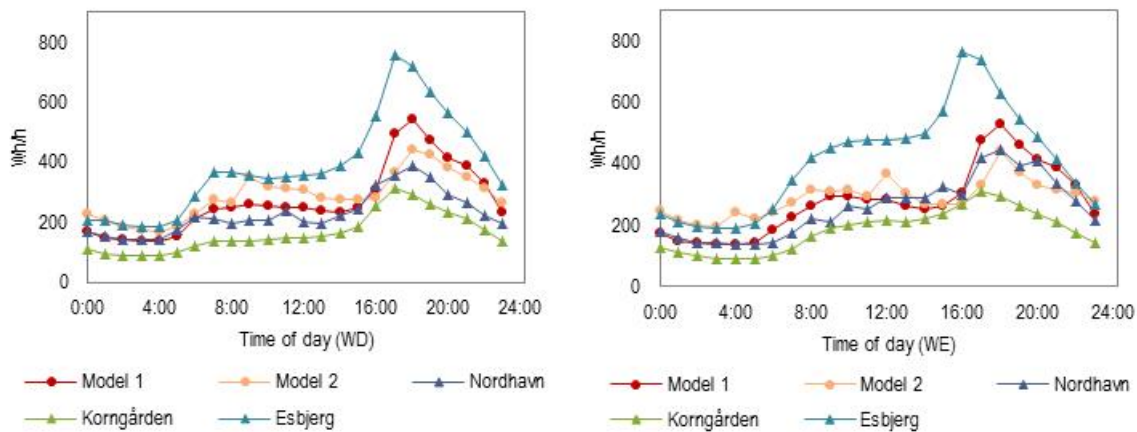
Figure 6: Average daily electricity load profile for weekdays (left) and weekends (right).

Overall the profiles followed a similar pattern. The lowest level of electricity use was during the night, followed by a morning increase during breakfast time. This level was, in general, maintained during the day until the late-afternoon, when the electricity use started to increase, reaching its highest peak in the evening. Subsequently, electricity use decreased towards the night level. During a weekend day, the morning increase in electricity use was shifted later in time and the consumption was higher during the day. Both in weekdays and weekends, the profiles had different magnitudes, which were in line with the differences in the annual consumption described previously. It can be noticed that the "Nordhavn_Tot" measurements had a less smooth curve, particularly for the weekend, which was attributed to the small sample size.

Regarding Model 1, although there were differences in scale between the measured and modelled profiles, the overall pattern was adequately represented. There was good correspondence of peaks and valleys during the day, both in terms of timing and magnitude, and the difference between a weekday and a weekend was captured as well. During the weekend, the profiles of both Model 1 and Model 2, were similar to that of "Nordhavn_Tot". In Model 2 there were some discrepancies between the measured and modelled data. An increase in consumption at 9:00 on a weekday and 12:00 on a weekend day were observed, which were not present in the measured profiles. Additionally, the evening peak was lower in magnitude compared to the other profiles, particularly at weekends.

The Root Mean Square Error (RMSE) between the modelled daily electricity load profiles and the measured values of individual households in the datasets was calculated, for weekdays (WD) and weekends (WE), and it is shown in Figure 7, Model 1 (left) and Model 2 (right). The measurements of individual households of "Esbjerg_Tot" dataset were not available, so it is not included in the figure.
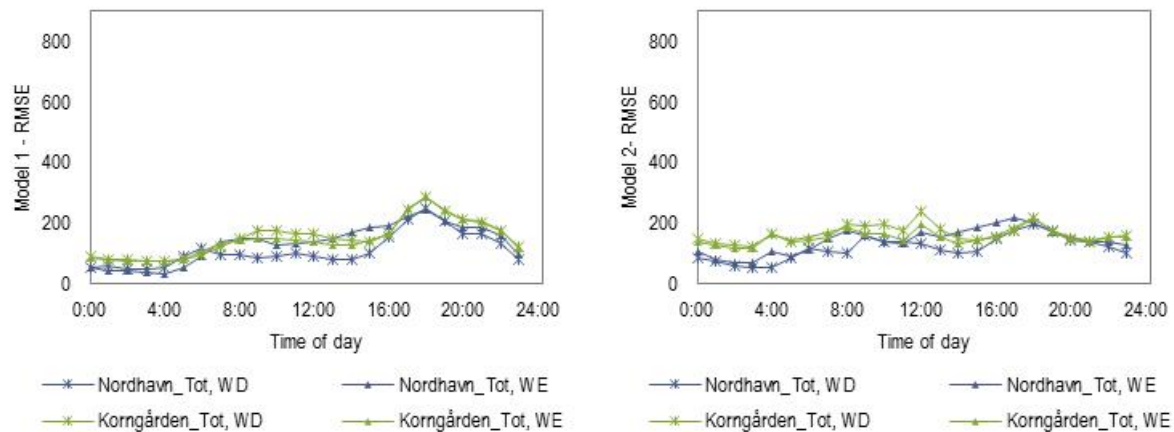
Figure 7: Root Mean Square Error (RMSE) between modelled daily electricity load profiles, Model 1 (left) and Model 2 (right) (WD = weekday, WE = Weekend), and measured profiles of individual households in the datasets.

The RMSE from the households of "Korngården_Tot" was higher than those from "Nordhavn_Tot". The RMSEs calculated for weekends were higher than those of weekdays, indicating higher variation in the profiles among households in weekends. In "Korngården_Tot" this is observed at a lower degree. The RMSE calculated for Model 1 for each hour showed a pattern relative to the electricity load profile, while for Model 2, the RMSE showed a similar pattern, but lower in magnitude.

Table 8 presents Pearson correlation coefficients and mean relative error between model and measurements, calculated for each model during weekdays and weekends based on the 1-hour average load profiles. The Pearson correlation coefficient is a measure of how well a linear function describes the correlation between the modelled and measured profiles. A perfect match between modelled and measured load profiles

would result in a Pearson correlation coefficient of 1. The mean relative error is the mean of the absolute relative difference between the modelled and measured load profiles.

Table 8: Correlation coefficient and mean relative error based on 1-hour average load profiles for Model 1 and Model 2 (WD = weekday, WE = Weekend).

	Pearson Correlation Coefficient		Mean Relative Error	
Model 1	WD	WE	WD	WE
Nordhavn_Tot	0.95	0.95	18.4	14.5
Korngården_Tot	0.95	0.90	64.9	51.5
Esbjerg_Tot	0.97	0.93	29.3	30.9
Model 2				
Nordhavn_Tot	0.85	0.83	29.5	31.5
Korngården_Tot	0.84	0.80	85.7	73.3
Esbjerg_Tot	0.88	0.82	20.8	26.1

The correlation of the measured datasets with Model 1 was above 0.95 for weekdays and above 0.90 for weekends, indicating that Model 1 was able to capture the shape of the load profile very well. The correlation with Model 2 was lower, yet still above 0.80. The magnitude of the mean relative errors was expected, as they reflect also the differences in scale of the load, which depends on the typology of measured households in each data set. The errors of Model 1 were overall lower compared to those of Model 2. The same measures of model quality were used in Fischer et al. 2015 [20]; the correlation of the measured and simulated mean daily electricity profiles was between 0.85 and 0.98. This indicates that with a less complex model implemented in this work, the general shape of the daily electricity load profile can be captured similarly well as in a more complex model implemented in Ref. [20].

The timing of peak loads is an important parameter, especially for tariff planning and load management, thus it was specifically evaluated. Figure 8 shows the average daily electricity load profile normalized against the individual maximum of each load profile, for weekdays and weekends.
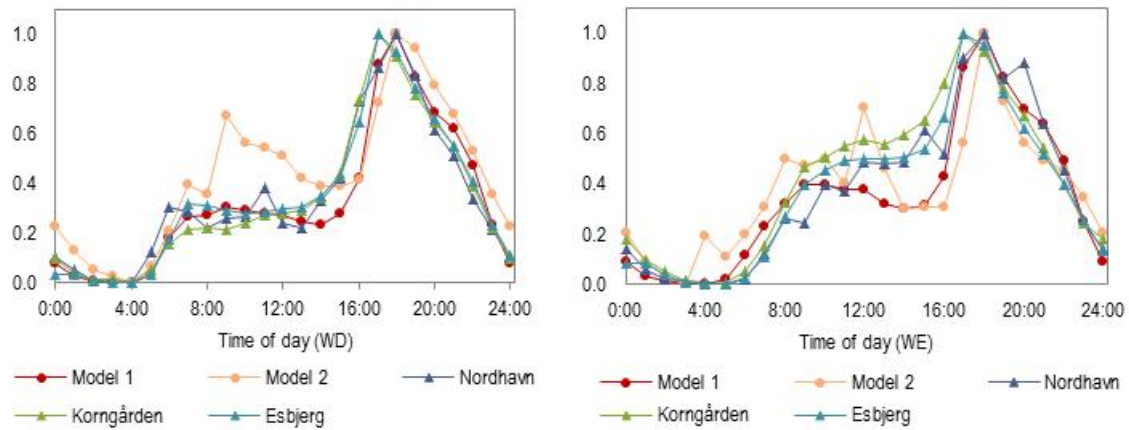
Figure 8: Average daily electricity load profile normalized on the individual maximum of each load profile for weekdays (left) and weekends (right).

During weekdays, the evening peaks occurred at different hours displaced by one hour for the different measured datasets. The peak was at 18:00 in the "Nordhavn_Tot" dataset and the two models. "Korngården_Tot" and "Esbjerg_Tot" peaked at 17:00, indicating differences in behavioural patterns between the datasets, possibly related to the occupation of the population of the latter two being more labour intensive than the average of Denmark [44]. There was a closer correspondence in the timing of the patterns in the weekdays compared to the weekends. Model 1 clearly captured the diurnal pattern in a weekday, while Model 2 presented a discrepancy. The electricity use was higher in the period 7:00-13:00, with a peak at 9:00 which was as high as approximately 65% of the main evening peak. The similarities in measured and modelled patterns during the weekend were not as clear as for the weekday. General patterns were still observed, starting with the morning load being shifted later in time. The following hours and until the late-afternoon the consumption was higher during weekend days compared to weekdays. Model 1 captured this difference, but at a lower magnitude compared to the "Korngården_Tot" and "Esbjerg_Tot" datasets and closer to the "Nordhavn_Tot" dataset. The time of the main evening peak was the same as for a weekday for all profiles. Both models presented a reduced use during midday (12:00-15:00), which was not observed in the measurements. Model 2 had a rather variable profile and could not reproduce a reliable pattern.

Although there were no measured data available for comparison, the models provide an estimation of the share of the different end-use loads in a household to the total electricity consumption. In Model 1, cold appliances had the highest consumption with 22.6%, followed by the lighting with 19.5%. Regarding the activity-related consumption, Activity 4 (cooking/washing dishes) had the highest consumption with 15.3%, followed by Activity 8 (relaxing/TV/IT) with 14.4% and lastly Activity 5 (cleaning/washing clothes) with 10.6%. The remaining 17.6% was consumption from the category "other devices". These results were similar to the typical share of

domestic electricity use in German households [45] and to those modelled and measured by Ref. [9] for the category "Apartments".

5. Discussion

The DTUS 2008/2009 used for the development of the models had a ten year gap with the dataset used for the calibration of some parameters. However, the DTUS 2008/2009 is the most recent survey of its type. Ref. [18] compared some attributes of the of the DTUS with national statistical data (dated 2008 and 2015) and confirmed its representativeness of the wider population in Denmark. Therefore, it was assumed that the data represented the overall geographical region of Denmark and that there have been no significant changes in the occupant activities patterns from the 2008/09 until 2018. The stock of appliances has probably changed (e.g. tablets, induction cookers, larger TV screens), but since the TUS determines the time and duration of the activities, it was assumed that the time gap is of marginal importance. An important deficiency of the DTUS is that only one activity could be reported in each time interval. Simultaneous activities could not, therefore, be represented in the analysis, as the respondents could not report for example cooking and watching TV at the same time. In addition, the 10 activities used in the models were clusters of a total of 35 activities reported by the respondents. The classification "at home" (Activities 1-8) or "not at home" (Activity 9) is not reported by the respondents, as that was not the purpose of the DTUS, but was consolidated in Ref. [18]. If a respondent, for example, occasionally works from home, this is not considered in the models. We hope future time use surveys can include specific questions and options towards energy.

Model 1 showed that the electricity load profile was a good fit and the overall pattern of the measured datasets was adequately represented. There were differences in scale between the measured and modelled profiles, which can be explained by the differences in the measured datasets, since they were not representative of the larger sample of DTUS that was used for the activity modelling. Nevertheless, there was good correspondence of peaks and valleys during the day and the main differences between a weekday and a weekend were captured.

Model 2 produced a less reliable profile of the electricity load compared to Model 1. There could be different sources of error in the process. Firstly, the responses recorded in diaries were not always well-reported, as the participants of the survey were solely responsible for filling in the diaries. Indicatively, in the graphs with the activities started (Figure 2), which were reported with 10-min resolution, it can be seen that the respondents tended to report the start of the activities primarily at the full or half of every hour. This created a variable profile

of the probability of starting an activity. In addition, in Ref. [18] Fig.6 it was shown that the number of activities started at each time interval had a pattern, with three peak times for initiation of activities: morning peak (07:00–09:00), the evening peak (18:00–20:00) and bedtime peak (23:00). This pattern was not taken into consideration in Model 2, since the start of the activities were selected based on the probabilities created by the maximum number of activities started in the specific time step. The mean daily occupant activities profile which was generated from Model 2 is shown in Figure 9. Comparing this with the respective of Model 1 (Figure 1), which was directly retrieved from the diary responses, it is apparent that the profiles vary significantly. The percentage of people "Sleeping" during the first hours of the day was lower in Model 2, while the percentage of people "Not at home" during day time was considerably higher. This was due to the shape of the survival curve of the activity "Not at home", which presented large variety in duration due to the assumption that the survival curves are time-independent. This led to lower percentages in the rest of activities that are energy-related, i.e. Activities 4, 5 and 8, which explains the lower evening peaks that were observed for Model 2. The model may be improved if the correlation of the survival functions of the activities with the starting time of the activities was defined and introduced.
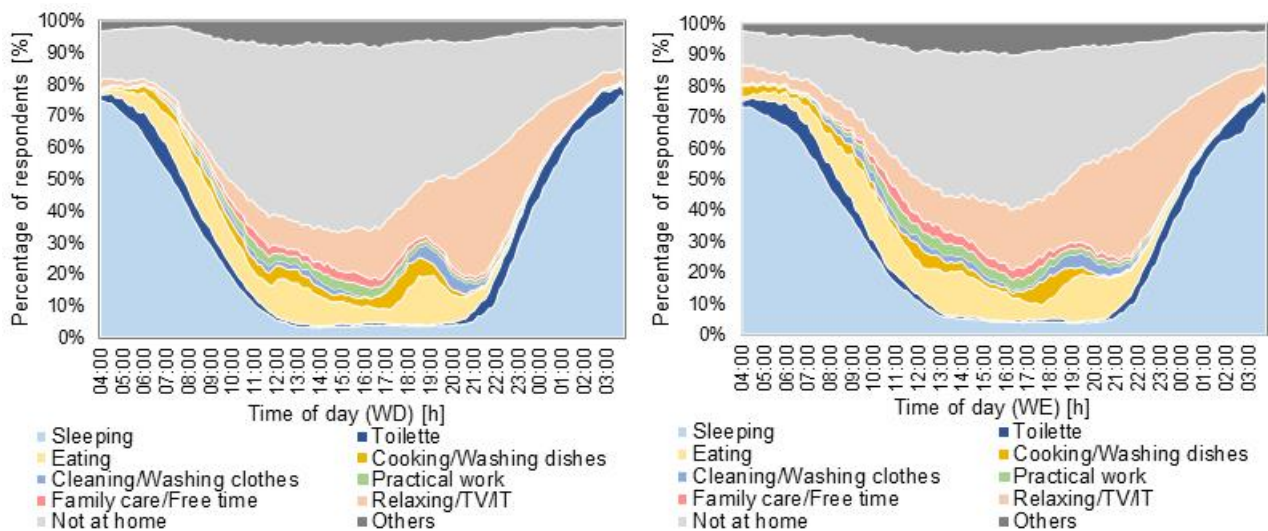
Figure 9: Occupant activities profile during weekdays (left) and weekends (right) as outcome from Model 2.

In both models, there were many modelling assumptions included in the process, especially the estimation of the parameters used, as the availability of relevant data was one of the most important constraints when developing the models. The appliances associated with the Activities 4, 5 and 8 and the cold appliances are the most common ones in a Danish household, but not all of them. Not only that every household is equipped with a different set of appliances, but also the characteristics and age of each appliance vary. It is complex to define the average power load of each appliance to be a representative mean for all households in Denmark. It is

indicative that various studies used different average power for the same appliances from a variety of sources, such as Refs. [10–12,16,20,23,25,35]. Some data for the appliances were available through measurements from one of the datasets, but for the most part standard parameters from literature were used. The models considered relatively large appliances, while smaller appliances, such as mobile phone chargers, wireless network router, hair dryer, etc., were aggregated in the category "other devices". As the number of smaller appliances used in the everyday life gradually grows, their consumption is expected to have a more significant contribution [46]. In addition, in this study the average power use during the operation of the appliances was used. Most appliances, however, operate on a cyclic load during the operation. A national database with this information for the stock of appliances would improve the models. The models were evaluated only by using mean daily profiles and variability in profiles between types of households was not included. Again, enhancement in those respects was not possible due to data unavailability. Depending on the available resources and the level of accuracy needed, the parameter estimation process in the models could be adjusted.

6. Conclusion

This paper presented the potential usefulness of the Danish time-use survey data for modelling household electricity load profiles. Using data about the timing of household activities from the DTUS 2008/2009 and data of appliances ownership at national level and power ratings, it was possible to model domestic electricity profiles. Two modelling approaches were implemented to model the occupants' energy-related activities: in the first approach, the occupant activities profiles from the DTUS were used directly to determine activities at 10 minute intervals. In the second approach, the probabilities of starting time and duration of the occupant activities were used to generate stochastic occupant activities profiles. In both approaches, the use of appliances was assigned to the energy-related activities. Both approaches aimed for reduced model complexity, to avoid introducing high input uncertainties. The modelled daily profile of electricity use was compared with three measured datasets of varying sizes and from different parts of Denmark.

Both approaches captured important qualitative characteristics of the measured electricity profiles. However, the first approach used a more simple method and resulted in smaller errors than the second approach. When both total electricity consumption and data of individual appliances was available for calibration, the models provided reliable profiles qualitatively both in the shape of the profile and in the magnitude. On the other hand, if only the total electricity consumption was available, the models were able to adequately provide qualitative features of the load profile. The correlations of the modelled daily profile of

electricity use with the measured datasets lied between 0.90 and 0.97 for Model 1 and between 0.80 – 0.88 for Model 2.

Overall, the models generated a representative electricity profile for Danish households, which included the important qualitative characteristics of the measured data. The detailed shape of the load profile was captured and there were high correlations between the modelled and measured profiles. The two approaches followed and compared contribute to the existing body of knowledge and add valuable input to the discussion of model complexity in bottom-up modelling for household electricity modelling, input data assumptions and possible simplifications.

References

[1]   European Commission, EU Reference Scenario 2016 - Energy, transport and GHG emissions - Trends to 2050, Energy, Transp. GHG Emiss. - Trends to 2050. (2016) 220. doi:10.2833/9127.

[2]   Y. Zhang, X. Bai, F.P. Mills, J.C.V. Pezzey, Rethinking the role of occupant behavior in building energy performance: A review, Energy Build. 172 (2018) 279–294. doi:10.1016/j.enbuild.2018.05.017.

[3]   I. EBCP, Final Report Annex 53. Total energy use in buildings Analysis and evaluation methods, 2016.

[4]   C. Isaksson, F. Karlsson, Indoor climate in low-energy houses-an interdisciplinary investigation, Build. Environ. 41 (2006) 1678–1690. doi:10.1016/j.buildenv.2005.06.022.

[5]   F. Karlsson, P. Rohdin, M.L. Persson, Measured and predicted energy demand of a low energy building: Important aspects when using building energy simulation, Build. Serv. Eng. Res. Technol. 28 (2007) 223–235. doi:10.1177/0143624407077393.

[6]   K. Foteinaki, R. Li, A. Heller, C. Rode, Heating system energy flexibility of low-energy residential buildings, Energy Build. 180 (2018) 95–108. doi:10.1016/j.enbuild.2018.09.030.

[7]   European Commission, European Council 23-24/10/2014 - Conclusions on 2030 Climate and Energy

Policy Framework, Brussels, Belgium, 2014.

[8]   L. Swan, V. Ugursal, Modeling of end-use energy consumption in the residential sector: A review of modeling techniques, Renew. Sustain. Energy Rev. (2009) 1819–1835.

[9]   J. Widén, E. Wäckelgård, A high-resolution stochastic model of domestic activity patterns and electricity demand, Appl. Energy. 87 (2010) 1880–1892. doi:10.1016/j.apenergy.2009.11.006.

[10]   S. Firth, K. Lomas, A. Wright, R. Wall, Identifying trends in the use of domestic appliances from household electricity consumption measurements, Energy Build. 40 (2008) 926–936. doi:10.1016/j.enbuild.2007.07.005.

[11]   A. Marszal-Pomianowska, P. Heiselberg, O. Kalyanova Larsen, Household electricity demand profiles - A high-resolution load model to facilitate modelling of energy flexible buildings, Energy. 103 (2016) 487–501. doi:10.1016/j.energy.2016.02.159.

[12]   J. Widén, M. Lundh, I. Vassileva, E. Dahlquist, K. Ellegård, E. Wäckelgård, Constructing load profiles for household electricity and hot water from time-use data-Modelling approach and validation, Energy Build. 41 (2009) 753–768. doi:10.1016/j.enbuild.2009.02.013.

[13]   J. Torriti, Understanding the timing of energy demand through time use data: Time of the day dependence of social practices, Energy Res. Soc. Sci. 25 (2017) 37–47. doi:10.1016/j.erss.2016.12.004.

[14]   U. Wilke, F. Haldi, J.L. Scartezzini, D. Robinson, A bottom-up stochastic model to predict building occupants' time-dependent activities, Build. Environ. 60 (2013) 254–264. doi:10.1016/j.buildenv.2012.10.021.

[15]   G. Buttitta, W. Turner, D. Finn, Clustering of Household Occupancy Profiles for Archetype Building Models, Energy Procedia. 111 (2017) 161–170. doi:10.1016/j.egypro.2017.03.018.

[16]   I. Richardson, M. Thomson, D. Infield, A high-resolution domestic building occupancy model for energy demand simulations, Energy Build. 40 (2008) 1560–1566. doi:10.1016/j.enbuild.2008.02.006.

[17]   D. Aerts, J. Minnen, I. Glorieux, I. Wouters, F. Descamps, A method for the identification and modelling of realistic domestic occupancy sequences for building energy demand simulations and peer comparison, Build. Environ. 75 (2014) 67–78. doi:10.1016/j.buildenv.2014.01.021.

[18]   V.M. Barthelmes, R. Li, R.K. Andersen, W. Bahnfleth, S.P. Corgnati, C. Rode, Profiling Occupant Behaviour in Danish Dwellings using Time Use Survey Data, Energy Build. 177 (2018) 329–340. doi:10.1016/j.enbuild.2018.07.044.

[19]   I. Richardson, M. Thomson, D. Infield, C. Clifford, Domestic electricity use: A high-resolution energy

demand model, Energy Build. 42 (2010) 1878–1887. doi:10.1016/j.enbuild.2010.05.023.

[20]   D. Fischer, A. Härtl, B. Wille-Haussmann, Model for electric load profiles with high time resolution for German households, Energy Build. 92 (2015) 170–179. doi:10.1016/j.enbuild.2015.01.058.

[21]   J. Widén, A.M. Nilsson, E. Wäckelgård, A combined Markov-chain and bottom-up approach to modelling of domestic lighting demand, Energy Build. 41 (2009) 1001–1012. doi:10.1016/j.enbuild.2009.05.002.

[22]   A. Capasso, W. Grattieri, R. Lamedica, A. Prudenzi, Bottom-up approach to residential load modeling, IEEE Trans. Power Syst. 9 (1994) 957–964. doi:10.1109/59.317650.

[23]   Y.S. Chiou, K.M. Carley, C.I. Davidson, M.P. Johnson, A high spatial resolution residential energy model based on American Time Use Survey data and the bootstrap sampling method, Energy Build. 43 (2011) 3528–3538. doi:10.1016/j.enbuild.2011.09.020.

[24]   B. Yu, J. Zhang, A. Fujiwara, A household time-use and energy-consumption model with multiple behavioral interactions and zero consumption, Environ. Plan. B Plan. Des. 40 (2013) 330–349. doi:10.1068/b38213.

[25]   M. Jalas, J.K. Juntunen, Energy intensive lifestyles: Time use, the activity patterns of consumers, and related energy demands in Finland, Ecol. Econ. 113 (2015) 51–59. doi:10.1016/j.ecolecon.2015.02.016.

[26]   A. Wang, R. Li, S. You, Development of a data driven approach to explore the energy flexibility potential of building clusters, Appl. Energy. (2018). doi:10.1016/j.apenergy.2018.09.187.

[27]   J. Bonke, Tax-reforms, normal and actual working hours and welfare in the beginning of the 20th's Denmark, Electron. Int. J. Time Use Res. 13 (2016) 91–108. doi:10.13085/eIJTUR.13.1.91-108.

[28]   J. Bonke, P. Fallesen, The impact of incentives and interview methods on response quantity and quality in diary-and booklet-based surveys, Surv. Res. Methods. 4 (2010) 91–101.

[29]   S. Jaboob, Stochastic Modelling of Occupants' Activities and Related Behaviours, University of Nottingham, 2015.

[30]   EnergyLab Nordhavn, EnergyLab Nordhavn – New Urban Energy Infrastructures, (2018). http://energylabnordhavn.weebly.com/.

[31]   A. Tureczek, P. Nielsen, H. Madsen, Electricity Consumption Clustering Using Smart Meter Data, Energies. 11 (2018) 859. doi:10.3390/en11040859.

[32]   J.K. Kristensen, Energy management and its influence on building energy performance and indoor environment, Technical University of Denmark, 2017. https://findit.dtu.dk/en/catalog/2385161880.

[33]   E.L. Kaplan, P. Meier, Nonparametric Estimation from Incomplete Observations, J. Am. Stat. Assoc. 53

(1958) 457–481. doi:10.1080/01621459.1958.10501452.

[34]   M.K. Goel, P. Khanna, J. Kishore, Understanding survival analysis: Kaplan-Meier estimate., Int. J. Ayurveda Res. 1 (2010) 274–278. doi:10.4103/0974-7788.76794.

[35]   Danish Energy Agency, Elmodelbolig Statistics, (2018). http://statistic.electric-demand.dk/ (accessed June 11, 2018).

[36]   I. Richardson, M. Thomson, Domestic Electricity Demand Model – Simulation Example, (2010). https://dspace.lboro.ac.uk/2134/5786.

[37]   EN/DS 15251, Indoor environmental input parameters for design and assessment of energy performance of buildings addressing indoor air quality, thermal environment, lighting and acoustics, Dansk Stand. (2007) 54.

[38]   Technical University of Denmark - Department of Civil Engineering, DTU Climate Station-Climate Data, (2018). http://climatestationdata.byg.dtu.dk.

[39]   K. Johnsen, K. Grau, tsbi3: Computer Program for Thermal Simulation of Buildings. User's Guide, (1994) The Danish Building Research Institute, Denmark.

[40]   EQUA Simulation AB, IDA Indoor Climate and Energy - A new generation building performance simulation software, IDA Indoor Clim. Energy. (2018). https://www.equa.se/en/ida-ice.

[41]   European Commission, End-use metering campaign in 400 households of the European Community, (2002) Project EURECO-SAVE PROGRAMME Contract N° 4.1031.

[42]   Energistyrelsen, Energistatistik 2010, (2010). http://www.b14cms.dk/users/klimakompasset.dk/www/files/pdf/Energistatistik_2010.pdf (accessed October 15, 2015).

[43]   Statistics Denmark, Statistics DenmarkByggeri og boligforhold, (2010). http://www.dst.dk/pukora/epub/upload/16217/headword/dk/282.pdf (accessed October 15, 2018).

[44]   Statistics Denmark, Living conditions/Education and knowledge/Labour, income and wealth, (2018). http://www.statistikbanken.dk (accessed June 10, 2018).

[45]   Erhebung 'Wo im Haushalt bleibt der Strom?,' (2011). http://www.energieagentur.nrw/content/anlagen/Erhebung_Wo_im_Haushalt_bleibt_der_Strom_20151 126.pdf.

[46]   A. Sancho-Tomás, M. Sumner, D. Robinson, A generalised model of electrical energy demand from small household appliances, Energy Build. 135 (2017) 350–366. doi:10.1016/j.enbuild.2016.10.044.

PAPER IV: <u>Foteinaki, K.</u>, Li, R., Heller, A., Christensen, M. H. and Rode, C. (2019) 'Dynamic thermal response of low-energy residential buildings based on in-wall measurements'. *Accepted to the 13th REHVA World Congress CLIMA 2019*. Bucharest, Romania.

Dynamic thermal response of low-energy residential buildings based on in-wall measurements

Kyriaki Foteinaki[1,*], *Rongling* Li [1], *Alfred* Heller [2], *Morten Herget* Christensen [3] and *Carsten* Rode [1]

[1]Technical University of Denmark, Department of Civil Engineering, Brovej, Building 118, 2800 Kgs. Lyngby, Denmark
[2]NIRAS, Østre Havnegade 12, 9000 Aalborg, Denmark
[3]Technical University of Denmark, Department of Electrical Engineering, Ørsteds Plads, Building 348, 2800 Kgs. Lyngby, Denmark

Abstract. This study analysed the dynamic thermal response of a low-energy building using measurement data from an apartment block in Copenhagen, Denmark. Measurements were collected during February and July 2018 on space heating energy use, setpoints, room air temperature and temperature from sensors integrated inside concrete elements, i.e. internal walls and ceiling in different heights and depths. The heating system was controlled entirely by the occupants. During February, there were unusually high setpoints for a period and a regular heating pattern for another. Overheating was observed during July. The significant effect of solar gains was noted both during winter and summer months. The room air temperature fluctuations were observed at a certain extent inside the concrete elements; higher in the non-bearing internal wall, followed by the load-bearing internal wall and lastly by the ceiling. The phenomenon of delayed thermal response of the concrete elements was apparent. All internal concrete masses examined were active elements and can contribute to the physically available heat storage potential of the building. The study provides deep insight into the thermal response of concrete elements in low-energy residential buildings, which should be considered when planning a flexible space heating energy use.

1 Introduction

In the future energy system a significant increase in the penetration of renewable energy is expected. As a consequence, the fluctuating energy production from renewable energy sources will challenge the controllability and stability of the power grid. Many studies propose energy flexibility as a solution to facilitate secure operation of the energy system while integrating a large share of renewables, as an example [1], [2]. The residential building sector, which constituted 27 % of the final energy consumption in Europe in 2016 [3], offers great potential for flexibility as the large thermal mass of the building stock could be utilized for energy storage. The new generation of buildings in Denmark are well-insulated and airtight, according to the Danish Building Regulation 2018 [4] and may be heavy-weight, thereby have large thermal storage capacity. There have been many studies showing the potential of the structural thermal mass of buildings to be utilized as storage medium to offer flexibility [5]–[12]. Most studies perform simulations aiming at moving load in time to avoid demand in peak load periods, or to promote demand in off-peak periods, imposing heating strategies that exploit the dynamic thermal response of the concrete mass. Some studies have performed analysis on the effect of the material properties pertaining to thermal mass on the flexibility potential [10], [12], and the contribution of different building components to

flexibility [5], [6]. To the knowledge of the authors, no recent full scale monitoring has been performed to document in detail the behaviour of the thermal mass.

The purpose of the present work is to analyse the dynamic thermal response of a low-energy building using measurement data. The case study building is a multi-family apartment block, located in Copenhagen, Denmark. Measurements are collected during the year 2018. Data on space heating energy use, indoor air temperature, CO_2 concentration and relative humidity are used to evaluate the energy performance and indoor environment of the apartments. In addition, a set of temperature sensors have been placed inside the prefabricated concrete walls and ceilings, in different depths from the surface to the middle of the concrete layer. This unique set of measurements allows for analysis of the dynamic thermal response of the thermal mass of the building, and it demonstrates which part of the thermal mass actively participates in the heat exchange with the indoor environment and can subsequently facilitate load shifting strategies.

The structure of this paper is organized as follows. Section 2 presents the case study building and the monitoring system, followed by the methodology of data analysis. In Section 3 the results of the measurements are presented and analysed, along with discussion of the outcomes. The main conclusions are summarized in Section 4.

---

* Corresponding author: email address

2 Methodology

2.1 Case study building

The case study building is a multi-family apartment block, which was completed in 2017 and is located in Nordhavn district, Copenhagen, Denmark. The building has 72 apartments and 11 town house units. 19 apartments and 1 town house unit have agreed to participate in the EnergyLab Nordhavn project [13], monitoring the energy use, indoor environment and temperatures inside the concrete elements. In the present analysis, one apartment has been chosen in order to analyse in depth the thermal response of concrete elements and develop the methodology that will be applied to the other apartments in future work.
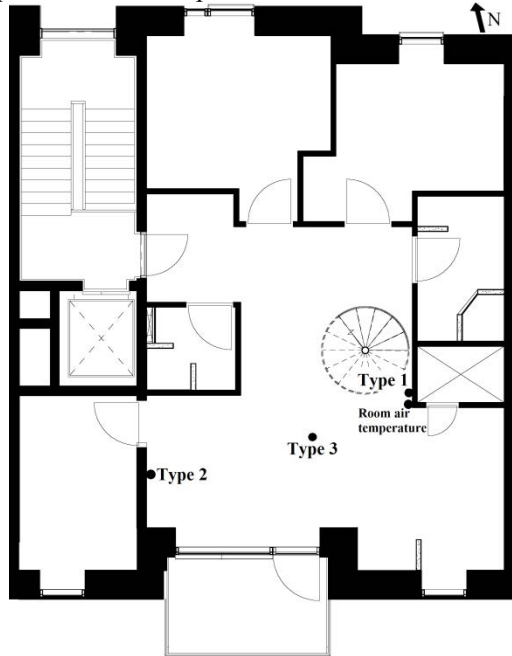

Fig. 1. Apartment floor plan and installed sensors [14].

The apartment has an area of 147 m^2. It is on the top floor (5th floor) of the building and has an attic. It is oriented south and north, while from the east and west sides there are adjacent apartments. Fig. 1 shows the floor plan of the apartment (excluding the attic). Table 1 presents the properties of the main building components.

Table 1. Properties of main building components.

The building is connected to the district heating system and the heat emission system in the apartment is floor heating. There is CAV mechanical ventilation with heat recovery of 85% efficiency. Fresh air is supplied in the living room and bedrooms and it is exhausted from the kitchen, bathroom and toilet.

2.2 Monitoring system

The apartment is equipped with sensors measuring air temperature, CO_2 concentration and relative humidity. There is a home management system which includes the control of the heating system via control panels with integrated room air temperature sensors placed in each room. Furthermore, for research purposes, there are custom-made concrete blocks of size (60 x 200 x 200 mm) with built-in sensors that measure the temperature in different depths. The concrete blocks were created in the laboratory of Technical University of Denmark (DTU), with three integrated temperature sensors, at the surface and at two depths into the material. The sensors used are PT 1000 (DIN EN 60751, CLASS DIN B). The sensors' heads are in direct contact with the concrete that surrounds them, while the sensor cables are covered with a flexible plastic pipe as they lead out of the concrete block, for them to be protected when the sensor block will be cast into the concrete wall and ceiling elements. Fig. 2 depicts the production process of the concrete blocks. These concrete blocks were subsequently casted in walls and ceilings during the production process of the latter. Three different types of setup have been created and are illustrated in Fig. 3.

- Type 1: Sensors were placed in the internal non-bearing wall made of 100 mm aerated concrete, at height 1.1 m in three depths: 0 mm, 25 mm and 50 mm from the surface.

- Type 2: Sensors were placed in the internal load-bearing wall made of 200 mm concrete, at height 1.1 m in three depths: 0 mm, 50 mm and 100 mm from the surface. Three more sensors were placed in the surface layer at heights 0.1 m, 0.6 m and 1.7 m.

- Type 3: Sensors were placed in the ceiling, in the layer made of 220 mm concrete, in three depths: 0 mm, 55 mm and 110 mm from the surface. On top of the concrete there is thermal insulation.

The sensors, which are presented in Table 2, were placed in elements facing the large open space (which includes

Components	Thickness [mm]	U-value [W/(m^2·K)]	Materials
External wall	580	0.122	Concrete (180 mm) Insulation class 38 (300 mm) Concrete (70 mm) Air gap (5 mm) Aluminium plates (25 mm)
Internal load-bearing wall	200	3.70	Concrete (200 mm)
Internal non-bearing wall	100	1.35	Aerated concrete (100 mm)
Floor/ceiling decks	407	0.34	Oak planks (14 mm) Concrete (80 mm) Insulation class 38 (93 mm) Hollow core concrete (220 mm)
Windows	3 pane glazing	0.72	g-value=0.5, frame fraction 15%, window frame U-value=0.85

the living room and kitchen, further referred to as living room), as depicted in Fig. 1.

All measurement data are received by a KNX system and are transferred to a central data management system at DTU. The time resolution of the data is 1 min. Ambient weather data are obtained from the Climate Station at DTU [15] for the respective months of the analysis. The weather station is located 10 km from the measured apartment, so a deviation in the weather data is expected. However, this is not considered critical for the present analysis.

Fig. 2. Production process of concrete blocks with integrated temperature sensors
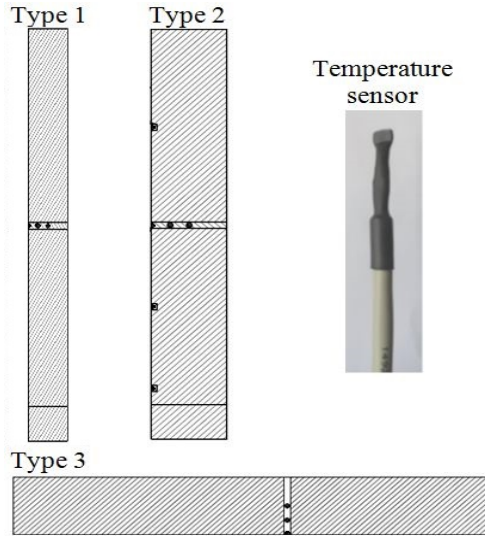

Fig. 3. Placement of temperature sensors in walls (Type 1 and Type 2) and ceiling (Type 3)

2.3 Data analysis

The analysis is performed for one winter month, February, and one summer month, July. The space heating energy use, CO_2 concentration and relative humidity are reported. The main goal of the analysis is the dynamic thermal response of the apartment. Thereby, the room air temperature is discussed, in relation to solar gains and subsequent heating patterns. In-depth analysis of temperature from the different nodes inside the concrete elements in different heights and depths is performed. The nodes inside each concrete element are examined in comparison to the room air temperature, to which the elements are exposed. The data presented are from the living room. For each month, two days are chosen, in order to deepen the analysis on the thermal response. The temperature fluctuations of all nodes in

the concrete elements are normalized, in order to evaluate what percentage of the room air temperature fluctuation is achieved in different depths of the concrete (Eq.1), as well as to evaluate their delay in the thermal response in comparison to the one of the room air temperature (Eq.2):

- $$T_{norm1} = \frac{T_{node} - T_{node(min)}}{T_{room(max)} - T_{room(min)}} \qquad \text{Eq. (1)}$$

- $$T_{norm2} = \frac{T_{node} - T_{node(min)}}{T_{node(max)} - T_{node(min)}} \qquad \text{Eq. (2)}$$

Table 2: Temperature sensors in walls and ceiling

Sensor	Element	Depth	Height
T1-0 mm	Wall	Surface	1.1 m
T1-25 mm	Wall	25mm	1.1 m
T1-50 mm	Wall	50mm	1.1 m
T2-0 mm-1.1 m height	Wall	Surface	1.1 m
T2-50 mm	Wall	50mm	1.1 m
T2-100 mm	Wall	100mm	1.1 m
T2-0 mm -0.1 m height	Wall	Surface	0.1 m
T2-0mm -0.6 m height	Wall	Surface	0.6 m
T2-0mm -1.7 m height	Wall	Surface	1.7 m
T3-0 mm	Ceiling	Surface	3.5 m
T3-55 mm	Ceiling	55mm	3.5 m
T3-110 mm	Ceiling	110mm	3.5 m

3 Results and discussion

3.1 Measurements during winter

The month of February 2018 has been relatively cold, with an average ambient temperature of -1 °C. Fig. 4(a) presents the ambient air temperature and the global irradiance for the whole month. The energy use for this month was 1252 kWh (8.5 kWh/m^2). Both the relative humidity and the CO_2 concentration were within the acceptable ranges according to EN/DS 15251 [16]; on average, relative humidity was 30 % and CO_2 concentration was 700 ppm. Fig. 4 (b) presents the heating power for the whole apartment, as well as the air temperature setpoint and air temperature in the living room. During the month there are periods with different heating patterns and respective thermal behaviour.

- At the beginning of the month, there was high heating use, despite the fact that the temperature setpoint in the living room was either 21 °C or the heating was turned off. The high energy use was due to unusually high setpoints in other rooms of the apartment, which also affected the air temperature in the living room. During the first three days of the month there were minimal solar gains, while from the 4th-9th there were considerable solar gains, which resulted in even higher air temperatures during middays, reaching up to 28 °C. Such temperatures are considered very high, especially for the month of February. Nevertheless, the system was

controlled entirely by the occupants based on their preferences, so extreme behaviors can be expected.

• From the 10th - 13th, the setpoints in the apartment were drastically decreased, while the setpoint in the living room was maintained constant at 21 °C. During these days the heating was turned off and there were very low solar gains. It took 4 days until the air temperature was decreased to 21°C.
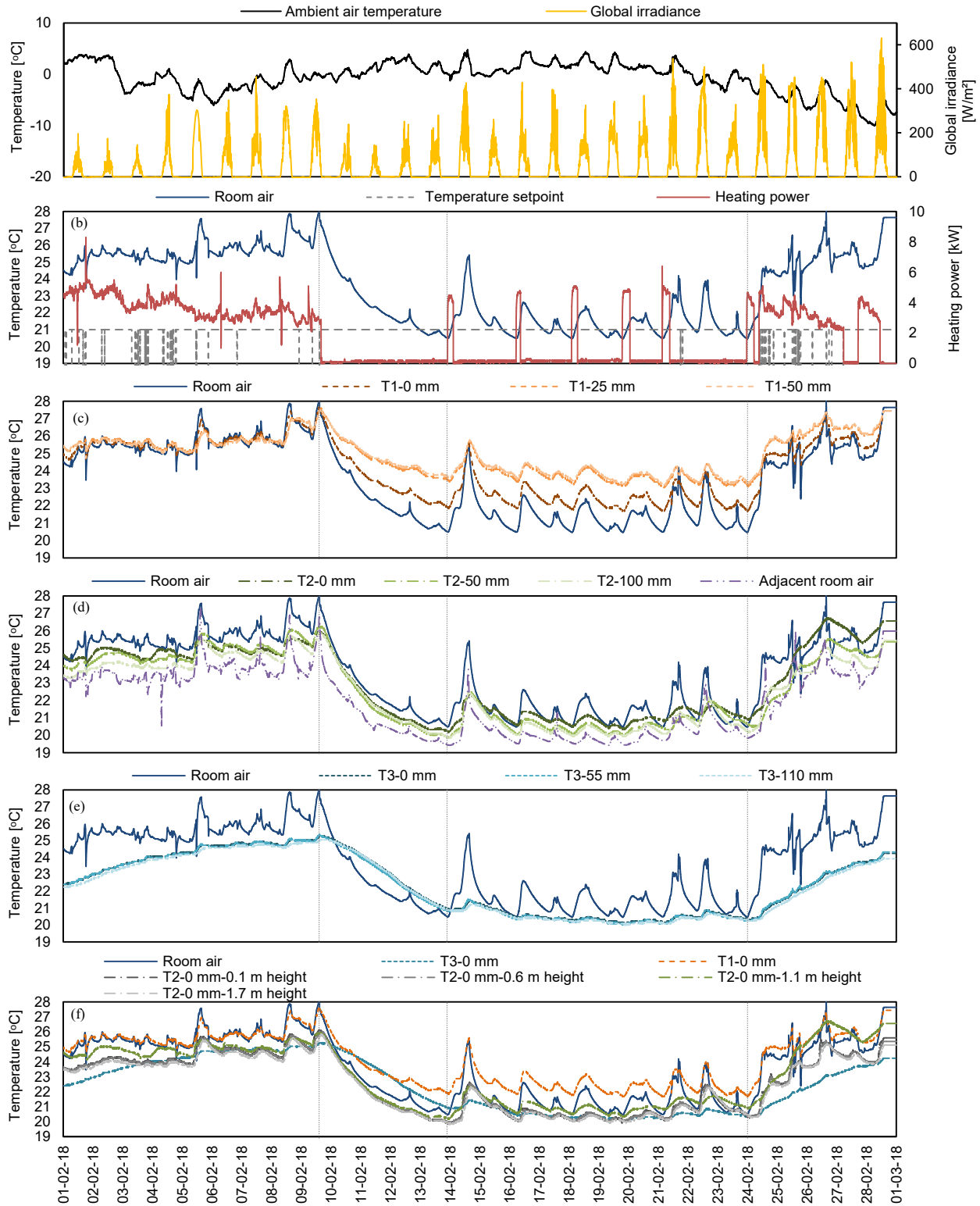
Fig. 4 Analysis of thermal response during February 2018: (a) Ambient air temperature and global irradiance. (b) Space heating power, temperature setpoint and room air temperature. (c) Temperature inside the non-bearing internal wall at 0 mm, 25 mm and 50 mm depth and the room air temperature. (d) Temperature inside the load-bearing internal wall at 0 mm, 50 mm and 100 mm depth and the room air temperature. (e) Temperature inside the ceiling at 0 mm, 55 mm and 110 mm depth and the room air temperature. (f) Surface temperature of the concrete elements and the room air temperature.

• With the setpoint maintained at 21 °C, in the period 14th – 24th the heating use was respective to the setpoint in the living room. A regular heating pattern was followed; the heating system was activated during the night, ran for 4.75 h on average and was subsequently turned off for two days. During this period, the solar gains were average for the season, and affected the air temperature, which increased every midday.

• Towards the end of the month, the temperature setpoints of other rooms were increased again and the thermal behavior resembled the one at the beginning of the month.

The aforementioned variations in the temperature setpoints and respective heating patterns have created significant changes in the room air temperature, which allows to better apprehend the thermal behavior inside the concrete elements.

Fig. 4(c) presents the temperatures inside the internal non-bearing wall (sensors Type 1) and the room air temperature. Fig. 4(d) presents the temperatures inside the internal load-bearing wall (sensors Type 2) and the room air temperature of the living room and the adjacent room. Fig. 4(e) presents the temperatures inside the ceiling (sensors Type 3) and the room air temperature. Fig. 4(f) presents the surface temperature of the concrete elements and the room air temperature.

Regarding the temperatures inside the internal non-bearing wall, all three sensors showed higher temperatures than the room air temperature. The one in the middle of the wall had the highest temperature, while the other two had almost the same temperature. The other side of the wall is the utility room, so it is most likely that hot pipes crossing the room were heating it up. At the beginning of the month, when the room air temperature was very high as well, this effect was not observed, but instead all the layers of the wall had an almost uniform temperature.

The temperatures inside the internal load-bearing wall had most of the time the expected behaviour, given that the adjacent room on the other side of the wall had lower temperature. They were mostly lower than the room air temperature, with the surface temperature being slightly closer to the room air temperature, followed by the temperatures in 50 mm and 100 mm depth in the concrete. Exceptions in this behaviour were the start of significant temperature changes (increase or decrease), when due to the delayed response of the different layers, the temperatures overlapped with each other. The delay of the thermal response in different elements and depths is analysed in depth onwards.

The thermal behaviour inside the ceiling was different than that in the walls. The three layers of the ceiling had almost the same temperature, with only negligible differences. The response to the room air temperature fluctuations was slow, and daily fluctuations could only marginally be observed, while the temperature curve was only smoothly responding cumulatively to the air temperature changes. This is explained as this element is exposed to room air temperature fluctuations only from one side as there is thermal insulation at the top of it, while the walls consist

of only concrete/aerated concrete and are exposed to room air temperature fluctuations from both sides. Furthermore, the ceiling is not directly exposed to solar radiation, as the wall can be.

Regarding the temperatures on the surface of the different elements, the surface temperature of the internal non-bearing wall was the highest, for the reasons previously explained. The temperatures on the surface of the internal load-bearing wall at the different heights, 0.1 m, 0.6 m and 1.7 m were almost the same, validating the expectation that the floor heating creates a uniform thermal environment with minimal vertical thermal asymmetries. However, the surface temperature at 1.1 m height was often higher than that of the other heights, which could possibly be attributed to direct solar radiation at this height. The surface temperature of the ceiling was, sometimes higher and sometimes lower than the rest of the surfaces, due to the slower thermal response. However, during the period with the regular heating pattern (14th – 24th), the temperature of the ceiling was very similar to those of the load-bearing internal wall. These results confirm the findings in [5], where a similar apartment was simulated and the thermal behaviour of different concrete elements was evaluated.
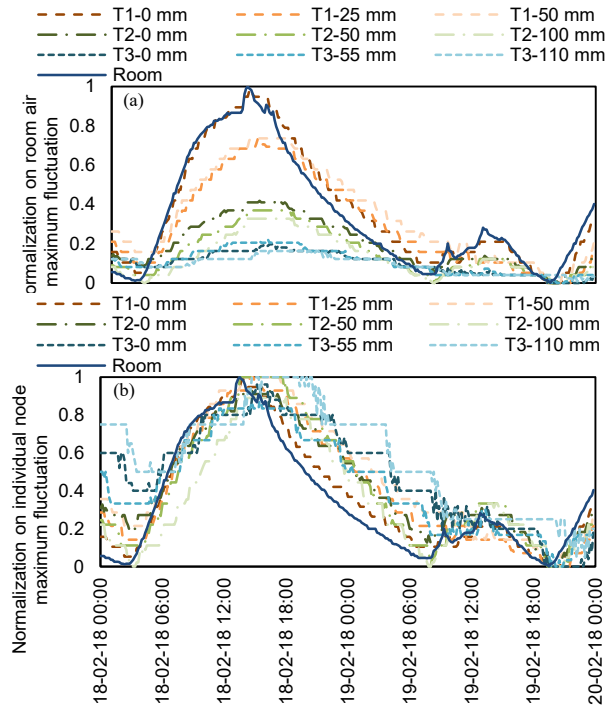
Fig. 5. Temperature fluctuations of all nodes between 18th–19th February. (a) Normalized on room air temperature maximum fluctuation. (b) Normalized on individual node temperature maximum fluctuation.

In order to deepen the understanding of the thermal response of the different layers of the concrete elements, two days were chosen, 18th – 19th February, for further analysis. Temperature fluctuations of each node (i.e. layer in each element) were normalized on the maximum fluctuation of the room air temperature for those two days. Thereby, the temperature fluctuation that was achieved in the different depths of the concrete elements is quantified as a percentage of the room temperature

fluctuation. This is presented in Fig. 5(a). For the two days analysed, the maximum room air temperature fluctuation was 2 °C. Comparing the temperature fluctuations achieved in the concrete elements to that of the room air temperature, the highest percentages were achieved in the non-bearing internal wall, followed by the load-bearing internal wall and lastly the ceiling. The surface node of the non-bearing internal wall had almost the same fluctuations as the room air temperature. The other two layers of this wall achieved a temperature increase as high as 74% of the room air temperature. The layers of the load-bearing internal wall achieved 43%, 37% and 33% for the surface, 50 mm and 100 mm node respectively. The layers of the ceiling achieved on average 19% of the room air temperature fluctuations. The room air temperature increase during the second day, which was 0.4 °C, was marginally observed inside the concrete of the ceiling.

Furthermore, temperature fluctuations of each node were normalized on the maximum temperature fluctuation of this node for those two days, such that the temperature fluctuation for each node varies between 0 and 1. Thereby, the timing of the fluctuations can be evaluated, quantifying the delay of the thermal response in different elements and depths. This is presented in Fig. 5(b). The delay of the thermal response in different elements and depths is apparent. During the temperature increase of the first day, the maximum delay was 2 h for the node 100 mm deep in the internal load-bearing wall. The delay in the non-bearing wall was negligible. The effect is more pronounced during the temperature decrease. This means that when the room is heated up by the heating system, the concrete elements react faster and this increase is observed to a certain degree in the nodes. On the contrary, when the heating system is turned off, the concrete elements react slower to the air temperature change, helping the apartment to cool down at a slower pace.

Fig. 6 Analysis of thermal response during July 2018: (a) Ambient air temperature and global irradiance. (b) Temperature inside the non-bearing internal wall at 0 mm, 25 mm and 50 mm depth and the room air 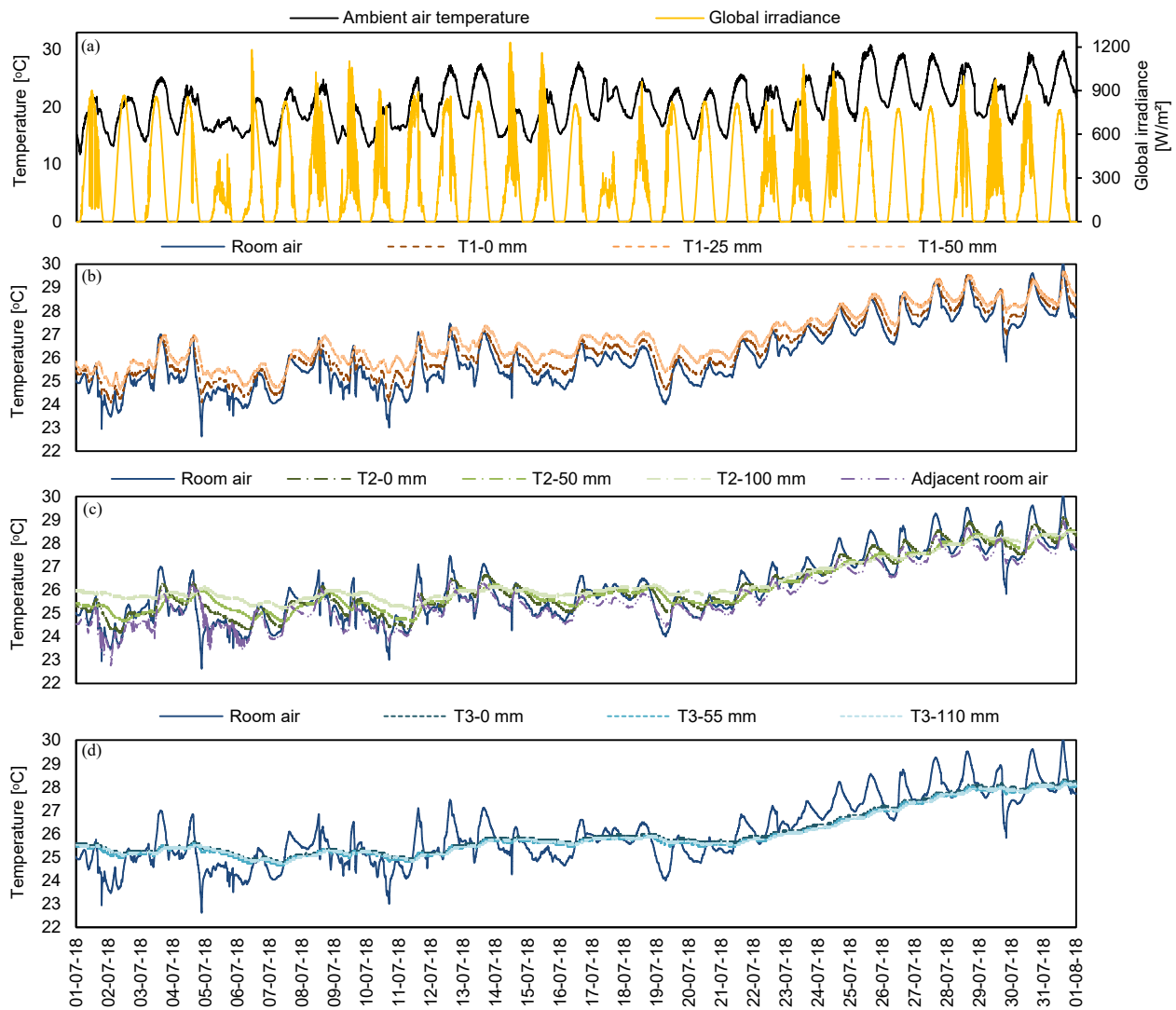temperature. (c) Temperature inside the load-bearing internal wall at 0 mm, 50 mm and 100 mm depth and the room air temperature. (d) Temperature inside the ceiling at 0 mm, 55 mm and 110 mm depth and the room air temperature.

3.2 Measurements during summer

The month of July 2018 had an average ambient temperature 20.4 °C. Fig. 6(a) presents the ambient air temperature and the global irradiance for the whole month. Both the relative humidity and the CO_2 concentration were within the acceptable ranges (EN/DS 15251 [16]), with the relative humidity being 50% and the CO_2 concentration 470 ppm on average. The room air temperature throughout the month indicates the problem of overheating observed in low-energy buildings, as the average temperature was 26 °C and reached a maximum of 30.1 °C.

The pattern of the temperatures in the internal non-bearing wall (Fig. 6(b)) was the same as the one in February, namely higher than the room air temperature, due to the adjacent room being the utility room. In the load-bearing internal wall (Fig. 6(c)), the temperatures were similar and occasionally slightly higher than the room air temperature. It should be noticed that the adjacent room had almost the same temperature as the living room, whereas during February the adjacent room had on average 2 °C lower room air temperature. The temperature in the ceiling (Fig. 6(d)) was rather stable, and approximately the average of the room air temperature, since daily fluctuations are not observed in the concrete of the ceiling. Towards the end of the month, when the room air temperature was constantly increasing, so did the temperature inside the ceiling but with a smoother development.
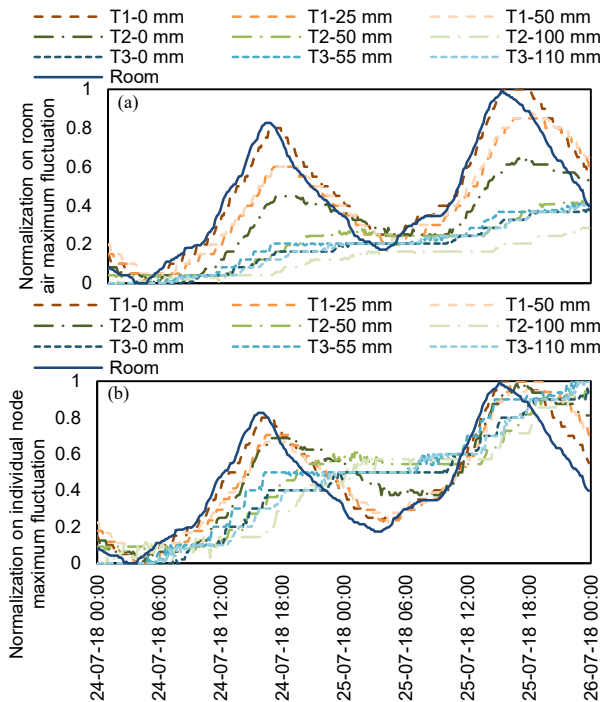

Fig. 7. Temperature fluctuations of all nodes between 24th–25th July. (a) Normalized on room air temperature maximum fluctuation. (b) Normalized on individual node temperature maximum fluctuation.

Two days were chosen for further analysis, 24th – 25th July (Fig. 7). For these two days, the maximum room air temperature fluctuation was 2 °C. Regarding

the temperature fluctuations achieved in the concrete elements compared to those of the room air temperature, the percentages achieved in the non-bearing internal wall were similar to those in February. For the layers of the load-bearing internal wall, there was larger distribution between the percentages achieved by each layer; 65%, 42% and 29% for the surface, 50 mm and 100 mm node respectively. The layers of the ceiling achieved on average 40% of the room air temperature fluctuations, namely double the percentage achieved during February, due to the difference between ceiling and air being smaller in summer than in winter and heat was accumulated in the ceiling. Regarding the delay in response of the concrete elements compared to the room air temperature, a difference in the behaviour can be noticed compared to the days in February. During the room air temperature increase due to solar gains, the delay in the response of the concrete elements was greater than that during February. Furthermore, in some nodes (i.e. 50 mm and 100 mm node in the load-bearing internal wall and all nodes in ceiling) the temperature decrease was not observed.

Nevertheless, both in February and July, the temperature fluctuations in all different depths and elements indicate that the concrete elements were effectively activated by the room air temperature fluctuations. Following the assumption also discussed by [17], in order for the thickness of a concrete element to be considered effective, higher than 10% of the room air temperature fluctuations should be achieved. According to this, all layers examined are effective, namely more than half of the concrete mass exposed to the room air temperature is effective and can actively facilitate load shifting strategies.

The conclusions of this study were based on measurements monitored while the heating system in the apartments was controlled by the occupants. The analysis clearly illustrated the importance of occupants' behavior on the space heating energy use and the respective thermal response. Data from the same case study building has been analysed in [18], where they focused on occupant interaction with heating systems and windows. Further investigations are planned for the upcoming heating season, when we plan to remotely control the heating temperature setpoints in the apartments.

4 Conclusions

This study analysed the dynamic thermal response of a low-energy building using measurement data from a multi-family apartment block located in Copenhagen, Denmark. Measurements collected during February and July 2018 were analysed, regarding space heating energy use, heating setpoints, room air temperature, CO_2 concentration, relative humidity, as well as a unique set of measurements from temperature sensors integrated inside concrete elements (internal walls and ceiling) in different heights and depths.

During the month of February there were periods with very different heating temperature setpoints and

respective heating patterns. Unusually high setpoints led to very high temperatures and heating energy use for some periods in the month of February. The significant effect of solar gains on indoor air temperature was observed both during winter and summer months. With the contribution of solar gains and the low heat losses, in order for the apartment to maintain the temperature at 21 °C, it was sufficient that the heating system was turned on for 4.75 h every other day. A problem of overheating was observed during July. The indoor air quality, in terms of CO_2 concentration and relative humidity was within the acceptable ranges and the thermal environment was uniform with minimal vertical thermal asymmetries.

Comparing the temperature fluctuations achieved in the concrete elements to that of the room air temperature (defining the 100%), the highest percentages/dynamics were achieved in the non-bearing internal wall (100 mm aerated concrete), i.e. 87% on average, followed by the load-bearing internal wall (200 mm concrete), i.e. 41%, and lastly by the ceiling (220 mm hollow core concrete), i.e. 30%. Thereby, all internal concrete masses examined were active elements and contribute to the physically available heat storage potential of the building. The phenomenon of delay in the thermal response of the concrete element was apparent.

The results of this study provide deep insight into the thermal response of concrete elements in low-energy residential buildings. Important information are presented about the behaviour of the structural mass of this type of buildings as a storage medium, which should be considered when planning a flexible space heating energy use to contribute to heat load shifting.

References

[1]   P. Denholm and M. Hand, Grid flexibility and storage required to achieve very high penetration of variable renewable electricity, Energy Policy, **vol. 39, no. 3**, pp. 1817–1830, (2011).

[2]   P. D. Lund, J. Lindgren, J. Mikkola, and J. Salpakari, Review of energy system flexibility measures to enable high levels of variable renewable electricity, Renew. Sustain. Energy Rev., **vol. 45**, pp. 785–807, (2015).

[3]   European Commission, EU Reference Scenario 2016 - Energy, transport and GHG emissions - Trends to 2050, *Energy, transport and GHG emissions - Trends to 2050*, (2016). Available: https://ec.europa.eu/energy/sites/ener/files/documents/ref2016_report_final-web.pdf.

[4]   Ministry of Transport Building and Housing, Executive order on building regulations 2018 (BR18), (2018). Available: http://bygningsreglementet.dk/~/media/Br/BR-English/BR18_Executive_order_on_building_regulations_2018.pdf.

[5]   K. Foteinaki, A. Heller, and C. Rode, Modeling energy flexibility of low energy buildings utilizing thermal mass, *Proceedings of IAQVEC*, (2016).

[6]   K. Foteinaki, R. Li, A. Heller, and C. Rode, Heating system energy flexibility of low-energy residential buildings, Energy Build., **vol. 180**, pp. 95–108, (2018).

[7]   J. Kensby, A. Trüschel, and J.-O. Dalenbäck, Potential of residential buildings as thermal energy storage in district heating systems – Results from a pilot test, Appl. Energy, **vol. 137**, pp. 773–781, (2015).

[8]   J. Le Dréau and P. Heiselberg, Energy flexibility of residential buildings using short term heat storage in the thermal mass, Energy, **vol. 111**, pp. 991–1002, (2016).

[9]   G. Masy, E. Georges, C. Verhelst, and V. Lemort, Smart grid energy flexible buildings through the use of heat pumps and building thermal mass as energy storage in the Belgian context, Sci. Technol. Built Environ., **vol. 4731**, pp. 800–811, (2015).

[10]   G. Reynders, T. Nuytten, and D. Saelens, Potential of structural thermal mass for demand-side management in dwellings, Build. Environ., **vol. 64**, pp. 187–199, (2013).

[11]   G. Reynders, J. Diriken, and D. Saelens, Generic characterization method for energy flexibility: Applied to structural thermal storage in residential buildings, Appl. Energy, **vol. 198**, pp. 192–202, (2017).

[12]   H. Wolisz, H. Harb, and P. Matthes, Dynamic simulation of thermal capacity and charging/discharging performance for sensible heat storage in building wall mass, *Proceedings of IBPSA*, (2013).

[13]   EnergyLab Nordhavn, EnergyLab Nordhavn – New Urban Energy Infrastructures, (2018). Available: http://energylabnordhavn.weebly.com/.

[14]   ARKITEMA ARCHITECTS, Architectural drawings. Århus, Denmark, 2015.

[15]   T. U. of D. DTU Climate Station, Department of Civil Engineering, Climate Data, (2018). Available: http://climatestationdata.byg.dtu.dk.

[16]   EN/DS 15251, Indoor environmental input parameters for design and assessment of energy performance of buildings addressing indoor air quality, thermal environment, lighting and acoustics, Dansk Stand., p. 54, (2007).

[17]   J. Babiak, M. Minarova, and B. W. Olesen, What is the effective thickness of a thermally activated concrete slab?, *Proceedings of ClLIMA*, (2007).

[18]   L. Sarran, M. H. Christensen, C. A. Hviid, A. M. Radoszynski, C. Rode, and P. Pinson, Data-driven study on individual occupant comfort using heating setpoints and window openings in new low-energy apartments – preliminary insights, *CLIMA 2019 (submitted)*, (2019).

PAPER V: Sarran, L., <u>Foteinaki, K.</u>, Gianniou, P. and Rode, C. (2017) 'Impact of Building Design Parameters on Thermal Energy Flexibility in a Low-Energy Building', *in the Proceedings of the 15th IBPSA Conference*. San Francisco, CA, USA, pp. 239–248.

Impact of Building Design Parameters on Thermal Energy Flexibility in a Low-Energy Building

Lucile Sarran[1], Kyriaki Foteinaki[1], Panagiota Gianniou[1], Carsten Rode[1]
[1]International Centre for Indoor Environment and Energy, Department of Civil Engineering, Technical University of Denmark, Kgs.Lyngby, Denmark

Abstract

This work focuses on demand-side management potential for the heating grid in residential buildings. The possibility to increase the flexibility provided to the heat network through specific building design is investigated. The role of different parts of the building structure on thermal flexibility is assessed through a parameter variation on a building model. Different building designs are subjected to heat cut-offs, and flexibility is evaluated with respect to comfort preservation and heating power peak creation.

Under the conditions of this study, the thermal transmittance of the envelope appears to have the largest impact on thermal flexibility. The importance of window design, namely the size, U-value and orientation, is underlined due to its critical influence on solar gains and heat losses. It is eventually observed that thermal mass has a secondary influence on the evaluated indicators; its variation only affects thermal flexibility if the thermal resistance of the envelope is sufficient.

Introduction

The share of renewable energy sources should represent at least 55% of the European gross energy consumption in 2050 (European Commission, 2011). Their production being inflexible and highly dependent on weather conditions, a high penetration of renewable sources might create a risk for energy security of supply. One of the solutions to this challenge is demand-side management as defined by Gellings (1985), which aims at adapting energy consumption to a fluctuating production rather than the opposite. This idea is particularly studied in the building sector, where implementation of demand-side management would permit to reduce the energy footprint of buildings, while providing flexibility to the energy grid as a whole (Kolokotsa, 2015).

EnergyLab Nordhavn is a full-scale research project investigating the possibility of intelligent energy operation across the neighbourhood of Nordhavn, Copenhagen. As a part of that project, the present study aims at understanding how energy efficient buildings can adapt perturbations in a city's heat and power grids. Focus is set here on thermal energy flexibility, specifically defined in this work as the capacity of a building to provide a good indoor comfort in spite of changes in delivered heating power. The understanding of this potential can then be used by the grid operator to optimise heating schedules. Thermal demand-side management is moreover seen as a tool to ensure electrical grid stability, via a coupling of the heat and power grids (EnergyLab Nordhavn, 2015; Müller et al., 2015).

An interest presented by low-energy buildings in the flexibility issue is their ability to retain heat for a long period of time, therefore acting as a storage medium in the heating grid. However, even though buildings' thermal flexibility potential is being investigated, few of the studies specifically evaluate the influence of design features on a building's flexible behaviour. The impact of different wall properties on their ability to store energy is well documented in literature (Asan, 2006; Borresen, 1973; Ma & Wang, 2012; Moffiet et al., 2014; Orosa et al., 2012; Wang et al., 2014) and their importance for load shifting was also specifically studied by Reynders (2015). Yet, it is valuable to extend the impact assessment to other building components than its sole thermal mass: all parameters having an influence on indoor comfort variations with time (through heat gains, losses and storage) are of interest when assessing a building's resilience to heating perturbations. Therefore, window parameters must also be investigated. Some researchers pay attention to the role of windows and solar gains (Orosa et al., 2012; Reynders, 2015; Wang et al., 2014), however more with respect to thermal buffering than flexibility. Similarly, research has been carried out on the role of window orientation in energy savings, but literature about its contribution to flexibility potential is rare (Reynders, 2015; Zhu et al., 2009).

Moreover, the achieved flexibility is often quantified in terms of financial savings (Masy et al., 2015; Reynders, 2015), shifted heating energy (De Coninck & Helsen, 2016) or capacity (Oldewurtel, 2013). The implications of heating control strategies on the occupants' comfort are generally not quantified.

This study is the first step of a larger project aiming at assessing the ability of low-energy buildings to ensure an active role in a city's heat and power grids. The goal of this preliminary study is to determine how the design parameters of a given low-energy

building can influence its capacity to adapt simple perturbations on the heating grid in which it is integrated. Focus was set on passive flexibility strategies, in particular heat storage in the building structure. A parameter variation was carried out on a simulation model of a dwelling, investigating the role of the different building components in the flexibility potential of the building regarding its heat load. This paper does not consider the role of building services systems, e.g. space heating and ventilation, on flexibility since this is the theme of a parallel work that will be published separately.

This work has two main outcomes. First, a set of two indicators was built, quantifying theoretical heat flexibility in a building in terms of indoor comfort and heating demand. Second, this work provides an understanding of the heat storage processes in a low-energy building, permitting to identify the issues related to heating power perturbations and the extent to which building design can respond to it.

Methodology

Investigated building

The impact of design features on thermal flexibility was evaluated on a model of an apartment created according to the geometry, materials and systems of an existing apartment in Copenhagen, Denmark. The modelled apartment is located in the northern district of Nordhavn, in a nearly-zero-energy building currently under construction. The chosen building is representative of the current and future constructions in Denmark, which are bound to low energy consumption due to the strict Danish Building Regulations. It was chosen to focus the study on a single apartment in order to be able to get a thorough understanding of the obtained results. This choice allows getting deeper into the heat transfer mechanisms occurring at a smaller scale and to give a straightforward explanation of the findings.

Parameter variation

As the output of a literature study, six design parameters were chosen to be investigated further. Several values were chosen for each of them, covering a realistic range of possibilities as found in the literature (Gianniou et al., 2016; Reynders, 2015) and which reflects the construction characteristics of Danish building stock. Even though the ranges of values investigated for the different parameters are heterogeneous, they can all be interpreted as the complete range from the worst to the best-performing building components currently available – or in the case of the glazing-to-wall ratio and building orientation, as the whole set of values observed in Danish buildings. The corresponding difference in flexibility potential between extreme design cases thus represents the overall potential improvement that can be triggered by a realistic change of the considered parameter.

Table 1 presents the chosen parameters, the value of these parameters in the investigated apartment, and the variation range for each of them.

Different versions of the original apartment model were created, each giving a different value to a single one of the investigated parameters. The goal here was to perform a local sensitivity analysis in order to isolate the impact of each of the parameters on thermal flexibility.

Table 1: Investigated parameters, value in the base apartment model and variation range

Parameter	Original value	Studied range
External wall concrete thickness (cm)	15	[2 ; 30]
External wall insulation thickness (cm)	27.5	[0 ; 32]
Floor concrete slab thickness (cm)	6	[3 ; 25]
Glazing-to-external-wall ratio[1] (-)	0.42	[0.1 ; 0.55]
Window U-value (W/m²K)	0.81	[0.75 ; 2.5]
Orientation of the main facade[2]	S	N; E; S; W

Flexibility assessment and indicators

The flexibility assessment performed on the different models included two elements: a protocol, and a set of indicators quantifying the apartment´s flexibility potential. The overall protocol was the following: a cut-off in the heating schedule was performed, and the consequences of this perturbation were measured with focus on two aspects: the occupants' comfort and the heating power profile. This led to the two flexibility indicators developed.

The first test, focusing on occupants' comfort, consisted of cutting heat off in the apartment at 7 AM on Monday, January 19th and observing the decrease in operative temperature in the living room. The climate files and schedules used in the simulation are detailed in the "Model description" section. The living room was chosen as the target of the study since it is assumed to be the space where occupants are the most present during daytime and therefore where thermal comfort is valued the most. Moreover, its large glazed surface makes it likely to suffer from large temperature swings. This heating control strategy corresponds to a peak shaving operation under its most extreme form: heat is completely cut off in the residential buildings to shave the morning heating peak. This scenario was chosen for its

---

[1] The glazing-to-external-wall ratio was modified by changing the size of the windows in the different rooms simultaneously and by the same factor.
[2] The orientation was changed by rotating the entire building model.

simplicity: indeed, implementing a preheating period of a specific duration or reducing heat supply by a certain percentage would create a bias on the results, while this bias is reduced when using a fundamental signal such as a total cut-off. The corresponding indicator was the time (measured from the cut-off) after which the operative temperature dropped below the lower bound of the occupants' acceptability range. In this work, this minimum acceptable temperature was set to 20°C, corresponding to Category II of EN/DS 15251. Figure 1 gives a simplified graphical representation of the indicator calculation.

In practice, given the large fluctuation of indoor temperature, temperature can drop for some minutes below 20°C and rise again, which is not a real threat to indoor comfort. Therefore, a tolerance factor was introduced, which made the indicator practically calculated as the duration of the time interval, starting from the cut-off, during which operative temperature in the living room has been above 20°C for 90% of the time since the cut-off.

This indicator was introduced to reflect in simple terms the degradation of indoor comfort in the living space. It is a tangible measure of occupants' perception. Following the variation of this indicator when modifying the apartment's design parameters permits to understand the theoretical ability of these investigated parameters to preserve indoor comfort, in case of a change in heating schedule ordered by the thermal grid operator. The simplicity of the protocol permits to obtain a fundamental comparison of the parameters' role – more complex control strategies will be implemented in a further study.

The second test consisted of cutting heat off in the apartment between 7 AM and 4 PM on Monday, January 19th, which corresponds to a heat prioritization strategy: dwellings are heated up in the evening and during the night, and offices during working hours. It was chosen to measure the maximum heating power level reached in the following two days (between the 19th and the 21st of January) in the simulation with heating cut-off and to compare it with the maximum power level in case of
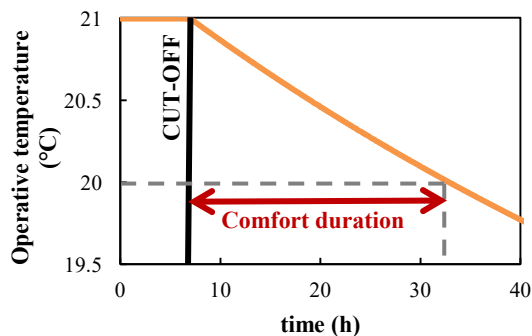
normal operation (with a setpoint at 21°C) during the same period. The heating power is defined as the heat input in the floor heating system for the whole apartment. This output constitutes the second flexibility indicator (1). Q_{max} and $Q_{max,ref}$ are represented in Figure 2.

$$Ind_2 = \frac{Q_{max} - Q_{max,\ ref}}{Q_{max,\ ref}} \qquad (1)$$
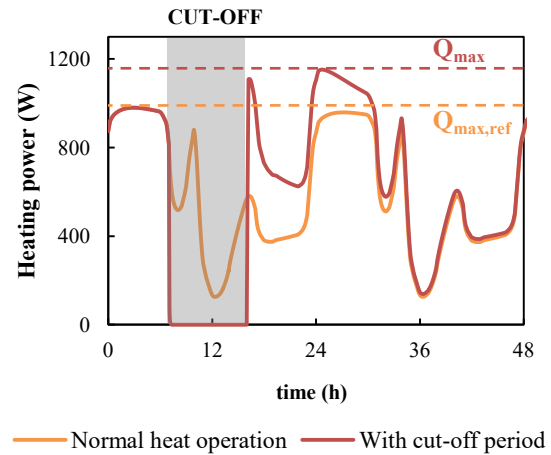
Figure 2: Peak power variation

The goal of this indicator is to assess the pressure set on the heating system when performing a heating control operation. Indeed, in order to satisfy indoor comfort requirements, there is a risk that the system reacts by a large increase in heating power when the cut-off period is over, which can in some cases go against the goals of performing a load-shifting strategy. Calculating this indicator under different design solutions permits to identify the magnitude of this potential problem; if the problem can be predicted; and if it is particularly affected by specific design parameters. In a future work, different controls strategies will be applied to mitigate this problem, in particular a ramp for the temperature setback rather than the simple on/off control tested here. In this indicator, the peak levels that are compared are not necessarily occurring at the same time: they are the overall maxima over the considered days. This approach gives information about the extra capacity that would be needed to accommodate the new peaks.

The two flexibility indicators were calculated for each of the models, and their variation was related to the change in the parameters' value by a graphical representation. The impact of the different parameters on the chosen indicators could then be appreciated.

Model description

This study was based on a set of numerical models created on the building performance simulation software IDA ICE 4.7.

Figure 1: Duration of the comfort period

Figure 3: Building overview (source: Alectia)

Geometry

The building that was investigated is a 5-floor low-energy residential building located on the waterfront, with the water-facing facade oriented 10° from South. One apartment of this building was modelled in this study. It is a 95m², 3-room apartment located on the 4th floor, with the main facade facing the waterfront.

The geometry of the IDA ICE model is shown in Figure 4. The rest of the building volume was included in the model, but only with regards to shading calculations: it was assumed that the adjacent apartments are similarly heated spaces, so there is no heat exchange with the rest of the building.

Figure 4: IDA ICE apartment model - floor plan

Building materials

The external walls of the building included a thick layer of concrete on the inside and a brick external façade, with mineral wool insulation in-between. Two sorts of internal walls were used: bearing walls made of a single concrete layer, and non-bearing walls made of aerate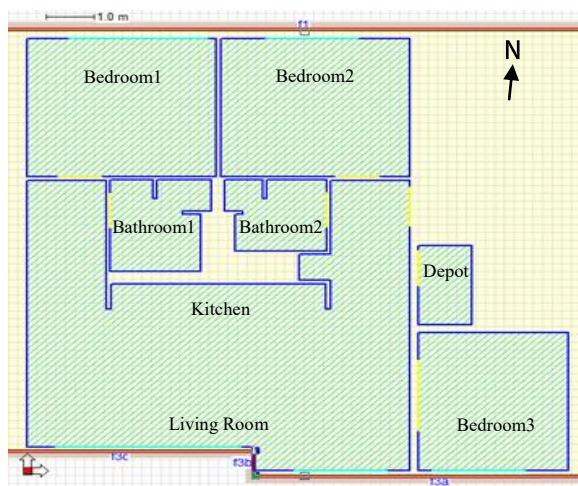d concrete, used to separate the bedrooms and in the kitchen corner. The floor of the bedrooms, living room and depot room was covered by oak planks lying on a concrete screed. The windows consisted of three glass panes filled with argon, with an aluminium and wood frame. The total

U-value of the apartment is equal to 0.49W/m²K. Table 2 details the different construction layers.

Systems

All the apartments were equipped with a floor heating system connected to the district heating network, with supply and return temperatures of respectively 40 and 35°C. The heating setpoint was chosen to be 21°C and no cooling system was included. The domestic hot water circuit was not modelled in this study due to its little influence on heat flexibility in the absence of individual hot water storage system for each apartment. The mechanical ventilation system was balanced CAV (constant air volume) with 80% heat recovery. Fresh air was supplied in the bedrooms and the living room with a setpoint of 17°C and the return air was exhausted from the kitchen and the bathrooms.

Outdoor conditions and internal gains

In order to isolate the results from the influence of fluctuating outdoor conditions, the base outdoor temperature was set constant to -5°C, representing a cold winter day, with 90% relative humidity. Due to the difficulty to predict the wind-driven infiltration in the context of a semi-exposed building, a constant value for infiltration of 0.1 L/s/m² floor area was used. Some solar gains were defined based on an average radiation in a short winter day. This pattern was repeated every day of the simulation period.

A standard pattern for the heat flux from occupants and electrical appliances was defined. The day was divided in four periods, and different uses were defined for weekdays and weekends in the different rooms. It was considered that four people live in the apartment, which is common for this specific building: Bedroom 1 was considered double. The four occupants were always present in the apartment from 5 PM to 9 AM, and all day during the weekends. None of them was present from 9 AM to 5 PM during workdays. Equipment units were positioned in every room apart from the depot room and the bathrooms.

A daylight-related control was designed for lighting

Table 2: Composition and U-value of building parts

Building part	Layers (from outside/from bottom)	Total U-value (W/m²K)
External wall	• Brick (10.8 cm) • Mineral wool (27.5 cm) • Concrete (15 cm)	0.13
Bearing internal wall	Concrete (20 cm)	3.43
Non-bearing internal wall	Aerated concrete (10 cm)	1.13
Floor	• Hollow concrete (22 cm) • Termotec insul. (14.6 cm) • Concrete screed (6 cm) • Oak planks (3 cm)	0.27
Window	Triple-pane Argon-filled	0.81

as advised in BR15 (The Danish Building Regulation, 2015). Shading devices were included and supposed to be manually activated by the occupants in case of excessive lighting conditions.

Simulation parameters

A dynamic simulation was chosen: the program made an initial guess and reached convergence while simulating from the 1st of January to the 18th of January, then started the simulation from the 19th of January, day of the cut-off. The maximum simulation time step was 12 minutes, but it was automatically reduced when more accuracy was needed.

Results

The graphical representation of the obtained flexibility results is shown in Figure 5. The two indicators (duration of the comfort period in the left graphs and peak power variation in the right graphs) are plotted against the different design parameters, which are gathered in three groups: material layers, window features and main facade orientation. In each of the graphs, the points representing the original building are darker and circled in black.

Material layers

As seen in Figure 5a and Figure 5b, the thickness of the concrete layer in the external walls shows impact on none of the two indicators under the considered conditions. Between a 2-cm and a 30-cm concrete layer, the duration of the comfort period in the living room varies between 72 and 74.5 hours, which is almost negligible in comparison to the impact observed for other parameters. Identically, the peak power in a period perturbed by a heat cut-off gets approximately 19% higher than under normal operation in the same period, independently of the concrete thickness in the external walls. This result questions the role of heat storage in the external walls in response to a heat cut-off: in this particular case, the increase in thermal storage capacity does not affect the apartment's energy flexibility potential.

On the contrary, the duration of the comfort period after cut-off in the living room shows a large dependence on the thickness of the insulation layer in the external walls. While a non-insulated external wall permits to retain heat in the living space for 21 hours before the comfort limit is reached, adding 10 centimeters of insulation brings this figure to 69 hours. Above 10 centimeters of insulation, the corresponding improvement in comfort conditions is relatively small, namely reaching 32 centimeters of insulation results in an increase in the comfort period duration from 69 to 81 hours. This result shows that a minimum thermal resistance is necessary to allow heat retention: if the insulation is too poor, energy is lost too rapidly towards the ambient to be stored in the building structure (external walls). The insulation thickness of the external walls also has a significant impact on the heat consumption peak: a heat cut-off in a non-insulated apartment leads to a rapid temperature decrease, and therefore to an important heating peak when heat is turned on again at 4 PM: the peak gets 60% higher than the maximum heating power in normal operation (with no cut-off). The peak power variation due to a cut-off gets less important when the insulation layer gets thicker: for an apartment with more than 18 centimeters insulation, the peak due to a cut-off is around 20% higher than the peak power in normal operation. Both tests show that even though a minimum level of insulation is required, the apartment's flexibility potential is not significantly improved for an insulation thickness higher than 20 centimeters, which is a valuable piece of information when drawing design guidelines.

Varying the thickness of the concrete slab that embeds the floor heating pipes from 3 to 12 centimeters leads to a change in the comfort period from 72 to 93 hours (Figure 5a), while increasing the slab thickness from 12 to 25 centimeters increases the comfort period duration by 3 hours only, from 93 to 96 hours. This result may be due to the fact that the pipes are located only one centimeter below the surface of the concrete slab in all of the cases, which limits the penetration of heat in the lower layers of the concrete. The study of the impact of the depth of the pipes into the concrete was not within the scope of this work. There is nevertheless room for improvement in the investigated building: increasing the concrete slab thickness from 6 cm to 12 cm could save up to 20 hours of heating in the living room. The analysis of the peak power variation due to a cut-off does not show a clear dependence on the slab thickness (Figure 5b). The results nevertheless show an optimal behaviour when the slab thickness approximates 12 centimeters.

Window features

Both the window U-value and the glazing-to-external-wall ratio show a large impact on the calculated flexibility indicators. As seen on Figure 5c, when varying the window U-value from 0.75 to 2.5 W/m²K, the duration of the comfort period is approximately divided by 4 (from 75 to 19 hours). This result demonstrates that the heat loss from windows has a large responsibility in the heat retention performance of the considered building, in this particular case of a large window surface (glazing-to-floor ratio of 0.42) and relatively cold outdoor conditions. It is also found that the higher the U-value of the windows, the higher the peak in heating power observed after a cut-off period (Figure 5d). This is due to the larger heat loss during the cut-off period when window U-value is increased, leading to a need for higher heating power when heat supply is re-established. The window size has a very clear influence on the flexibility results. The larger the share of glazed surface in the external walls, the shorter time can heat be retained indoors, as seen in Figure 5c. It has to be noticed that the scale of Figure

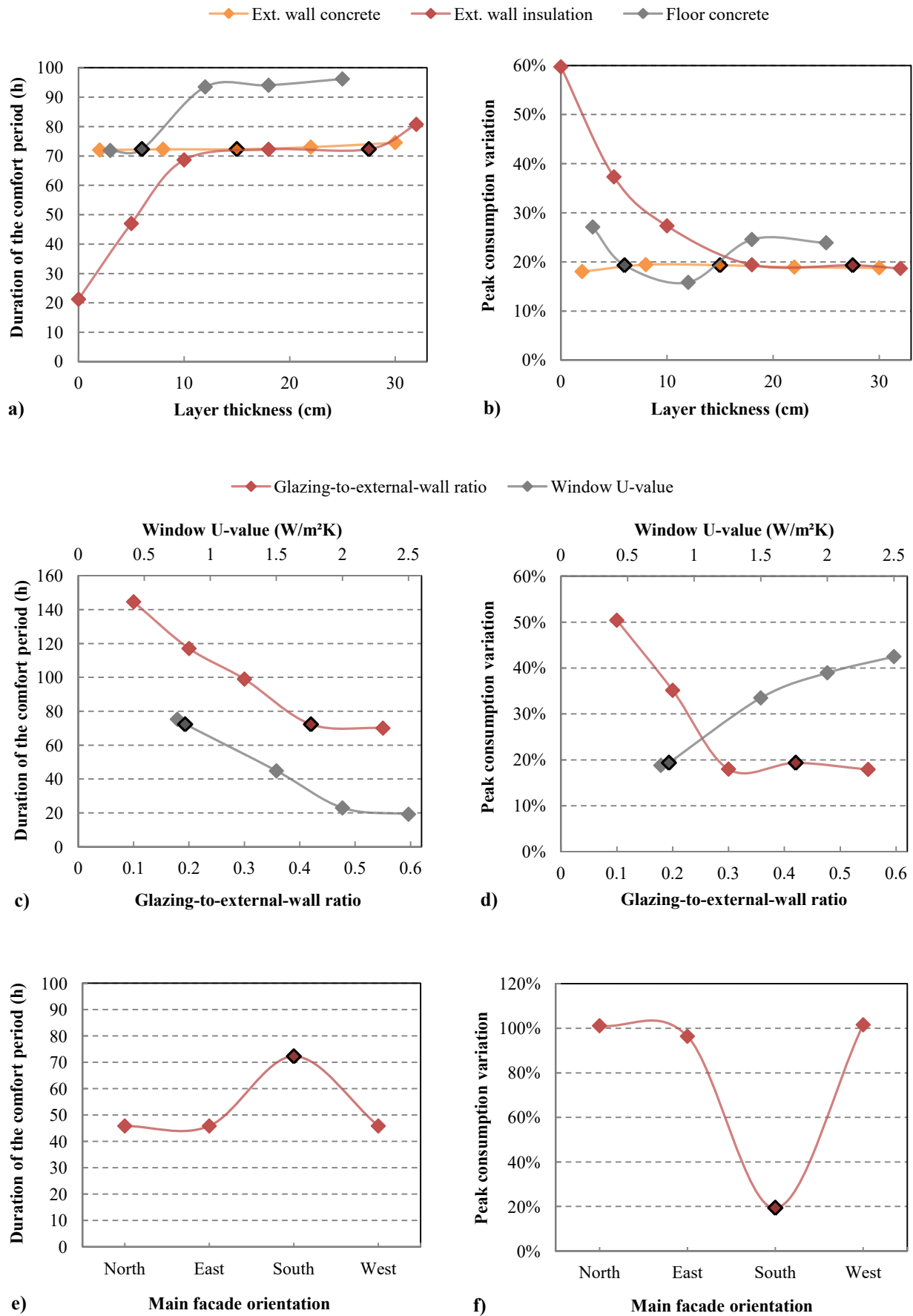*Figure 5: Parameter variation results: duration of the comfort period (**a,c,e**) and peak consumption variation (**b,d,f**) in function of the thickness of different wall and floor layers (**a,b**), window properties (**c,d**) and orientation (**e,f**)*

5c has been extended, since for a glazing-to-wall ratio lower than 30%, good comfort conditions can be kept in the living room for more than 100 hours.

This result also confirms the predominance of thermal resistance in the flexibility issue: indeed, windows are both a source of heat loss and of solar gains, but the losses seem to have a much larger impact on flexibility in this apartment since reducing the window size has such a positive effect on heat retention. However, a further analysis has to be carried out investigating whether this effect is due to the greater wall volume when window size is reduced, increasing the apartment's thermal mass. The analysis of the heating peak gives different results (Figure 5d). For glazing-to-wall ratios below 30%, the solar intake is low and does not contribute much to heating up the space. Consequently, the impact of cutting heat off is larger and the change more brutal, leading to a relatively high peak when heat is turned on at 4 PM (up to 50% higher than normal). For glazing-to-wall ratios higher than 30%, the height of the peak stabilizes between 18 and 19% above its level in absence of a cut-off. Solar gains constitute an immediate source of heat able to balance heat losses, hence their impact on the heating power required after a heating control operation. For large window sizes, the positive impact of solar gains is balanced by the increased heat loss from the extra surface, keeping the peak power surplus constant for glazing-to-wall ratios of 30 to 50%. The Danish BR15 building regulation sets a minimum of 15% for the glazing-to-floor ratio, which corresponds in the present apartment to a glazing-to-wall ratio of 24%. Going above this value shows to be beneficial from the point of view of peak power minimization, but leads to a shorter comfort period in case of a cut-off. However, daylight being an important component of indoor comfort, it is not advisable to introduce a lower threshold for window size in a new version of the building regulation.

Main facade orientation

As seen on Figure 5e and Figure 5f, all orientations but the South give similar flexibility results in the studied apartment for both indicators: the comfort period lasts around 45 hours, and a several-hour long heat cut-off triggers a heating power peak twice the height of the maximum power in normal operation. Orienting the facade 10° to the South, as done in the existing building, permits to extend the comfort period up to 72 hours, which is a favourable scenario when considering energy flexibility. This result permits to qualify the interpretation of the findings from the window size investigation. Indeed, even though solar gains show to have, in the present case, a smaller impact than heat losses through windows on thermal comfort preservation after a heating control operation, their absence significantly degrades the performance described by the indicator.

A South orientation permits to greatly limit the heating peak, making it only 20% higher than the maximum power in normal operation. This result confirms the finding from the glazing-to-wall ratio investigation: solar gains have a prevailing moderating impact on the heating power increase following a cut-off.

Holistic analysis

In order to get a better understanding of the findings, all the investigated cases were gathered. The two flexibility indicators were plotted over both the UA-value of the apartment and its total effective internal heat capacity, giving a point for each of the different design cases. The latter was calculated including the thermal mass of external and internal walls, floors and ceilings, calculated accordingly to DS/EN ISO 13790 (2008). The results can be seen in Figure 6.

The thermal resistance of the envelope appears as the primary factor able to guarantee a satisfactory response to a control operation in terms of indoor comfort. As shown in Figure 6a, the duration of the comfort period shows a clear dependency on the apartment's total UA-value, with little dispersion. As highlighted in the study, the insulation level of the external walls and the U-value of the windows are critical parameters in the preservation of thermal comfort during a heating control operation such as, in the most extreme case, a complete heat cut-off. Reducing the window size also permits to preserve comfort for a longer time, even though this results in a lower solar energy intake. These three parameters impact the heat loss rate through the envelope, thus influencing the duration of the comfort period.

The conducted parameter analysis shows that the envelope's thermal performance has a decisive impact on the possible extreme heat power peaks following a heat cut-off. Indeed, a poor thermal performance leads to high heat losses during the cut-off period, thus the need to quickly increase heating power to satisfy indoor comfort requirements. However, Figure 6b makes it clear that even though an increase in UA-value globally leads to an increase in peak surplus, another factor has a much higher influence on this parameter: the facade orientation, responsible for a doubling of the peak height when changed from the South to any other direction. Solar gains show to strongly attenuate the risk of creating heat consumption peaks after a cut-off period.

Through the analysis of different orientations and windows sizes, it is made clear that solar gains participate in preserving indoor comfort after a heating perturbation, but that in the current case, the amount of heat lost through windows is higher than the amount gained from solar radiation, which limits the relevance of increasing the window size. In the studied apartment, heat accumulation in the thermal mass (specifically external walls and floor) plays a limited role, as highlighted by the study and confirmed by Figure 6c. Increasing the heat storage capacity in the external walls triggers no change in
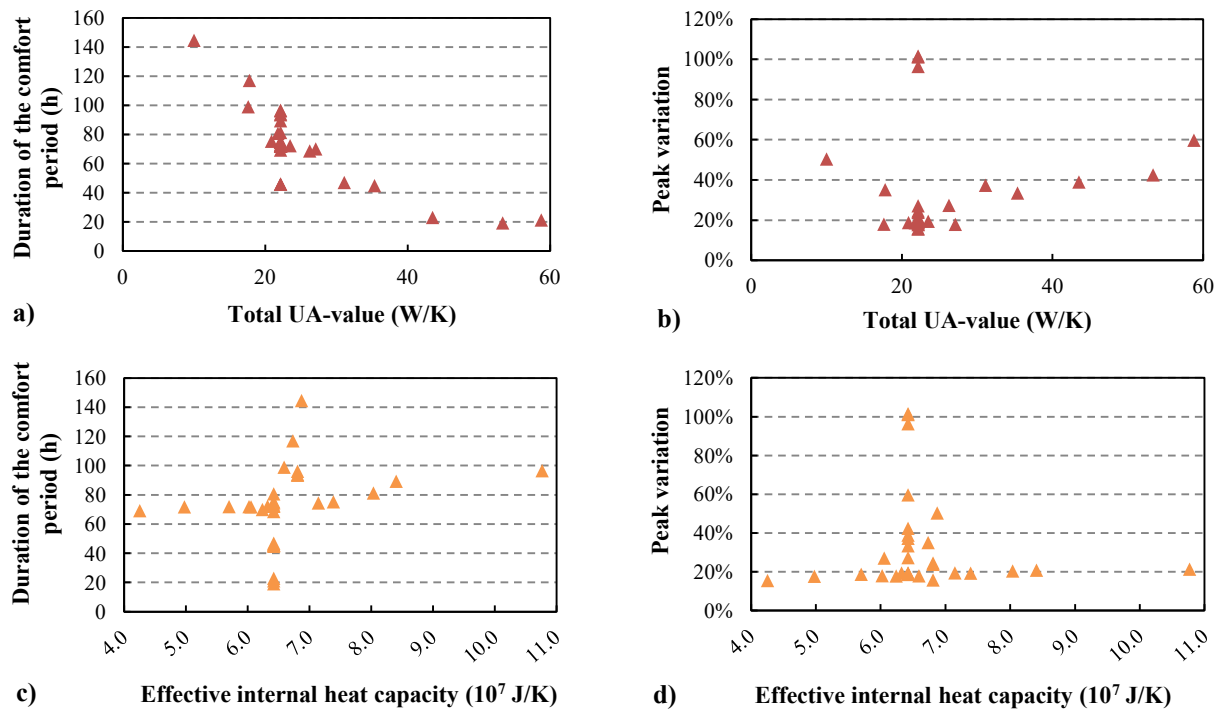
Figure 6: Flexibility indicators as function of total UA-value (a,b) and effective internal heat capacity (c,d)

the duration of the comfort period, while increasing the available storage volume in the floor slab that contains the floor heating pipes helps counteract heat losses in the space up to a certain volume (Figure 5a). Figure 6c shows a globally flat profile with a high dispersion, demonstrating that internal heat capacity is not a decisive parameter in this case. This result could find an explanation in the large window surface resulting in a limited external wall volume. In order to confirm this hypothesis, the impact on the indicators of a simultaneous change in the window area and in the heat storage capacity should be investigated. Identically, the building's thermal mass shows no direct impact on heat power peaks following a cut-off (Figure 6d). As an example, the different design cases that keep an internal heat capacity of around 6.5×10^7 show a large variability in peak power variation, which indicates no correlation between the indicator and the internal heat capacity. The value of the indicator is rather sensitive to other parameters such as the window orientation or the insulation thickness, which variations have no influence on the internal thermal capacity.

Discussion

This study is based on simulations that aim at understanding and comparing the influence of different design parameters on heat flexibility. Assumptions and simplifications were used in order to be able to isolate the influence of the investigated parameters from other factors. Thus, the results cannot be used as such to establish a heating control strategy for example, since they have been obtained in a context that could deviate from other cases. The

purpose of the obtained flexibility results is rather to show the evolution of the flexibility potential when varying a parameter and to observe the different impact that they would have. The results have to be read in relative terms, the trend being more interesting and reliable than the level itself. Among the main simplifications are the constant outdoor temperature and infiltration, the periodic heat gains and the scheduled occupants' behaviour. An analysis of the sensitivity of the present flexibility results to these assumptions is available in a complementary publication by Zilio et al. (2017).

Moreover, this paper describes a local sensitivity analysis, which has the advantage of isolating every parameter's impact while requiring a limited number of simulation runs. The influence of one of the parameters on the results given by the other, through a multi-parameter analysis, is under investigation for some particular parameter combinations and the results are to be published in a coming article. This complementary analysis is expected to permit to make the whole analysis applicable to a wider range of buildings.

Another assumption having an impact on the results is the choice of the cut-off time. In particular, the choice of the cut-off period in the heat power investigation is likely to give a bias to the role of solar gains in the peak power height, since the cut-off period includes the whole solar radiation period. The heating control strategies themselves include a bias in the obtained results: as an example, Wolisz at al. (2013) show that in the case where a pre-heating period is performed before the heat cut-off, the building's thermal mass plays a more important role.

However, even though the investigation mode itself induces some bias in the result, the difference in result presented by the two studies gives some valuable information. While the first indicator is an index of building performance from the occupants' point of view, the second indicator can rather be used when focusing on grid stability. Moreover, both measurements give information about the ability of the apartment to retain heat indoors, but under different angles. Measuring the duration of the comfort period after a cut-off answers the following question: how long can the building provide an acceptable temperature indoors without heating? Focusing on the heating peak after a temporary cut-off rather answers this question: after 9 hours without heating, how far is the temperature in the living room from acceptable conditions (namely the heating setpoint)? This difference in time span explains in particular why increasing the window size has such a positive impact on reducing the heating peak while its effect on the comfort period is overall negative: solar gains help increasing indoor temperature on the short term but thermal losses are predominant on a longer term.

Eventually, it would have been of great interest to be able to couple this study, which is based on a simulation model of the apartment, to actual measurements in the investigated building. The edifice still being under construction, it was impossible. However, measurements are scheduled in the context of the EnergyLab Nordhavn project and this aspect will be the topic of a further study. The influence of the occupants and of the outdoor conditions will in particular be made more clear and the evaluation of indoor comfort more detailed by distributing questionnaires to the occupants.

Conclusion

The present study deals with design of buildings as a tool to improve their ability to retain heat and thus adapt changes in heating schedule, the end goal being to provide energy flexibility to the heating network. In order to understand which of the building design parameters influence its flexibility potential and in which way each of them contributes to it, two investigations were performed on a number of design solutions for the building model. In the first investigation, a complete heat cut-off was performed at 7AM, and the time during which the operative temperature in the living room remained above 20°C was measured, constituting the first flexibility indicator. In the second investigation, heating was cut off between 7AM and 4PM and the heating power peak around that period was measured. Its relative difference with the peak level under normal heating operation constituted the second flexibility indicator. By comparing the results under different design versions, the influence of design parameters on heat flexibility in the present building was assessed.

It was found that the design parameters with the most influence on the temperature drop in the inhabited space after a heat cut-off are those impacting the heat losses through the building envelope. The insulation of the external walls is the parameter showing the largest impact on flexibility. Improving the U-value of the windows can multiply the duration of the comfort period by up to a factor of 4. Heat retention time strongly decreases when the glazing-to-external-wall ratio increases, showing that the losses due to a larger glazed surface impact more the indoor temperature than the increased solar gains when the window gets larger. The orientation of the apartment shows a moderated but clear impact on heat retention: any other orientation than South significantly reduces the time in the comfort range after a cut-off.

As to the thickness of the concrete layers of the different building components, its impact is less important than expected. The layer which thickness has the most significant influence on flexibility is the floor slab, since it embeds the heating pipes, but this is only true up to a certain thickness. The thickness of the concrete layer of the external walls shows a negligible influence under the conditions of this study.

A temporary heat cut-off performed during the day is followed by a heat power consumption peak that is influenced by the building design. The relative height of this peak with respect to the peak power in normal conditions is not affected at all by thermal storage in the building structure, but is greatly influenced by the thermal resistance of the envelope, namely by the insulation thickness and U-value. However, according to the present calculation methods, the main influence on the peak power seems to come from the presence of solar gains: orienting the main facade in any other direction than South greatly increases the heating power peak. Similarly, while smaller windows guarantee a better heat retention, they also lead to an important increase of the peak power.

This work has permitted to understand the mechanisms that lead to transmission and retention of heat indoors, which give the district heating operator the possibility to apply restrictions on heat supply when best for the system as a whole. The importance of an optimal building design is now obvious, and the role of the main building components has been clarified.

The present work is a preliminary theoretical comparison of the role of different building components in heat perturbations adaptation. This work also aims at giving an estimate of the energy flexibility potential that these newly-constructed apartment blocks can offer to the grid and which can be further utilized by the future heat supply of the area. Some multi-parameter investigations as well as analyses with different building shapes and indoor

space organisation will complete this work, and help forming a set of guidelines for an optimal building design with focus on heat flexibility. An impact assessment of outdoor conditions and internal gains on the present flexibility results is developed by Zilio et al. (2017). The following steps of this work include yearly simulations using realistic weather data permitting to assess the building's response to both summer and winter conditions. Moreover, field measurements are being collected on the studied building and will be used to support the present simulation work. Finally, a study of different heating schedules is planned, including price-dependent scenarios.

Acknowledgements

References

Asan, H. (2006). Numerical computation of time lags and decrement factors for different building materials. *Building and Environment*, *41*(5), 615–620.

Borresen, B. A. (1973). Heat storage in walls. *Build Serv Eng*, *41*, 17 – 18.

De Coninck, R., & Helsen, L. (2016). Quantification of flexibility in buildings by cost curves - Methodology and application. *Applied Energy*, *162*, 653–665.

DS/EN ISO 13790 - Energy performance of buildings – Calculation of energy use for space heating and cooling. (2008).

EnergyLab Nordhavn. (2015). EnergyLab Nordhavn - public project description. Retrieved January 11, 2016, from http://energylabnordhavn.dk

European Commission. (2011). Energy Roadmap 2050 (Vol. 53, pp. 1689–1699).

Gellings, C. W. (1985). The concept of demand-side management for electric utilities. *Proceedings of the IEEE*, *73*(10), 1468–1470.

Gianniou, P., Heller, A., Nielsen, P. S., & Rode, C. (2016). Identification of Parameters Affecting the Variability of Energy Use in Residential Buildings. In *Proceedings of CLIMA Conference, Aalborg*.

Kolokotsa, D. (2015). The role of smart grids in the building sector. *Energy and Buildings*, *116*, 703–708.

Le Dréau, J., & Heiselberg, P. (2016). Energy flexibility of residential buildings using short term heat storage in the thermal mass, *111*, 991–1002.

Ma, P., & Wang, L. S. (2012). Effective heat capacity of interior planar thermal mass (iPTM) subject to periodic heating and cooling.

Energy and Buildings, *47*, 44–52.

Masy, G., Georges, E., Verhelst, C., & Lemort, V. (2015). Smart grid energy flexible buildings through the use of heat pumps and building thermal mass as energy storage in the Belgian context. *Science and Technology for the Built Environment*, *4731*(August), 800–811.

Moffiet, T., Alterman, D., Hands, S., Colyvas, K., Page, A., & Moghtaderi, B. (2014). A statistical study on the combined effects of wall thermal mass and thermal resistance on internal air temperatures. *Journal of Building Physics*, *38*(5), 419–443.

Müller, D., Monti, A., Stinner, S., Schlösser, T., Schütz, T., Matthes, P., … Streblow, R. (2015). Demand side management for city districts. *Building and Environment*, *91*, 283–293.

Oldewurtel, F., Sturzenegger, D., Andersson, G., Morari, M., & Smith, R. S. (2013). Towards a standardized building assessment for demand response. *Proceedings of the IEEE Conference on Decision and Control*, 7083–7088.

Orosa, J. A., & Oliveira, A. C. (2012). A field study on building inertia and its effects on indoor thermal environment. *Renewable Energy*, *37*(1), 89–96.

Reynders, G. (2015). *Quantifying the impact of building design on the potential of structural storage for active demand response in residential buildings*. KU Leuven.

The Danish Building Regulation. (2015). Executive Order amending the Executive Order on the Publication of the Danish Building Regulations 2010 (BR10).

Wang, L.-S., Ma, P., Hu, E., Giza-Sisson, D., Mueller, G., & Guo, N. (2014). A study of building envelope and thermal mass requirements for achieving thermal autonomy in an office building. *Energy and Buildings*, *78*, 79–88.

Wolisz, H., Harb, H., Matthes, P., Streblow, R., & Müller, D. (2013). Dynamic simulation of thermal capacity and charging / discharging performance for sensible heat storage in building wall mass. In *13th Conference of International Bulding Performance Simulation Association* (pp. 2716–2723).

Zhu, L., Hurt, R., Correia, D., & Boehm, R. (2009). Detailed energy saving performance analyses on thermal mass walls demonstrated in a zero energy house. *Energy and Buildings*, *41*(3), 303–310.

Zilio, E., Foteinaki, K., Gianniou, P., & Rode, C. (2017). Impact of Weather and Occupancy on Energy Flexibility Potential of a Low-energy Building.

PAPER VI: Zilio, E., Foteinaki, K., Gianniou, P. and Rode, C. (2017) 'Impact of Weather and Occupancy on Energy Flexibility Potential of a Low-energy Building', *in the Proceedings of the 15th IBPSA Conference*. San Francisco, CA, USA, pp. 1493–1502.

Impact of Weather and Occupancy on Energy Flexibility Potential of a Low-energy Building

Emanuele Zilio[1], Kyriaki Foteinaki[1], Panagiota Gianniou[1], Carsten Rode[1]
[1]International Centre for Indoor Environment and Energy, Department of Civil Engineering,
Technical University of Denmark, Kgs. Lyngby, Denmark

Abstract

The introduction of renewable energy sources in the energy market leads to instability of the energy system itself; therefore, new solutions to increase its flexibility will become more common in the coming years. In this context the implementation of energy flexibility in buildings is evaluated, using heat storage in the building mass. This study focuses on the influence of weather conditions and internal gains on the energy flexibility potential of a nearly-zero-energy building in Denmark. A specific six hours heating program is used to reach the scope. The main findings showed that the direct solar radiation and the outdoor temperature appeared to have the larger impact on the thermal flexibility of the building. Specifically, the energy flexibility potential of the examined apartment can ensure its thermal autonomy up to 200 h in a typical sunny winter day.

Introduction

The high share of Renewable Energy Sources (RES) expected in the energy market for the coming years will lead to lower stability of the energy system itself due to the high dependence on weather conditions (e.g. solar radiation and wind). Consequently, there will be problems with matching the production side with the demand side. To overcome this issue, new solutions have to be implemented to increase the energy flexibility of the energy system (Lund and Lindgren et al., 2015) (Rotger-Griful and Hylsberg Jacobsen, 2015). Few decades ago, Gelling coined the term "Demand-Side Management" (DSM) to indicate all actions that can be taken to influence the users' consumption profile in order to adapt it to the energy production (Gellings and Parmenter, 1985). Such solutions (e.g. peak shaving or load shifting) are becoming more relevant in the energy management field. For instance, energy storage devices can be implemented at final-user level, in this way, when there is surplus of energy from renewable production, it can be stored and used in a second moment when there is a lack of it (Lund and Lindgren et al., 2015).

The integration of RES in the energy system also leads to a more decentralized structure, since these sources are distributed in the territory. For this reason, a "smart city" model has to be used to allow communication between energy producers, loads and components (Aduda et al., 2016) (Lund and Lindgren et al., 2015). The aim of the new energy system is to improve the flexibility on the demand side, since, due to the high maintenance and operational costs, it would be more expensive to act on the supplier side (Aduda et al., 2016) (X. Xue et al., 2015) (Labeodan et al., 2015). In the building sector, a certain amount of storage capacity can be installed while ensuring good indoor comfort for the occupants (Zheng et al., 2015). Referring to the Danish energy market, its correlation between energy price and amount of renewables production ensures that flexible consumers can benefit from lower electricity prices (Neupane et al., 2015).

As the previous studies presented by Marin et al. (2016) and Ling et al. (2006) state, the thermal mass of buildings can be used to store energy. For example, the thermal inertia of the floor heating system allows the use of intermittent heating strategies, achieving load shifting. On the other hand, the envelopes of refurbished or new buildings lead to lower heating demand and higher influence of internal gains on the heating consumption. Firlåg et al. (2013) presents a first assessment of the influence of the internal gains on the energy consumption. In new buildings, heat gains can cover up to 60% of the heat losses and therefore considerably affect the energy consumption. They can affect the indoor comfort and with a dedicated heating control strategy, it is possible to take advantage of them, with the consequent reduction in energy consumption, up to 30%. In Lazos et al. (2014) it is described how heat gains prediction from occupancy and weather conditions could be used to reduce the energy consumption in a range 15-30%, highlighting the importance of heat gains prediction in the energy management of a building. Sikula et al. (2012) found that the highest impact is given by solar gains that can affect the energy consumption around 20%. In Chen et al. (2012) it is explained that the energy consumption of a building could be forecasted based on weather forecast. Le Dréau and Heiselberg (2016) showed that a single-family passive house can be totally autonomous in terms of heating demand up to 48 h, while ensuring the operative temperature was always kept above 20 °C. In the same way, Ingvarson and Werner (2008) investigated the energy storage capacity in the building mass. The results show that the heating system can be switched-off in newly built or renovated dwellings, while ensuring acceptable indoor temperature for more than 24 h.

The aim of this paper is to investigate energy flexibility in a newly constructed building through energy storage in building mass during the heating period. The building investigated follows the Danish building regulation (BR10) for a low energy building in class 2015. The energy supply for heating, ventilation, cooling and domestic hot water per m^2 of heated floor area does not exceed 30.1 kWh/m^2/year. An important step of the evaluation is the definition of a dedicated flexibility indicator, evaluated with regards to different weather conditions and internal gains. Furthermore, two heating strategies are implemented: the first one is used to define the flexibility indicator and the second one is used to assess the effect of achieving energy storage on a daily basis with a specific heating program. The relevance of this study is based on the type of building chosen for the investigation. Due to its design characteristics, it ensures a unique contribution in terms of energy flexibility.

Methodology

Model description

The reference building is located in Copenhagen, Denmark, and is newly constructed. It consists of 85 apartments of different sizes, divided in five storeys. In this case study, a reference apartment is chosen, which is 95 m^2, located at the 4th floor and facing the waterfront on the south-east façade. The apartment has three bedrooms, a kitchen-living room, two bathrooms and a storage room. Figure 1 gives an overview of the apartment.
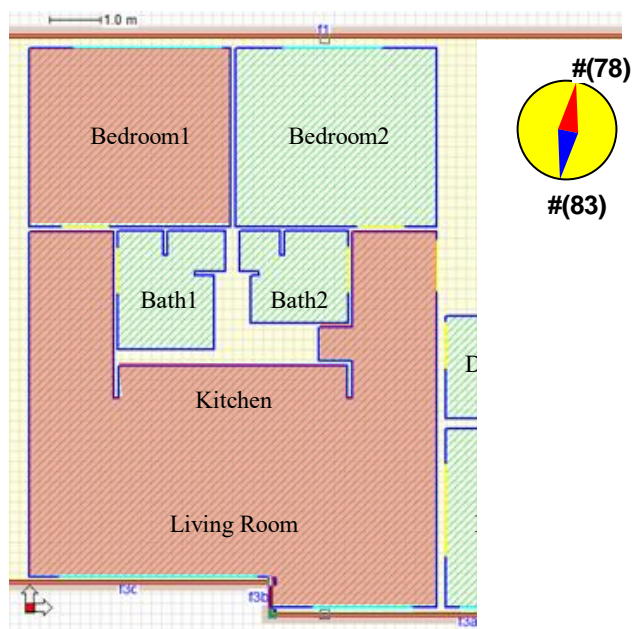
Figure 1: Floor plan of the apartment in

The rooms used for the analysis in this s... Kitchen-Living Room (45 m^2) and bedroo... highlighted in red in Figure 1. The buildin... concrete-structure, where both internal ... bearing walls are reinforced concrete walls ... about the composition of the building's co...

be found in Table 1. The external walls have a U-value of 0.12 W/m^{2}K, while for the internal walls is 3.43 W/m^{2}K. Triple glazing windows are used with an overall U-value equal to 0.8 W/m^{2}K. The glazing-to-wall ratio is 0.42.

Table 1: Material layers

	Layer material	Thickness (m)
External walls	Concrete (inside)	0.150
	Mineral wool	0.275
	Air gap	0.025
	Brick (outside)	0.108
Internal floor	Oak planks (top)	0.030
	Concrete	0.060
	Termotec insulation	0.146
	Hollow concrete (bottom)	0.220
Bathroom floor	Concrete (top)	0.100
	Air	0.126
	Hollow concrete	0.220
	Lightweight concrete (bottom)	0.060
Bearing internal wall	Concrete	0.200
Non-bearing internal wall	Aerated concrete	0.100
Bathroom wall	Lightweight concrete	0.080

The building is connected to the local district heating network with supply water temperature at 60 °C and return at 40 °C. The space heating (SH) system is a

Weather file

To assess the influence of the weather conditions on the flexibility potential, it is decided to vary only two weather parameters (outdoor temperature and solar radiation). For each case, three specific weather files are created based on realistic conditions of Denmark's heating season. The Test Reference Year (TRY) file representing the weather conditions in Vanløse, suburb of Copenhagen, is used as reference file to create the new ones. The outdoor temperature pattern during the heating period is analysed and three representative constant temperatures are selected. The temperatures chosen are 5 °C, 0 °C and -12 °C, respectively the highest, the average and the lowest temperature in January (coldest month in Denmark). In order to limit the influence of temperature variations, the three selected temperatures are kept constant during the simulation period.

The second parameter considered is the direct solar radiation. Similar to the temperature profile, three typical conditions are selected from the TRY file: large solar radiation, narrow solar radiation and no direct solar radiation, based on the hours that direct solar radiation is available. The large solar radiation considers 8 h of direct solar radiation, with a peak of 500 W/m^2 in the middle of the day and 0 W/m^2 at the beginning and the end of it; the narrow solar radiation considers 4 h of direct solar radiation with the same pattern. Regarding the diffuse radiation, it is assumed to have a peak of 50 W/m^2 in the middle of the day, in accordance with the direct solar radiation. These three cases are considered to occur on daily basis throughout the simulation period. The relative humidity is kept constant at 80% in all cases and absence of wind is considered.

Internal gains

In addition to solar radiation, the influence of the occupancy is investigated, simulating with two, three and four occupants. Table 2 gives a detailed description of the schedule applied to the occupants

Table 2: Schedule for four occupants working

| Room | Time | No. People [MET] | |
		Weekdays	Weekend
Living Room-Kitchen	7:00 - 9:00	2.1 [1]	2.1 [1]
	9:00 - 17:00	0 [0]	1.2 [1]
	17:00 -23:00	2.1 [1]	2.1 [1]
	23:00 - 7:00	0 [0]	0 [0]
Bedroom 1	7:00 - 17:00	0 [0]	0.4 [1]
	17:00 - 23:00	0 [0]	0.4 [1]
	23:00 - 7:00	2 [0.7]	2 [0.7]
Bedroom 2/3	7:00 - 17:00	0 [0]	0.2 [1]
	17:00 - 23:00	0 [0]	0.2 [1]
	23:00 - 7:00	1 [0.7]	1 [0.7]
Bathrooms	7:00 - 9:00	0.5 [1.2]	0.5 [1.2]
	9:00 - 17:00	0 [1.2]	0.2 [1.2]
	17:00 -23:00	0.5 [1.2]	0.5 [1.2]
	23:00 - 7:00	0 [0]	0 [0]

The occupancy schedule applied to the occupants evaluates two different configurations. The first one considers working people that are not at home during weekdays and the second one considers retired people that spend more time at home throughout the week. For the schedule of retired people, the weekend pattern is applied for all the weekdays.

Heating program

The aim of the heating program is to allow the possibility of load shifting. Two cases are created in order to achieve two different aims during the investigations:

- Cut-off program
- Daily heating program

The first one is used to assess the flexibility potential in terms of the number of hours of acceptable indoor comfort that can be maintained in the apartment once the heating is switched-off. It is related to the first flexibility indicator explained in the next paragraph, and it is used to evaluate the flexibility potential using different internal gains. This heating program is called "cut-off program" since it considers the complete switch-off of the SH system. More specifically, it considers a continuous control of the heating from the 1st of January until the 14th of January, with the room set point at 20 °C. Afterwards, on the 15th of January, from 0:00 until 6:00, the heating set point in the rooms is risen to higher values (21 °C, 22 °C, 23 °C and 24 °C), in order to enable heat storage in the building mass. Afterwards, the heating is switched-off and the temperature drop in the apartment is analysed.

The second program implemented considers a daily pattern. It is used to determine whether a daily heating program could provide flexibility by storing heat into the building mass. The heating pattern used is the same as the one used for the cut-off program, but in this case after the 15th of January, the SH system is set to work every day from 0:00 to 6:00. As previously, different set points are tested during the six hours heating period (21 °C, 22 °C, 23 °C and 24 °C).

Flexibility indicator

In a residential apartment, it is necessary to guarantee the occupants' comfort. In this study, the thermal comfort, and in particular the operative temperature is used as indicator to evaluate the flexibility potential of the building. The requirements provided by the European Standard DS/EN 15251 (Dansk Standard, 2007) for a building in comfort category II are followed, that require minimum operative temperature at 20 °C during the heating season.

The first flexibility indicator represents the number of hours that the operative temperature is kept above the lowest limit recommended by the standard (20 °C), once the heating is switched-off according to the cut-off program. Figure 2 shows a simplified representation of the first flexibility indicator.
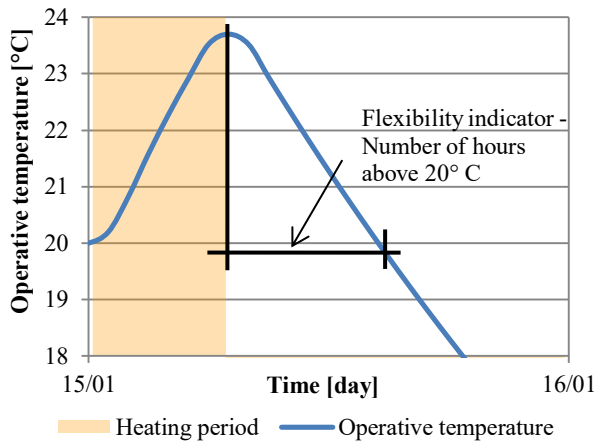
Figure 2: Representation of the flexibility indicator

The following formula (1) explains the concept adopted.

$$Ind_1 = min \{t \mid T_{op}(t) \geq 20 \text{ °C}\} \quad (1)$$

where,

t is the time with a temperature above 20 °C after the heating cut-off,

T_{op} is the operative temperature in the room.

The indicator quantifies the time that the building can be independent of the heating supply, which corresponds to a period when the renewable energy is not available.

A second indicator is defined to evaluate the effect of implementing a dedicated heating program to take advantage of the flexibility potential in terms of power peaks. In fact, the new heating program created, considers raising the set point for a limited period and then switching-off the heating system. Usually, in buildings the heating set point is constant and the SH system controls the indoor temperature throughout the day. The consumption peak obtained when implementing a continuous control of the SH system is compared with the one obtained using the daily heating program presented in the previous paragraph. The indicator is defined as:

$$Ind_2 = \frac{P_{\max\_daily}}{P_{\max\_cont}} \quad (2)$$

where,

P_{max_daily} is the consumption peak obtained with the daily heating program,

P_{max_cont} is the consumption peak obtained with the continuous control.

The flexibility indicator gives an evaluation of the impact that the implementation of energy flexibility has on the dimensioning of the heating system.

Results

Flexibility potential

The results of two reference rooms are plotted in the following graphs, Bedroom 1 and Kitchen-Living Room, since they have opposite orientation and they represent two "end-use" cases, with different occupancy

schedules. In terms of thermal comfort, they represent the best and worst case respectively. The results shown refer to heating set point of 21 °C, since for higher set points, the same pattern is found and the difference is only in the magnitude of the indicator. It is important to mention that a basic case is created, and every time a single parameter is changed. The basic case considers narrow solar radiation, outdoor temperature at 0 °C and three occupants following the schedule for working people.

Figure 3 presents the flexibility indicator as number of hours above 20 °C. In this particular case, it quantifies the time that the building can be independent of the heating supply for the three different direct solar radiation cases.
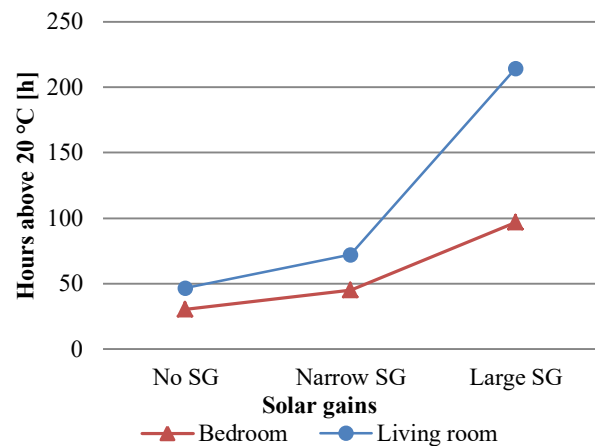

Figure 3: Flexibility indicator with different solar radiation

The impact of solar gains in the two rooms is presented with regards to the first indicator. This impact is higher in the living room than in the bedroom, mainly due to the orientation of the room that is facing south. Moreover, the glazing area is larger in the living room. It can be seen that the impact of the narrow solar gains compared to the absence of solar gains, increases the number of hours above 20 °C with a factor of 1.47 in the bedroom, while in the living room with 1.54. On the other hand, when considering the transition from narrow solar gains to large solar gains, the increasing factor is 2.14 in the bedroom and 2.96 in the living room. Therefore, it can be deduced that the indicator is affected more in case of large solar gains and that the living room is more sensitive to this change since it faces south.

In Figure 4, the results of the first flexibility indicator for different outdoor temperatures are presented. It is noticeable that the outdoor temperature influences the indicator with an exponential pattern. The results obtained with the outdoor temperature at -12 °C show that the temperature in the rooms drops rather faster and a lower flexibility can be achieved compared with the other temperatures tested. The decrease of the flexibility indicator, when the temperature at -12 °C is considered, is about 4.51 times for the bedroom and 3.93 times for the living room. On the other hand, when the temperature is changed to 5 °C, the indicator increased

with a factor of 2.14 for the bedroom and 2.05 for the living room. Therefore, it is seen that the outdoor temperature is an important factor for the thermal comfort in the rooms as it was expected, and this is revealed from the flexibility indicator. In extreme outdoor conditions (-12 °C), the flexibility of the building is limited (i.e. 10 hours in the bedroom). As it is noticed also in the solar gains analysis, the living room always ensures a higher indicator due to the fact it faces south and it is more affected by the solar radiation.
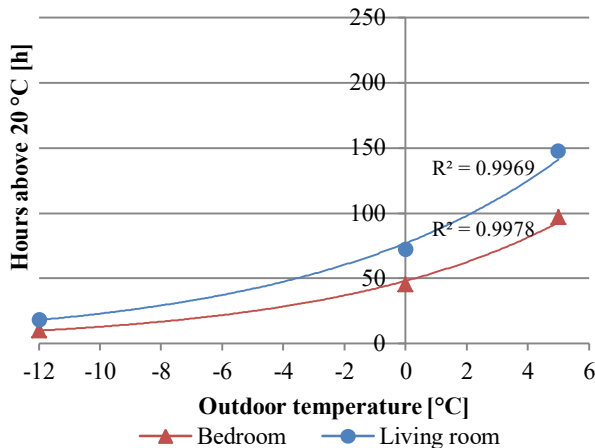

Figure 4: Flexibility indicator with different outdoor temperatures

Figure 5 shows the flexibility indicator results when different numbers of occupants are present in the apartment.
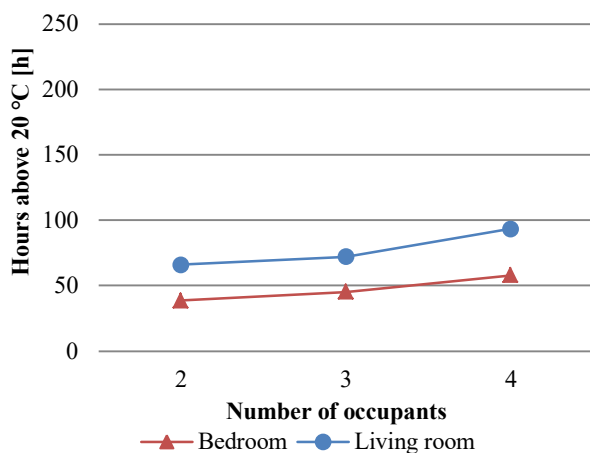

Figure 5: Flexibility indicator with different number of occupants

It can be seen that the increase in number of hours above 20 °C is almost linear for different number of occupants. The decrease of the flexibility indicator is about 1.18 times in the bedroom, when it is considered to decrease from three to two occupants, while it is about 1.09 in the living room. On the other hand, when four people are considered, compared to the case of three occupants, the flexibility indicator increased with a factor of 1.28 in the bedroom and 1.29 in the living room. It can be deduced that increasing the number of occupants by one unit can influence almost linearly the indicator. As it is seen in

the previous cases, the living room guarantees a higher indicator due to the higher solar gains.

Figure 6 shows the results of the first flexibility indicator for the two different occupancy schedules. It is observed that for the schedule of retired people the flexibility indicator is higher. In particular, it increases with a factor 1.44 in the bedroom and approximately 1.26 in the living room. This is due to the time that the people spend in the apartment, which is assumed longer for retired people.
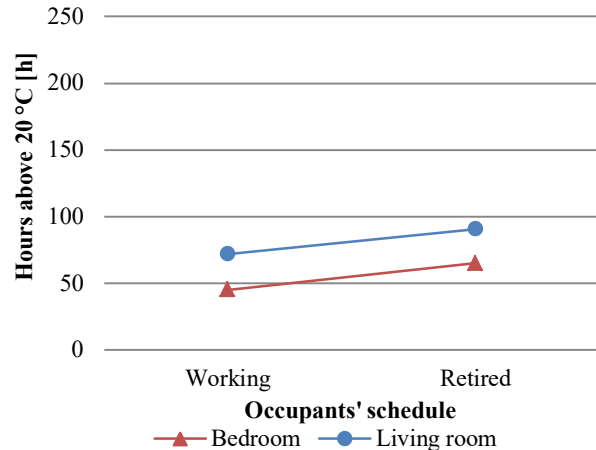
Figure 6: Flexibility indicator with different occupancy schedule

The following two analyses give an overview in case a different apartment in the same block is chosen as reference. In the first case, the building is rotated by 180°, in order to have the main façade oriented towards the north, while keeping the same allocation of the rooms. In the second one, the reference apartment is moved from the fourth floor to the ground floor and the top floor.

Figure 7 shows the flexibility indicator for two different orientation of the building.
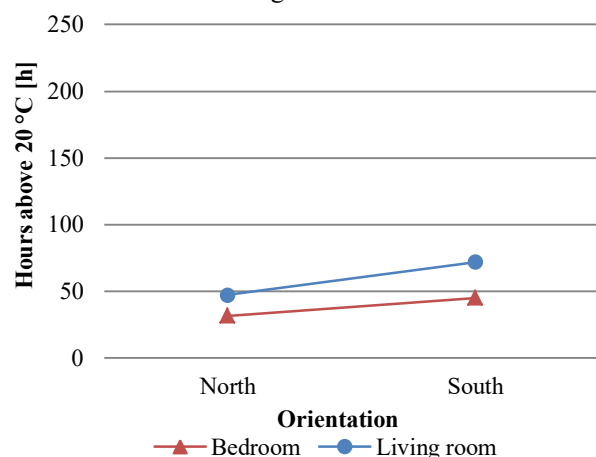
Figure 7: Flexibility indicator with different orientation of the building

When the main façade is oriented towards the south, the living room faces south and the bedroom faces north. The large glazing area of the first room guarantees the highest flexibility indicator, due to the high solar gains in

the apartment. Consequently, the highest flexibility indicator is found in the living room. On the other hand, when the main façade faces north, the solar gains in the apartment are lower, resulting in a lower flexibility indicator. In this case, it is expected to get a higher indicator in the bedroom, since it is facing south. However, the room faces the internal yard, and the opposite side of the building creates shading thus reducing the solar gains in the room and attenuating the effect of being oriented to the south. Furthermore, higher internal gains in the living room still ensure a higher flexibility indicator in this room. This can be seen in Figure 7, where the indicator increases for the south orientation, 1.52 times higher than the north once, while in the bedroom the difference is lower, where the indicator is 1.43 times higher in the south oriented case.

Figure 8 represents the flexibility indicator when the apartment is moved at different floor levels.
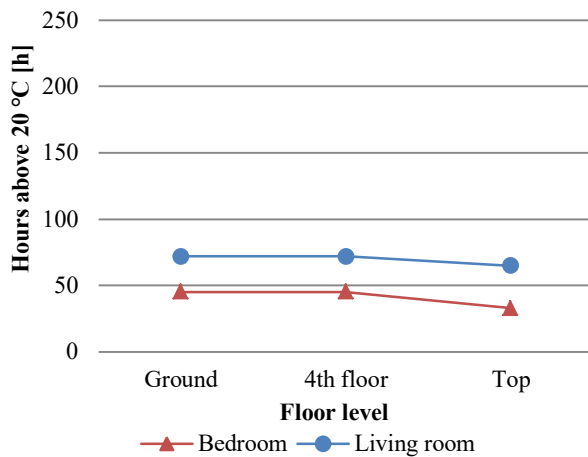

Figure 8: Flexibility indicator with different heights of the apartment

It is noticeable that for the cases at the ground floor and in the fourth floor, the results obtained are the same. Since the building has a heated basement, the losses in the ground floor are limited. However, the flexibility potential decreases 1.12 times in the living room and 1.37 times in the bedroom, when the apartment is located at the top floor. In this case, the apartment has higher heat losses since the exposed wall and roof area towards the ambient are bigger compared to the other cases.

Heating programs

In the second part of the study, the flexibility potential is investigated with particular attention to the heating system. Firstly, the flexibility potential is tested for different heating set points (20 °C – 24 °C) with the cut-off program for the basic case. Afterwards, the daily heating program is implemented and the possibility of implementing load shifting is investigated. Figure 9 shows the results of the flexibility indicator *Ind1* when the cut-off program is applied.
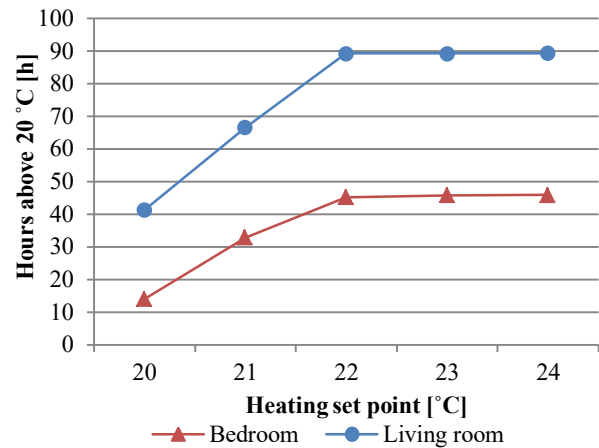
Figure 9: Flexibility indicator obtained with the cut-off program at different heating set points

It can be noticed that the heating set point used in the rooms during the heating period influences the flexibility indicator. In particular, for both the bedroom and the living room, the maximum amount of hours is reached with a set point of 22 °C, namely 89 h for the living room and 45 h for the bedroom. When higher set points are used (23 °C or 24 °C), the same results in terms of flexibility indicator are achieved, due to the thermal inertia of the floor heating system, namely that the temperature set point cannot be reached within the six hours of pre-heating. Thus, higher set points would not make any difference in the energy stored in the thermal mass. On the other hand, a set point lower than 22 °C, i.e. 20 °C and 21 °C, leads to a lower number of hours above the comfort limit. When the set point is increased from 20 °C to 22 °C in order to obtain the maximum result in terms of flexibility, the indicator increases with a factor of 3.22 for the bedroom and 2.16 for the living room.

Figure 10 shows the operative temperature pattern from January 14th until January 20th in the bedroom when the cut-off program is applied.

Figure 10: Temperature pattern in the bedroom for the cut-off program

BUILDING
SIMULATION 2017

INTERNATIONAL
BUILDING
PERFORMANCE
SIMULATION
ASSOCIATION

As expected from the evaluation of the flexibility indicator, for set points 22 °C, 23 °C and 24 °C set points, the temperature pattern overlaps. It is possible to notice the influence of the solar radiation, which can be observed in the temperature peak in the middle of each day. The weekend is highlighted (grey area) and it can be seen that the operative temperature drop slightly decreases, due to the fact that the occupancy schedule considered that people spend more time at home. It is also noticed that the initial temperature in the beginning of the heating program is 20.4 °C. This is a bit higher 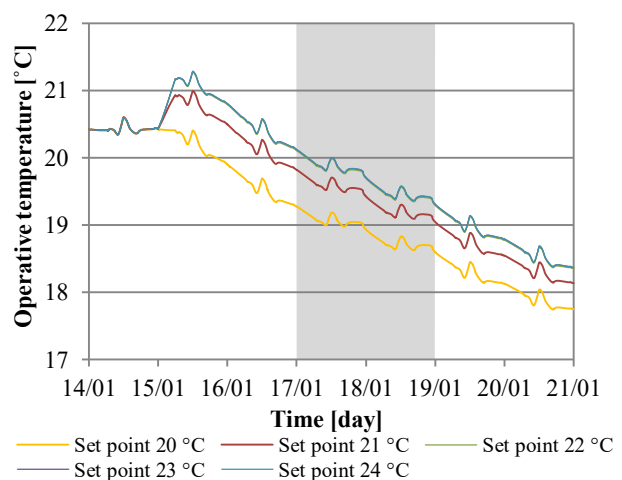than the set point (20 °C) for the period before the 15th of January. The reason is the proportional controller implemented in the model that introduces this error. It has a bandwidth of 2 °C and it stops the heating supply only when the operative temperature reaches the set point plus half of the bandwidth. The temperature pattern in the living room shows similar behaviour to the one in the bedroom with the only difference of higher temperatures, due to larger influence of the solar gains.

In the second step of the investigation, the heating program is applied on a daily basis. Figure 11 shows the temperature patterns in the bedroom at different heating set points when the daily heating program is applied. For the set points above 21 °C the six hours heating period guarantees acceptable thermal comfort in the rooms, thanks to the heat storage in the building mass. In fact, for all set points higher than 20 °C the temperature increases day by day. This means that during the heating period, the energy accumulated in the concrete slab increases day by day. Only for the set point at 20 °C, the temperature drops below the limit since the energy stored during the heating period is not sufficient to keep the temperature above the limit during the period with no heating. The grey area highlight the weekend, where the occupants spend more time in the apartment.
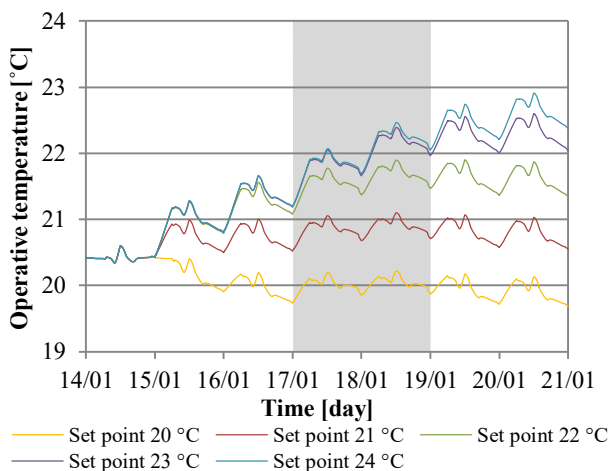

Figure 11: Temperature pattern in the bedroom for the daily heating program

The change of heating program is considered as a DSM solution and it is important to evaluate the effect of its implementation. A higher set point leads to higher power peak, compared to the continuous control of the heating system. Table 3 shows the consumption peaks for the cut-off program on the 15th of January.

Table 3: Consumption peaks for the cut-off program for different heating set points

Continuous control	
Heating set point [°C]	Peak consumption [W]
20	743
Cut-off program	
20	709
21	3785
22	4829
23	4877
24	4877

As it is expected from the operative temperature trends, the highest peak is obtained for the set points of 22 °C, 23 °C and 24 °C. This is due to the higher temperature difference between the operative temperature in the room and the set point temperature which influence the use of the proportional control. For this reason, in case of the 21 °C set point, the consumption is significantly lower, since the room temperature is closer to the set point. The highest peaks measured are slightly lower than 4900 W while for the set point of 21 °C it is approximately 3785 W. For the set point of 20 °C, the peak consumption is much lower, 743 W, but as previously shown, it provides lower flexibility. It can be concluded that, in order to enable the maximum energy storage and flexibility potential in the building mass with the increase of the heating set point, a higher power peak is required. Comparing the highest peak, (set point at 23 °C or 24 °C), with the one obtained with the continuous control of the SH system (set point 20 °C), the increase factor is approximately 6.56 times.

Regarding the daily heating program, in order to assess energy flexibility on a daily basis, the primary energy consumption of the heating system is evaluated. In this case, only the set point at 21 °C is considered, since it is the lowest one that guarantees an operative temperature above 20 °C in all the rooms. Table 4 shows the results in terms of primary energy consumption after one month.

Table 4: Primary energy consumption after one-month simulation

Primary Energy Consumption [kWh/m²]	
Continuous control	2.89
Daily heating program	2.99

The primary energy consumption obtained with the continuous control is compared with the one obtained with the daily heating program. As it is noticed, the daily heating program leads to 3.5% higher energy consumption. Thus, in order to implement energy flexibility measures in buildings, an overconsumption of the SH system might need to be faced.

Discussion

The results obtained in this study highlighted the energy flexibility potential obtained in a newly constructed building in Denmark. The most updated construction

technologies ensure lower energy consumption, lower heat losses and lower infiltration, leading to higher flexibility potential of new buildings, compared to buildings built following older legislations.

As explained also in the work presented by Le Dréau and Heiselberg (2016), which showed heating demand autonomy up to 48 h in a new passive house, new buildings can largely contribute to increase the flexibility of the energy system. In this study, the high amount of hours above 20° C (about 200 h) is found with a specific weather file, where the solar radiation and the outdoor temperature highly contribute to keep an acceptable indoor temperature. The higher flexibility potential, besides the differences in the weather condition, is due to the type of house considered in the two studies. In fact, a single family house, with higher external wall surface, has higher heat losses compared to an apartment.

During the investigation procedure, many assumptions had to be made in order to simplify the comprehension of the parameters changed. For this reason, the results need to be treated carefully according to the specific study case. However, they represent a starting point for further investigations, in which all assumptions can be sharpened in order to evolve it to a more generic model.

The specific heating program used during the investigation is based on the evaluation of consumption patterns found in the literature. According to (Fischer et al., 2016) in the daily heating demand, two peaks can be identified: the first one in the morning around 6 a.m. and the second one around 6 p.m. Since the building investigated is located in a district, where there are both residential and office buildings, synergies between the two types of buildings could be developed. The heating operator would supply the two types of buildings at different moments during the day, in order to reduce the peak consumption. Since the lowest consumption of the offices is during night, in this paper it is decided to implement a heating program that ensures the energy supply during night for the residential buildings. This solution could also be applied in case of electrical flexibility, since during the night the electricity price is usually lower due to the night tariffs regulations.

The results obtained from the investigations refer to a new low-energy building; therefore, using different type of buildings (different age of construction or not refurbished) to run the same simulations would lead to different flexibility potentials. In particular, with the perspective of extending the smart grid concept to a larger area, other types of buildings need to be studied to evaluate the impact and the relation of different constructions on the flexibility potential.

The main part of the investigations conducted is based on a simulation model that considered the weather conditions, i.e. outdoor temperature and solar radiation, constant throughout the period. This assumption was made in order to limit the influence of external parameters and it is possible to isolate the effect of each parameter. Definitely, variable weather conditions would have led to different results in terms of flexibility.

However, the constant temperature and solar radiation are estimated based on the average conditions during the heating season. This makes the assumption consistent and the results more indicative.

The number of occupants and the schedule that regulate their presence are defined equally for each weekday and for each weekend. In reality, people behave in a random way and this could influence the results. In a further study, it would worth implementing a stochastic model. Moreover, to simplify the investigations, the occupied hours are not distinguished from the non-occupied ones when analysing the results and the minimum indoor temperature is set at 20 °C all times. Finally, the minimum temperature was set according to Category II of the Standard DS/EN 15251, while in reality, each occupant has a different level of acceptability and it could be interesting for further analysis to investigate if different set point temperatures in the rooms can influence the flexibility (i.e. lower set point than 20 °C in bedrooms).

Regarding the apartment's position, it emerged that a different orientation can affect its energy flexibility potential. In the same way, the floor level at which the apartment is located, can affect the indicator due to the different heat losses. Apartment and rooms oriented to the south can ensure higher flexibility as expected, while apartment located at the last floor or at the corners have a lower potential. Therefore, in order to take advantage of the flexibility potential in an apartment block, a dynamic system has to be considered, which evaluates the spatial differences and adapts the heating supply in order to ensure the desirable indoor temperature.

Conclusion

This study gives a first evaluation of how the flexibility potential depends on internal gains and weather conditions. To reach the aim, two flexibility indicators are defined and applied during the investigation. The study highlighted the high influence of solar radiation and outdoor temperature on the indicator, while showed a lower impact of the number of occupants and the occupant's schedule. The analyses about the apartment's position demonstrated that the orientation influences the flexibility indicator the most, while the floor level has a lower impact on it.

The south oriented rooms proved to be more sensitive to solar radiation, as the first indicator is found to be always higher compared to the rooms facing north. The highest impact on the flexibility indicator is given by the large solar radiation and the highest number is found at 215 hours in the living room. In this study case, the number of hours increased around four times compared to the lowest case obtained with no solar radiation. In the same way, the outdoor temperature is found to have high influence on the indoor comfort and therefore, on the possibility of using the flexibility of the building. In particular, for the extreme outdoor condition of -12 °C, the indicator showed the lowest result equal to 10 hours above 20 °C. Regarding the internal gains related to the number of occupants in the apartment and their

schedules, it is noticed that increasing the number of occupants by one unit, the increase in hours is almost linear. From the study appears that solar radiation and outdoor temperature have high impact on the indoor comfort in buildings. Therefore, weather forecasts can be used as means to predict the flexibility potential of buildings and if integrated in a smart city network they can be used to achieve results in terms of energy consumption reduction, while maximizing the use of renewable energy.

Implementing flexibility with a dedicated heating program, such as the cut-off program, shows that higher power peaks have to be faced. In fact, the power peak found for the heating systems results 6 times higher than in case of continuous control. This result has to be treated carefully, since it is dependent on the heating control used, as well as it has to be taken into account that only the coldest month was considered. However, despite of the good results in terms of flexibility, changes in heating program need to be evaluated carefully, since due to the higher power peaks, the building's systems might have to be designed accordingly. Furthermore, the primary energy consumption of the heating system with the daily heating program is found to be 3.5 % higher than the continuous control. Therefore, implementing energy storage in the building mass with dedicated heating programs leads to a slight overconsumption, which can be justified if this ensures higher use of energy from RES.

Acknowledgements

References

Aduda, K.O., Labeodan, T., Zeiler, W., Boxem, G. and Zhao, Y. (2016). Demand side flexibility: Potentials and building performance implications. *Sustainable Cities and Society*, 22, 146–163.

Chen, D., Wang, X. and Ren, Z. (2012). Selection of climatic variables and time scales for future weather preparation in building heating and cooling energy predictions. *Energy and Buildings*, 51, 223–233.

Dansk Standard. (2007). DS/EN 15251 indoor environmental input parameters for design and assessment of energy performance of buildings addressing indoor air quality, thermal environment, lighting and acoustics. *Danish Standard*, 1st ed.

Firląg, S. and Murray, S. (2013). Impacts of airflows, internal heat and moisture gains on accuracy of modeling energy consumption and indoor parameters in passive building. *Energy and Buildings*, 64, 372–383.

Fischer, D., Wolf, T., Scherer, J. and Wille-Haussmann, B. (2016). A stochastic bottom-up model for space heating and domestic hot water load profiles for German households. *Energy and Buildings*, 124, 120–128.

Gellings, C. W. (1985). The concept of demand-side management for electric utilities. *Proceedings of the IEEE*, 73(10), 1468–1470.

Labeodan, T., Zeiler, W., Boxem, G. and Zhao, Y. (2015). Occupancy measurement in commercial office buildings for demand-driven control applications - A survey and detection system evaluation. *Energy and Buildings*, 93, 303–314.

Lazos, D., Sproul, A. B. and Kay, M. (2014). Optimisation of energy management in commercial buildings with weather forecasting inputs: A review. *Renewable and Sustainable Energy Reviews*, 39, 587–603.

Le Dréau, J. and Heiselberg, P. (2016). Energy flexibility of residential buildings using short term heat storage in the thermal mass. *Energy*, 111, 991–1002.

Ling, Z.G., Zhang, S.Y., Fu, X.Z. and Wang, Y. (2006). Investigation of floor heating with thermal storage, *Journal OSUT* 13(4), 1974–1975.

Lund, P.D., Lindgren, J., Mikkola, J. and Salpakari, J. (2015). Review of energy system flexibility measures to enable high levels of variable renewable electricity. *Renewable & Sustainable Energy Reviews*, Elsevier Ltd, 45, 785–807.

Marin, P., Saffari, M., de Gracia, A., Zhu, X., Farid, M. M., Cabeza, L. F. and Ushak, S. (2016). Energy savings due to the use of PCM for relocatable lightweight buildings passive heating and cooling in different weather conditions. *Energy and Buildings*, 129, 274–283.

Neupane, B., Bach, T. and Thiesson, B. (2014). Towards Flexibility Detection in Device-Level Energy Consumption. *Lecture Notes in Computer Science (Including Subseries Lecture Notes in Artificial Intelligence and Lecture Notes in Bioinformatics)*, 8817, 1–16.

Rotger-Griful, S. and Hylsberg Jacobsen, R. (2015). Control of Smart Grid ResidentialBuildings with Demand Response. Chaos Modelling and Control Systems Design. (A. T. Azar & S. Vaidyanathan, Eds.). *Studies in Computational Intelligence* (Vol. 581), 133-161, Springer International Publishing.

Sikula, O., Plasek, J. and Hirs, J. (2012). Numerical simulation of the effect of heat gains in the heating season. *Energy Procedia*, 14, 906–912.

Werner, S. and Olsson Ingvarsson, L. (2008). Building mass used as short term heat storage. *In Proceedings of the 11th International Symposium on District Heating and Cooling*. Reykjavik, Iceland.

Xue, X., Wang, S., Yan, C. and Cui, B. (2015). A fast chiller power demand response control strategy for

buildings connected to smart grid. *Applied Energy*, 137(Jan), 77–87.

Zheng, M., Meinrenken, C.J. and Lackner, K.S. (2015). Smart households: Dispatch strategies and economic analysis of distributed energy storage for residential peak saving. *Applied Energy*, 147, 246–257.

PAPER VII: Gianniou, P., <u>Foteinaki, K.</u>, Heller, A. and Rode, C. (2017) 'Intelligent Scheduling of a Grid-Connected Heat Pump in a Danish Detached House, *in the Proceedings of the 15th IBPSA Conference*. San Francisco, CA, USA, pp. 95–102.

Intelligent Scheduling of a Grid-Connected Heat Pump in a Danish Detached House

Panagiota Gianniou[1], Kyriaki Foteinaki[1], Alfred Heller[1], Carsten Rode[1]
[1]Department of Civil Engineering, DTU, Kgs. Lyngby, Denmark
Contact: pagian@byg.dtu.dk

Abstract

This study proposes a methodology for intelligent scheduling of a heat pump installed in a refurbished grid-connected detached house in Denmark. This scheduling is conducted through the coupling of a dynamic building simulation tool with an optimization tool. The optimization of the operation of the system is based on a price-signal considering a three-day period for different weather cases. The results show that the optimal scheduling of the system is successful in terms of reducing the peak load during times when electricity prices are high, thus achieving cost savings as well as maintaining good thermal comfort conditions. The proposed methodology bridges dynamic building modelling with optimization of real-time operation of HVAC systems offering a detailed model for building physics, especially regarding thermal mass and a stochastic price-based control.

Introduction

As the share of renewable energy sources (RES) in power generation is constantly increasing in many countries, imbalances arise between the supply and demand side. Specifically for Denmark, renewable energy is expected to cover about 80-85% of electricity consumption and up to 65% of district heating in 2020 (Danish Energy Agency, 2015). One of the main goals is that the entire energy supply is covered by RES by 2050. That calls for demand-side management (DSM) approaches that can facilitate the operation of the smart grid while enabling controllability of the electric loads.

The potential of buildings' participation in DSM approaches has been investigated, implementing strategies to reduce power consumption during peak periods (peak-shaving) and/or to shift the power consumption from peak periods to off-peak periods (load-shifting). There is a number of studies indicating the importance of the structural thermal mass of buildings, for example Reynders et al. (2013), while some others implemented DSM by adjusting the HVAC systems of the building, for example Arteconi et al. (2013) and Masy et al. (2015). There are also a few studies that tried to reschedule the operation of shiftable plug loads, such as dishwashers, washing machines and tumble dryers, as in D'hulst et al. (2015).

The two main types of control are direct control and indirect or price-based control. Schibuola et al. (2015) concluded that HVAC systems will not undergo direct control in future smart grids due to discomfort issues that this might bring to the occupants. Thus, price response strategies will be the main focus of this study. Particularly in countries like Denmark, where power generation achieved by RES accounted for 25% of the adjusted gross energy consumption, which describes total observed energy consumption adjusted for fluctuations in climate with respect to a normal weather year (Danish Energy Agency, 2015), this leads to very low electricity spot prices or even negative ones. Thus, price-based control can achieve peak-shaving that is much needed by the grid to ensure decrease or displacement of peak loads.

Computational methods of design optimization have proven to be advantageous in several building studies according to Evins (2013). Optimization algorithms are mainly categorized into heuristic and meta-heuristic when it comes to building co-simulation. Heuristic algorithms include direct search such as pattern search and linear or non-linear programming. Meta-heuristic algorithms consist of evolutionary algorithms such as genetic algorithms (GA) or particle swarm optimization (PSO). So far, optimization in building modelling has been used with regards to building envelope, systems, energy generation and holistic approaches considering many aspects in building operation (Evins, 2013). Extensive studies have focused on optimizing the building envelope and dimensioning of the systems mostly during the design phase. The optimization of the control of the HVAC systems has been implemented in some studies. Particularly Zhou et al. (2003) investigated the minimization of electricity cost of varying cooling set-points for different algorithms and concluded on a most suitable one. Miara et al. (2014) investigated how heat pumps provided with heat storage and floor heating system may take advantage of real-time pricing. The authors determined that the most important parameter to ensure this was the water heat storage tank. However, the flexibility that thermal mass, which is embedded into the building structure, can offer along with demand response management of the heating systems, have not been thoroughly discussed. Especially when using reduced order models or grey-box models, many optimization techniques and algorithms can ensure their feasibility. Their application has not been extensively highlighted though, in cases of flexible operation of HVAC systems in residential buildings. Particularly in the case of white-box building models, which describe building physics and

heat transfer mechanisms in full detail, little effort has been made to use them as basis for optimal scheduling of the HVAC systems based on electricity pricing. This is mainly due to their complexity, which impedes their coupling with advanced optimization tools. However, the potential that the thermal mass of the building gives with regards to energy flexibility is crucial to such studies and should be modelled with every detail possible.

The current study aims at developing a methodology for optimally scheduling the systems of a grid-connected single-family house equipped with an air-to-water heat pump and low temperature radiators based on a price response strategy. This strategy will indicate the potential of the systems for optimization, which will define a generic methodology while enabling the utilization of the building's thermal mass that can be applied in every residential building with similar HVAC systems.

Model description

The current analysis was conducted by use of a building model. This corresponds to a typical Danish single-family house (SFH) built between 1961-1972 (Figure 1), which is the most common type of SFH in Denmark according to Danmarks Statistik (2016). The properties of the building envelope and systems have been created according to TABULA database (2016). The building area is 153m^2, while the glazing covers an area of 34m^2. Its building envelope has been extensively renovated and the average U-value of the building is 0.27 W/m^{2}K. The material layers that consist the building components can be seen in Table 1. The house contains an air-to-water heat pump (HP) of 13 kW with COP of 3.5. The heat emission system installed is a hydronic one with low-temperature water radiators. The controller of the hydronic system is a thermostat set at 21°C with 2°C deadband based on the operative temperature.

Table 1: Material layers

Building component	Layer material	Thickness (m)	U-value (W/m^{2}K)
External walls	Brick	0.05	0.13
	Light insulation	0.25	
	Brick	0.05	
Roof	Light insulation	0.34	0.10
	Wood	0.03	
	Gypsum	0.013	
Floor	Wood	0.02	0.12
	Light insulation	0.28	
	Gypsum	0.02	

Deterministic profiles were created for the internal gains. The occupants living in the house were assumed to be two according to data from Danish Statistics (Danmarks Statistik, 2016) following a typical house living profile (Figure 2) and with sedentary activity level (met-value=1.2) according to DS/EN 15251 (2007). Their clothing was variable ranging from 1 during the winter season to 0.5 for the summer season. The schedules of

equipment and lighting can also be found in Figure 2. Internal blinds were drawn in cases of excessive solar radiation. It was also assumed that windows started to open when indoor temperature reaches 25°C and opened fully at 27°C. There was no mechanical ventilation or cooling installed in the building. The infiltration rate was 0.2 ACH representing a quite air-tight refurbished envelope. The location was set to Copenhagen, Denmark. The main façade of the house was assumed to be oriented towards the south. The weather file used was the Danish Design Reference Year (DRY) (DMI, 2013).
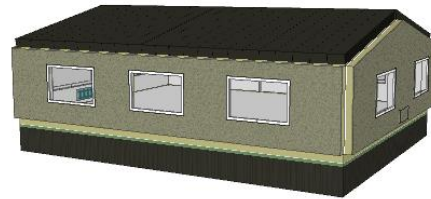

Figure 1: Design of examined SFH
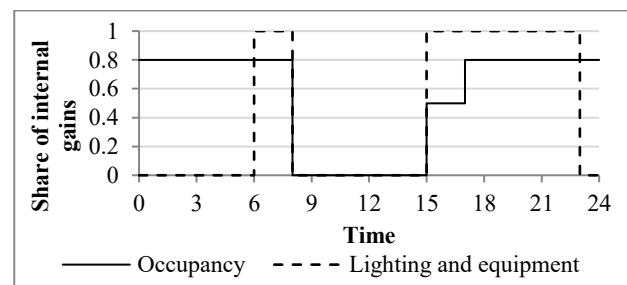
Figure 2: Daily schedule for internal gains

Since emphasis will be placed on the utilization of the thermal mass of the building in the present study, the heat transfer mechanisms taking place inside the building structure are important. The wall model used is a finite difference model of multi-layered components. Each material layer is discretized into four nodes. Thus, it can provide accuracy when alternative models, such as RC-networks, fail to. Furthermore, nonlinear effects in the thermal dynamics of buildings, which are usually oversimplified in RC-networks (Thavlov and Bindner, 2015), (Zong et al., 2017), are described in detail in the current model.

Methodology

In this paper, a price-based control strategy for the management of the heat pump was implemented that enabled the exploitation of dynamic electricity prices and thus management of the energy load according to the grid's imbalances. In this way, the interaction of the detached house with the grid was improved. The scheduling of the HP comprised two parts: the control of the system, and its optimization.

The scheduling of the heat pump was carried out considering an advanced controller for the radiators. This can be seen in Figure 3. The base heating setpoint was set to 20°C. An additional controller, which contained an algorithm to smooth its output as an approximation to a P-

controller so that no events (abrupt turn-ons and offs) were created, was added in the loop to allow for the system's flexibility when the electricity prices were low. Therefore, the operation of the HP was forced to increase during low-tariff hours. The hourly tariff concept was assumed to reflect the lack of or excess of RES energy in the grid and thus represent the stress on the grid (Dar et al., 2014). The low electricity prices were defined as the ones that were lower than the average electricity price of the specific month. This means that when the electricity price was low, a positive deadband of 3°C was added to the base setpoint, resulting in 23°C upper threshold, which allowed the system to take advantage of the low prices. In this way, the increase in the heating setpoint would enable heat to be stored into the thermal mass during low price periods, and be released back to the room when prices were higher. The electricity price signal was imported into the model as a source file connected to the P-controller. The proportional band of the P-controller was set to -0.5 as this referred to heating mode. The capability of the system to keep the indoor environment within comfort conditions was a significant advantage of the selected control strategy. According to EN/DS 15251 (2007), Category II of acceptable thermal comfort ranges from 20-25°C.

The optimization was defined as minimization of the operating cost of the HP. This cost depended on the variable electricity prices and on the consumption of the HP. The cost-optimal control of the heat pump on a 3-day horizon would ensure cost savings in the electricity bill along with the desired peak shavings in the heat load of the building. Also, the 3-day horizon was selected so that any phenomena of cumulative heat storage into the thermal mass can be observed. Due to increased computation time, it was not selected to investigate a longer period. It has to be clarified that no electricity was assumed to be sold back to the grid or modelled in this case for simplification reasons.
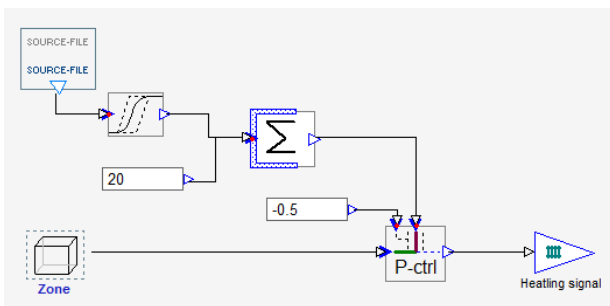

Figure 3: Control of heating system based on price signal

The optimization problem of the intelligent scheduling of the heat pump according to the price signal was formulated as following:

$$Minimize\ C_{HP} \qquad (1)$$

where C_{HP} is the operating cost of the HP, calculated as following:

$$C_{HP}=p_{el} \cdot W \qquad (2)$$

where p_{el} is the total electricity price and W is the energy consumption of the HP.

The optimization of the system operation was conducted through the boiler schedule which was characterized by ten variables per day, b_i, corresponding to the schedule of the part load operation of the HP. This means that a different schedule of the HP operation was optimized for each day.

$$b_i \in [0,1]\ for\ i = 1 \dots 30 \qquad (3)$$

The optimization was conducted with the use of the open-source software MOBO. MOBO is a generic freeware designed to handle single-objective and multi-objective optimization problems with continuous or discrete variables (Rosli et al., 2016). It provides the possibility to be coupled to building performance simulation tools, while selecting different algorithms to perform the calculations. Furthermore, MOBO has the feature of running multiple simulations in parallel, thus reducing the overall computation time with a factor equal to the number of threads available in the computer. In this case, different optimization algorithms were selected, and they were compared upon the optimal solution and the number of runs. In particular, a deterministic algorithm (Hooke-Jeeves), two genetic algorithms (NSGA-II, Omni-optimizer) and a hybrid one (GA and Hooke-Jeeves) were tested. As defined in Wetter and Wright (2004), GA are algorithms that operate on a finite set of points, called a population. The different populations are called generations. They are derived on the principles of natural selection and incorporate operators for fitness assignment, selection of points for recombination, recombination of points, and mutation of a point. The simple GA iterates either until a user-specified number of generations is exceeded, or until all iterates of the current generation have the same cost function value (Wetter and Wright, 2004). Initially, the optimization algorithms were implemented having the same solver settings. These were 8 populations, 20 generations, 0.05 mutation probability and 0.9 cross-over probability. The meaning of the cross-over probability is that when this is not met, the individuals do not continue to the new population as explained in Evins et al. (2010). The crossover process continues until the new population is full. The reason for using a small population size was to reduce computation time. The deterministic algorithm that was tested does not enable parallel computing, thus being significantly slower. The settings of the deterministic algorithm were ρ=0.05 (convergence parameter) and ε=0.01 (minimum criterion to stop the search).

Furthermore, different solver settings were applied to determine their effect on achieving the optimal solution. Based on the cost-optimal solution and the number of simulations carried out until convergence was reached, one optimization algorithm was selected and tested upon its accuracy for various numbers of generations. Then, the solver settings that reached the biggest cost reduction were selected and implemented into the building model. The schedule for the boiler/HP operation was thus defined according to the optimal solution. These results were

compared to the ones of the reference case with normal operation of the HP, as previously described in the model description.

Simulation

The simulation was run in IDA ICE Version 4.7 (EQUA, 2013) using MOBO. The building was simulated as a single-zone model. The reference model was initially run with the DRY weather file. Three climate cases were selected out of the entire simulation period, the coldest 3-day period of the heating season (January) with a mean ambient temperature of -4°C, the warmest 3-day period of the heating season (September) with a mean ambient temperature of 11°C and an intermediate one (April) when the average ambient temperature was 3°C.
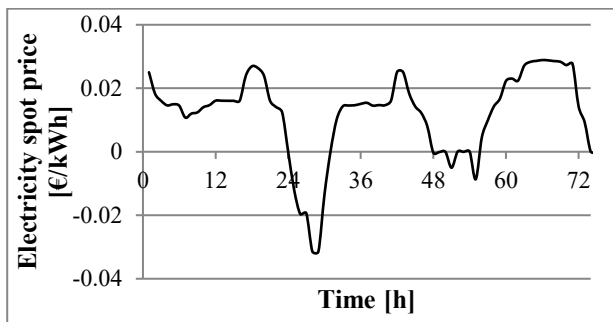

Figure 4: Electricity spot prices over 3 days

The prices for electricity were set in the model through a stochastic profile reflecting real electricity prices in 2015 according to the Nordic electricity market Nord Pool for East Denmark. During this period, wind power generation accounted for 74% of the total electricity production, which explains the low electricity prices that comprise the price signal that was coupled to the IDA ICE model. These prices reflect the total electricity prices consisting of variable el-spot prices (commercial), which account for 32% of the total price in Denmark, while the remaining 68% are fixed taxes for local network, grid and system tariffs, public service obligation tariff and further subscriptions to electrical companies based on the Association of Danish Energy Companies (2015). The total electricity prices were used in the model so that they correspond to the ones that electricity customers have to

pay. The same price-signal was used for all three cases of weather data to ensure comparability, so it has not been correlated to the climate data. Figure 4 presents the electricity spot prices during this 3-day period. The negative prices indicate the surplus of wind power generation during these days.

Result analysis and discussion

As mentioned before, different optimization algorithms were tested in MOBO in order to determine which one to select based on the biggest cost reduction they could achieve. The selected genetic and deterministic algorithms were implemented and tested for the three different weather data having the same solver settings, as described in the Methodology section. The implemented algorithms are presented in Table 2. A detailed explanation of all the algorithm parameters is beyond the scope of this paper and we refer the readers to Wetter and Wright (2003). The cost-optimal solution refers to the minimum cost (€) that each optimization algorithm achieved which means the total operating cost of the HP needed to heat up the building for the examined 3 days.

Due to the increased number of variables used in the optimization problem, some discontinuities could be expected in the cost function which would make optimization rather difficult to be achieved (Wetter, 2004). For this reason, different optimization algorithms were tested, some of which (i.e. Hooke-Jeeves) are less likely to converge to a discontinuity far from the optimal solution (Wetter, 2011). Moreover, the total cost reduction observed might be limited for the above-described reasons and is not assessed per se but in comparison with the rest of the results. Furthermore, some uncertainty in the results has to be considered due to randomness of the optimization. The hybrid algorithm, GA and Hooke-Jeeves, proved to be the best one among the rest, even though the differences were very small, calculating the biggest cost reduction in all three weather cases. It has to be noticed that the hybrid algorithm led to a higher number of simulations, due to which it converged to a lower cost-optimal solution. Thus, it was selected to run some further analysis on the impact that the number of generations has on achieving the optimal solution.

Table 2: Results of different optimization algorithms

Optimization algorithm	Type of algorithm	Cost-optimal solution [€]	Simulations until convergence (output)	Weather data
NSGA-II	Genetic (evolutionary)	1.802	144	Cold
		0.787	152	Intermediate
		0.008	152	Warm
Hooke-Jeeves	Deterministic (pattern-search)	1.775	221	Cold
		0.778	166	Intermediate
		0.008	60	Warm
GA and Hooke-Jeeves	Hybrid	1.774	311	Cold
		0.778	363	Intermediate
		0.007	311	Warm
Omni-optimizer	Genetic (evolutionary)	1.806	152	Cold
		0.780	152	Intermediate
		0.007	152	Warm

Three numbers of generations were applied to the hybrid algorithm being comprised of GA and Hooke-Jeeves, and are presented in Table 3 along with the number of simulations and the solution they resulted in. It can be observed that the higher the number of generations and the more simulations conducted, the bigger cost reduction was achieved, as it was expected. Therefore, the optimal solution found with 100 generations for each weather case was used for the following analysis. However, it has to be pointed out that even though a scenario of 100 generations leads to approximately twice as many simulations as the one of 50 generations, the cost reduction is not significantly bigger. Specifically, this was 2% for the cold and intermediate weather data and 1% for the warm case, (Table 3). Therefore, it was decided not to investigate an even bigger number of generations.

Table 3: Impact of generations on optimal solution

GA and Hooke-Jeeves	Cost-optimal solution [€] (Number of simulations)		
Generations	Cold	Intermediate	Warm
25	1.7741 (311)	0.7778 (363)	0.0075 (311)
50	1.7727 (512)	0.7771 (568)	0.0074 (800)
100	1.7418 (913)	0.7612 (909)	0.0073 (1491)

Figure 5 shows the power consumption for the reference and optimized case for each of the weather cases. As it was expected, the pattern is different for the different climate cases examined. For the cold weather, when using the thermostat as in the reference case, the HP turned on and off in very small intervals, in order to cover the high demand, which results in high power peaks. On the other hand, for the optimal case, the power consumption presented a considerably more smooth pattern, which was fully in line with the price signal. This is also attributed to the smoothing effect that the controller applied in the optimal scenario has. There were small parts of the load that were shifted towards a different timing than in the

reference case, but this schedule mainly achieved considerable peak shaving. It is clear that the optimization was conducted successfully, as during times with low electricity prices, the HP was forced to increase its part load and vice versa. For the intermediate climate case, it can be seen that the power consumption pattern is similar for the reference and optimal cases. The time when the power consumption peaks is almost identical, but still there was peak shaving achieved with the optimal case and the operation pattern of the HP is more smooth. This means that continuous on/offs are avoided, which would lead to a decrease in HP's lifetime and inefficient operation. For the warm climate case, it is obvious that the energy demand is amost zero, so the difference between the two cases is marginal. This minimum heat load left no room for the optimization to take place.

Table 4. Total energy consumption results

Weather data	Total energy consumption (kWh)	
	Reference case	Optimal case
Cold	191	180
Intermediate	92	104
Warm	8.80E-05	8.70E-05

Regarding the total energy consumption, the results were different for the different climate cases. These are presented in Table 4. For the cold climate, there was an energy consumption reduction of 6% with the optimal case, while for the intermediate climate there was a 13% increase for the optimal case. This indicates that when implementing a DSM strategy, i.e. peak shaving, this might result in an overall over-consumption. However, the goal of this strategy is to use the energy produced from RES, which is, in this study, reflected in the low prices. So, the focus is not to achieve energy minimization, but to "force" the operation of the HP to follow the production pattern of renewable energy in the energy system, while maintaining the thermal comfort and achieving cost savings for the occupants. As previously mentioned, the heat demand for the warm climate is minor, so there is only 1% decrease in the total energy consumption after the optimal case was applied.
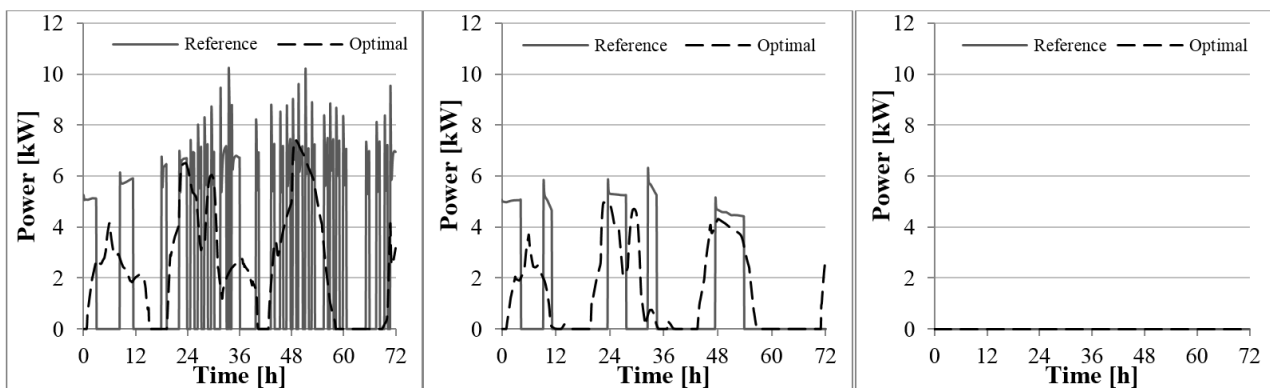

Figure 5: Power results for the optimized scheduling of the HP and the reference operation for cold weather data (left), intermediate (middle) and warm (right)
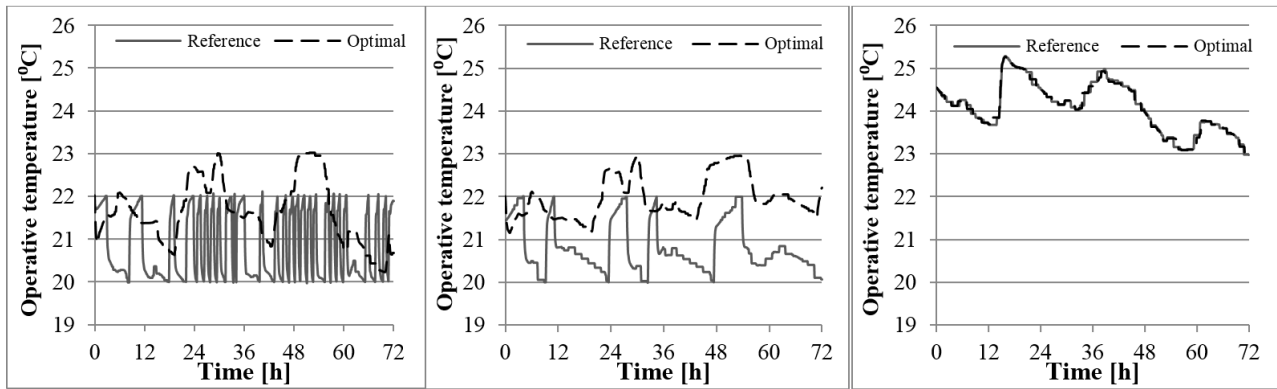
Figure 6: Operative temperature results for the optimized scheduling of the HP and the reference operation for cold weather data (left), intermediate (middle) and warm (right)

As far as cost reduction is concerned, the results varied, too, with regards to the different climate cases and can be seen in Table 5. In the cold weather case, optimally scheduling the HP resulted in 42% decrease in the total operating cost of the HP for the examined 3-day period. In the intermediate case, the cost savings were 22% compared to the reference operation of the HP, while in the warm weather case these were significantly lower, approximately 13%, as it was expected.

Table 5. Operating cost results of the HP for 3 days

Weather data	Total operating cost (€)	
	Reference case	Optimal case
Cold	2.998	1.742
Intermediate	0.979	0.761
Warm	0.008	0.007

Regarding peak shavings, which is the main goal of this demand side management approach, the results showed a clear decrease in peak consumption at the optimal case both for the cold and the intermediate weather. Taking the highest peak in power for each case, there was a reduction of 27% (2.75 kW) for the cold weather and 21% (1.32 kW) for the intermediate weather (Figure 5). This was achieved due to the smoother operation pattern of the heat pump that shifted parts of the load in time, which led to reduced peak demand. The magnitude of the potential peak decrease would always depend on the price signal, but the main outcome is that the implemented control is an effective peak shaving strategy.

Figure 6 presents the operative temperature for the reference and optimized cases for each of the weather cases. It can be observed that there is a trend for the optimal cases to have higher operative temperature than the respective of the reference cases at all climate cases. This can be explained by the control of the heating system, which was able to increase the setpoint up to 23ºC when the electricity prices were low. It has to be pointed out that the electricity prices according to which the optimal scheduling of the HP was conducted in the three weather cases were found to be low compared to the average monthly price, which resulted in utilization of the increased heating setpoint most of the time. If a different threshold was used instead of the monthly average

electricity price, the price signal might not be characterized as low most of the time and the results would be somewhat different as the decision to add the deadband to the base setpoint would alter. The lowest threshold of the thermal setpoint (considering the given deadband) was set to be equal for the reference and the optimal cases (20ºC), so that they both retain similar thermal comfort conditions. Furthermore, there is a clear correlation between the power consumption pattern and the operative temperature pattern. This explains why the temperature of the reference case of the cold climate had frequent fluctuations, whereas the temperature of the optimal case of the cold climate and both cases of the intermediate climate had a smooth pattern. Due to the cold external temperatures that reached -18ºC, the HP was forced to switch on and off very frequently creating high peaks in order to maintain the desired indoor temperature. In the intermediate weather case, the significantly higher ambient temperatures allowed a more flexible operation of the HP. In the warm climate case, there was almost no difference observed in the operative temperatures between the optimal and the reference case since the HP operated for a very short time. In all cases, the operative temperature stayed within the acceptable limits of EN/DS 15251 ensuring that with the applied control and cost optimization, the thermal comfort for the occupants was not compromised.

This can be verified by the amount of occupancy hours into the different comfort categories, which were in all cases within the acceptable categories according to EN/DS 15251, as it can be seen in Table 6. In particular, Table 6 indicates the cumulative share of occupancy hours that fell into the three comfort categories according to EN/DS 15251. Category IV is not presented since no occupancy hours belonged to that. The optimized scheduling of the HP increased the amount of occupancy hours belonging to comfort Category I for the cold and intermediate weather case, while slightly decreased these for the warm weather case. Overall, the optimized operation of the HP maintained the good thermal comfort corresponding to the design conditions of the heating system in all three weather cases.

Table 6: Thermal comfort assessment for optimal scheduling of HP

Weather data	Cold		Intermediate		Warm	
Case	Opt.	Ref.	Opt.	Ref.	Opt.	Ref.
Comfort category	Share of occupancy hours (%)					
I (best) (21-25ºC)	71	40	100	26	78	100
II (good) (20-25ºC)	100	98	100	100	100	100
III (acceptable) (18-25ºC)	100	100	100	100	100	100

Summing up, the optimization problem has been solved using MOBO coupled with IDA ICE. The simulations were performed on a computer with Intel i7 4-core processor clocking at 2.1 GHz and 8 GB of RAM. The average total time of solving was 7250 seconds for the cold and warm weather case and 7460 seconds for the intermediate one. In this specific case, the optimization problem was solved for a three-day period.

It has to be pointed out that the goal of this study was the proposal of a methodology to schedule the HP operation intelligently using building performance simulation tools according to the grid's imbalances that are reflected on the price signal and not the investigation of optimization techniques. In addition to this, the complicated building model and the large number of continuous variables used in the optimization problem increased significantly the computation time. On the other hand, the advanced building model that was used modelled accurately the thermal building physics mainly of the thermal mass and the complicated heat transfer mechanisms that take place during the charging or discharging of the thermal mass. These were critical to estimate the flexible operation of the HP.

Due to increased computation time, it was chosen to investigate a three-day design period for each weather case instead of a whole-year simulation that would be more representative. The optimization horizon was not restricted to one day, since the authors wanted to investigate any heat storage mechanisms into the thermal mass of the building, which are cumulative over time. Furthermore, the proposed methodology refers to future energy market designs, where the optimization of individual buildings' heating or cooling systems based on price signals will be possible. In this case, day-ahead prices will be available, so the optimization problem will be solved only for the following day, which will result in shorter computation time. However, attention should be paid to the initial and final conditions of the thermal model, so that they are consistent with the ones of the previous and following day.

Computationally expensive simulations also led to tight solver settings (small number of populations and low mutation probability), which increased the chances of not converging to a stationary minimum point of the cost function.

The positive 3ºC deadband provided to the base heating setpoint that allowed for the system flexibility was selected such that the thermal comfort of occupants was not compromised with the optimized scheduling of the heating system. If a looser comfort threshold was to be achieved, this deadband could be further expanded so that lower operative temperatures than 20ºC should be allowed. Furthermore, different price signals could have been applied to the case so that an estimate of the range of peak and power savings could be made and also a realistic correlation to the weather data would be possible. Lastly, the use of historical weather data for the examined period would have resulted in much more clear optimization results and would have avoided uncertainty. Hence, they ought to replace the DRY weather file as a next step to this study.

Conclusion

In this study, the cost optimization of the control of a HP in a detached Danish house was investigated. A dynamic building performance simulation tool was coupled to an optimization software. A hybrid genetic algorithm was selected as the most suitable one to achieve the biggest cost reduction of the operation of the HP. The optimal scheduling of the HP that was achieved based on a price signal for three weather data was compared to the reference case, which was normal operation of the HP system. The comparison was made with regards to power peak shavings, cost savings, operative temperature and thermal comfort. The results showed that the optimization was conducted successfully, as the price-based control managed to reduce the peak loads during high price times and increase the energy load during the low price times. This resulted in a smoother pattern for the operation of the HP for the cold and intermediate weather data. In the warm weather case, the very low heating demand left no room for optimization. Furthermore, the optimal scheduling of the HP maintained good thermal comfort of the occupants with regards to the operative temperature. The operative temperatures during the optimal scheduling of the system were maintained in a good comfort category according to EN/DS 15251. Even though the detailed building model that was used increased the number of variables in the optimization problem and the computation time, it modelled the heat dynamics into the thermal mass sufficiently well, which allowed for the flexible operation of the HP.

Finally, the three selected weather cases represented different climatic conditions during a heating season in Denmark. The cold and the intermediate weather cases proved to be representative of extreme and mild winter weather conditions and enabled the optimization of the HP. The warm weather data could not be considered for the optimal scheduling of the HP, since the heat demand was very low. Therefore, should a holistic overview of the intelligent scheduling of a HP in a similar building and climate be given, a combination of the two afore-mentioned weather data has to be considered.

Acknowledgements

References

Arteconi, A., Hewitt, N. J., Polonara, F. (2013). Domestic demand-side management (DSM): Role of heat pumps and thermal energy storage (TES) systems. *Applied Thermal Engineering*, *51*(1–2), 155–165.

Association of Danish Energy Companies (2015). Electric Utility tariffs and electricity prices (Danish title: Dansk Energi. Elforsyningens tariffer & elpriser)

D'hulst, R., Labeeuw, W., Beusen, B., Claessens, S., Deconinck, G., Vanthournout, K. (2015). Demand response flexibility and flexibility potential of residential smart appliances: Experiences from large pilot test in Belgium. *Applied Energy*, *155*, 79–90.

Danish Energy Agency (2015). Danish energy and climate outlook. Published in December 2015 by the Danish Energy Agency, Copenhagen, Denmark.

Danmarks Statistik (accessed 2nd December 2016). https://www.statbank.dk/statbank5a/default.asp?w=1920

Dar, U. I., Sartori, I., Georges, L., Novakovic, V. (2014). Advanced control of heat pumps for improved flexibility of Net-ZEB towards the grid. *Energy and Buildings*, *69*, 74–84.

DMI, Danish Meteorological Institute (2013). Danish Ministry of Climate, Energy and Building: 2001-2010 Danish Design Reference Year. Technical Report 13-19.

EN/DS 15251 (2007). Indoor environmental input parameters for design and assessment of energy performance of buildings addressing indoor air quality, thermal environment, lighting and acoustics.

Evins, R. (2013). A review of computational optimisation methods applied to sustainable building design. Renewable and Sustainable Energy Reviews, 22, 230–245.

Evins, R., Pointer, P.,Vaidyanathan, R. (2010). Configuration of a genetic algorithm for multi-objective optimisation of solar gain to buildings. In: Proceedings of the genetic and evolutionary computation (GECCO). NewYork, NY, USA, 1327–1328.

EQUA (2013). IDA Indoor Climate and Energy. User Manual. Version 4.5. http://www.equaonline.com/iceuser/pdf/ICE45eng.pdf .

Masy, G., Georges, E., Verhelst, C., Lemort, V., Andre, P. (2015). Smart grid energy flexible buildings through the use of heat pumps and building thermal mass as energy storage in the Belgian context. *Science and Technology for the Built Environment*, *4731*(August), 800–811.

Miara, M., Günther, D., Leitner, Z. L., Wapler, J. (2014). Simulation of an Air-to-Water Heat Pump System to Evaluate the Impact of Demand-Side-Management Measures on Efficiency and Load-Shifting Potential. Energy Technology, 2(1), 90–99.

Reynders, G., Nuytten, T., Saelens, D. (2013). Potential of structural thermal mass for demand-side management in dwellings. *Building and Environment*, *64*, 187–199.

Rosli, E. M.A.M., Sopian, K., Mat, S., Sulaiman, M. Y. (2016). Renewable Energy in the Service of Mankind Vol II. *Selected Topics from the World Renewable Energy Congress WREC 2014*, *I*, 583–590.

Schibuola, L., Scarpa, M., Tambani, C. (2015). Demand response management by means of heat pumps controlled via real time pricing. Energy and Buildings, 90, 15–28.

TABULA WebTool (accessed 30th November 2016). http://webtool.building-typology.eu/#bm .

Thavlov, A., Bindner, H. (2015). A Heat Dynamic Model for Intelligent Heating of Buildings. International Journal of Green Energy, 12, 240–247.

Wetter, M. and Wright, J. (2003). Comparison of a generalized pattern search and a genetic algorithm optimization method. In Augenbroe, G. and Hensen, J., editors, Proc. of the 8-th IBPSA Conference, volume III, pages 1401-1408, Eindhoven, NL.

Wetter, M. and Wright, J. (2004). A comparison of deterministic and probabilistic optimization algorithms for nonsmooth simulation-based optimization. Building and Environment, 39, 989-999.

Wetter, M. (2011). GenOpt, generic optimization program, user manual, version 3.1.0. Lawrence Berkeley National Laboratory, Berkeley, CA, USA.

Zhou, G., Ihm, P., Krarti, M., Liu, S., Henze, G. (2003). Integration of an internal optimization module within EnergyPlus. In: Proceedings of the building simulation, Eindhoven, Netherlands.

Zong, H., Bönning, G. M., Santos, R. M., You, S., Hu, J., Han, X. (2017). Challenges of implementing economic model predictive control strategy for buildings interacting with smart energy systems. Applied Thermal Engineering, 114, 1476–1486.

PAPER VIII: Foteinaki, K., Heller, A. and Rode, C. (2016) 'Modeling energy flexibility of low energy buildings utilizing thermal mass', *in the Proceedings of* the *9th International Conference on Indoor Air Quality Ventilation & Energy Conservation In Buildings (IAQVEC)*. Songdo, Incheon. Republic of Korea.

Modeling energy flexibility of low energy buildings utilizing thermal mass

Kyriaki Foteinaki[*], Alfred Heller and Carsten Rode

Technical University of Denmark, Kgs.Lyngby, Denmark

[*]*Corresponding email: kyfote@byg.dtu.dk*

ABSTRACT
In the future energy system a considerable increase in the penetration of renewable energy is expected, challenging the stability of the system, as both production and consumption will have fluctuating patterns. Hence, the concept of energy flexibility will be necessary in order for the consumption to match the production patterns, shifting demand from on-peak hours to off-peak hours. Buildings could act as flexibility suppliers to the energy system, through load shifting potential, provided that the large thermal mass of the building stock could be utilized for energy storage. In the present study the load shifting potential of an apartment of a low energy building in Copenhagen is assessed, utilizing the heat storage capacity of the thermal mass when the heating system is switched off for relieving the energy system. It is shown that when using a 4-hour preheating period before switching off the heating system, the thermal mass of the building releases sufficient heat to maintain the operative temperature above 20^0C for 15 hours. This potential increases with longer preheating period. The thermal behaviour of the external envelope and internal walls is examined, identifying the heat losses of the external envelope and the thermal capacity of the internal walls as the main parameters that affect the load shifting potential of the apartment.

KEYWORDS
energy flexibility, load shifting, thermal mass, low energy buildings, energy simulation

INTRODUCTION
In the future energy system a considerable increase in the penetration of renewable energy is expected. The fluctuating pattern of sources like solar and wind would create peaks and deficiencies in the energy production, which would challenge the stability of the system, as both the production and the consumption side would have fluctuating patterns. This would lead to imbalances of the electricity grid requiring changes to the balancing strategies (Hermanns and Wiechmann, 2009). Initially, the focus of such strategies was on the electrical system, but recently a multi-carrier energy system is of interest, including electricity grids, gas grids and district heating and cooling. Energy storage (Beaudin et al., 2010) and Demand Side Management (DSM) (Mohsenian-Rad et al., 2010) and would have a key role facilitating the future energy system. Typical methods to achieve DSM include peak load reduction, shifting demand from on-peak hours to off-peak hours (load shifting), introduction of flexible load shape and energy consumption reduction (strategic conservation) (Müller, 2015).

The building sector appears to have great potential for load shifting, due to the large mass of the building stock, and studies have been performed so as to utilize this mass for thermal energy storage (Wolisz et al., 2013; Reynders et al., 2013; Kensby et al., 2015; Ma and Guo, 2015; Masy et al., 2015).

The purpose of the present study is to perform a building energy simulation of an apartment of a low energy building in Copenhagen and evaluate the heat load shifting potential by

utilizing the thermal mass. A scenario is examined, in which the apartment is preheated before the heat supply is cut off to avoid a peak in the operation of the system. In the next section, the scenario examined is described and the basic inputs for the model are given. Afterwards, the results from the simulated cases are presented. Eventually, the main outcomes are discussed and final conclusions are given.

METHODS
In the multi-carrier future energy system the demand patterns will have to become flexible in order to facilitate the system to integrate a large share of renewables. It has been indicated by the district heating operators that in the future it might be favourable for the district heating system to stop supplying specific districts for certain time intervals. The purpose of the simulated scenario was to identify the effect such a stop would have in an apartment. The focus was on the impact of the thermal mass on the apartment's thermal behaviour. One of the key parameters investigated was the duration of the time that the apartment would need to be preheated before such a stop, in order for the thermal comfort to be maintained. The apartment modelled for this study belongs to a multi-family house building, which was built in 2016 in Copenhagen, Demark, and is connected to the local district heating system. The apartment was modelled in IDA Indoor Climate and Energy (ICE, version 4.7), and dynamic simulations were performed with a time resolution of 5 minutes.

The thermal behaviour of a building consists of a complicated mechanism and is affected by various parameters. This study had a focus on the thermal mass of the building, isolating it from exogenous parameters, such as the daily operation of the building, users' patterns and ambient weather conditions. Thereby, a synthetic weather file was created with stable ambient conditions. Using the Design Reference Year data for Denmark (DRY, 2013), an average day of the heating season for Denmark was estimated, having 3^0C temperature, 4.7m/s wind speed and 85% relative humidity. The solar radiation was not included in the study, as solar gains could account for an amount of energy added uncontrollably into a building, which would not allow for the thermal mass to be isolated. Internal gains from occupants, equipment and lighting were not included, as they depend on occupants' behaviour and there could be a range of amplitude and patterns, which would impede the isolation of the thermal mass. Internal masses for furniture and interior constructions were not included as well.

The scenario examined was divided in three periods; the steady state conditions, the preheating period and the cool down period with heating being switched off. Initially, the model was simulated for 5 days to ensure steady state conditions inside the zone and within the walls (days #1 - #5). During the steady state period the operative temperature setpoint was set to 20^0C according to EN/DS 15251 (2007), Category II, which corresponds to "normal level of expectations and should be used for new and renovated buildings". Operative temperature above 20^0C was considered as minimal comfort temperature. In day #6, the operative temperature setpoint was increased to 22^0C, which lasted for 4 hours, as a preheating period in order for the thermal mass to absorb heat. Then, the heating system was turned off and the apartment was left to cool down for the next days (until day #10). During the cool down process, the focus was at the first day of this cooling period, observing the thermal response of the apartment.

The simulated apartment had an area of 81 m^2 and 2.6 m height. The north and south walls were exposed to the ambient, while the east and west walls, as well as the floor and ceiling were attached to similarly heated spaces. The building was designed according to the Danish design regulations for 2020. Table 1 shows the properties of main components and materials.

Table 1: Properties of main components and materials

Components	Thickness [m]	U-value [W/(m^2·K)]	Surface [m^2]	Materials
External wall	0.55	0.12	25.7	Concrete Insulation Brick
Internal wall	0.2	3.43	49.4	Concrete
Internal floor/ceiling	0.45	0.27	161.5	Wood Concrete Insulation
Windows	3 pane glazing	0.81	18.51	-

Materials	Thermal conductivity [W/(m·K)]	Specific heat [J/(kg·K)]	Density [kg/m^3]
Concrete	1.65	1000	2200
Insulation	0.037	750	20
Brick	1.2	840	1600
Wood	0.17	2000	750

Mechanical ventilation was included in the system with constant flow of 0.5 ach, according to EN/DS 15251 (2007), using heat recovery with efficiency 0.8. Infiltration was accounted as constant flow of 0.1 ach, according to DS 418 (2011) for new buildings. Regarding the heating system, the building was connected to the district heating system and the heating emission system inside the apartment was floor heating of 16 W/m^2, supplied with 40^{0}C water temperature and controlled with a proportional controller on the room operative temperature.

RESULTS
As a reference value, the time constant of the apartment was calculated as the ratio of the thermal capacity to the steady-state heat losses (Antonopoulos and Koronaki, 2000), including transmission, ventilation with heat recovery and infiltration. The thermal capacity was approximately 108 MJ/K and the heat losses 34 W/K, leading to a time constant for the apartment of 878 hours. This is a very high value compared to a typical Danish building. The limited losses were attributed, firstly, to the fact that the apartment had a relatively small façade compared to the total wall area and secondly, as previously explained, the examined apartment was built according to the 2020 regulations, so it was an airtight building with very low values of heat transfer coefficients, both for the external walls and the windows.

Dynamic simulations were performed for the scenario explained in the METHODS section. During the steady state conditions, the operative temperature was maintained at 20 ^{0}C. Subsequently, the temperature was allowed to increase until 22 ^{0}C during the 4-hours preheating period. Since the heating system of the apartment was floor heating, the system had a slow response, so the operative temperature was increased only until 20.6 ^{0}C. The operative temperature increase achieved was small, so the temperature increase of the ceiling, internal and external wall surfaces was minor, as depicted in Figure 1a. The floor surface had the highest surface temperature at all times and achieved a distinct temperature increase during the preheating period, as expected. Figure 1b depicts the surface heat fluxes for the ceiling, one of the external walls and one of the internal walls. Negative values indicate that heat was absorbed in the walls, while positive values indicate that heat was released from the walls to the room. It may be seen that the ceiling and the internal wall behaved similarly, absorbing heat during the preheating hours and emitting back to the room, shortly after the

cooling down phase began. Although the external wall absorbed heat within the preheating hours, heat was never released back in the apartment.
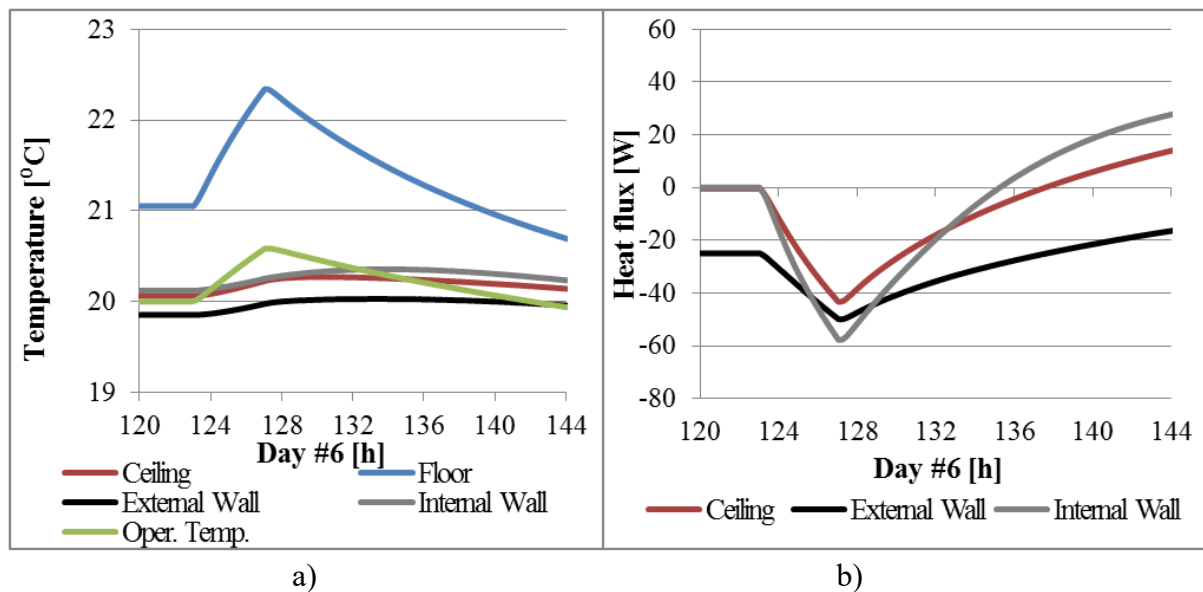

a) b)

Figure 1. a) Surface temperatures during day #6 (hours counted since day #1). b) Surface heat fluxes during day #6 (hours counted since day #1).

During the steady state conditions, the heating system ran uninterrupted generating 1.15 kWh for a duration of 2h, as it is depicted in the energy balance in Figure 2a. During the first two hours of the cool down period the internal walls, including floor and ceiling, released 0.81 kWh. This accounted for 61% of the demand, namely heat losses from the windows, external walls and thermal bridges, mechanical ventilation and infiltration.
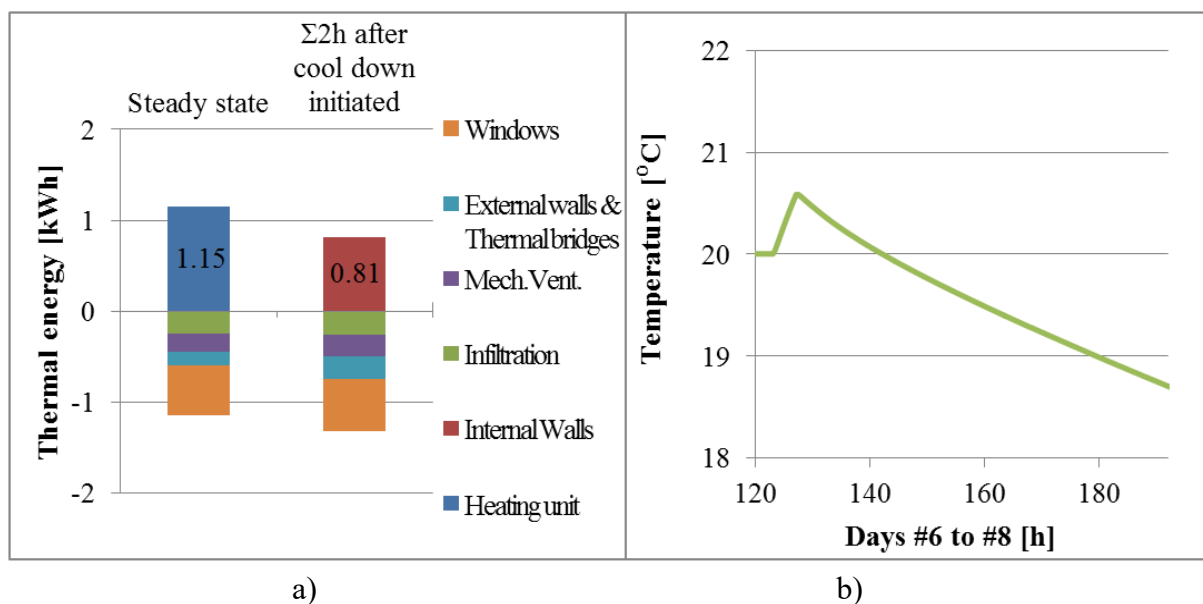

a) b)

Figure 2. a) Energy balance for a duration of 2h. b) Operative temperature during days #6-#8 (hours counted since day #1).

Letting the apartment cool down for the following days, it may be observed from Figure 2b that the operative temperature still remained above 20 ^{0}C for a considerable amount of hours. In this case, with 4 hours of preheating, the operative temperature remained above 20 ^{0}C for 15 hours after the heating system stopped working, only by recovering heat from the internal walls, ceiling and floor. During these 15 hours, 7 kWh were recovered from the thermal mass of the apartment. This indicates that the heat flows released are sufficient for a load shifting to be planned.

In order to investigate the effect of the duration of preheating, simulations were performed for different preheating periods, decreasing to 2 hours and increasing to 6 hours of preheating. The results may be seen in Table 2.

Table 2. Thermal response of the apartment for different preheating periods

Basic case apartment	Preheating duration		
	2 h	4 h	6 h
Max operative temperature difference during preheating [^{0}C]	0.3	0.6	0.8
No. of hours operative temperature above 20^{0}C [h]	8.3	15.1	21.2
Energy recovered from thermal mass during above hours [kWh]	3.79	7.04	10.09

It can be observed from the table that the slow response of the heating system did not allow the operative temperature to increase considerably in any of the preheating periods, hence thermal comfort is almost not affected. However, one may notice the effect of the different preheating periods on the number of hours that the operative temperature can be maintained above 20^{0}C, being approximately 8 h, 15 h and 21 h for the different preheating periods. Respectively, the thermal energy recovered during these hours varied between 3.8 kWh, 7 kWh and 10.1 kWh.

It could be observed that the heat recovered from the thermal mass came from the internal walls, including the ceiling and the floor. Thereby, the capacity of the thermal mass of the internal walls, should be considered as one of the main contributors to the load shifting potential of the apartment. On the other hand, the building envelope did not contribute to the heat recovery. Nevertheless, the external envelope is of equal importance for the load shifting potential of the apartment, since it governs the losses to the ambient. Thereby, it should be investigated in terms of total heat loss, rather than the capacity of its thermal mass. In addition, the total surface area of the external walls was rather small compared to the total surface area of the internal walls, ceiling and floor. Therefore, in order to examine the different behaviour of the internal and external walls, two scenario cases were created.

In the first case, the effect of thermal capacity of the internal walls on the load shifting potential was investigated. The material of the internal walls was changed from concrete to aerated concrete, with the following thermal properties; thermal conductivity of 0.2 W/(m·K), density of 500 kg/m^3 and specific heat of 800 J/(kg·K). This apartment would have a thermal capacity of 29 MJ/K, the same heat losses as the base case apartment (34W/K), leading to a time constant of 238 hours, namely 640 hours less than the base case apartment. In the second case, the effect of the heat losses of the building envelope on the load shifting potential was investigated. The windows were replaced with windows of a U-value of 2.8 W/(m^2·K) and the infiltration was increased to 0.87 ach, both typical values of Danish existing buildings.

This apartment would have a thermal capacity of 108 MJ/K, heat losses of 126 W/K, leading to a time constant of 238 hours, equal to the first case. The results are presented in Table 3.

Table 3. Thermal response of the apartment for the two scenario cases examined

	Case 1: Aerated concrete for internal walls			Case 2: Increased heat losses from building envelope		
	Preheating duration			Preheating duration		
	2 h	4 h	6 h	2 h	4 h	6 h
Max operative temp. difference during preheating [^{0}C]	1.1	1.7	2.0	0.2	0.3	0.5
No. of hours operative temp. above 20^{0}C [h]	6.1	9.5	11.2	1.7	2.9	3.9
Energy recovered from thermal mass during above hours [kWh]	0.36	2.49	3.37	2.08	4.90	6.61

As expected, in both cases the hours that the operative temperature remained above 20^{0}C were reduced, and so was the difference between the different preheating periods. In the first case, the temperature increase achieved during the preheating periods was considerably higher, but since the thermal capacity of the internal walls was reduced, the energy recovered from thermal mass was considerably lower, namely from 0.4 kWh to 3.4 kWh for the different preheating periods. Taking, for example, the 4 h preheating period, the internal walls managed to cover only 8% of the demand in the first 2 hours of the cool down period, compared to the 61% which was presented in the base case apartment.

In the second case, the apartment behaved similarly to the base case apartment. A very small temperature increase was observed during the preheating periods, but the high capacity of the internal walls recovered from 2.1 kWh to 6.6 kWh for the different preheating periods. This corresponds to the internal walls covering 76% of the demand in the first 2 hours of the cool down period for the 4 h preheating period scenario. However, the hours that the minimal comfort temperature was maintained were considerably reduced, due to the increased losses through the building envelope.

DISCUSSIONS
The operative temperature setpoint of 20^{0}C used as minimal comfort temperature corresponds to a "normal level of expectations" and should be used for new buildings, according to EN/DS 15251 (Category II). However, a lower temperature of 18^{0}C could also be used corresponding to "moderate, acceptable level of expectations". In this case, the potential for load shifting would be considerably increased. Furthermore, the upper limit of 22^{0}C was not reached in most cases, due to short preheating periods and slow response of the floor heating system. Different control of the floor heating system, for example supplying higher water temperatures, could achieve higher temperature increase during the preheating period. This would yield a higher amount of heat being stored and released back in the apartment, thus better load shifting potential. Even further, the upper limit could be increased if the preheating period would be during the time that occupants are not present in the apartment.

Regarding the two scenario cases, they resulted in limited load shifting potential. In the case of the decreased thermal capacity of the internal walls, the hours that the minimal comfort temperature was maintained were reduced by 37% for the preheating period of 4 hours, while in the case of the increased heat losses of the building envelope, the hours that the minimal comfort temperature was maintained were reduced by 80% for the same preheating period.

The duration of the preheating period had a considerable impact on the number of hours that the minimal comfort temperature was maintained, varying from 8h to 21h for 2h to 6h preheating period for the base case scenario. This provides different possibilities for Demand Side Management, adjusting to projections of the system's needs. The duration of the period that heating can be switched off could be used as an indicator for the flexibility performance of a building. This report has shown that it would depend strongly on the thermal mass of the apartment, but not exclusively. The degree of insulation of the building envelope is also substantive.

Finally, it should be noted that for this study, the time of the switch off of the heating was not influential, as there were no solar or internal gains, since the target was to isolate the effect of the thermal mass. Further on, more realistic cases should be studied including solar and internal gains, using different occupancy schedules and identifying the impact on load shifting potential.

CONCLUSIONS

It has been shown that for an apartment of a low energy building in Copenhagen the thermal mass can be utilized as thermal energy storage, thus facilitating heat load shifting for several hours, without the contribution from internal or solar gains. This potential increases with longer preheating periods.

Two cases were examined, first changing the thermal capacity of the internal walls and second the heat losses of the external envelope such that the static time constant became equal in both cases. It was shown that the external and internal walls, including floor and ceiling, contributed to the load shifting potential of the apartment, though in different terms. The internal walls recovered the heat that was absorbed during the preheating period, covering for a certain amount of hours part of the demand. The properties of the materials used in the internal walls defined the heat capacity of the internal walls, which governed the potential for load shifting of the apartment. On the other hand, the building envelope affected the potential for load shifting, only in terms of heat losses to the ambient. The heat that was absorbed in the external walls during the preheating period was not released in the apartment, but it was gradually lost to the ambient due to heat conduction. Thereby, in the second case, the heat losses of the external envelope governed the potential for load shifting of the apartment.

Finally, the relative size of the internal versus the external walls partly defines the impact of the two types of walls. In the present case the area of the outer walls was so small that thermal capacity of the external walls had infinitesimal impact on the load shifting potential.

REFERENCES

Antonopoulos, K. and Koronaki, E., 2000. Effect of indoor mass on the time constant and thermal delay of buildings. Fuel and Energy Abstracts, 41(May 1999), p.408.

Beaudin, M. et al., 2010. Energy storage for mitigating the variability of renewable electricity sources: An updated review. Energy for Sustainable Development, 14(4), pp.302–314.

Danish Ministry of Climate, Energy and Building, 2013. 2001-2010 Danish Design Reference Year. Technical Report 13-19. Danish Meteorological Institute, Copenhagen.

Dansk Standard, 2007. DS/EN 15251:2007: Input-parametre til indeklimaet ved design og bestemmelse af bygningers energimæssige ydeevne vedrørende indendørs luftkvalitet, termisk miljø, belysning og akustik. - Indoor environmental input parameters for design and assessment of energy performance of buildings addressing indoor air quality, thermal environment, lighting and acoustics.

Dansk Standard, 2011. Beregning af bygningers varmetab. - Calculation of heat loss from buildings.

Hermanns, H. and Wiechmann, H. 2009. Future Design Challenges for Electric Energy Supply. Emerging Technologies & Factory Automation, 2009. IEEE Conference, p. 1-8.

IDA Indoor Climate and Energy (ICE), version 4.7, EQUA Simulation AB, http://www.equa.se/en/ , accessed 02/03/2016.

Kensby, J., Trüschel, A. and Dalenbäck, J.-O., 2015. Potential of residential buildings as thermal energy storage in district heating systems – Results from a pilot test. Applied Energy, 137, pp.773–781.

Ma, P. and Guo, N., 2015. Modeling of Thermal Mass in a Small Commercial Building and Potential Improvement by Applying TABS. American Journal of Mechanical Engineering, 3(2), pp.55–62.

Masy, G. et al., 2015. Smart grid energy flexible buildings through the use of heat pumps and building thermal mass as energy storage in the Belgian context. Science and Technology for the Built Environment, 4731(August), pp.800–811.

Mohsenian-Rad, A.H. et al., 2010. Autonomous demand-side management based on game-theoretic energy consumption scheduling for the future smart grid. IEEE Transactions on Smart Grid, 1(3), pp.320–331.

Müller, D. et al., 2015. Demand side management for city districts. Building and Environment, 91, pp.283–293.

Reynders, G., Nuytten, T. and Saelens, D., 2013. Potential of structural thermal mass for demand-side management in dwellings. Building and Environment, 64, pp.187–199.

Wolisz, H., Harb, H. and Matthes, P., 2013. Dynamic simulation of thermal capacity and charging/discharging performance for sensible heat storage in building wall mass. In 13th Conference of International Building Performance Simulation Association. Chambery, France, pp. 2716–2723.

Energy flexibility is proposed as a way to facilitate the management of the energy system while integrating a large proportion of renewable energy sources. The residential building sector has a great potential for flexibility, as it is responsible for a large share of all energy use, and part of this energy demand can, with appropriate control, be shifted in time, in order to increase the flexibility of the demand side. The aim of the thesis was to investigate the physical potential of low-energy buildings to facilitate flexible heating operation by using the thermal mass of the buildings as heat storage, while maintaining thermal comfort. The operational flexibility potential of low-energy buildings was investigated and methodologies were proposed that made it possible for the heating system to be operated in such a way as to meet the flexibility requirements of the local district heating system. In addition, creating daily electricity demand profiles representative for Danish households was undertaken as the basis for flexibility modelling of electricity household loads, i.e. rescheduling the use of domestic appliances and electricity-based heating systems.